Profiling the molecular mechanisms underlying negative cross-resistance to insecticides using *Drosophila melanogaster*

Mohamad Fakhrur Razi Ghazali

ORCID ID: 0000-0002-2647-2204

Submitted in total fulfilment of the requirements of the degree of

Doctor of Philosophy

April 2020

School of BioSciences
Faculty of Science
The University of Melbourne

Abstract

Nicotinic acetylcholine receptors (nAChRs) are ligand-gated ion channels that mediate neurotransmission at cholinergic synapses. The nAChRs are mainly expressed in the central nervous system and are highly conserved across a wide range of insect species. Neonicotinoids and spinosyns are two classes of insecticide that target nAChR subunits to kill pest insects. Mutations in genes encoding several nAChR subunits in various insect species, as well as in *Drosophila melanogaster*, have been documented as conferring insecticide resistance.

Chemical control including insecticides has been a key tool in controlling pest insects. The cycle of insecticide use, resistance evolution and insecticide replacement has been continuing for the past decade, leading to many pest species carrying resistance to multiple classes of insecticides. This thesis examines the interplay between different insecticides and nAChR mutations that are associated with resistance to one insecticide but result in hypersensitivity to another, a phenomenon called negative cross-resistance. The negative cross-resistance relationship presents insecticides that could complement current rotation strategies for resistance management, and this warrants further analysis to understand the mechanism.

Examination of loss-of-function mutations on the nAChR subunits in this thesis, confirmed the previous identification of the Dα1 and Dβ2 subunits as targets for neonicotinoids, as well as the Dα6 subunit as a target for spinosyns. This study also identifies the Dα2 subunit as an additional target for imidacloprid. Importantly, mutations on these subunits were also associated with insecticide hypersensitivity, suggesting negative cross-resistance. The neonicotinoid-resistant, *Dα1* mutants were hypersensitive to spinosyn, except for a full knockout allele, while the spinosyn-resistant, *Dα6* mutants were all hypersensitive to neonicotinoids. Additionally, negative cross-resistance was found between two

neonicotinoids, nitenpyram and imidacloprid in the *Dα2* mutants. Analysis of different allelic variations at the gene encoding these subunits indicates that this is not an allele specific phenotype.

Combining the negative cross-resistance relationship and analyses of molecular changes induced in the nAChR subunits mutants, our study initiated to characterise the changes at the synapse that underlie the negative cross-resistance phenotype. A mechanism involving nAChR compensatory changes in levels of another receptor subunit/subtype was hypothesised to cause the phenotype. Following measurement of transcriptional changes and subunit protein changes, the study classified few correlations between nAChR subunit expressions and the negative cross-resistance, and these vary between the mutants suggesting other possible route(s) for the insecticide hypersensitivity.

A genome-wide differential gene expression analysis in specific neuronal cell types of larval brain revealed differentially expressed genes in the *Dα1* and *Dα6* mutants. Interestingly, gene ontology enrichment analysis indicates dysregulation of cellular processes, including oxidative stress, protein trafficking and proteasomal degradation pathways in the mutants, that may contribute to the insecticide hypersensitivity. Dysregulation of oxidative stress may predispose the nAChR mutants to further insecticide-induced increase in oxidative levels. Finally, blocking dynamin-mediated endocytosis and proteasome activity, using chemical inhibitors, showed protection against larval movement reduction following imidacloprid and/or spinosad exposure. These findings indicate that the relatively straightforward phenotypic observation of insecticide hypersensitivity in response to loss of a receptor subunit is most likely underpinned by several complex changes in neurons, altering the sensitivity of their response to insecticides and their capacity to cope with downstream effects of insecticide exposure.

Declaration

This is to certify that:

i. the thesis comprises only my original work towards the PhD except where indicated in the Preface;

ii. due acknowledgement has been made in the text to all other material used;

iii. the thesis is fewer than 100,000 words in length, exclusive of tables, maps, bibliographies and appendices.

Signed:

Mohamad Fakhrur Razi Ghazali

20 April 2020

Preface

This thesis is made up of my own work under the supervision of my supervisory panel (Dr Trent Perry and Professor Philip Batterham) except, where indicated below:

Chapter 2

- CRISPR-generated nAChR subunit mutant strains were made by Dr Trent Perry, Ying Ting (Tinna) Yang, Dr Hang Ngoc Bao (Jenny) Luong, Danielle Christesen and Wei Chen
- *Dα1*^{P141S} strain were made by Dr Trent Perry and Ying Ting (Tinna) Yang

Chapter 3

- Fly strains containing UAS-LT3-NDam or UAS-LT3-NDam-RpII215 construct for targeted DamID were contributed by Professor Andrea Brand from University of Cambridge, UK
- Dr Owen Marshall and Dr Michael Murray helped to set up an analysis pipeline for targeted DamID
- RNA extraction for RNA-seq analysis were performed with the assistance from Ying Ting (Tinna) Yang, Felipe Martelli and Danielle Christesen

Chapter 4

- T2AGAL4 strain for *Dα1* was made by Wei Chen
- Fly strains containing UAS-Dα1-YFP or UAS-Dα6-YFP were made and screened on insecticides by Dr Jason Somers and Joseph Nguyen

All chapters presented in this thesis are unpublished materials not submitted for publication.

Scholarships and funding

The following awards funded me during the course of my PhD candidature:

- Melbourne Research Scholarship (stipend and fee offset) to undertake a doctoral degree from April 2016 to April 2020
- Bio21 Institute Student Travel Award to aid travel to conferences and/or to visit labs to discuss or develop research (2018)
- Science Abroad Travelling Scholarships by the Faculty of Science, the University of Melbourne to undertake travel to attend conferences, fieldwork, etc (2019)
- F H Drummond Travel Award to undertake study and/or research at an overseas university or other academic institution (2019)
- BioSciences GR Travel Grant by the School of Biosciences, the University of Melbourne to participate in domestic or international meetings and/or conferences (2019)

Acknowledgements

My journey in completing this PhD thesis would have not been possible without the huge help, support and encouragement from the people around me, to only some of whom it is possible to give particular mention here.

Above all, I would like to express my unending gratitude to my supervisors, Dr Trent Perry and Professor Phil Batterham, not only for direct guidance, knowledge and expertise throughout the research project but also for being intellectual inspirations and emotional strongholds through the greatest opportunity of a lifetime, that is my PhD. Trent has been an excellent supervisor, guiding me through every technicality from experiments to research analysis. Phil has been a true expert in scientific knowledge and literature of the field. I will always be thankful for both of you for always being available to talk and who were never short to provide the support I needed, despite the challenges of a busy schedule. I would also like to extend my appreciation to my PhD advisory panel, Professor Andrew Pask and Dr Michael Murray for the valuable input into the research and in ensuring steady progress throughout my candidature.

A big thank you to Dr Andrea Brand (University of Cambridge, UK), Dr Owen Marshall (University of Tasmania, Australia) and Dr Michael Murray to whom without would not have made the analysis in my thesis possible. They contributed a wealth of resources and ideas to the targeted DamID experiments.

I would also like to express my gratitude to the Perry/Batterham lab members, past and present, not only for lending a helping hand in the experiments but also, all the good and relaxing times that we spent together in making sure that everyone is not overwhelmed at work. I would like to particularly mention Tinna Yang who was my go-to person in the lab, when learning molecular techniques and lab instrument procedures, and also, Joseph, Danielle, Wei, Felipe and Alex who introduced me to various experimental techniques in the lab that have made lab work more convenient.

To all the PhD peers who shared the same journey with me, you have done well. Particularly, to my close group of friends at the University of Melbourne – Azri, Suffian, Hidaya, Yudha, Yichao and Thy, I will always be thankful for the endless support and encouragement through the challenging times as well as along this journey. To my other friends in Malaysia and Australia, thanks for the unmatched encouragement for the past eight years whilst I was in Melbourne.

Last but certainly not the least, I want to dedicate this journey to my family. I'm grateful that they have always been there for me, for supporting me in the good as well as the troubling times in my life. Especially, to both my parents for the endless support and prayers, and to my siblings for the advice and encouragement, thank you. Also, thanks to my extended family and friends for keeping in touch and caring for my well-being throughout these years.

It has been an incredible journey completing this PhD thesis. Thank you!

Table of Contents

List of Figures

List of Tables

Abbreviations

5-HT_3 receptor	type 3 5-hydroxytryptamine receptor
α-BTX	α-bungarotoxin
αCTXMII	α4/7 conotoxin
ACh	Acetylcholine
AChBP	Acetylcholine binding protein
AChE	Acetylcholinesterase
BDSC	Bloomington Drosophila Stock Centre
ChAT	Choline acetyltransferase
ChIP	Chromatin immunoprecipitation
CI	Confidence intervals
CNS	Central nervous system
CRIMIC	CRISPR-Mediated Integration Cassette
CRISPR	Clustered Regularly Interspaced Short Palindromic Repeats
Dam	DNA adenine methyltransferase
DamID	Dam (DNA adenine methyltransferase) Identification
DDT	Dichlorodiphenyltrichloroethane
DEG(s)	Differentially expressed gene(s)
DMSO	Dimethyl sulfoxide
EMS	Ethyl methane sulfonate

ER	Endoplasmic reticulum
ERAD	Endoplasmic reticulum-associated degradation
FDR	False discovery rate
FL	Fiducial limits
GFP	Green fluorescent protein
GO term	Gene Ontology term
IPM	Integrated Pest Management
IRAC	Insecticide Resistance Action Committee
IRM	Insecticide Resistance Management
IUPAC	International Union of Pure and Applied Chemistry
nAChR(s)	Nicotinic acetylcholine receptor(s)
LC_{50}	Lethal concentration 50
LGIC	Ligand-gated ion channels
LNvs	Ventral lateral neurons
MiMIC	Minos-Mediated Integration Cassette
NDGA	Nordihydroguaiaretic acid
NMJ	Neuromuscular junction
ORF	Open reading frame
PBS	Phosphate-buffered saline
PCR	Polymerase Chain Reaction
PDB	Protein Data Bank
ppm	parts per million

qPCR	Quantitative real-time PCR
RMR	Relative movement ratio
RNAi	RNA interference
RNA Pol II	RNA polymerase II
RNAseq	RNA sequencing
ROS	Reactive oxygen species
RR	Resistance ratio
SEM	Standard error of mean
SDS	Sodium dodecyl sulphate
ssODN	Single-stranded oligodeoxynucleotide
TF	Transcription factor
TM	Transmembrane domain
UAS	Upstream activating sequence
UPS	Ubiquitin–proteasome system
UTR	Untranslated region
VGSC	Voltage-gated sodium channel
VNC	Ventral nerve cord
YFP	Yellow fluorescent protein

Chapter 1 : Introduction

1.1 Nicotinic acetylcholine receptor (nAChR)

1.1.1 nAChRs are Cys-loop ligand-gated ion channels

Neurons pass information as electrical or chemical signals at synapses, a close contact point between two neurons where they communicate to each other. These signals are typically propagated as action potentials that requires exchange of ions such as Na^+, K^+, Ca^{2+} and Cl^-, across cellular membranes via protein channels or receptors. When an action potential reaches the presynaptic terminal of a neuron, chemical messengers or ligands called neurotransmitters are released, which later bind and activate the receptors at the postsynaptic membrane (Borst and Sakmann 1996; Lee and Sine 2005). This opens up the channels resulting in an influx of ions into the neuron, converting the chemical signal back to action potential. This whole process is known as neurotransmission. The channel receptors, including the nicotinic acetylcholine receptors (nAChRs) are essential in mediating rapid transduction of chemical signals into electrical signals in the nervous system, allowing organisms to quickly respond to stimuli.

nAChRs are members of the Cys-loop subfamily of the ligand-gated ion channels (LGIC), which are a superfamily of oligomeric ionotropic receptors that respond to ligands. They are commonly transmembrane ion-channels that become permeable to ion flows in response to the binding of their native ligand. Members of the Cys-loop LGIC subfamily are usually similar in structure and related through evolution (Lester et al. 2004; Ortells and Lunt 1995). The subfamily includes other receptor classes such as γ-aminobutyric-acid (GABA) receptors, 5-hydroxytryptamine type 3 ($5\text{-}HT_3$) receptors and glycine receptors (Lester et al. 2004). While all receptors under the Cys-loop LGIC subfamily are ionotropic

receptors, nAChRs and 5-HT_3 receptors have excitatory effects and are selective for cation flow, while GABA and glycine receptors exhibit inhibitory effects and are permeable to anions when open (Ortells and Lunt 1995). Insect nAChRs are mainly expressed in the central and peripheral nervous system, while in vertebrates they are also expressed in neuromuscular junctions, NMJ (Millar and Gotti 2009; Unwin 2013).

1.1.2 nAChR identification and characterisation

Acetylcholine (ACh) was the first neurotransmitter to be discovered and its receptor, the first pharmacological receptor to be characterised (Loewi 1921). This characterisation of nAChRs was initiated by isolation from electric organ of the electric eel, *Electrophorus electricus*, which is packed with nAChRs. Later, the discovery of α-bungarotoxin (α-BTX) provided a method for nAChR purification. α-BTX, a toxin from venom of Taiwanese krait snake, *Bungarus multicinctus*, has high binding affinity for nAChRs at the NMJ. It inhibits nAChR function leading to respiratory failure and paralysis (Changeux, Kasai, and Lee 1970; Lee and Chang 1966). The integration of these discoveries allowed for the nAChR to be purified from the electric organs using affinity chromatography with beads labelled with α-BTX (Meunier et al. 1971).

Currently, only nuclear magnetic resonance (NMR) structures of human nAChRs have been reported and these have been limited to the transmembrane domain of the receptor (Bondarenko et al. 2012, 2014). The crystal structure of a complete neuronal nAChRs is not yet available, however predictions of their general tertiary and quaternary structure have been inferred from the muscle-type nAChRs due to the high homology between the two receptor proteins (reviewed in Karlin 2002). Muscle nAChRs are mainly expressed postsynaptically at the NMJ, connecting the nervous and muscular system to control muscle contraction (Fagerlund and Eriksson 2009; Wang, McIntosh, and Rich 2018). It was demonstrated that nAChRs isolated from electric organs of Torpedo genus are very similar to the mammalian muscle nAChRs (Conti-Tronconi and Raftery 1982). Because of the high degree of conservation between these nAChRs,

studies using X-ray crystallography and electron microscopy have provided insight into the protein structure.

Examination of muscle nAChRs purified from *Torpedo marmorata* using electron microscopy revealed ring-like particles made up of several subunits surrounding a central hydrophilic core (Cartaud et al. 1973). Later, detailed 4Å resolution crystal structure of the *Torpedo* nAChR revealed the 3D structure and arrangement of the receptor subunits (Figure 1.1A) (Unwin 2005). Purified polypeptides were then sequenced to reveal several distinct, yet related, receptor subunits. X-ray crystallographic structures of ACh binding protein (AChBP) isolated from snail, *Lymnaea stagnalis* were also becoming available around the same time (Brejc et al. 2001). AChBP is a homolog of the nAChR extracellular amino-terminus domain (24% sequence identity with human α7 extracellular domain). These AChBPs are secreted by glial cells as homopentamers that resemble nAChRs but lacking the transmembrane and intracellular domains (Celie et al. 2005; Hansen et al. 2004; Smit et al. 2001). The resolved AChBP structure helped to define the ligand-binding domain of nAChR (Figure 1.1B).

1.1.3 nAChR structure

Like all members of Cys-loop LGIC family, nAChRs are pentameric channel receptors composed of five nAChR subunits which form a barrel-like arrangement around a central pore (Figure 1.2A). Each of these highly conserved subunits commonly consists of a large extracellular amino-terminus domain which contains a signal peptide and the ligand-binding domain, followed by four transmembrane domains (TM1 to TM4) with a large intracellular loop of variable length between TM3 and TM4. The subunit ends with a short extracellular carboxy-terminus (Figure 1.2B).

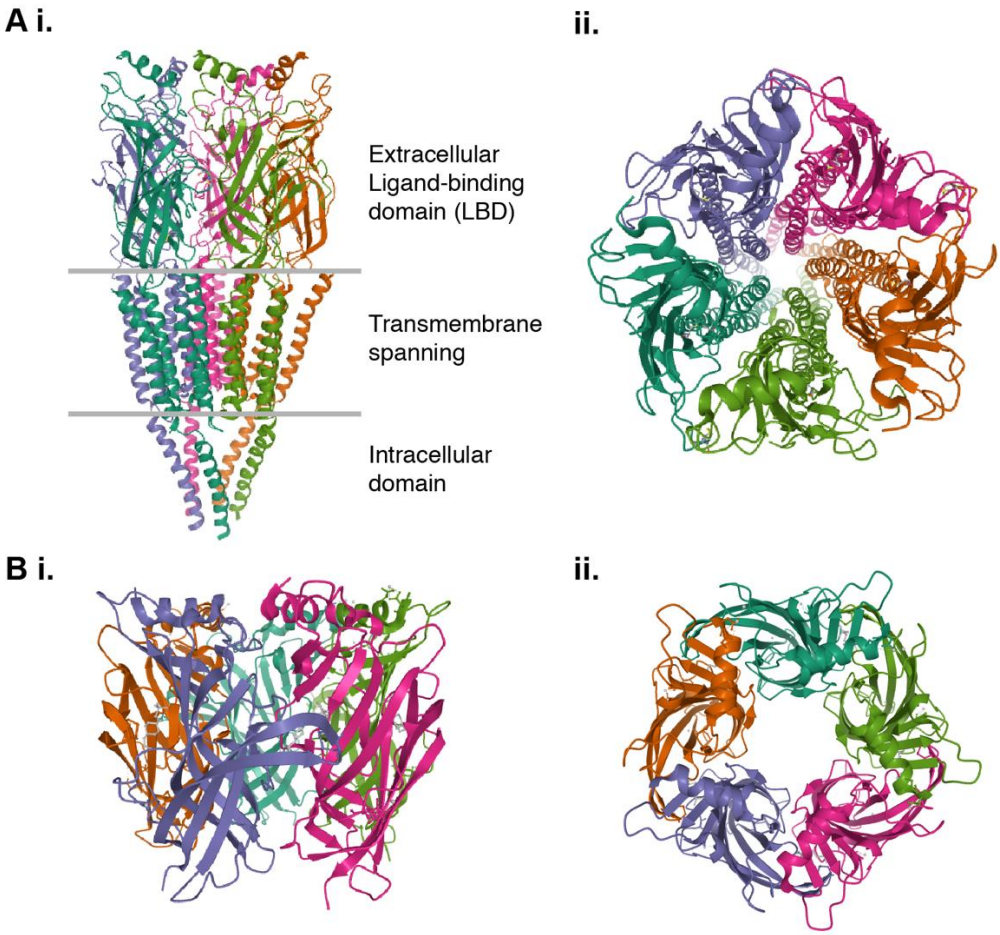

Figure 1.1 Early 3D structures revealed pentameric arrangement of nAChR

(A)(i) Side and (ii) top down view of the *Torpedo* receptor highlighting pentameric structure of $\alpha_2\beta\delta\gamma$ nAChR (α, purple and light green; β, pink; δ, orange; γ, dark green). The 3D structure highlights the extracellular ligand-binding region, the transmembrane spanning domain and the intracellular region of the receptor. PDB 2BG9. (B)(i) Side and (ii) top down view of the molluscan AChBP α-subunit homopentamer that helped to resolve the ligand-binding region of nAChR. PDB 1I9B.

Figure 1.2 nAChR structure and arrangement

Opposite (A) Pentameric nAChR highlighting barrel-like arrangement of five individual subunits around a central pore. Note, two molecules of acetylcholine (ACh) are required to efficiently activate the receptor. (B) Each individual subunit is composed of extracellular-binding domain, followed by four transmembrane domains (TM1-TM4) with a large intracellular loop connecting the TM3 and TM4. (C) The principle face contributes loops A, B and C, while the complementary face contributes loops D, E and F to ligand binding. Important, conserved residues for the ligand binding are also highlighted.

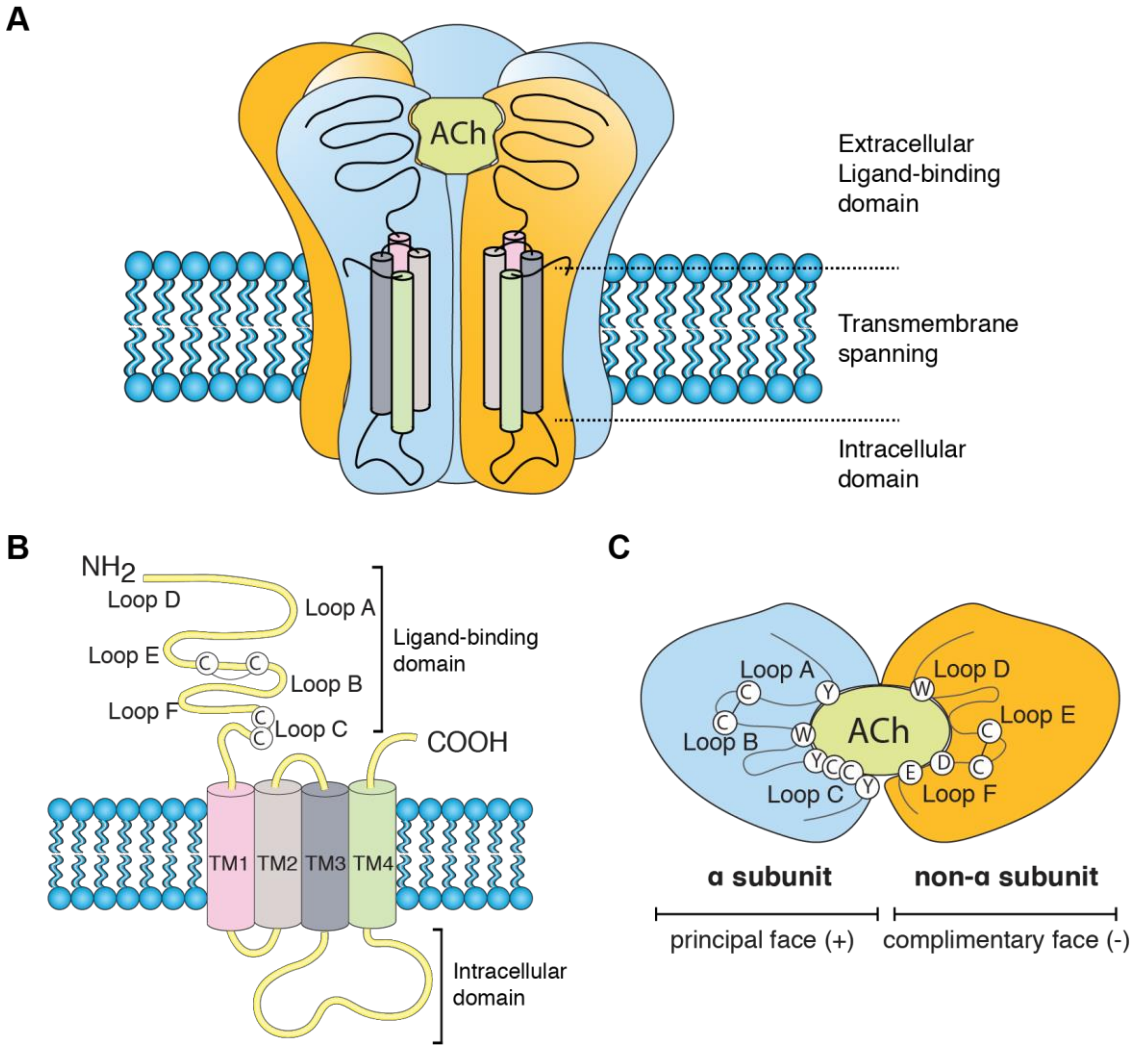

Each nAChR subunit has four transmembrane domains. TM2 contributes to the lining of the central ion pore (Hucho, Oberthür, and Lottspeich 1986). Meanwhile, TM1 and TM3 form an outer circle, and TM4 is furthest away from the central channel. All TM domains protect TM2 from the phospholipid environment (Tierney and Unwin 2000). TM2 is an alpha-helical domain with conserved residues at both ends of the helix. These well-conserved residues govern cation selectivity of the channel (Corringer, Le Novere, and Changeux 2000), which is also contributed to by residues of the short intracellular linker between TM1-TM2 (Jensen, Schousboe, and Ahring 2005). Unlike the short linkers between TM1-TM2 and TM2-TM3, TM3-TM4 is separated by a large intracellular domain (Figure 1.2B). This intracellular domain is varied in length and not conserved among the different subunits. This region contains predicted sites for phosphorylation that are important for the receptor function (Nashmi et al. 2003).

Thus, the variability of these domains might have functional consequences on the hypothesised roles in subunit/receptor maturation, trafficking, assembly, distribution, clustering and gating (Breitinger et al. 2009; Kracun et al. 2008; Mukherjee et al. 2009; Pollock, Pastoor, and Wecker 2007).

The extracellular nAChR ligand-binding domain contains six loops (loops A-F) and a characteristic Cys-loop motif. Loops A-F contribute to the orthosteric pocket for ligand binding (Figure 1.2C). nAChR subunits are grouped into either α subunit or non-α subunit (β, δ, ε or γ) with the defining difference being that the α subunit contains two conserved adjacent cysteines (YXCC motif) in loop C which non-α subunits lack (Corringer et al. 2000). The two cysteines of the YXCC motif form a disulphide bond which is important for ligand binding. Upon ligand binding, rearrangement of the disulphide bond in loop C will initiate a series of conformational changes leading to receptor activation. The orthosteric pocket for ligand binding usually occurs between the cleft of two nAChR subunits where the principal face is always provided by an α subunit. The principal face contributes loops A, B and C, while the complementary face contributes loops D, E and F to the binding pocket (Figure 1.2C)(Sine, Wang, and Bren 2002). Given the important of the loop C YXCC motif, functional ACh-binding nAChRs are only predicted to form from α-subunit homopentamers while heteromeric nAChRs require at least one α subunit (Corringer et al. 2000).

The characteristic Cys-loop defining the LGIC subfamily consists of two disulphide bond-forming cysteines which are separated by thirteen highly conserved amino acid residues. The Cys-loop is located in proximity to the transmembrane domain and has a functional role in mediating conformational changes from the ligand-binding domain to the transmembrane domains for channel opening (Miller and Smart 2010).

1.1.4 nAChR gating and function

nAChRs adopt three main functional states; a closed resting state, an open ion-conductive state upon ligand binding, and a closed desensitised state that is insensitive to further ligand activation (Figure 1.3A-B). Binding of chemical messengers, which have been referred to by several different terms including ligand, transmitter or agonist, can cause the opening of the nAChR channel. The neurotransmitter ACh, the endogenous ligand for nAChR, binds to the ligand-binding site leading to a conformational shift of all subunits present in the receptor complex to trigger channel opening (Wells 2008; Yamodo et al. 2010). This usually happens in microseconds, and thus the entire receptor structure is thought to be well tuned to accommodate for the rapid conformational changes, which also explains why the subunit structures are well-conserved.

The exact conformational changes involved in the process remain unclear, however, evidence suggests they involve the anchoring of the ligand-binding domain to the TM2-TM3 linker through mediation by the Cys-loop (Unwin 2005). This leads to rotation of the TM2 helices, removing the hydrophobic residues from the central pore and increasing the diameter of the pore for ion flow (Althoff et al. 2014; Miyazawa, Fujiyoshi, and Unwin 2003). Mutations at the interface between the ligand-binding domain and the transmembrane domain were described to affect, not only the channel opening, but also the rate of receptor desensitisation (Bouzat et al. 2008). Other ligands of nAChR include agonists (nicotine, epibatidine, and choline) which activate the receptors and antagonists (mecamylamine, dihydro-β-erythroidine, and hexamethonium) which block the receptor, preventing ion flow. The varying subunit combinations that form nAChRs were shown to influence receptor pharmacology (Figure 1.3C)(Ihara et al. 2003; Lansdell et al. 2012).

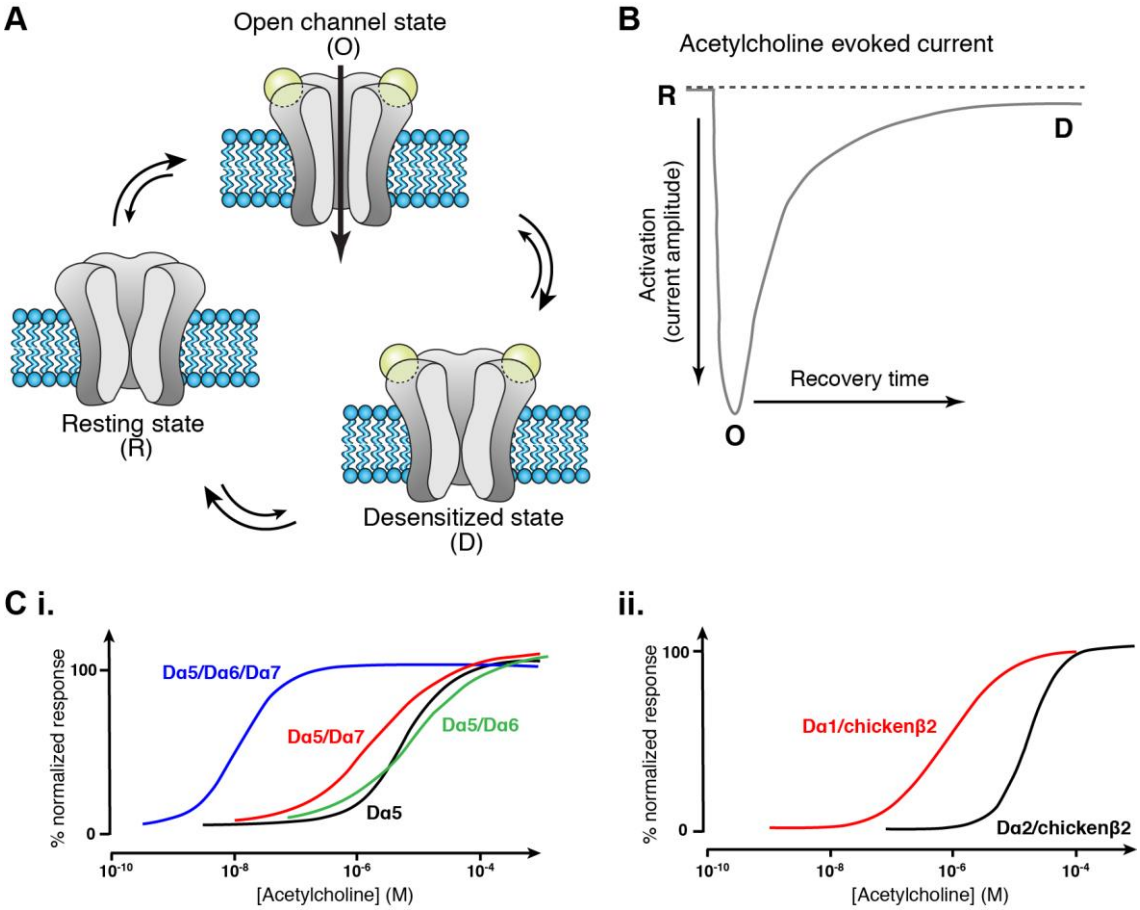

Figure 1.3 Three conformational states for nAChRs

Illustrations highlight changes in (A) conformational state of an nAChR and (B) changes in inward current in response to ACh. Prior to ligand activation, the nAChR exists in the resting state, R with the channel closed. Activation of the nAChR in response to ligand binding, leads to an open conformation, O, associated with ion flow through the channel, a fast, inward current. A decay in current back to initial (zero current) indicates inactivation of the receptor, entering its desensitised state, D. (C) Heterologous expression studies have demonstrated that nAChRs differing in subunit composition differ in receptor gating and responses to ligand (Ihara et al. 2003; Lansdell et al. 2012).

nAChRs mainly function to transmit rapid neurotransmitter signals, typically in neuronal tissues, from the presynaptic to the postsynaptic cells. In general, the activation of nAChRs leads to membrane depolarisation via influx of cations (K^+, Na^+ and Ca^{2+}) through the receptor channels, and thus, changes the extracellular and intracellular cation concentration (Letz et al. 1997). When expressed presynaptically, nAChRs can also directly or indirectly increase neurotransmitter release (Marchi and Grilli 2010). Muscle nAChR functions postsynaptically at the

NMJ, between neurons and skeletal muscles, mediating an ACh signal to generate a muscular response.

Although mainly expressed in neurons, nAChRs are also expressed in other cell types including glia, endothelial cells, skin cells and multiple cell types in lungs, digestive system and immune system, with many of these cells also releasing ACh (Fujii et al. 2017; Gahring, Persiyanov, and Rogers 2004; Grando et al. 1995; Heeschen et al. 2001; Wang et al. 2002; Wessler and Kirkpatrick 2008). Similarly, other components of cholinergic system were found to be expressed in considerable amounts in many of these tissues (Fujii et al. 2017; Wessler and Kirkpatrick 2008). Taken together, these indicate involvement of cholinergic activity in modulation of cellular functions in non-neuronal cells. For instance, there is evidence that nAChRs regulate an inflammatory signal in the immune system through distinct intracellular pathways. It was suggested that cholinergic activity is involved in the regulation of cytokines for inflammatory response (Fujii et al. 2017). Meanwhile in the epidermis, nAChRs potentially regulate cell adhesion and lateral cell migration (Grando et al. 1995; Grando, Pittelkow, and Schallreuter 2006). Nicotine-mediated angiogenesis and tumour growth were also associated with nAChR expression in endothelial cells and lungs (Heeschen et al. 2001). Note that many of these potential nAChR functions in non-neuronal tissues are still not well-understood and thus, require further characterisation.

Due to important nAChR roles in these systems, it has been found that in humans, mutations in nAChRs are associated with neurological disorders such as epilepsy, muscular disorders such as congenital myasthenia and autoimmune disorders such as myasthenia gravis (Bertrand et al. 2002; Engel and Sine 2005; Noridomi et al. 2017; Webster et al. 2014). The importance of nAChR function in the central nervous system also has led to interest in the receptors as potential drug targets to treat nicotine addiction, Alzheimer's disease, Parkinson's disease and schizophrenia (Crooks, Bardo, and Dwoskin 2014; Dineley, Pandya, and Yakel 2015; Gotti, Zoli, and Clementi 2006; Quik, Bordia, and O'Leary 2007).

1.1.5 Regulation of nAChR expression

1.1.5.1 Transcriptional and post-transcriptional regulation

nAChR biogenesis is complex and involves multiple levels of regulation. The first level of nAChR expression is controlled by transcriptional regulation of the genes encoding subunits. Cell-specific expression of nAChR transcripts was reported in early studies where the composition of nAChRs was observed to differ, qualitatively and quantitatively, in different mammalian cell-types tissues, at different stages of cells differentiation and during development (Boulter et al. 1990; Kues, Sakmann, and Witzemann 1995; Nery et al. 2010). In mammals, the *α3* and *β4* transcripts are abundantly expressed in the autonomic nervous system while the *α4* and *β2* transcripts predominate in the central nervous system (Albuquerque et al. 1995). Different regions of the brain were also found to have different levels of nAChR subunit transcripts, which could indicate distinct roles of different nAChR subtypes in the brain (Albuquerque et al. 1995; Alkondon and Albuquerque 2004; Gotti and Clementi 2004).

Similarly, transcriptional regulation was reported in insects, where specific nAChR subunit transcripts were enriched in different types of neurons. Dα1 and Dα6 were suggested to be the main functional subunits in *Drosophila melanogaster* ventral lateral neurons as their transcripts were more abundantly expressed than the other subunits (Rosenthal et al. 2019). The study also indicated that while both *Dα1* and *Dα6* transcripts expression change throughout larval development, only *Dα1* transcript level can be modulated via external factors such as light conditions (Rosenthal et al. 2019). Modulation of nAChR transcripts in response to external factors such as neuronal injury has also been described in mice (Kelso et al. 2006). These changes in transcript expression could imply that transcriptional regulation of nAChRs can be altered in response to external factors, however, the role of post-transcriptional modification on protein levels was not investigated in the studies, and thus, its involvement should not be excluded.

Post-transcriptional modification may provide an additional level of regulation to nAChR subcellular localisation. microRNA (miRNA) which generally target 3’

UTR of mRNA transcript leading to mRNA degradation or protein translation inhibition, is among the significant regulators of gene expression at the post-transcriptional level (Ambros 2004). As miRNA machinery has been shown to be involved in broad range of biological processes, it is likely that they also mediate nAChR expression changes. It was previously shown that miRNA is involved in nicotine-induced nAChR upregulation in *Caenorhabditis elegans*. The normal induction fails to occur in a mutant of *alg-1* gene that encodes a key Argonaute-family member involved in miRNA-mediated inhibition (Rauthan et al. 2017). Further, nicotine treatment leads to the downregulation of an miRNA predicted to regulate *β2* mRNA, miR-542-3p. In turn, when miR-542-3p is over-expressed in a cell line, it leads to reduced *β2* expression (Hogan et al. 2014). Other post-transcriptional processes that are important for regulation of receptor expression include translation, phosphorylation, glycosylation, trafficking, assembly, ubiquitination and degradation.

1.1.5.2 Trafficking, assembly and degradation

Assembly of ion channels, including nAChRs, is relatively slow and inefficient. Only about 30% of synthesised subunits assemble into functional nAChR receptors upon acquiring correct subunit folding and undergoing post-translational modifications (Govind, Walsh, and Green 2012; Wanamaker, Christianson, and Green 2003). The rules that govern nAChR subunit assembly into functional receptors have not yet been fully understood. The assembly of the pentameric structure is likely to be tightly regulated by multiple mechanisms. Various studies have shown multiple combinations of nAChR subunits in heterologous systems, some of which are not observed *in vivo*. For instance, the mammalian α7 subunit has been successfully co-expressed with α5, β2, or β3 subunits to form heteromeric receptors in heterologous system (Khiroug et al. 2002; Palma et al. 1999; Yu and Role 1998), while only homomeric α7 have been observed in neurons (Drisdel and Green 2000). If indeed many of the subunits can assemble to form functional receptors that are not formed *in vivo*, then rules governing nAChRs assembly and expression must be tightly regulated. Several accessory or chaperone proteins have also been described to assist with nAChR maturation, assembly and trafficking. The importance of these proteins is clearly

illustrated as several studies have shown there are difficulties in expressing recombinant nAChRs in non-neuronal cell lines (Cooper and Millar 1997; Kassner and Berg 1997; Millar 2009).

Studies on vertebrate nAChR subunits have demonstrated the requirement of protein chaperones such as RIC-3 in facilitating nAChR maturation (folding and assembly) and for the heterologous expression of functional nAChRs (Ben-David et al. 2016; Halevi et al. 2002; Lansdell et al. 2005). Mutations in the *ric-3* gene were initially characterised as impacting cholinergic transmission (Nguyen et al. 1995). Later, a screen for genes required for ACh receptor activity in *C. elegans* revealed that RIC-3 is specifically needed for receptor maturation (Halevi et al. 2002). RIC-3 chaperone activity has been described as highly specific to nAChRs and 5-HT_3 receptors (Halevi et al. 2002, 2003). Other chaperone proteins found to interact with nAChR subunits to facilitate their maturation include UNC-50 and 14-3-3eta (Eimer et al. 2007; Jeanclos et al. 2001). In addition, proper glycosylation was also reported to be necessary for nAChR folding as well as insertion into the plasma membrane (Gehle et al. 1997; Sumikawa and Gehle 1992).

Endoplasmic reticulum (ER) processes including synthesis, degradation and ER-exit play important roles in the regulation of any membrane receptor, including neurotransmitter receptors at the neuron (Ramírez and Couve 2011). ER associated degradation (ERAD) for example, is highly important in continuously clearing unassembled protein subunits in ER, and thus, regulating concentrations of assembling receptor pools. A study has shown that blocking proteasome involved in the degradation process accumulates nAChR subunits in the ER membrane, which in turn increases receptor assembly and delivery to cell membrane (Christianson and Green 2004). This is supported by another study showing that proteasome inhibitor PS-341 treatment increases the levels of α3, β2 and β4 subunits in rat cell lysates enriched for the ER/Golgi content (Rezvani, Teng, and De Biasi 2010).

Ubiquitination also serves an important role in nAChR regulation. UBXD4 (also known as UBXN2A), a ubiquitin regulatory X (UBX)-containing protein present in the ER and Golgi, was found to interact with α3 and α4 subunits (Rezvani et al.

2009). Reduction in α3 ubiquitination and its degradation were demonstrated when UBXD4 binds to the subunit. Overexpression of the protein was described to increase the cell surface expression of α3-containing nAChR subtypes (Rezvani et al. 2010). UBXD4 was then found to interact with an E3 ubiquitin ligase, modulating its function in the ubiquitination of nAChR subunits (Teng, Rezvani, and De Biasi 2015).

nAChRs expression is also critically dependent on its trafficking from the ER to the cell surface. VILIP-1 is a myristoylated neuronal calcium-sensor protein in human, that has a role in signal transduction and is known to regulate clathrin-dependent receptor recycling (Brackmann et al. 2005). The protein has been described to be an interacting partner for α4β2 nAChRs. VILIP-1 co-expression with recombinant α4β2 nAChRs in *Xenopus laevis* oocytes was shown to double the receptor expression levels and triple their agonist sensitivity (Lin et al. 2002).

Several other nAChR-interacting proteins have also been described in *Drosophila melanogaster.* A study identified Hasp (Hig-anchoring scaffold protein), a synaptic matrix protein in *D. melanogaster* brain with a domain similar to LEV-9 of *C. elegans* (Nakayama et al. 2016). LEV-9 was previously reported to be required for the clustering of levamisole-sensitive ACh receptors in the nematode species (Briseño-Roa and Bessereau 2014). Hasp regulates *Drosophila* nAChRs synaptic localisation via a matrix component (Hig) by one of two possible mechanisms; (1) by physical interaction with the nAChR subunits which either maintains the receptor clustering or prevents their degradation or (2) by signal transduction into the cytoplasm of postsynaptic terminals which induces clustering of nAChRs. Analysis of loss-of-function *Hig* or *Hasp* mutants demonstrated a reduction in synaptic distribution of Dα6 and Dα7 leading to compromised cholinergic synaptic activity (Nakayama et al. 2016). Therefore, it is clear that additional cofactors are critical for correct nAChR function and maintenance and alterations in their expression levels could influence how an insect may respond to compounds that bind nAChRs.

1.1.5.3 Changes in nAChR expression

nAChRs do not behave like other receptors which are generally downregulated in expression in response to chronic stimulation by an agonist. As described by their name, nAChRs are targets for nicotine which binds to the ACh-binding site and acts in a similar manner, activating the receptors (Gotti et al. 2009). Extended exposure to the agonist nicotine results in upregulation of nAChRs in the brains of human, mice and rats. Benwell et al. has shown higher levels of nAChRs in smokers post mortem brains compared to non-smokers, especially in brain areas associated with smoking (Benwell, Balfour, and Anderson 1988). The same observations were described in earlier studies using brains from rats and mice (Marks, Burch, and Collins 1983; Schwartz and Kellar 1983), where extended exposure to nicotine increased levels of α4β2 nAChRs. However, transcriptome analysis performed using the mouse brain exposed to nicotine revealed no changes in *α2, α3, α4, α5* or *β2* mRNA levels suggesting the upregulation was due to post-transcriptional mechanisms (Marks et al. 1992). Subsequent studies showed a decrease in nicotine binding when the extended nicotine exposure is ceased (Breese et al. 1997; Collins, Romm, and Wehner 1990; Mamede et al. 2007; Marks, Stitzel, and Collins 1985). Significantly, this upregulation is specific to certain subtypes of nAChRs, especially some α4β2-containing nAChRs (Flores et al. 1992; Zhang et al. 1995); the α5 subunit in the α4β2-containing nAChRs did not lead to the same outcome (Mao et al. 2008). An autoradiographic study demonstrated a different situation where chronic exposure of nicotine decreases α6-containing nAChRs, but not in the presence of β3 subunits (Perry, Mao, Gold, et al. 2007).

Most evidence of nAChR upregulation in the literature has been demonstrated via chronic nicotine exposure, to the extent that nicotine has been described as the best-known pharmacological chaperone of the receptors (Lester et al. 2009). As suggested by the term pharmacological chaperone, nicotine is likely triggering intracellular process that selectively changes the receptor number. Various studies conducted to identify the underpinning mechanism have produced evidence for the involvement of processes including increased nAChR subunit maturation and assembly (Harkness and Millar 2002; Sallette et al. 2005),

reduced subunit degradation (Rezvani et al. 2007), enhanced nAChR trafficking (Darsow et al. 2005), and activation of second messenger pathway involving protein kinase C, PKC (Gopalakrishnan, Molinari, and Sullivan 1997; Nashmi et al. 2003). Although these studies suggested different mechanisms, many of them are not mutually exclusive and it is likely that more than one process is involved. It is also possible that the nAChR upregulation is activity dependent. Exposure to other agonists and antagonists of nAChR have been found to upregulate receptor expression, however the mechanism by which this was mediated is still not known (Zambrano et al. 2015, Nguyen et al. manuscript in preparation).

Another recent study demonstrated that *Drosophila* Dα6-containing nAChRs were downregulated when acutely or chronically exposed to spinosyn, an insecticide that binds to nAChRs in insects (Nguyen et al. manuscript in preparation). When the proteasomal degradation pathway was blocked, the spinosyn-induced Dα6 downregulation was inhibited, suggesting involvement of protein degradation in the process (Nguyen et al. manuscript in preparation). In other studies (refer Section 1.1.5.2), blocking the proteasomal degradation pathway has also been reported to upregulate nAChR expression. This highlights the complex nature of nAChR regulation and how it can vary between different subunits.

1.1.6 nAChRs are conserved across various species including insects

Genomic sequence data revealed that features of nAChR subunits are evolutionary conserved across animal phyla. For instance, genes encoding *Drosophila melanogaster* α5-α7 subunits share more than 50% sequence identity to vertebrate *α7* gene, and the sequence identity is even higher when compared to the gene ortholog in other invertebrate species such as *Heliothis virescens* (Grauso et al. 2002). Soon after the identification of nAChR subunit from *T. marmorata*, DNA probes were used to isolate cDNA clones from other animal species. The completion of many genome projects has led to identification of all nAChR family members in a wide variety of species, including insects. The high conservation of nAChR families also has allowed for comparison between various studies of nAChRs from different animal species.

The largest known vertebrate nAChR family belongs to the pufferfish, *Fugu rubripes*, with 28 subunits identified (Jones, Elgar, and Sattelle 2003). Meanwhile, the most extensive nAChR gene family belongs to *C. elegans*, which has at least 29 subunits described so far (Jones and Sattelle 2004). Mammals generally have approximately 16 genes encoding α1-α7, α9-α10, β1-β4, δ, ε or γ subunits, while chicken has an additional α8 subunit (Millar 2003; Millar and Gotti 2009). By comparison, insect nAChR families are smaller, with only 10-12 subunit genes on average. For example, *D. melanogaster* has 10 subunit genes (Jones and Sattelle 2010). Despite overall homologies with their vertebrate counterparts, insect nAChRs show distinct pharmacological characteristics (Tornøe et al. 1995). The differences in binding and sensitivity to certain chemical toxins are of particular interest in studying their differences in structure and function.

1.2 *Drosophila melanogaster* as a model to study insect nAChR family

1.2.1 *Drosophila melanogaster* as model organism

The vinegar fly, *D. melanogaster* serves as a powerful genetic model given the ability to systematically manipulate its genome and the availability of a massive array of genetic resources. The ease and low cost of maintaining stocks in the lab, coupled with a short generation time make this an easy organism to work with. Many biological and cellular processes have been characterised through investigation in *Drosophila*, including studies in the area of animal development and behaviour, neurobiology, and human genetic diseases. *D. melanogaster* is exposed to insecticides in the field. Resistance strains of various classes of insecticides have been identified in the field (Perry, Batterham, and Daborn 2011), and/or generated in the lab through mutagenesis or gene manipulation (Perry and Batterham 2018).

The extensive molecular tools available for this model organism has been kept up to date with the latest advances. Generation of new mutations to study various phenotypes has been conducted in *Drosophila* for many years through chemical mutagenesis. This followed by the availability of techniques for genetic mapping, gene cloning and gene overexpression. The research community was later

introduced with *Minos*-mediated integration cassette (MiMIC) transposon system which has utilised cassette swapping approach to generate gene disruption mutations, gene tagging as well as protein tagging (Venken et al. 2011). Recent advancement introduced Clustered Regularly Interspaced Short Palindromic Repeats (CRISPR) also known as CRISPR/Cas9 editing in *Drosophila*, making genome editing as well as other genetics strategies a lot faster and easier (Gratz et al. 2013). Other toolkits available in this model organism include the libraries of various gene disruption mutants as well as RNAi lines for gene knockdown, UAS/GAL4 system and many more.

1.2.2 *Drosophila* nAChR subunits and subtypes diversity

To date ten neuronal nAChR subunits have been identified from *D. melanogaster* representing the smallest nAChR family currently known (Table 1.1). These include seven α subunits (Dα1-Dα7) and three non-α subunits, classified as β subunits (Dβ1-Dβ3). nAChR subunit genes from the fruit fly and other insect species were previously compared to reveal that each of the insect species has equivalent nAChR subunits to those in *D. melanogaster* with greater than 60% identity in their amino acid sequences (Jones and Sattelle 2010). The distinct features of the subunits are also conserved. Majority of insect nAChR families consist of nine core and well-conserved subunits, α1-α8 and β1, where in *Drosophila* the α8 orthologue lacks the YXCC motif in loop C, thus referred to as Dβ2 subunit (Figure 1.4A). It was also shown that each of these insects owns at least one subunit with low sequence homology (less than 29% identity) to rest of the subunits. These particular subunits are described as divergent subunits which represent species-specific nAChR subtypes and Dβ3 is the only divergent subunit identified in *D. melanogaster* (Figure 1.4B)(Lansdell and Millar 2002).

Table 1.1 Ten neuronal nAChR subunits of *D. melanogaster*

Subunit	Alias	Gene ID	Identification/Reference
Dα1	ALS, nAChRα1, nAcRα-96Aa	CG5610, FBgn0000036	Bossy et al. 1988
Dα2	SAD, nAChRα2, nAcRα-96Ab	CG6844, FBgn0000039	Sawruk 1990
Dα3	nAChRα3, nAcRα-7E	CG2302, FBgn0015519	Schulz et al. 1998
Dα4	nAChRα4, nAcRα-80B	CG12414, FBgn0266347	Lansdell and Millar 2000a
Dα5	nAChRα5, nAcRα-34E	CG32975, FBgn0028875	Grauso et al. 2002
Dα6	nAChRα6, nAcRα-30D	CG4128, FBgn003215	Grauso et al. 2002
Dα7	nAChRα7, nAcRα-18C, gfA	CG32538, FBgn0086778	Grauso et al. 2002
Dβ1	ARD, nAChRβ1, nAcRβ-64B	CG11348, FBgn0000038	Hermans-Borgmeyer et al. 1986
Dβ2	SBD, nAChRβ2, nAcRβ-96A	CG6798, FBgn0004118	Sawruk et al. 1990
Dβ3	nAChRβ3, nAcRβ-21C	CG11822, FBgn0031261	Lansdell and Millar 2002

Figure 1.4 nAChR subunits are conserved in various insect species

Opposite (A) Amino acid alignment spanning Loop E to TM1 domain of ten *Drosophila* nAChR subunits showing the conserved Cys-loop motif that consists of two disulphide bond-forming cysteines (purple shading) which are separated by thirteen highly conserved residues. Yellow shading highlights the two conserved adjacent cysteines (YXCC motif) in loop C present α, but not β subunits. (B) Phylogenetic tree of insect nAChR subunits grouped according to subunits present in *D. melanogaster*. The majority of insect nAChR families have orthologues of nine core subunits (α1-α8 and β1). In *D. melanogaster* the α8 orthologue lacks the YXCC motif in loop C and is thus referred to as the Dβ2 subunit. Commonly there are 1-6 divergent subunits in insect nAChR families; Dβ3 is the only divergent subunit identified in in *D. melanogaster*. The nAChR tree is adapted from Somers (2015). Species; Ag, *A. gambiae*; Am, *A. mellifera*; Bm, *B. mori*; Dm, *D. melanogaster*; Ha, *H. armigera*; Nv, *N. vitripennis*; Tc, *T. castaneum*. *D. melanogaster* GABA receptor, Rdl was used as an outgroup.

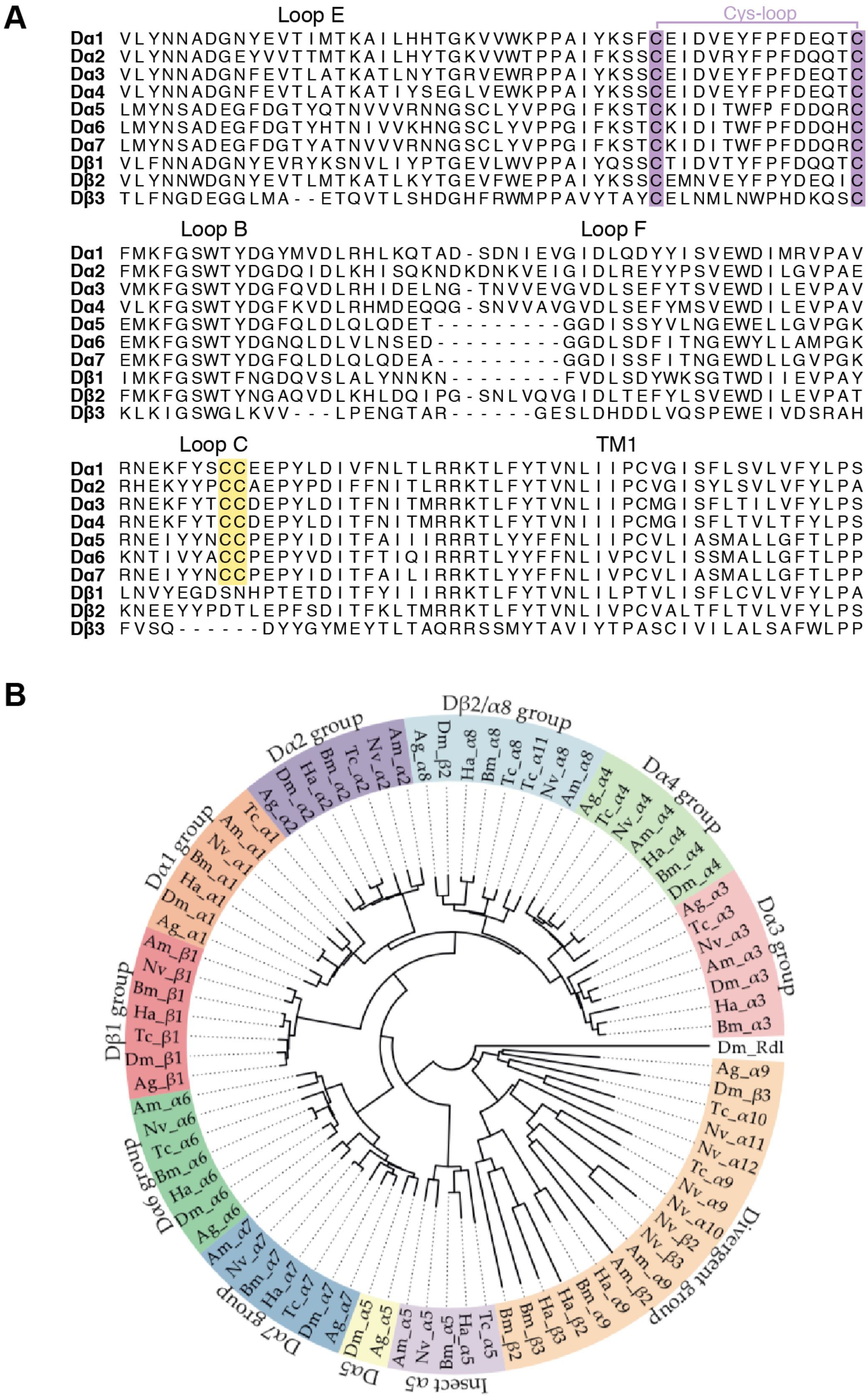
A
Loop E
Cys-loop
Dα1 VLYNNADGNYEVTIMTKAILHHTGKVVWKPPAIYKSFCEIDVEYFPFDEQTC
Dα2 VLYNNADGEYYVVTTMTKAILHYTGKVVWTPPAIFKSSCEIDVRYFPFDQQTC
Dα3 VLYNNADGNFEVTLATKATLNYTGRVEWRPPAIYKSSCEIDVEYFPFDEQTC
Dα4 VLYNNADGNFEVTLATKATIYSEGLVEWKPPAIYKSSCEIDVEYFPFDEQTC
Dα5 LMYNSADEGFDGTYQTNVVVRNNGSCLYVPPGIFKSTCKIDITWFPFDDQRC
Dα6 LMYNSADEGFDGTYHTNIVVKHNGSCLYVPPGIFKSTCKIDITWFPFDDQHC
Dα7 LMYNSADEGFDGTYATNVVVRNNGSCLYVPPGIFKSTCKIDITWFPFDDQRC
Dβ1 VLFNNADGNYEVRYKSNVLIYPTGEVLWVPPAIYQSSCTIDVTYFPFDQQTC
Dβ2 VLYNNWDGNYEVTLMTKATLKYTGEVFWEPPAIYKSSCEMNVEYFPYDEQIC
Dβ3 TLFNGDEGGLMA--ETQVTLSHDGHFRWMPPAVYTAYCELNMLNWPHDKQSC
Loop B
Loop F
Dα1 FMKFGSWTYDGYMVDLRHLKQTAD-SDNIEVGIDLQDYYISVEWDIMRVPAV
Dα2 FMKFGSWTYDGDQIDLKHISQKNDKDNKVEIGIDLREYYPSVEWDILGVPAE
Dα3 VMKFGSWTYDGFQVDLRHIDELNG-TNVVEVGVDLSEFYTSVEWDILEVPAV
Dα4 VLKFGSWTYDGFKVDLRHMDEQQG-SNVVAVGVDLSEFYMSVEWDILEVPAV
Dα5 EMKFGSWTYDGFQLDLQLQDET---------GGDISSYVLNGEWELLGVPGK
Dα6 EMKFGSWTYDGNQLDLVLNSED---------GGDLSDFITNGEWYLLAMPGK
Dα7 EMKFGSWTYDGFQLDLQLQDEA---------GGDISSFITNGEWDLLGVPGK
Dβ1 IMKFGSWTFNGDQVSLALYNNKN--------FVDLSDYWKSGTWDIIEVPAY
Dβ2 FMKFGSWTYNGAQVDLKHLDQIPG-SNLVQVGIDLTEFYLSVEWDILEVPAT
Dβ3 KLKIGSWGLKVV---LPENGTAR------GESLDHDDLVQSPEWEIVDSRAH
Loop C
TM1
Dα1 RNEKFYSCCEEPYLDIVFNLTLRRKTLFYTVNLIIPCVGISFLSVLVFYLPS
Dα2 RHEKYYPCCAEPYPDIFFNITLRRKTLFYTVNLIIPCVGISYLSVLVFYLPA
Dα3 RNEKFYTCCDEPYLDITFNITMRRKTLFYTVNLIIPCMGISFLTILVFYLPS
Dα4 RNEKFYTCCDEPYLDITFNITMRRKTLFYTVNIIIPCMGISFLTVLTFYLPS
Dα5 RNEIYYNCCPEPYIDITFAIIIRRRTLYYFFNLIIPCVLIASMALLGFTLPP
Dα6 KNTIVYACCPEPYVDITFTIQIRRRTLYYFFNLIVPCVLISSMALLGFTLPP
Dα7 RNEIYYNCCPEPYIDITFAILIRRKTLYYFFNLIVPCVLIASMALLGFTLPP
Dβ1 LNVYEGDSNHPTETDITFYIIIRRKTLFYTVNLILPTVLISFLCVLVFYLPA
Dβ2 KNEEYYPDTLEPFSDITFKLTMRRKTLFYTVNLIVPCVALTFLTVLVFYLPS
Dβ3 FVSQ------DYYGYMEYTLTAQRRSSMYTAVIYTPASCIVILALSAFWLPP
B
Dα2 group
Dβ2/α8 group
Dα4 group
Dα3 group
Dα1 group
Dβ1 group
Dα6 group
Dα7 group
Dα5
Insect α5
Divergent group
Dm_Rdl

Even though insect nAChR subunit family including *Drosophila*'s is considered limited compared to the large number of nAChR subunits in the vertebrate or the nematode species, post-transcriptional modifications including alternative splicing, RNA editing and other alteration such as truncation of the nAChR subunit gene transcripts have considerably broadened the subunit diversity (Grauso et al. 2002; Jones and Sattelle 2010; Lansdell and Millar 2000a). While some of these changes are conserved across insect species, others are not, resulting in species-specific nAChR subunit isoforms (Jones and Sattelle 2010; Yao et al. 2009). Alternative splicing for insect nAChR genes has been described in species including *A. melifera*, *B. mori* and *T. castaneum* where multiple isoforms have been observed for the α3, α4, α6 and α7 nAChR subunits (Dupuis et al. 2012; Rinkevich and Scott 2009; Shao, Dong, and Zhang 2007). In *Drosophila*, alternative splicing occurs commonly in two nAChR subunits; Dα4 and Dα6, generating species-specific isoforms with variations in the Cys-loop, loops E and B of the subunits. These variant isoforms effectively diversify the nAChRs function by modulating the assembly of the receptor and their ligand binding properties (Grauso et al. 2002; Lansdell and Millar 2000a). Another post-transcriptional modification, RNA A-to-I editing of nAChR subunit transcript, particularly for the α6 subunit, has also been described for several insect species including *D. melanogaster* (Jin et al. 2007). For instance, the modification of specific adenosine (A) residues to inosine (I) in the extracellular N-terminal region of Dα6 pre-mRNA transcripts has the potential to result in altered ligand binding properties (Jin et al. 2007; Jones and Sattelle 2010). These post-transcriptional modifications have largely contributed to the diversification of insect nAChRs to counterpart the compact gene families.

In combination with the diverse subunit availability, a vast array of nAChR subtypes can be formed. However, like in many other species, the combination of nAChR subunits that comprise natively expressed nAChRs in *D. melanogaster* is still largely unknown. Efforts to investigate this have found difficulty expressing functional insect nAChRs in heterologous systems (Millar and Lansdell 2010). To eliminate issues with the expression of functional nAChR in heterologous system altogether, many studies have also resorted to approaches such as

immunoprecipitation to characterise nAChR complex composition. Using this method, a study confirmed co-assembly of Dα1 and Dα2 into the same receptor complex (Schulz et al. 2000). Later, another study using two-step immunoaffinity chromatography and co-immunoprecipitation revealed the existence of receptor complex that includes Dα1, Dα2 and Dβ2 or, Dβ1 and Dβ2 (Chamaon et al. 2002). Dα3 and Dβ1 were also previously co-immunoprecipitated together suggesting existence of nAChR complex that contain the two subunits (Chamaon et al. 2000).

Later, successful attempts of heterologous co-expression of insect nAChR subunits in combination with vertebrate β subunit or chimeric subunit were reported (Huang et al. 1999; Lansdell and Millar 2000a, 2000b). Heterologous expression of *Drosophila*-only receptors containing certain combinations of α-subunits (Dα5, Dα6 and Dα7) were successfully demonstrated in *Xenopus* oocytes. These subunits generated different combinations of homomeric and heteromeric nAChRs (Lansdell et al. 2012). In addition, these heterologous expressions of insect nAChRs have also provided advances in the investigation of pharmacological properties of *Drosophila* nAChRs. For example, individual Dα1, Dα2 and Dα3 subunits were demonstrated to form functional nAChR with different binding affinity for imidacloprid, an insecticide that binds nAChRs, when co-expressed with rat β2 subunits in *Drosophila* S2 cells (Lansdell and Millar 2000b). The study provided an overview on subunit combinations and their properties, although these hybrid receptors might not reflect the pharmacology of native insect-only receptors. Table 1.2 summarises possible nAChR subtype combinations in *D. melanogaster,* pointed out by the literature. However, despite these findings, the combinations of subunits assembled into native *Drosophila* nAChR are still not clear.

Table 1.2 Summary of published evidence for the assembly of particular nAChR subunit combinations

Combination	Radioligand	Experiment	Reference
Dα1+Dα2	-	Co-IP	Schulz et al. 2000
Dα3+Dβ1	-	Co-IP	Chamaon et al. 2000
Dα1+Dα2+Dβ2; Dβ1+Dβ2	-	Co-IP, immunoaffinity chromatography	Chamaon et al. 2002
Dα1+ratβ; Dα2+ratβ2; Dα3+ratβ2; Dα3+ratβ4	Epibatidine, α-BTX, imidacloprid, MCCh	Heterologous expression in *Drosophila* S2 cells	Lansdell and Millar 2000b
Dα4+ratβ2	Epibatidine, α-BTX	Heterologous expression in *Drosophila* S2 cells	Lansdell and Millar 2000a
Dα1+chickenβ2; Dα2+chickenβ2	Nitenpyram, imidacloprid, CH-IMI, DN-IMI	Heterologous expression in *Xenopus* oocytes	Ihara et al. 2003
Dα5+Dα6*	Nicotine, ACh, Spinosyn	Heterologous expression in *Xenopus* oocytes	Watson et al. 2010
Dα5*; Dα7*; Dα5+Dα6*; Dα5+Dα7*; Dα5+Dα6+Dα7*	Epibatidine, α-BTX	Heterologous expression in *Xenopus* oocytes	Lansdell et al. 2012

*co-expression with RIC-3
MCCh, methylcarbamylcholine; CH-IMI, nitromethylene analogue of imidacloprid; DN-IMI, denitrated derivative of imidacloprid; Co-IP, co-immunoprecipitation

1.2.3 Functional roles of nAChRs in *D. melanogaster*

The contributions that specific subunits make to particular functions in *D. melanogaster*, or insects more generally, are largely unknown. However, some functions have recently been associated with these subunits in studies using loss-of-function mutations. Loss-of-function mutants have been reported for eight out of ten *D. melanogaster* nAChR subunits. These include Dα1*,* Dα2*,* Dα3, Dα4*,* Dα7*,* Dα6, Dβ2 and Dβ3 (Luong 2018; Perry et al. 2008, 2012; Perry, McKenzie, and Batterham 2007; Somers et al. 2015; Somers, Luong, Batterham, et al. 2017; Watson et al. 2010). That homozygous mutants are viable suggests that none of these subunits are by themselves essential for life. Similar observations have

been made in knockout mice where the lack of any one of the nAChR subunits, including α4, α5, α6, α7, α9, β2, β3 and β4 did not show any obvious external abnormality or lethality (Champtiaux and Changeux 2004). However, some of the nAChR subunits have proven otherwise. A study using RNAi to reduce *Dα5* expression in the Drosophila prothoracic gland, a major tissue for hormone production resulted in an embryonic lethal phenotype suggesting a role for this gene in development (Mitchell 2012). Difficulty in generating a loss-of-function mutant for Dα5 subunit was attributed to lethality (Christesen et al. manuscript in preparation). Where functional redundancy does exist, double- or triple-knockout mutants may be useful in detecting the involvement of multiple subunits in undetected functions (Müller 1999). For example, *β2* and *β4* single-mutant mice did not show any visible abnormalities in terms of survival and growth while the double-mutant mice displayed severe phenotypes (Xu et al. 1999).

In contrast to viability, other functions have been associated with specific subunits. Analysis of *Drosophila Dα7* mutants has demonstrated that this subunit is necessary for giant fiber-mediated escape behaviour (Fayyazuddin et al. 2006). Several subunits have been shown to contribute to various aspects of sleep behaviour. Knockouts of *Dα1* and *Dα2* presented with significantly shorter bouts of sleep and reduced lifespan (Luong 2018). The Dα3 subunit was associated with a protein factor that promotes sleep, Sleepless (SSS); RNAi knockdown of Dα3 was shown to increase sleep duration of SSS mutant strains (Wu, Robinson, and Joiner 2014). A full knockout of *Dα1* was reported to have reduced motility and reduced mating (Somers 2015; Somers, Luong, Mitchell, et al. 2017).

A variety of chemical insecticides exert control over insect pests by targeting nAChRs and perturbing their function (Raymond-Delpech et al. 2005). Unlike the endogenous ligand, ACh, which is tightly regulated by balancing the levels of enzymes that synthesize (choline acetyltransferase, ChAT) and degrade (acetylcholinesterase, AChE) ACh, the level of these insecticides is not regulated by the endogenous system. Most of them bind to nAChRs constitutively, leading to overstimulation of the central nervous system (Figure 1.5). The topics of pests,

insecticides and resistance management are among the main foci of the thesis and this will be addressed in the following sections.

1.3 Insecticides and resistance

1.3.1 Development of insecticide for pest managements

Human populations are growing rapidly. Concurrent with a decline in arable land available for agriculture, the world's population is estimated to reach nine billion by 2050. Increasing food production on less land poses a huge challenge. Pest species pose a constant threat because they cause substantial crop losses and directly threaten human health. Insects cause a loss of 18% to 20% of annual global crop production at a cost of approximately US$470 billion (Sharma, Kooner, and Arora 2017). These losses are expected to rise with global warming. For example, it has been predicted that there will be large yield losses for three major grain crops (wheat (46%), maize (31%) and rice (19%)) with a 2°C increase in global temperature (Deutsch et al. 2018). Under such circumstances, the total yield losses for these crops would be reduced by about 200 metric megatons per year (Deutsch et al. 2018). In terms of human health, many insect species spread diseases. Pest species such as cockroaches and flies spread bacteria that cause diseases including salmonellosis, shigellosis and trachoma, while mosquitos vector pathogens that cause diseases such as Malaria and Dengue (Khamesipour et al. 2018; Tatfeng et al. 2005).

Various strategies have been deployed with the aim of achieving sustainable insect pest control. Non-chemical approaches have included the use of natural predators, physical barriers such as netting, non-pest competitor species and meiotic drive to spread a deleterious allele within populations (Fishel 2013; Hoffmann et al. 2011; Lindholm et al. 2016). More recently this armoury has been expanded with the use of endosymbionts including Wolbachia (Hoffmann et al. 2011) and the potential to use gene drive if regulatory approval is given. To date, these pest control strategies have been generally less effective than application of chemical pesticides (National Research Council 2000).

Nicotine and dichlorodiphenyltrichloroethane (DDT) were among the first chemical compounds introduced for pest management. We know nicotine as an active ingredient in tobacco products, but its native biological role is as a plant defence compound for plants of the Solanaceae family. Nicotine was once widely used as an insecticide, ceasing with the increasing realisation of the extent of its human health impacts (Mishra et al. 2015). Synthetic pesticides were developed to fulfil the need for better chemical control. DDT was the first synthetic pesticide introduced in the 1940s. Upon its introduction, DDT became a popular choice and used widely in crop protection due to its effectiveness and low toxicity towards humans (Jarman and Ballschmiter 2012). Later, DDT was found to cause chronic toxicity to non-target wildlife (Carson et al. 1962), but its usage was only officially banned in 2001 at the Stockholm Convention.

In the 1950s, integrated pest management (IPM) was introduced to maximise pest control while minimising the usage of pesticides, thus reducing its harmful effects to humans and the environment (Smith et al. 1967). IPM integrates biological, cultural and chemical approaches to achieve the best outcomes, weighing up the economic and environmental effects. While IPM has great value and is widely touted, global insecticide usage remains high. Approximately 4.4 billion pounds of global pesticide usage are recorded each year, where the highest usage contributed by China and the USA, while over 88 million pounds are contributed by the usage in Australia alone (Grube et al. 2011; Sharma et al. 2019). The global pesticide usage is estimated to reach 7.8 billion pounds by end of 2020 (Sharma et al. 2019).

1.3.2 Neonicotinoids and spinosyns target nAChRs

nAChRs are targeted by five groups of insecticides neonicotinoids, nicotine, sulfoximines, butenolides and spinosyns (Sparks and Nauen 2015). The primary focus here is on the neonicotinoids and spinosyns and their nAChR targets as these insecticides are used in the research to be described. The neonicotinoids are the most widely used class of insecticides (Sparks, Hahn, and Garizi 2017), and the spinosyns are an increasingly used organic alternative.

1.3.2.1 Neonicotinoids

Pest control has improved greatly with the discovery of the neonicotinoid class of insecticides. It started with the discoveries of nitromethylene and nithiazine in 1970 and continued with the introduction of chloropyridinyl and nitroimine moieties in the 1980s which have considerably increased insecticidal activity (Foster 1990). These discoveries led to the introduction of a more stable compound, imidacloprid by Kagabu and coworkers in the early 1990s which became the top-selling insecticide for many years (Kagabu 1999). Imidacloprid has more than 3000-fold-higher insecticidal activity compared to nicotine, depending on species (Jeschke and Nauen 2008). Following imidacloprid, other compounds with a similar structure were developed; the resemblance of all these insecticides to nicotine and nicotinoids gave rise to the name, neonicotinoids (Figure 1.5B-C). Neonicotinoids including imidacloprid, nitenpyram, cycloxaprid, clothianidin, thiamethoxam, dinotefuran, thiacloprid, and acetamiprid represented more than 26.6% of the global insecticide market, valued over US$4.9 billion in 2016 (Sparks et al. 2017). The market value of imidacloprid sales exceeded US$1 billion of the market, making it the top selling insecticide in 2008 (Pollak 2011).

Neonicotinoids act as agonists for postsynaptic nAChRs, binding with much higher affinity than nicotine (Brown et al. 2006; Yamamoto et al. 1995). They act on nAChRs in a similar way to ACh, binding to the extracellular interface between two nAChR subunits, activating the receptor. However, unlike ACh, they are not hydrolysed by the enzyme AChE (Thany 2010). They are persistent in modulating the receptors, leading to a constitutive influx of cations into neurons (Brown et al. 2006). At appropriate insecticide concentrations, this over-stimulation of the nervous system leads to the death of an insect (Figure 1.6). The neonicotinoid binding site was first determined using [^{3}H]Imidacloprid as the radioligand (Latli and Casida 1992). A high affinity binding site was shown to be conserved across a broad range of insect species (Chao, Dennehy, and Casida 1997; Lind et al. 1998; Nauen, Ebbinghaus-Kintscher, and Schmuck 2001; Tomizawa and Casida 2001; Tomizawa, Latli, and Casida 1996; Wiesner and Kayser 2000; Zhang et al. 2000). Vertebrate nAChRs bind neonicotinoids with low affinity compared to insect nAChRs (Matsuda et al. 2005; Matsuda and Sattelle 2004). This explains

the higher level of neonicotinoid toxicity for insects compared to vertebrates (Tomizawa and Casida 2004).

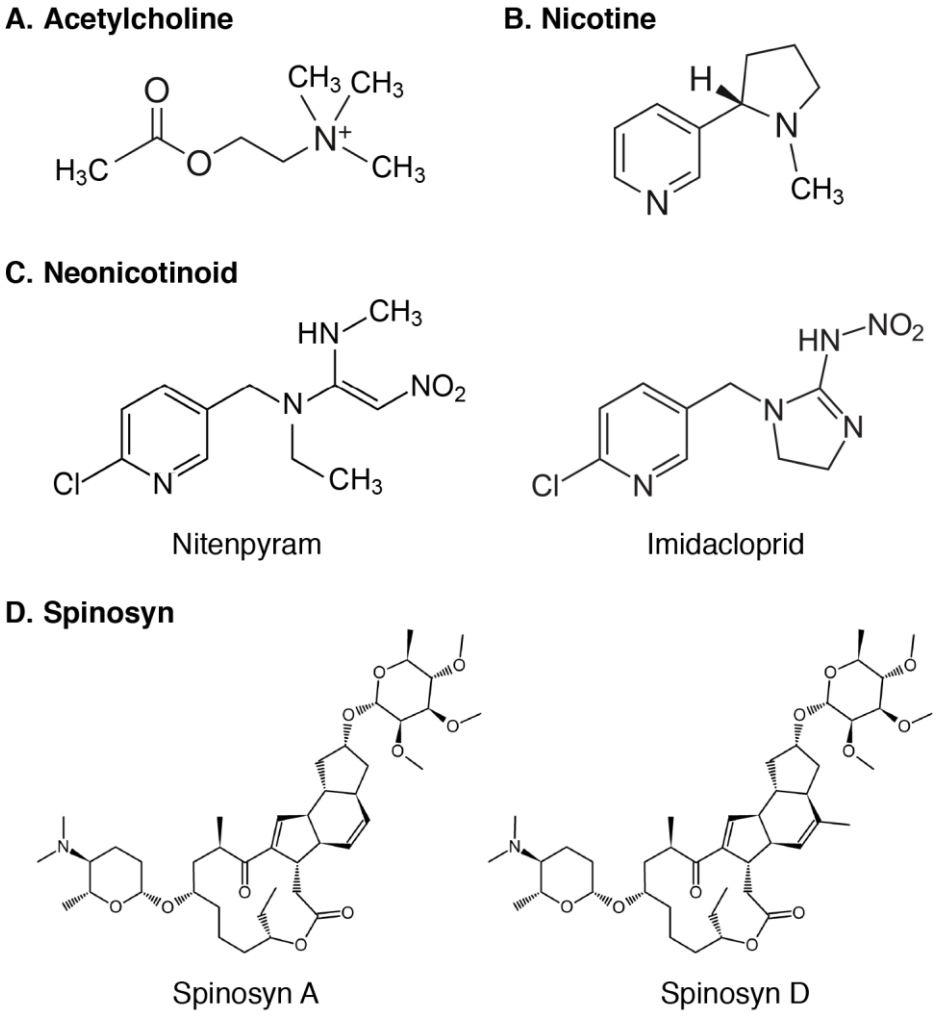

Figure 1.5 Chemical structure of nAChR ligands

Structure of (A) acetylcholine, ACh, (B) nicotine, (C) neonicotinoids and (D) spinosyns. ACh is the neurotransmitter for cholinergic neurons. It binds and activates nAChRs. Neonicotinoids including nitenpyram and imidacloprid are derivative of nicotine, while spinosyns such as spinosad (spinosyn A/D mixture) are macro lactone products of bacterial fermentation. They are commercialised as insecticides targeting nAChRs.

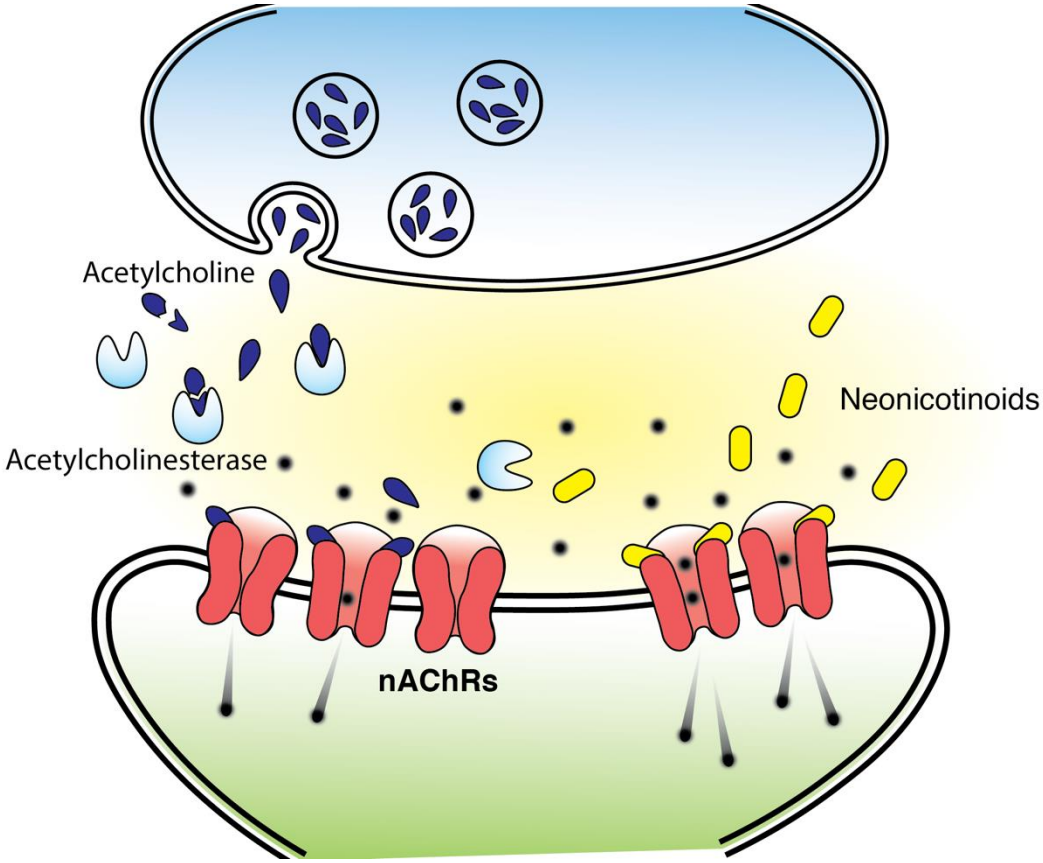

Figure 1.6 Acetylcholine action versus insecticides action on nAChR

Neurotransmitter acetylcholine (ACh) activates postsynaptic nAChRs, mediating channel opening, and thus, neurotransmission in a form of cation flow through the receptors. This is tightly regulated by the rate of neurotransmitter release from pre-synaptic vesicles and level of enzymes that regulate ACh levels, including acetylcholinesterase, AChE. Neonicotinoids bind nAChRs in a similar manner to ACh.

Neonicotinoids were previously classified as safe for agricultural use because of their low toxicity to vertebrates. More recently, concerns have been raised about the impact of low dose neonicotinoid exposures on populations of non-targeted, non-pest insects. Population sizes for many non-pest insects have been plummeting over the last decade (Henry et al. 2012; Morrissey et al. 2015; Pistorius et al. 2009). While many factors could contribute to population crashes and there is no evidence of neonicotinoids being responsible, there is evidence of neonicotinoid impacts on the behaviour of non-pest insects, particularly honeybees, *Apis mellifera*. Imidacloprid and two other insecticides of neonicotinoid class have been banned in the European Union since 2018 due to

the concerns about their impact on this species which is so vital for pollination of crops (European Commission 2018). In addition, increasing studies were linked imidacloprid to the poisoning of bird species including songbirds, partridges and pigeons around the world (Millot et al. 2017; Rogers et al. 2019). Thus, it has become more important now to understand the selectivity of neonicotinoids for nAChRs. As a starting point the nAChRs to which neonicotinoids bind need to be identified.

In *Drosophila*, neonicotinoids have been found to mainly target nAChRs that include Dα1 and Dβ2 subunits based on the insecticide resistance strains (Perry et al. 2008, 2012; Somers, Luong, Batterham, et al. 2017), which will be discussed further under the topic of insecticide resistance. Individual nAChR combinations of Dα1, Dα2 and Dα3 subunits co-expressed with rat β2 subunits, were all demonstrated to form a binding site for imidacloprid (Table 1.2)(Lansdell and Millar 2000b). Later, co-expression of *Drosophila* Dα1 and Dα2 subunits in *Xenopus* oocytes with chicken β2 subunits showed that Dα2/β2 receptors can be activated by imidacloprid and nitenpyram, however, only nitenpyram strongly activates Dα1/β2 receptors (Ihara et al. 2003). These findings suggest that the α-subunits play an important role in the selectivity of neonicotinoids on nAChR. The difference in residues between these α-subunits could be important for affinity enhancement of selective neonicotinoid. Interestingly, the heterologous expressions of Dα1 with distinct vertebrate β2 subunits showed different receptor pharmacology to imidacloprid (Table 1.2)(Ihara et al. 2003; Lansdell and Millar 2000b). When the rat β2 subunits were swapped with alternative vertebrate non-α subunit including the rat β4 subunits, the hybrid receptors showed lower binding affinity for imidacloprid (Lansdell and Millar 2000b). This indicates that the β-subunits can also play an important role in neonicotinoid sensitivity. The importance of the β-subunit was further supported by another study where a vertebrate β2 subunit, with its amino acid residues mutated to be more insect-like, showed higher sensitivity to imidacloprid (Shimomura et al. 2006).

1.3.2.2 Spinosyns

Another highly valued class of insecticide, spinosyns, are naturally derived macrocyclic lactones produced as fermentation products of actinomycete bacterial species, *Saccharopolyspora spinosa* (Mertz and Yao 1990; Salgado and Sparks 2005). Spinosad is a natural mixture of two spinosyns, A and D, with chemical structure comprised of a tetracyclic ring system attached to a neutral sugar and an amino sugar moiety (Figure 1.5D) (Kirst 2010; Mertz and Yao 1990). Spinosad has been used widely in crop protection since it was first registered in the US in 1997. In 2007 spinoteram, another mixture of semi-synthetic spinosyn derivatives, was commercialised (Sparks et al. 2012).

Studies to date have deduced that spinosyns act on the insect nervous system in a different manner from other insecticide classes (Somers et al. 2015; Watson et al. 2010; Martelli et al. manuscript in preparation; Nguyen et al. manuscript in preparation). While incompletely defined, the mode of action for spinosyns is considered unique. Available evidence suggests that spinosad mainly acts on insect nAChRs as an allosteric agonist, and that it may also have some effect on the GABA receptor function (Salgado 1998; Watson et al. 2010). Spinosyns have been found to bind to a different binding site from the ACh ligand binding domain on nAChRs, unlike neonicotinoids. Spinosyn A was demonstrated to activate nAChRs that have been simultaneously bounded by α-BTX, suggesting synergistic activity with ACh (Salgado and Saar 2004). It was initially thought that spinosad binding led to hyperexcitation of nAChRs (Salgado 1998), but subsequent studies have indicated inhibition (Martelli 2020; Salgado and Saar 2004).

Spinosyns and neonicotinoids appear to target different nAChR subunits. The evidence for this is a lack of cross resistance to spinosyns in neonicotinoid resistant strains and vice versa (Perry et al. 2008, 2012; Perry, McKenzie and Batterham 2007; Salgado and Saar 2004; Watson et al. 2010). To date, the Dα6 nAChR subunit provides the only known target site for spinosad in *D. melanogaster*. Dα6 null mutants are highly resistant to spinosad (Perry, McKenzie and Batterham 2007). Radioligand binding studies indicate that

neonicotinoids do not bind to Dα6-containing nAChRs (Lansdell and Millar 2004), underlining further selectivity and specificity of these two classes of insecticides for different α-subunits. There is no evidence of any involvement of β-subunits in spinosad sensitivity. While the precise binding site of spinosad remain unknown, Somers et al. (2015) found that it is located between the TM3 and C-terminal region of the Dα6 subunit. This was demonstrated in an *in vivo* system where only a Dα6/Dα7 chimeric subunit containing the Dα6 C-terminal region was able to rescue spinosad susceptibility in a *Drosophila Dα6* null mutant (Somers et al. 2015). This correlated well with observations of spinosad resistance in strains of the melon thrip, *Thrips palmi* and the western flower thrip, *Frankliniella occidentalis* that had a G275E amino acid replacement in their respective Dα6 orthologues (Bao et al. 2014; Puinean et al. 2013). This amino acid is located 4 residues away from TM3 segment.

1.3.3 Insecticide resistance

The extensive and persistent application of insecticides in crop protection has led to the appearance of resistance in many insect pest species due to increased selection pressure. Pests become resistant by evolving physiological modifications to protect them from the insecticide. Various protective mechanisms implicated in insecticide resistance have been reported. These include (1) increased insecticide metabolism (Markussen and Kristensen 2010a; Schmidt et al. 2017), (2) behavioural modification for insecticide avoidance (Zalucki and Furlong 2017), (3) enhanced transport of the insecticide including rapid excretion of the toxic compounds or secretion of the insecticide away from vulnerable tissues (Fusetto et al. 2017; Gott et al. 2017), (4) inefficient penetration of the insecticide through cuticle (Gott et al. 2017), and (5) modification/loss of the target receptors that bind to the insecticide (Pedra et al. 2004; Perry et al. 2008, 2015; Watson et al. 2010). Although all these mechanisms may contribute to insecticide resistance, target receptor modification/loss often leads to highest level of resistance that render the insecticide ineffective. Lower levels of resistance associated with the other mechanisms that can often be overcome by using higher doses or increased application frequencies. The following section

will focus on target site modification/loss considering studies using lab-based mutants and field derived resistant strains.

Mutations in genes encoding multiple nAChR subunits have been implicated in neonicotinoid resistance (Table 1.3). A study on a resistant strain of brown planthopper, *Nilaparvata lugens* identified a Y151S amino acid replacement in two nAChR α-subunits, Nlα1 and Nlα3 (encoded by genes orthologous to *Dα1* and *Dα3,* respectively) that result in reduced binding affinity for imidacloprid (Table 1.3)(Liu et al. 2005). In *D. melanogaster*, multiple studies on lab generated mutants have also discovered more than one nAChR subunit gene can confer neonicotinoid resistance when mutated. Selection for nitenpyram resistance in the progeny of flies exposed to the chemical mutagen EMS led to the identification of a mutation in *Dα1* that disrupts the C-terminal structure of Dα1, including the TM4 domain of the protein (Perry et al. 2008). This study also identified several mutations in *Dβ2* which result in resistance to nitenpyram (Table 1.3)(Perry et al. 2008). Compared to a specific amino acid substitution in *N. lugens*, all the mutations in *Drosophila* resulted in more drastic loss of function and some are distant from the ACh binding site. When the levels of resistance were quantified, the *Dα1* and *Dβ2* mutants demonstrated cross-resistance to other neonicotinoids, including imidacloprid (Perry et al. 2012). Later, Somers and colleagues reported a full knockout of *Dα1* that shows similar resistance level to imidacloprid, compared to the EMS-generated mutant, but even higher levels for nitenpyram (~50-fold resistance)(Somers, Luong, Batterham, et al. 2017). However, there were interesting differences in responses of these *Dα1* and *Dβ2* mutants to the insecticide dinotefuran, suggesting the involvement of other nAChR subunits as dinotefuran target (Perry et al. 2012; Somers, Luong, Batterham, et al. 2017). While individual combination of Dα2 or Dα3 subunits with rat β2 subunits were previously mentioned to form imidacloprid-binding site (refer to Section 1.3.2.1), whether or not mutation to these subunits implicates insecticide resistance has not been explored.

Recent evidence indicates that the *Drosophila* Dβ1 subunit also contributes to nAChRs targeted by neonicotinoids; elevated imidacloprid and nitenpyram resistance was observed in flies where the Dβ1 subunit was knocked out in the

brain using a somatic CRISPR/CAS9 technique (Perry et al. manuscript in preparation). The involvement of nAChR β1 as a neonicotinoid target was also demonstrated in other insect species. Earlier study in *N. lugens* identified N133D substitution in the nAChR β-subunit, Nlβ1 (encoded by gene orthologous to *Dβ1*) following RNA A-to-I editing results in imidacloprid insensitivity (Yao et al. 2009). Later, a novel R81T replacement in the β-subunit of aphid *Myzus persicae* was identified to be the causal mutation for one of imidacloprid resistant strains isolated from field populations (Bass et al. 2011). The analogous R81T replacement in the β1 subunit was demonstrated to also confer neonicotinoid resistance in *Aphis gosypii* and *D. melanogaster* (Homem et al. 2020; Shi et al. 2012). The amino acid threonine residue at this position was described to be important for imidacloprid binding at the binding pocket of the receptor (Shi et al. 2012).

Thus far, only mutations in Dα6 have been associated with resistance to spinosyns in *D. melanogaster* (Table 1.3). These include a knockout mutant identified over a deficiency chromosome in a resistant strain showing elevated resistance to spinosad. The null mutation of Dα6 subunit causes over 1000-fold of resistance to spinosad, a significantly higher level of resistance compared to those found for target site mutations associated with neonicotinoid resistance (Perry, McKenzie and Batterham 2007). Various other *Dα6* mutations induced by chemical mutagenesis have also been associated with spinosad resistance, with the majority of them leading to premature truncation of the Dα6 subunit (Somers et al. 2015; Watson et al. 2010). The high level of resistance observed in these mutants are consistent with Dα6 being the major target for spinosyn insecticides. In comparison, the lower levels of resistance observed for neonicotinoid target site mutants is consistent with the evidence that multiple subunits are targeted by these insecticides.

Table 1.3 nAChR mutations implicated in resistance to neonicotinoids and spinosyns

Gene	Mutation	Resistance	Reference
Nlα1 (*Dα1* ortholog)	Y151S substitution	Imidacloprid	Liu et al. 2005
Nlα3 (*Dα1* ortholog)	Y151S substitution	Imidacloprid	Liu et al. 2005
Dα1	11bp deletion resulting in altered TM4	Neonicotinoids - nitenpyram, imidacloprid	Perry et al. 2008, 2012
Dβ2	*EMS2*, 352* truncation; *EMS3,* L351Q substitution; *EMS4;* L118 replacement	Neonicotinoids - nitenpyram, imidacloprid	Perry et al. 2008, 2012
Mpβ1 (*Dβ1* ortholog)	R81T substitution	Imidacloprid	Bass et al. 2011
Agβ1 (*Dβ1* ortholog)	R81T substitution	Imidacloprid	Shi et al. 2012
Dβ1	R81T substitution	Neonicotinoids - acetamiprid, imidacloprid	Homem et al. 2020
Dα6	Null mutation resulting in no detectable transcript	Spinosad	Perry, McKenzie and Batterham 2007
Dα6	Various mutation alleles, i.e., *DAS1*, *DAS2*	Spinosad	Watson et al. 2010
Dα6	P146S substitution	Spinosad	Somers et al. 2015; Watson et al. 2010
Tpα6 (*Dα6* ortholog)	G275E substitution	Spinosad	Bao et al. 2014
Foα6 (*Dα6* ortholog)	G275E substitution	Spinosad	Puinean et al. 2013
Pxα6 (*Dα6* ortholog)	Mis-splicing resulting in TM3/TM4 truncation	Spinosad	Baxter et al. 2010
Pxα6 (*Dα6* ortholog)	3 amino acids deletion in TM4	Spinosad	Wang et al. 2016
Bdα6 (*Dα6* ortholog)	Various mutations alleles, i.e., truncated transcripts	Spinosad	Hsu et al. 2012

Nl, *Nilaparvata lugens*; D, *Drosophila melanogaster*; Tp, *Thrips palmi*; Fo, *Frankliniella occidentalis*; Px, *Plutella xylostella*; Bd, *Bactrocera dorsalis*

As the Dα6 subunit is highly conserved in insect species, it is not surprising that mutations in orthologues have been described with the same resistance phenotype (Perry, McKenzie and Batterham 2007). Besides the G275E replacement in the Dα6 subunit orthologues of *T. palmi* and *F. occidentalis* (Bao et al. 2014; Puinean et al. 2013), mutations in the *Dα6* orthologues of many other species have also been associated with resistant to spinosad (Table 1.3)(Baxter et al. 2010; Hsu et al. 2012; Wang et al. 2016).

1.3.4 Phenomenon of negative cross-resistance

Negative cross-resistance is a phenomenon where a mutant allele that confers resistance to one insecticide, confers hypersensitivity to another insecticide (Pittendrigh et al. 2014). By the term hypersensitivity or hyper-susceptibility, it means that the mutant strain now has increased susceptibility to one insecticide compared to the existing susceptible strain. This is of interest given that, where it exists, negative cross-resistance could be exploited to maintain control in populations that are resistant to an insecticide. Negative cross-resistance has been reported in various pest insect species as well as in the model insect, *D. melanogaster* (Table 1.4).

One of the best studied examples, the $para^{ts\text{-}1}$ mutant of *D. melanogaster,* was shown to be resistant to DDT while having increased susceptibility to deltamethrin, a pyrethroid class insecticide (Pedra et al. 2004). Both DDT and pyrethroid insecticides target the voltage-gated sodium channel, VGSC (Lee et al. 1999; Pittendrigh et al. 1997; Vijverberg, van der Zalm, and van der Bercken 1982). The $para^{ts\text{-}1}$ allele introduced a single mutation in the α-subunit of the channel. In the case of the *para* sodium channel, negative cross-resistance was shown to be allele specific – other DDT resistant $para^{ts}$ mutants did not show negative cross-resistance with deltamethrin (Pittendrigh et al. 1997). Negative cross-resistance has also been associated with VGSC mutations in several other insects including the house fly *Musca domestica* and tobacco budworm *Heliothis virescens* (Elliott et al. 1986; Khambay et al. 2001; McCutchen et al. 1997). *kdr* and *super-kdr* are pyrethroid-resistant mutations that lead to, one or two amino acid replacements, respectively. *kdr* strains of both *M. domestica* and *H.*

virescens have increased sensitivity to neurotoxic peptide, AaIT (Elliott et al. 1986; McCutchen et al. 1997). *super-kdr* strains of *M. domestica* have increased sensitivity to N-alkylamides (Khambay et al. 2001).

Negative cross-resistance can also occur due to mutations that impact insecticide metabolism. *D. melanogaster* strains with metabolic resistance to DDT were reported to be more sensitive to phenylthiourea than control strains. It was hypothesised that these DDT-resistant strains have an increased capacity to metabolize phenylthiourea into phenylurea, a more toxic compound, and thus, leading to greater toxicity in the resistant insects (Ogita 1961b, 1961a). Increased cytochrome P450 activity was also invoked to explain the hypersensitivity to diazinon in a pyrethroid resistant strain of the horn fly, *Haematobia irritans* (Barros et al. 2002; Cilek, Dahlman, and Knapp 1995; Sheppard and Marchiondo 1987). Similarly, omethoate-resistant strains of *Aphis gossypii* were described with increased sensitivity to bifenthrin, which may be attributed by reduced AChE sensitivity or increased cytochrome P450 activity (Shang et al. 2012).

Table 1.4 Summary of mutations implicated with negative cross-resistance in insect species

Insect	Mutation/factor	Insecticide/ toxin pair	Reference
D. melanogaster	*para*$^{ts\text{-}1}$ mutation in VGSC	DDT and deltamethrin	Pedra et al. 2004
M. domestica	*super-kdr* mutation in VGSC	Pyrethroids and N-alkylamides	Khambay et al. 2001
M. domestica	*kdr* mutation in VGSC	AaIT and pyrethroids	Elliott et al. 1986
H. virescens	*kdr* mutation in VGSC	AaIT and pyrethroids	McCutchen et al. 1997
H. irritans	Hypothesis of increased cytochrome P450 activity	Pyrethroids and diazinon	Sheppard and Marchiondo, 1987
D. melanogaster	Hypothesis of increased capacity to metabolize phenylthiourea	DDT and phenylthiourea	Ogita 1961b, 1961a
A. gossypii	Reduced AChE sensitivity or increased cytochrome P450 activity	Omethoate and bifenthrin	Shang et al. 2012

1.3.4.1 Mechanisms for negative cross-resistance

Based on these reported cases, negative cross-resistance can be explained by several different mechanisms (Figure 1.7). It can be generated by (1) a single mutation in a gene encoding an insecticide target. This occurs if the mutation decreases the capacity for one insecticide to bind target, while increasing the capacity of a different insecticide to bind at the same time. This includes the mutations in *D. melanogaster*, *M. domestica* and *H. virescens* that all involved a mutation in the gene encoding VGSC. However, exact changes at the target site that responsible for the insecticide hypersensitivity were never characterised. Additionally, negative cross-resistance can occur due to (2) a mutation that changes metabolic response to multiple insecticides. Here the changes in metabolic processes involved increased detoxification of one insecticide while reducing the detoxification capacity for a different insecticide. However, again, the exact molecular changes that impact this metabolic response are still not clear.

Mutations at two distinct loci could also produce resistance to one insecticide and hypersensitivity to another. This is more accurately classified as negatively correlated resistance (Pittendrigh et al. 2014). While negative cross-resistance has been of interest for resistance management as it provides hypersensitivity of the resistant strain to a different compound, negatively correlated resistance will be less effective for this purpose. The reason for this is that the two mutations for negatively correlated resistance may not necessarily be inherited through generations, depending on how tightly linked the two loci are.

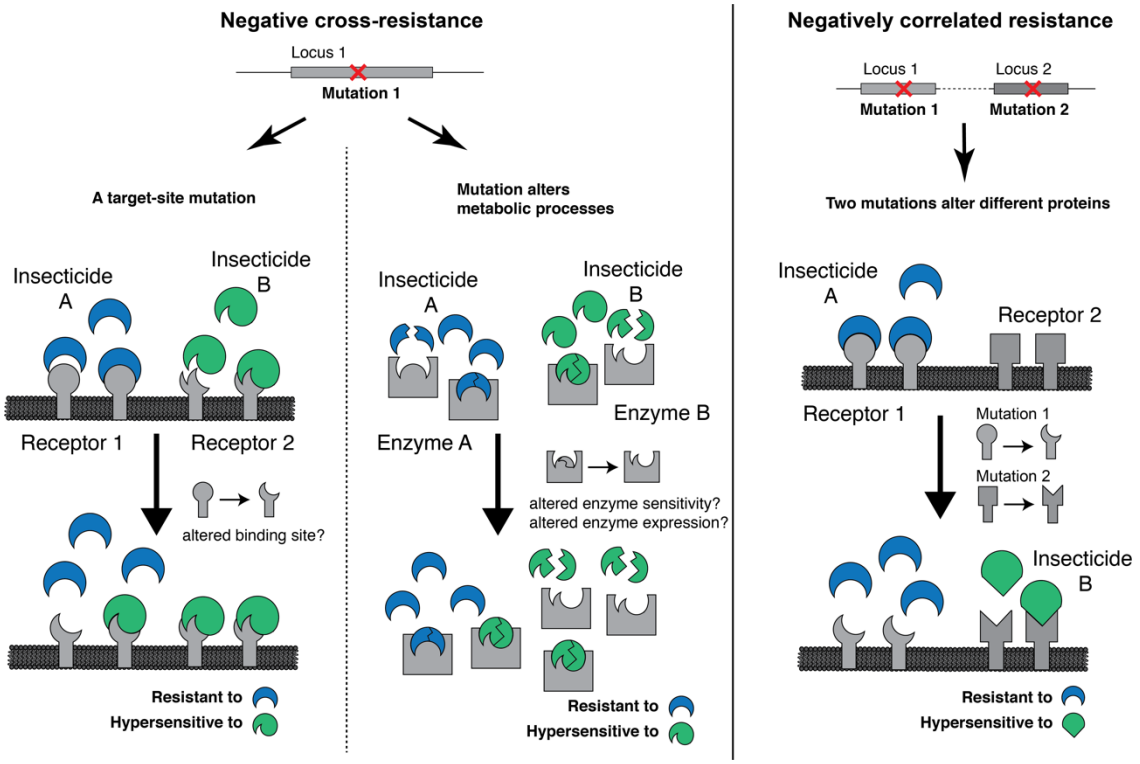

Figure 1.7 Negative cross-resistance versus negatively correlated resistance

Negative cross-resistance occurs if a mutation in a single gene that affects an insecticide target site or alters metabolic responses to insecticides, leading to resistance to insecticide A and increased sensitivity to an insecticide B. A negatively correlated resistance involves mutations at two distinct sites where ‘mutation 1’ confers resistance to insecticide A and ‘mutation 2’ confers hypersensitivity to insecticide B.

1.3.5 Insect resistance management

The evolution of resistance is almost inevitable and, in many cases, occurs rapidly in the absence of carefully designed Insecticide Resistance Management (IRM) strategies. IRM is a component of IPM intended for forecasting and delaying of resistance development to all insecticides (Vorley and Dittrich 1994). Various strategies have been investigated to find a best way to use the available insecticides considering application options such as rotations, mixtures, and mosaics (Roush 1989) and the use of insecticides with differing modes of action (Sparks and Nauen 2015).

Negative cross-resistance has provided new opportunities for IRM. As the frequency of resistance to one insecticide rises, the second insecticide can be deployed to maintain control. Theoretically, sustainable control could be achieved by timely rotations of two different insecticides. There are examples that underscore this approach. Following the identification of the DDT-resistant, *para*$^{ts-1}$ mutation, Pedra et al. (2004) showed that after five generations of selection using the negative cross-resistance compound, deltamethrin, *para*$^{ts-1}$ allele frequency was reduced significantly in the population compared to control (Pedra et al. 2004). Yamamoto et al. (1993) were able to reduce the frequency of N-methylcarbamate resistance in *Nephotettix cincticeps* populations using another carbamate, N-propylcarbamate, for which there was negative cross-resistance. Resistance was attributed to a mutation in AChE that simultaneously increased sensitivity to N-propylcarbamate. Alternating these carbamates application was demonstrated to shift the resistant allele frequencies back and forth in the population (Yamamoto, Kyomura, and Takahashi 1993). A similar strategy was used to control tick infestations by applying acaracides, chlorfenvinphos, and amitraz to resistant tick population affecting a Kenyan cattle herd (Kamidi and Kamidi 2005).

1.4 Rationale for the study

Insecticide resistance poses a major threat to human health and food production, rendering insecticides ineffective, requiring the costly development of new chemicals that can satisfy ever stricter regulatory constraints being applied due to the environmental concerns. In theory, the identification of negative cross-resistance relationships between insecticides would give a huge advantage in the management of resistance in the population, extending the lifespan of available insecticides. Rotation or mixtures of appropriate insecticides could be effective in reducing resistant allele frequencies in field populations although the effectiveness of such approaches would depend on various factors that require further investigation. No company has marketed products that take advantage of negative cross-resistance. The limited number of examples of the phenomenon could be a reason for this, but there are other factors. A given agrochemical

company may not have the two suitable insecticides required to control a given pest in their product range. Nonetheless, the appropriate agencies and consultants could advise growers on choices of suitable products that would be available from different companies. In reality, such advice would depend on negative cross-resistance research which has, thus far, been limited in scope in terms of the number of examples investigated and the extent to which the underlying mechanisms have been investigated. Filling these gaps is vital if negative cross-resistance is to fulfil its potential for sustained insect pest control.

nAChRs continue to be a popular target for increasing numbers of insecticides. Mutations conferring resistance have been characterised in pest populations and have been recovered following mutagenesis and gene manipulation in the lab in the *D. melanogaster* model system. A number of examples of negative cross-resistance have been observed in these mutants (described in Chapter 2, Section 2.1.1) affording the opportunity to investigate the underlying mechanism(s) and possibly opening up fresh avenues for pest control in the field. In probing mechanism, a deeper understanding of the biology of nAChRs and the functions of individual subunits is required. The identity of the individual subunits that combine to form nAChRs is largely unknown as are the mechanisms controlling correct trafficking and localisation to the plasma membrane. The observation that homozygous loss-of-function mutants for some of the subunits are viable provides evidence some of these subunits are not required. Further characterisation of insect nAChR subunits to test for possible functional redundancy between some of the subunits and to better understand the 'redundancy rules' could be instructive for future insecticide design. Resistance is more likely to evolve if it targets a single redundant nAChR subunit than if it targets combinations of subunits that are non-redundant. Negative cross-resistance could be totally explained in terms due to differences in the way in which two insecticides respond to a mutant target (as suggested for the $para^{ts-1}$ mutant). Alternatively, given that there is a family of nAChR subunit genes, there is the possibility that it could be explained by a compensatory regulatory mechanism whereby a mutation impacting one subunit alters the expression of others. These possibilities will be explored in this thesis.

1.5 Research questions

This thesis will address some of the gaps in our understanding of target site resistance and how the insect nervous system adapts to mutations that can confer resistance and negative cross-resistance. It investigates the redundancy rules and investigates changes in gene expression in resistant mutants and under conditions of insecticide exposure. Much of the research to be described would only be possible in the *Drosophila* model system due to the variety of powerful tools available for the manipulation of genes and gene expression. Although *Drosophila* is not a pest species it has long been utilised as model to study insecticide mode of action as well as mechanisms of resistance (reviewed in Perry et al. 2011). The nAChR genes to be studied here have conserved orthologues in pest species, so the findings of this research are likely to have wider application.

This thesis will address the following questions:

Chapter 2

1. Which nAChR subunits and which insecticides are involved in negative cross-resistance relationships?
2. Is the negative cross-resistance phenotype an allele specific event? If it is, does a particular type of nAChR subunit mutation lead to the negative cross-resistance phenotype?
3. What are the likely mechanisms involved in negative cross-resistance?

Chapter 3

1. What are the nAChR subunit gene expression changes in backgrounds that have the negative cross-resistance phenotype?
2. How does nAChR subunit expression change and does it support the nAChR compensation hypothesis for negative cross-resistance?
3. What functional pathways are affected in the mutants?
4. Do the findings from different transcriptional analyses (RNAseq and Targeted DamID) performed correlate with each other?

Chapter 4

1. Where in the brain are the nAChR subunits involved with the negative cross-resistance phenotype being expressed? Are they expressed in the same cells?
2. Is there any change in protein level of nAChR subunits that could explain the negative cross-resistance phenotype?
3. Can other pathways possibly involved in negative cross-resistance be targeted for further investigation?

1.6 Thesis structure

The thesis continues with Chapter 2, which examines negative cross-resistance profiles in various nAChR subunit mutants of *D. melanogaster*. CRISPR-generated mutants for eight nAChR subunit genes were investigated for altered toxicity to two neonicotinoids, nitenpyram and imidacloprid, as well as a spinosyn, spinosad, using larvae-to-adult toxicology bioassay. Mutants for the Dα1, Dα2 and Dα6 subunits displayed negative cross-resistance. With the exception of a single allele of *Dα1*, the negative cross-resistance phenotypes observed are not allele specific. This chapter discusses the variation in insecticide toxicity observed for the different mutant alleles and highlights possible changes in the nAChR subunit population that could mediate the negative cross-resistance.

Chapter 3 describes changes at transcriptional level that could be responsible for negative cross-resistance phenotype in the nAChR subunit mutants. Genome wide transcriptome analysis were performed in first instar larvae using RNAseq to reveal differentially expressed genes in *Dα1*, *Dα2* and *Dα6* mutants. A cell-specific transcriptomic approach utilising targeted Dam Identification (DamID) was also used to analyse transcriptional changes in specific neuronal cells that are expressing *Dα6*, in *Dα1* and *Dα6* mutants. This chapter discusses the biological pathways identified from differentially expressed genes and their possible contribution to the negative cross-resistance.

Chapter 4 investigates localisation of the nAChR subunits in the larval brain and measures subunit protein expression in *Dα1* and *Dα6* mutants that may explain

the negative cross-resistance phenotype. T2AGAL4 system was utilised to allow for GAL4 expression under the control of endogenous nAChR gene. An approach using a fluorescently tagged nAChR subunit was later used to measure changes in subunit levels in the mutant backgrounds. Additionally, the chapter analyses involvement of previously identified biological pathways in the mechanism of negative cross-resistance using commercial chemical inhibitors, assayed with a larval movement assay, the Wiggle Index.

Finally, Chapter 5 brings together the observed negative cross-resistance profiles and the findings of altered transcription and protein expression in nAChR subunit mutants. It presents mechanisms that may contribute to the insecticide hypersensitivity and considers the importance of these findings for future resistance management.

Chapter 2 : Identification of negative cross-resistance between insecticides in nAChR subunit mutants

2.1 Introduction

The widespread use of insecticides in agriculture has been a key factor in the control of insect pests. However, this control is almost inevitably compromised by the evolution of insecticide resistance, which in turn, drives a search for alternative chemical compounds with different mode of actions. This cycle of *resistance and replacement* has led to many pest species developing resistance to multiple classes of insecticides. It is now becoming more difficult and expensive to discover and develop novel insecticides (Sparks and Nauen 2015). Given these challenging circumstances, the phenomenon of negative cross-resistance between insecticides would be extremely valuable for resistance management. Application of insecticides in the context of a negative cross-resistance phenotype theoretically has the ability to overcome the impact of existing resistant alleles, extending the period over which some current generation insecticides may be used to control pests. An understanding of the mechanism underpinning negative cross-resistance may assist in optimising control strategies but the mechanisms for the known examples have not been defined in detail (refer Section 1.3.4).

2.1.1 Negative cross-resistance in nAChR mutants

Previous studies have implicated the Dα1 and Dβ2 nAChR subunits as targets for neonicotinoids while current evidence suggests that spinosyns only target the Dα6 nAChR subunit (Perry et al. 2008, 2012, 2015; Perry, McKenzie and

Batterham 2007; Somers et al. 2015; Somers, Luong, Batterham, et al. 2017; Watson et al. 2010). Studies on *D. melanogaster* have identified neonicotinoid-resistant and spinosyn-resistant strains, characterising loss-of-function mutations in these nAChR subunits (refer Section 1.3.3). Importantly, the two insecticides are classified by IRAC as having distinct modes of action (Sparks and Nauen 2015) and published cross resistance data provides evidence supporting the hypothesis that the subunits that they target are not co-assembled into the same receptor, i.e. they have distinct targets (Perry et al. 2012, 2015; Perry and Batterham 2018). Therefore, as might be expected, insects resistant to one of these insecticide classes due to a target site mutation are not cross resistant to the other insecticide class (Perry et al. 2008, 2012; Salgado and Saar 2004; Watson et al. 2010). In fact, the opposite may be true.

A closer examination of the insecticide resistance phenotypes observed for different nAChR subunit loss-of-function mutants suggests that there are at least some mutations that confer resistance to one compound and hypersensitivity to another (Perry et al. 2012; Perry, McKenzie and Batterham 2007). This leads to the possibility that there exists a negative cross-resistance relationship between these insecticide classes. Negative cross-resistance is defined as a phenotypic characteristic based on insecticide toxicity where a mutant allele is observed with increased resistance to one insecticide and increased susceptibility to another insecticide at the same time (refer to Section 1.3.4). The nitenpyram-resistant strain, $D\alpha1^{EMS1}$, was shown to have increased susceptibility to spinosad as compared to the control (Perry et al. 2012) and the *D. melanogaster* strain used to identify Dα6 as a spinosad target has increased sensitivity to nitenpyram (Perry, McKenzie and Batterham 2007; Trent Perry, personal communication). This relationship is however not always observed. A full knockout of *Dα1*, $D\alpha1^{KO}$ that is resistant to neonicotinoids, shows wildtype susceptibility (LC_{50}) to spinosad (Somers 2015). Taken together, these data suggest that this phenomenon could be allele specific or influenced by the genetic background.

Studies on insects other than *D. melanogaster*, also appear to provide evidence for a negative cross-resistance relationship between neonicotinoids and spinosyns. In *H. virescens,* a spinosad-resistant strain was shown to be more

susceptible to a neonicotionid, acetamiprid (Roe et al. 2010). The basis of the spinosad resistance in this species has not yet been determined. Additionally, a spinosad-resistant strain of *M. domestica*, characterised with dysregulated expression of cytochrome P450 genes, was also indicated with negative cross-resistance to neonicotinoids (Markussen and Kristensen 2012), however it was not clear which genes were involved. For the examples involving mutations in nAChR subunit genes, the observation of negative cross-resistance has led to the hypothesis that a change in one nAChR subunit may affect the susceptibility of a compound that binds to another subunit. Roe et al. suggested that there might be some degree of interaction between the target sites of the two insecticides (Roe et al. 2010). Given that we now know that neonicotinoid and spinosyn insecticides have distinct targets, this hypothesis can be elaborated to suggest that a mutation in a gene encoding a subunit targets by one insecticide, leads to a compensatory change in the expression of a subunit(s) targeted by the other. Changes in expression could mean differences at the transcriptional or post-transcriptional level. Alternatively, compensation could arise through changes in metabolic responses to the insecticides (Section 1.3.4.1).

2.1.2 Chapter overview

This chapter builds on earlier research and the published literature, examining mutations in nAChR subunits targeted by neonicotinoid and spinosyn classes of insecticide. In contrast to earlier studies, by examining a range of mutant alleles the extent to which the negative cross-resistance phenomena is allele specific will be ascertained. By establishing which nAChR subunit mutations confer negative cross-resistance, a platform will be established for further studies to investigate the mechanism(s) that might be responsible for the phenomenon. Given neonicotinoids alone account for the largest portion of 26.6% from the total global insecticide sales and spinosyns contribute a substantial portion of 1.6% (Sparks et al. 2017), understanding the nature of the negative cross-resistance relationship between the two insecticide classes may be valuable in informing insecticide resistance management strategies. This potential would be maximised if negative cross-resistance proves not to be allele specific.

2.1.2.1 Research questions

This chapter will answer the following research questions:

1. Which nAChR subunits and which insecticides are involved in negative cross-resistance relationships?
2. Is the negative cross-resistance phenotype an allele specific event? If it is, does a particular type of nAChR subunit mutation lead to the negative cross-resistance phenotype?
3. What are the likely mechanisms involved in negative cross-resistance?

2.2 Materials and Methods

2.2.1 Fly strains

Previously generated *D. melanogaster* loss-of-function mutant strain for eight of the ten known nAChR subunits and their corresponding background strains were used in the first part of the study. The fly stocks and corresponding gene mutations are listed in Table 2.1. *Dα1$^{\Delta DH}$, Dα2$^{\Delta(3)4E}$, Dα3$^{\Delta 1020}$, Dα4$^{\Delta BA}$, Dα6^{KO}, Dα7$^{\Delta D6}$, Dβ2^{E145A}* and *Dβ3$^{\Delta B4.2}$* mutants were generated in the genetic background of an *actin>Cas9* expressing strain (Bloomington Drosophila Stock Centre, BDSC #54590) using CRISPR/Cas9 genome editing (Perry et al. manuscript in preparation). The X chromosome was later replaced with the X chromosome from a white-eyed strain, *w^{1118}* (BDSC #5905) to eliminate Cas9 expression in all the mutants (the control background strain is renamed as *wAC9* in comparison to the original control, *AC9*) except for two, the *Dα3$^{\Delta 1020}$* and *Dα7$^{\Delta D6}$* mutants. These genes are located on the X chromosome and so Cas9 is still expressed in these flies.

Other fly strains with different alleles for *Dα1, Dα2* and *Dα6* were also included in this study (Table 2.2). Specifically, these were: -

1. *Dα1^{EMS1}* and *Dα1^{Nit11}* (*Dα1^{Q533*}*) were generated by ethyl methane-sulfonate (EMS) mutagenesis of *Armenia^{14}* (Perry, McKenzie and Batterham 2007).

2. *Dα6^{EMS6}* (*Dα6^{W337*}*) and *Dα6^{EMS7} (Dα6^{nx})*, also generated by the EMS mutagenesis of *Armenia^{14},* each carrying a *Dα6* mutation that confers spinosad-resistance (Perry et al. 2015).

3. A *Dα1* full knockout mutant, *Dα1^{KO}*, that was previously generated in the *w^{1118}* background using ends-out gene targeting (Somers, Luong, Batterham, et al. 2017).

4. A *Dα6* amino acid replacement mutant (P146S), *Dα6^{P146S}*, generated on the background of *RAL059* (BDSC #28129). This allele exhibits incomplete dominance for spinosad resistance (Somers et al. 2015).

5. *Dα1^{P141S}* was generated by introducing the P141S amino acid change to an analogous site in Dα1, in the background of *wAC9* as described in Section 2.2.2.

6. A *Dα2* full knockout mutant, *Dα2^{KO}*, generated using CRISPR/Cas9 editing in the background of *wAC9* (Luong 2018).

Table 2.1 List of CRISPR/Cas9-generated mutant strains of various nAChR subunits in the study

Strain	Background	Inheritance	Mutation and protein alteration
Dα1$^{\Delta DH}$	*wAC9*	Recessive	partial deletion inside exon 6; altered extracellular ligand-binding domain
Dα2$^{\Delta(3)4E}$	*wAC9*	Recessive	deletion spanning exon 2-5; truncated peptide inside extracellular ligand-binding domain
Dα3$^{\Delta1020}$	*AC9*	Recessive	two partial deletions at the 3' end and 5' end of the gene
Dα4$^{\Delta BA}$	*wAC9*	Recessive	full gene deletion; null mutation
Dα6^{KO}	*wAC9*	Recessive	full gene deletion; null mutation
Dα7$^{\Delta D6}$	*AC9*	Recessive	full gene deletion; null mutation
Dβ2^{E145A}	*wAC9*	Recessive	E145A; single amino acid change in extracellular ligand-binding domain
Dβ3$^{\Delta B4.2}$	*wAC9*	Recessive	full gene deletion; null mutation

Table 2.2 List of different *Dα1, Dα2* and *Dα6* subunit alleles in the study

Allele	Background	Inheritance	Mutation and protein alteration
Dα1^{EMS1}	*Armenia^{14}*	Recessive	11bp deletion; altered TM4 domain
Dα1^{Nit11}	*Armenia^{14}*	Recessive	Q533stop; truncated peptide right after TM4 domain
Dα1^{P141S}	*wAC9*	Dominant	P141S; single amino acid change in extracellular ligand-binding domain
Dα1^{KO}	*w^{1118}*	Recessive	full gene deletion; null mutation
Dα2^{KO}	*wAC9*	Recessive	full gene deletion; null mutation
Dα6^{EMS6}	*Armenia^{14}*	Recessive	W337stop; truncated peptide 13 residues after TM3
Dα6^{EMS7}	*Armenia^{14}*	Recessive	unknown; no detectable transcript
Dα6^{P146S}	*RAL059*	Dominant	P146S; single amino acid change in extracellular ligand-binding domain

2.2.2 Generation of *Dα1*^{P141S}

The CRISPR/Cas9 system guided by a small guide RNA (sgRNA) was used to create the *Dα1* P141S mutation in the *AC9* background. Two sgRNAs flanking the codon for residue 141, GATGGAAAATATGTTAGATT and GAAACATGTC-TGCTCGTCGA, were designed and cloned into U6b-sgRNA-short plasmids following digestion with BbsI (Ren et al. 2013). To introduce the P141S mutation, a single-stranded oligodeoxynucleotide (ssODN) was used as a homology repair template for the CRISPR-mediated mutation. The ssODN was designed to span 3R:24,407,199 – 24,407,517 and includes the GCC to ACT mutation at base position of 3R:24,407,423 – 24,407,425, taking account that *Dα1* gene is transcribed from a negative direction. The mutation also introduced an additional restriction fragment length polymorphism (RFLP) site, which is recognised by the restriction enzyme, *HphI*. DNA sequence for the ~500bp ssODN is provided as follow, where the introduced P141S mutation is highlighted in blue while the *HphI* recognition sites are underlined:

5′-GTGGAGAAAAAAACTTTCTATCGCCAACAAAATGCTTTACAAAAAAAATTT
AAGTCCTGATATATATTTGAAAGTTAAATCATTGAAAGATAACATTAAAGGATA
TCACATTGATATACCTAAAATATTAGTTCAATCAATATGTAAATCGTTAGTAAA
TCCAATATCTTCTCCATCGTTTTTTTTTTCCATTTCAGCGCCGATGGCAACTAT
GAAGTGACAATAATGACAAAAGCAATTCTTCATCACACGGGCAAAGTGGTGTGG
AAATCACCCGCCATTTACAAATCCTTCTGCGAAATTGATGTCGAGTACTTTCCC
TTTGATGAACAAACCTGTTTCATGAAGTTCGGATCCTGGACCTACGATGGTTAC
ATGGTGAGTTGGGGATTTGATGGCGGGGATGACCCAGAAGCCATCATCCGAAGG
GAGGCAACAGCTGGCAGCTCTGGCCACGAACAGATTATCCCCCGGCCCATCAAT
CAAAATCGAAGCAA-3′

150 ng/uL of each sgRNA and 500 ng/uL of ssODN were co-injected into *AC9* embryos using a standard *Drosophila* microinjection protocol (Gratz et al. 2015). Positive CRISPR events were identified using insecticide screening. Briefly, individual survivors were mated to virgin double balancer flies. This strain has balancer chromosomes for the major autosomes in *Drosophila*, chromosomes II and III. Balancer chromosomes carry multiple inversions to suppress

recombination and a dominant phenotypic marker that allows the presence of the balancer chromosome to be detected in heterozygotes. The *F1* male progeny of cross were backcrossed to the double balancer virgin females and their progeny was screened on a discriminating dose of imidacloprid. Survivor males were crossed back to the virgin double balancer females before being made homozygous.

The presence of P141S mutation was checked via the introduced RFLP site described earlier. DNA was extracted using a standard single fly prep protocol (Gloor and Engles 1992) and fragments containing the P141S mutation were amplified using GTTCGGCACTTTTAGTCGATTTCG forward and CGAGTCA-AGGCAACGTTTG reverse primer. Restriction enzyme *HphI* (New England Biolabs) cut the PCR product twice, instead of once, when the introduced sequence is present. The PCR product was also sequenced to confirm the P141S mutation. Off-target sites for each sgRNA were checked online (http://tools.flycrispr.molbio.wisc.edu/targetFinder) and the off-target regions were sequenced to make sure that no off-target mutations were present.

2.2.3 Fly media

All fly media containing ingredients has been previously described (Perry et al. 2012). The standard fly media used for fly rearing contained 7.9 g of potassium tartrate, 0.5 g of calcium chloride, 5.25 g of agar, 11.8 g of dried yeast, 52.6 g of glucose, 26.3 g of sucrose, 65.8 g of semolina, 11 mL of acid mix (412 mL/L of propionic acid and 42 mL/L of orthophosphoric acid in distilled water) and 16 mL of tegosept (50g of tegosept dissolved in 950 mL of 95% ethanol) per litre, topped up using water.

Apple juice plates of varying size (50 mm or 90 mm clear petri dish plate) were used for the collection embryos and larvae. They contained 200 mL of apple juice, 20 g of agar, 7 g of dried yeast, 26 g of sucrose, 52 g of glucose and 6 mL of tegosept per litre, topped up using water.

2.2.4 Insecticide compounds

Nitenpyram (270.72 $gmol^{-1}$ Pestanal®; Sigma-Aldrich), Imidacloprid (255.66 $gmol^{-1}$ Pestanal®; Sigma-Aldrich) and Spinosad (10 gL^{-1} Success®; Yates) were purchased commercially. For media preparation, nitenpyram and spinosad were diluted in distilled water, whereas imidacloprid was diluted in dimethyl sulfoxide (DMSO). Each insecticide was diluted to make a stock solution containing 1000 ppm of the active ingredient. All stock solutions were stored at 4°C in the dark because, to varying degrees, these insecticides are light sensitive.

2.2.5 Insecticide toxicology bioassay

Insecticide toxicology bioassays were performed on first instar *D. melanogaster* larvae as described previously (Perry et al. 2012). Flies were allowed to lay eggs on 50 mm apple juice plates, in mass-bred cages for up to 24 hours. Embryos were collected, washed and spread onto 90 mm apple juice plates. After 24 hours, for each vial, 50 first instar larvae were transferred onto standard fly media containing varying doses of insecticide. The insecticide was pre-mixed into freshly cooked, molten fly media to achieve the desired final concentration and the fly media was allowed to set in vials for several hours. Fly media containing only the solvent for the insecticide being tested (distilled water or DMSO) served as a control. Vials containing the first instar larvae being assayed were kept in the dark at 25°C. The total number of adult flies eclosed were counted and recorded after 18 days. Typically, three replicates of five different doses of each insecticide were used in a series of bioassays for each mutant and its appropriate genetic background control strain, i.e., an average total of 750 larvae per strain, per insecticide were tested.

2.2.6 Data analysis

Analyses were performed in R software using a custom R script for the insecticide toxicology bioassay (Appendix 1). The mortality data from the toxicology bioassay was corrected for control mortality using Abbott's correction (Abbott 1925). Probit analysis of the corrected mortality data was used to develop regression lines and determine the $LC_{50,}$ the concentration that was lethal to 50% of the tested larvae

(Finney 1947). The Student's t-test was used to test for statistical significance between LC_{50} values for a given mutant and its appropriate genetic background control strain, *wAC9* or *AC9*. The resistance ratio and its 95% confidence limits were calculated, comparing the LC_{50} of each mutant strain and its respective control strain (Robertson et al. 2009). A resistance ratio that had 95% confidence limits that did not include 1.0 were considered statistically significant ($\alpha = 0.05$). When required, the level of dominance (D_{LC}) based on the LC_{50} values, and effective dominance (D_{ML}) at several insecticide concentrations were calculated (Bourguet et al. 2000; Roush and McKenzie 1987).

2.3 Results

2.3.1 Profiling mutants of different nAChR subunits for insecticide cross-resistance and negative cross-resistance

To profile the toxicity of neonicotinoid and spinosyn insecticides against flies with different nAChR subunit mutations, first instar larval toxicology bioassays were performed on available mutants of nAChR subunits Dα1, Dα2, Dα3, Dα4, Dα6, Dα7, Dβ2 and Dβ3 generated using the CRISPR/Cas9 system (Perry et al. manuscript in preparation). The analyses were conducted, comparing each mutant to their wildtype background strains, *wAC9* and *AC9*. Toxicity levels of three insecticides, nitenpyram, imidacloprid and spinosad were determined by dosage mortality analysis where LC_{50} values for each of *Drosophila* strains tested were calculated. In addition, a resistance ratio comparing each mutant and its respective wildtype strain was determined to compare resistance levels between the different mutant strains.

The two wildtype strains, *wAC9* and *AC9* showed very similar response levels to all three insecticides (Figure 2.1A-C). LC_{50} values for *wAC9* and *AC9* were not significantly different in terms of the toxicity to nitenpyram, imidacloprid or spinosad. Comparing the nitenpyram toxicity levels on the nAChR subunit mutants, the $D\alpha1^{\Delta DH}$ and $D\beta2^{E145A}$ mutants showed the highest levels of resistance, ~7.5-fold and ~12-fold resistance respectively (Figure 2.1A & D). As expected, these mutants also showed cross-resistance to imidacloprid. Interestingly, the level of resistance level to imidacloprid (more than 20-fold) was higher than that observed for nitenpyram (Figure 2.1B & D). Another mutant, $D\alpha2^{\Delta(3)4E}$, was also observed to have a noteworthy level of imidacloprid resistance (~8-fold). *Dα2* has not been previously associated with neonicotinoid resistance. Looking at spinosad toxicity levels, only the *Dα6* mutant is expected to be resistant based on the literature. Accordingly, only the $D\alpha6^{KO}$ mutant showed a strikingly high level of resistance (~2100-fold)(Figure 2.1C-D). These data are consistent with published findings for resistance testing of Dα1, Dα6 or Dβ2 loss-of-function mutants (Perry et al. 2008, 2012, 2015; Watson et al. 2010).

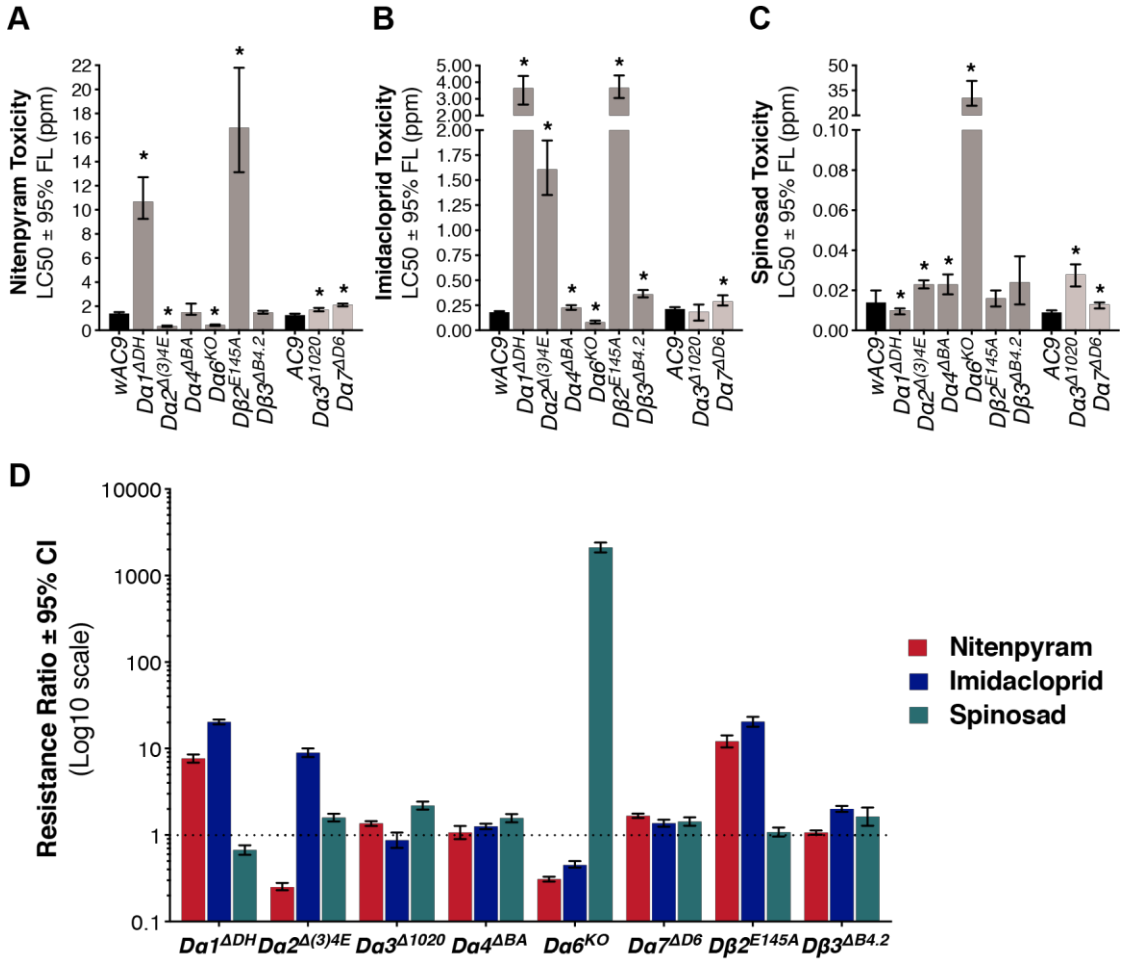

Figure 2.1 Relative toxicity of nitenpyram, imidacloprid and spinosad on nAChR subunit mutants

Bar graphs showing LC_{50} values for mutants for each of eight nAChR subunits exposed to (A) nitenpyram, (B) imidacloprid and (C) spinosad in larval-to-adult toxicology bioassays. Error bars indicate 95% fiducial limits. Statistical analysis was performed using the Student's t-test where (*) denotes $P < 0.05$. (D) Bar graph summarised resistance ratio in $\log_{10}$ scale for the mutant strains compared to their respective genetic background control strain. Error bars indicate 95% confidence limits of the ratio where intervals excluding 1 (dotted line) are considered statistically significant.

The *Dα2*$^{\Delta(3)4E}$, *Dα3*$^{\Delta1020}$, *Dα4*$^{\Delta BA}$, *Dα7*$^{\Delta D6}$ and *Dβ3*$^{\Delta B4.2}$ strains also showed a statistically significant level of spinosad resistance, but the levels were very low (less than 2-fold) compared to the over 2000 fold observed for *Dα6* mutant (Figure 2.1D). Similarly, a slight increase in nitenpyram resistance levels (less than 2-fold) were recorded for some of the mutants (*Dα3*$^{\Delta1020}$, *Dα7*$^{\Delta D6}$), and the same for imidacloprid (*Dα4*$^{\Delta BA}$, *Dα7*$^{\Delta D6}$, *Dβ3*$^{\Delta B4.2}$).

Three of the mutants showed negative cross-resistance. *Dα1*$^{\Delta DH}$ was approximately 1.5-fold more sensitive to spinosad compared to the control strain *wAC9*, indicating negative cross-resistance between neonicotinoids and spinosad (Figure 2.1D). *Dα6*^{KO} was 3-fold more sensitive to nitenpyram and 2.2-fold more sensitive to imidacloprid, showing an opposite negative cross-resistance relationship between neonicotinoids and spinosad. These observations were consistent with other studies. Interestingly, *Dα2*$^{\Delta(3)4E}$ showed a significant hypersensitivity (4-fold) to nitenpyram, while being ~8-fold resistant to imidacloprid. This is the first observation of negative cross-resistance involving a mutant for a single nAChR subunit and two insecticides from the same chemical class.

2.3.2 Generation and characterisation of *Dα1*^{P146S}

Somers et al. (2015) have demonstrated that a mutation which resulted in a single amino acid replacement, P146S, in the Dα6 subunit led to spinosad resistance. The spinosad-resistance was found to be an incompletely dominant trait where *F1* generation from the cross between *Dα6*^{P146S} and the wildtype (susceptible) background parent had an intermediate level of spinosad resistance (Somers et al. 2015). Here the same amino acid replacement was introduced into analogous site, P141S in the Dα1 subunit to test whether dominant resistance could occur via other subunits, targeted by neonicotinoid insecticides. Utilising the CRISPR/Cas9 system, in combination with a homology repair template, a targeted CCG to TCA mutation in exon 6 of *Dα1* that leads to Proline to Serine replacement at residue P141 in Dα1 (analogous site of P146 in Dα6) was introduced in the background of *wAC9* (Figure 2.2). Positive genome editing events were isolated by screening for a dominant imidacloprid phenotype. The events were made homozygous for sequence analysis to confirm that the desired mutation had been created. None of the predicted off-target changes were detected on chromosome III, while the non-targeted chromosomes were replaced with ones from *wAC9* to eliminate any off-target events. The mutant *Drosophila* strain is referred to as *Dα1*^{P141S}.

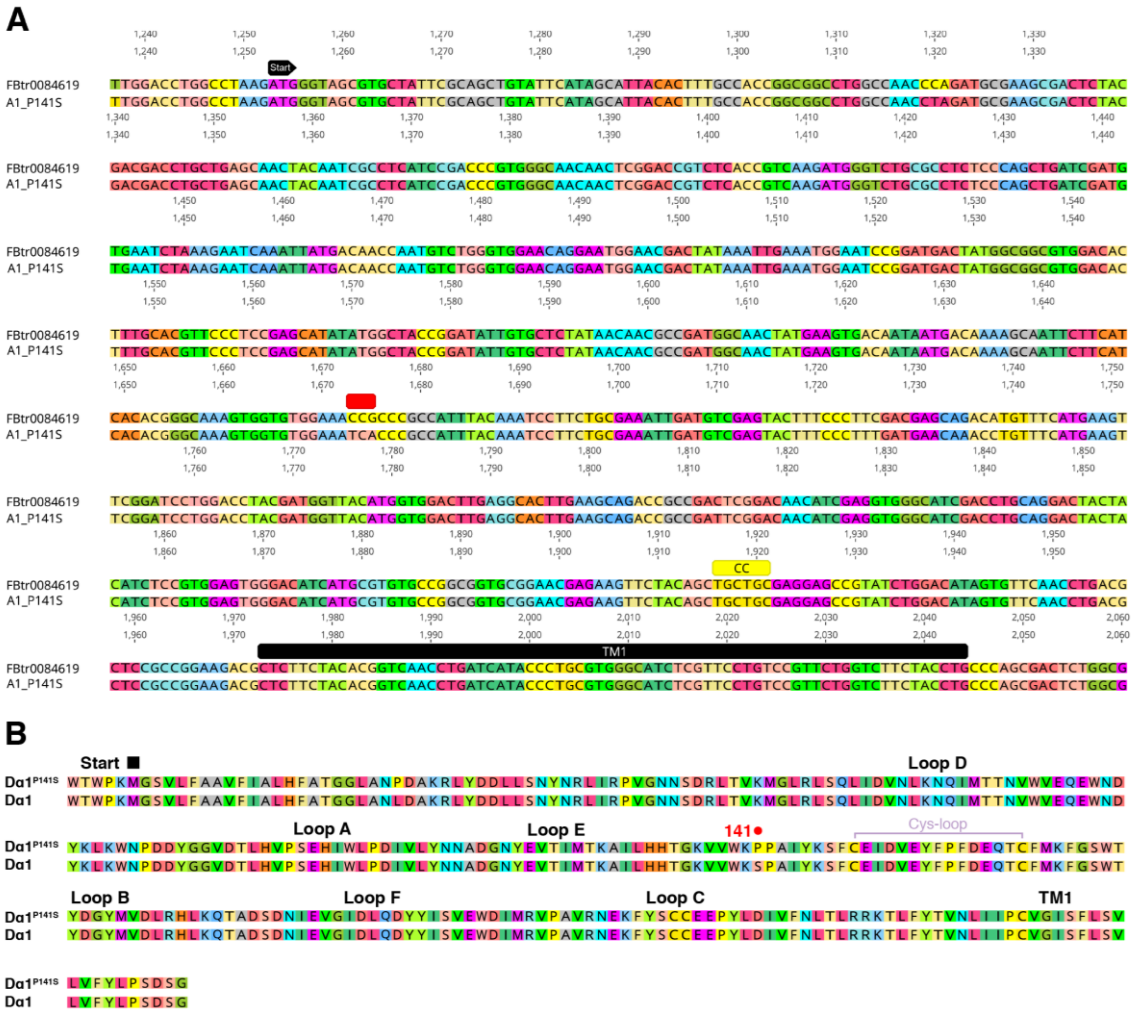

Figure 2.2 Alignment of *Dα1*^{P141S} and *Dα1* transcripts

(A) The amplified region of *Dα1*^{P141S} transcript (A1_P141S) was sequenced and aligned to the consensus *Dα1* transcript (FBtr0084619). The targeted CCG to TCA that led to Proline to Serine replacement at residue P141 is indicated by the red box. (B) Colour-coded amino acid residues encoded by both transcripts showed no other amino acid changes introduced in the region.

To characterise the insecticide resistance level of this newly generated strain, the individual strains *Dα1*^{P141S}, *wAC9* as well as their *F1* progeny were screened on nitenpyram and imidacloprid using the first instar larval toxicology bioassay. LC_{50} values and the corresponding resistance ratio (RR) were determined and summarised in Table 2.3. *Dα1*^{P141S} and the *F1* had significantly higher LC_{50} values than *wAC9*, for both nitenpyram and imidacloprid. Notably, the *F1* had an intermediate level of resistance between the two parental strains, indicating that the allele is not completely recessive or dominant. *Dα1*^{P141S} was 3.2-fold more

resistant to nitenpyram while the *F1* showed only 1.2-fold resistance compared to wildtype. Similarly, *Dα1*^{P141S} was 9.5-fold more resistant to imidacloprid while the *F1* showed only 2-fold resistance compared to wildtype. The level of dominance (D_{LC}) was calculated from the LC50 values as previously described (Bourguet et al. 2000), and D_{LC} values were presented at 0.19 and 0.27 for nitenpyram and imidacloprid, respectively, indicating that both resistance phenotypes were inherited as an incomplete recessive trait.

Table 2.3 Nitenpyram and imidacloprid toxicity level in the *Dα1*^{P141S} mutant

Strain	Nitenpyram LC_{50} (95% FL)[a]	Nitenpyram RR (95% CI)[b]	Imidacloprid LC_{50} (95% FL)[a]	Imidacloprid RR (95% CI)[b]
wAC9	1.39 (1.29-1.51)	1.00 (0.95-1.05)	0.18 (0.15-0.23)	1.00 (0.90-1.12)
F1 of Dα1^{P141S} x *wAC9*	1.73 (1.59-1.90)	1.24 (1.18-1.31)	0.33 (0.30-0.37)	1.98 (1.78-2.20)
Dα1^{P146S}	4.45 (3.99-4.89)	3.20 (2.97-3.44)	1.74 (1.40-2.14)	9.46 (8.14-11.00)

[a] Lethal insecticide concentration (ppm) for 50% mortality with its 95% fiducial limits
[b] Resistance ratio relative to *wAC9* with 95% confidence limits of ratio

The dominance level of these insecticide resistance traits is dependent of insecticide dose. Hence, the effective dominance (D_{ML}) was calculated using corrected mortality data at a range of different insecticide doses (Bourguet et al. 2000; Roush and McKenzie 1987). The D_{ML} values decrease with increasing insecticide concentration. Nitenpyram resistance ranged from being incompletely dominant at the lowest dose to completely recessive at the highest dose tested (Table 2.4). Similarly, imidacloprid resistance was incompletely dominant at the lowest dose and completely recessive at the highest dose tested (Table 2.5).

Table 2.4 Effective dominance level of *Dα1^{P141S}* over nitenpyram doses

Concentration (ppm)	Strain	Corrected mortality[a]	D_{ML}[b]
1.2	*wAC9*	22.4	0.60
	F_1	9.3	
	Dα1^{P141S}	0.0	
1.8	*wAC9*	84.3	0.40
	F_1	52.6	
	Dα1^{P141S}	7.0	
2.1	*wAC9*	94.1	0.20
	F_1	78.8	
	Dα1^{P141S}	16.4	
4.0	*wAC9*	100.0	0.10
	F_1	95.9	
	Dα1^{P141S}	47.7	
6.0	*wAC9*	100.0	0.00
	F_1	99.8	
	Dα1^{P141S}	66.0	

[a] Percentage mortality corrected for control mortality using Abbott's formula

[b] Effective dominance at a particular nitenpyram concentration

Table 2.5 Effective dominance level of *Dα1^{P141S}* over imidacloprid doses

Concentration (ppm)	Strain	Corrected mortality[a]	D_{ML}[b]
0.2	*wAC9*	49.6	0.50
	F_1	33.1	
	Dα1^{P141S}	17.6	
0.3	*wAC9*	76.3	0.40
	F_1	47.6	
	Dα1^{P141S}	17.6	
0.5	*wAC9*	92.4	0.30
	F_1	72.6	
	Dα1^{P141S}	30.2	
1.0	*wAC9*	100.0	0.20
	F_1	89.5	
	Dα1^{P141S}	30.2	
1.5	*wAC9*	100.0	0.01
	F_1	99.2	
	Dα1^{P141S}	33.6	
2.5	*wAC9*	100.0	0.00
	F_1	100.0	
	Dα1^{P141S}	57.1	

[a] Percentage mortality corrected for control mortality using Abbott's formula

[b] Effective dominance at a particular imidacloprid concentration

2.3.3 Analysis of allelic specific variation for nAChR subunits associated with negative cross-resistance

To further investigate the observed negative cross-resistance phenotype, we tested various mutant alleles for the three nAChR subunits that showed negative cross-resistance, Dα1, Dα2 and Dα6. Screening was conducted on the three insecticides – nitenpyram, imidacloprid and spinosad. Insecticide LC_{50} values for each of these strains and their genetic background controls are summarised in Table 2.6.

2.3.3.1 Susceptibility level of background strains

Four wildtype background strains, *Armenia*^{14}, *wAC9*, *w*^{1118} and *RAL059,* in which the mutants being tested were generated, were tested. *Armenia*^{14} and *w*^{1118} had similar susceptibility levels to nitenpyram (LC_{50} 0.84 ppm and 0.54 ppm respectively), while *wAC9* and *RAL059* showed significantly reduced susceptibility to nitenpyram compared to the other two strains (LC_{50} 1.39 ppm and 1.73 ppm, respectively). *wAC9* showed a slightly higher LC_{50} for imidacloprid compared to *Armenia*^{14} and *w*^{1118}, while *RAL059* was observed with 40-fold higher LC_{50} compared to the other three wildtype strains on average. In terms of relative toxicity of spinosad to these strains, *Armenia*^{14}, *w*^{1118} and *RAL059* all showed comparable susceptibility levels (LC_{50} 0.024 ppm, 0.024 ppm and 0.022 ppm, respectively). However, the LC_{50} of spinosad for the *wAC9* was significantly lower (0.013 ppm). As the susceptibility levels were varied between the background control strains, it was essential to take account of these differences when comparing the toxicity levels of each insecticide on the mutant strains generated from these different backgrounds. Hence, the resistance ratio was calculated by comparing the LC_{50} for each mutant to their corresponding wildtype background strain.

Table 2.6 Toxicity of nitenpyram, imidacloprid and spinosad to the *Dα1*, *Dα2* and *Dα6* mutants and their respective background control strains

	Allele	Nitenpyram LC_{50} (95% FL)[a]	Imidacloprid LC_{50} (95% FL)[a]	Spinosad LC_{50} (95% FL)[a]
Background strain	*Armenia*^{14}	0.84 (0.73-0.93)	0.11 (0.09-0.13)	0.024 (0.020-0.029)
	wAC9	1.39 (1.29-1.51)	0.18 (0.15-0.23)	0.013 (0.011-0.015)
	w^{1118}	0.54 (0.48-0.60)	0.12 (0.11-0.12)	0.024 (0.021-0.027)
	RAL059	1.73 (1.52-1.94)	5.40 (4.68-6.57)	0.022 (0.019-0.026)
Dα1 mutant	*Dα1*^{EMS1}	12.33 (10.65-17.00)	2.13 (1.57-2.83)	0.006 (0.005-0.007)
	Dα1^{Nit11}	6.45 (5.17-8.13)	1.60 (1.34-1.84)	0.014 (0.012-0.016)
	Dα1^{DH}	10.67 (9.25-12.71)	3.56 (3.26-3.86)	0.007 (0.006-0.009)
	Dα1^{P141S}	4.45 (3.99-4.89)	1.74 (1.40-2.14)	0.008 (0.007-0.009)
	Dα1^{KO}	26.41 (23.06-30.52)	2.74 (2.34-3.13)	0.021 (0.019-0.023)
Dα2 mutant	*Dα2*$^{\Delta 3(4E)}$	0.35 (0.28-0.40)	1.49 (1.22-1.72)	0.011 (0.007-0.014)
	Dα2^{KO}	0.83 (0.11-0.89)	2.46 (2.20-2.72)	0.015 (0.012-0.019)
Dα6 mutant	*Dα6*^{EMS6}	0.30 (0.27-0.33)	0.069 (0.043-0.085)	4.67 (3.11-6.79)
	Dα6^{EMS7}	0.39 (0.35-0.44)	0.070 (0.061-0.079)	24.96 (19.30-29.91)
	Dα6^{P146S}	0.66 (0.52-0.78)	0.79 (0.65-0.97)	1.27 (1.02-1.76)
	Dα6^{KO}	0.43 (0.36-0.48)	0.077 (0.064-0.091)	30.50 (25.82-40.69)

[a] Lethal insecticide concentration (ppm) for 50% mortality with its 95% fiducial limits
Blue shading indicates that the LC_{50} of the mutant strain is significantly higher than LC_{50} of the respective background control strain, whereas red shading indicates that it is significantly lower.

2.3.3.2 Dα1 mutant alleles

This study includes five mutant alleles of the Dα1 subunit; *Dα1*^{EMS1}, *Dα1*^{Nit11}, *Dα1*^{P141S}, *Dα1*^{DH} and *Dα1*^{KO} strain. The results consistently showed that all *Dα1* mutation alleles were resistant to nitenpyram, at resistance levels ranging from 3-fold to 50-fold (Figure 2.3A). The full knockout allele, *Dα1*^{KO} showed the highest resistance level to nitenpyram (over 40-fold higher than the other *Dα1* alleles on average). All the alleles were also cross-resistant to imidacloprid with resistance level ranging from 10-fold to 23-fold (Figure 2.3B). This time, similar level of resistance was recorded between *Dα1*^{KO} and other *Dα1* mutation alleles. The resistance levels presented are consistent with the previously reported toxicity levels (Perry et al. 2012; Somers, Luong, Batterham, et al. 2017).

Four of the *Dα1* mutants showed a hypersensitivity to spinosad (2.7-fold to 4-fold more sensitive) when compared to their background controls (Figure 2.3C), reflecting the same negative cross-resistance relationship indicated previously (Section 2.3.1). *Dα1*^{KO} showed a slightly lower LC_{50} compared to its background strain, *w*^{1118}, but this difference was not statistically significant. In order to verify if the negative cross-resistance phenotype is dominant, flies carrying the *Dα1*^{EMS1} truncation allele were crossed to the *Dα1*^{KO} strain. The F_1 generation of the crosses showed a similar spinosad sensitivity level to the one observed for the homozygous *Dα1*^{EMS1} mutant (Table 2.7), indicating that the hypersensitivity to spinosad is dominant.

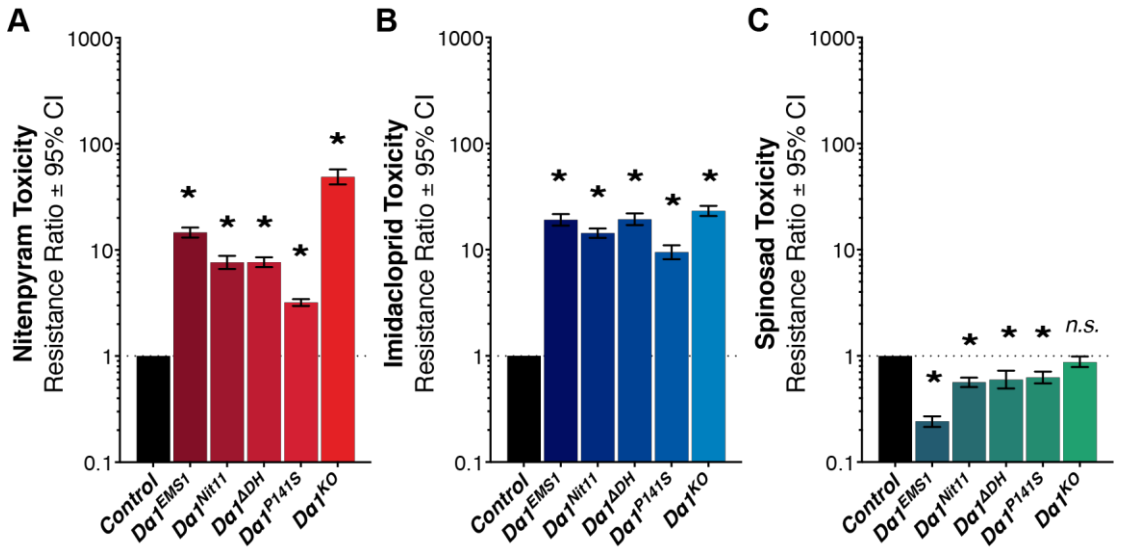

Figure 2.3 Insecticide toxicity for five *Dα1* mutants

Bar graphs showed resistance ratio for (A) nitenpyram, (B) imidacloprid and (C) spinosad, measured using first instar larval toxicology bioassays on five *Dα1* mutant strains compared to their respective background control strains. Graphs were plotted on $\log_{10}$ scale and error bars indicate 95% confidence limits of the ratio. Intervals that exclude 1 (dotted line) are considered statistically significant (*). *n.s.*, not significant

Table 2.7 Spinosad toxicity level in *Dα1^{EMS1}*, *Dα1KO,* and *F1* generations of the two strains

Strain	LC_{50} (95% FL)[a]	RR (95% CI)[b]
Armenia^{14}	0.024 (0.020-0.029)	1.00 (0.89-1.10)
Dα1^{EMS1}	0.006 (0.005-0.007)	0.24 (0.22-0.27)
Dα1^{KO}	0.021 (0.019-0.023)	0.87 (0.78-0.97)
F_1 of ♀*Dα1*^{EMS1} x ♂*Dα1*^{KO}	0.005 (0.004-0.006)	0.21 (0.19-0.24)
F_1 of ♂*Dα1*^{EMS1} x ♀*Dα1*^{KO}	0.006 (0.006-0.007)	0.26 (0.24-0.29)

[a] Lethal insecticide concentration (ppm) for 50% mortality with its 95% fiducial limits
[b] Resistance ratio relative to Armenia14 with 95% confidence limits of ratio

2.3.3.3 Dα2 mutant alleles

Two *Dα2* mutants were examined, the previously examined $D\alpha2^{\Delta(3)4E}$ and another full knockout mutant, $D\alpha2^{KO}$. Both mutants were resistant to imidacloprid and negatively cross-resistant to nitenpyram. The $D\alpha2^{\Delta(3)4E}$ mutant was approximately 7-fold resistant to imidacloprid and the $D\alpha2^{KO}$ showed even higher resistance level to imidacloprid (approximately 14-fold in magnitude), compared to the background strain, *wAC9* (Figure 2.4B). In terms of hypersensitivity to nitenpyram, $D\alpha2^{\Delta(3)4E}$ was 3-fold more sensitive to nitenpyram, while $D\alpha2^{KO}$ showing a modest, but significant, level of hypersensitivity (1.2-fold) compared to the control (Figure 2.4A). Neither mutant showed any significant difference in response to spinosad (Figure 2.4C).

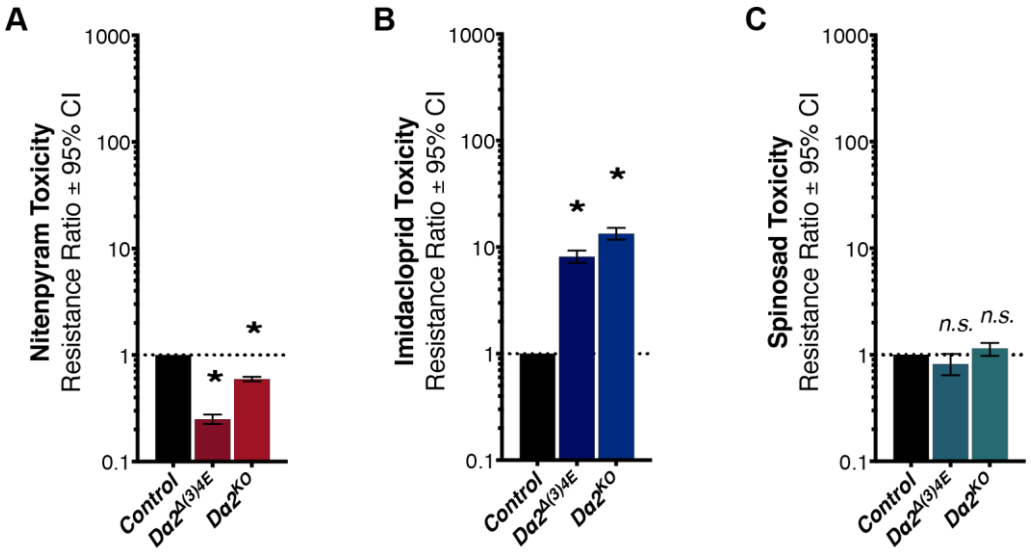

Figure 2.4 Insecticide toxicity for two *Dα2* mutants

Bar graphs showed resistance ratio for (A) nitenpyram, (B) imidacloprid and (C) spinosad, measured using toxicology bioassays on first instar larvae of two *Dα2* mutant strains, compared to their respective background strains. Graphs were plotted on $\log_{10}$ scale and error bars indicate 95% confidence limits of the ratio where intervals that exclude 1 (dotted line) are considered statistically significant (*). *n.s.*, not significant

2.3.3.4 Dα6 mutant alleles

Four *Dα6* mutants were examined, *Dα6*^{EMS6}, *Dα6*^{EMS7}, *Dα6*^{P146S} and the previously examined *Dα6*^{KO}. As expected, all the *Dα6* alleles showed high levels of resistance to spinosad ranging from 58-fold to 2100-fold, when compared to their background controls (Figure 2.5C). This strongly supports prior findings in the literature, demonstrating that *Dα6* gene is the main target for spinosad (Somers et al. 2015; Watson et al. 2010). The spinosad resistance levels for *Dα6* alleles were also similar to the previously reported values, except for *Dα6*^{P146S} (Luong 2018; Perry et al. 2012). Somers and colleagues reported 28-fold resistance to spinosad for the *Dα6*^{P146S} mutant in comparison to the background strain, *RAL059* (Somers et al. 2015). The difference between the two studies is that spinosad LC_{50} for *RAL059* measured here was lower than that measured by Somers et al. (2015). Similar LC_{50} values for *Dα6*^{P146S} were measured in both studies.

All four of the *Dα6* mutants showed a significant elevation in sensitivity to both nitenpyram and imidacloprid. The mutants showed a similar level of hypersensitivity to nitenpyram, ranging from 2-fold to 3-fold compared to their background controls (Figure 2.5A). However, the hypersensitivity levels to imidacloprid were more varied between the different mutants. *Dα6*^{EMS6} and *Dα6*^{EMS7} showed a 1.6-fold increase in sensitivity to imidacloprid, while *Dα6*^{P146S} and *Dα6*^{KO} were 6.8-fold and 2.3-fold more sensitive to imidacloprid respectively, when compared to the background controls (Figure 2.5B). In summary, every *Dα6* mutant showed spinosad resistance and neonicotinoid hypersensitivity, a noteworthy inverse of the negative cross-resistance relationship observed for the *Dα1* mutants.

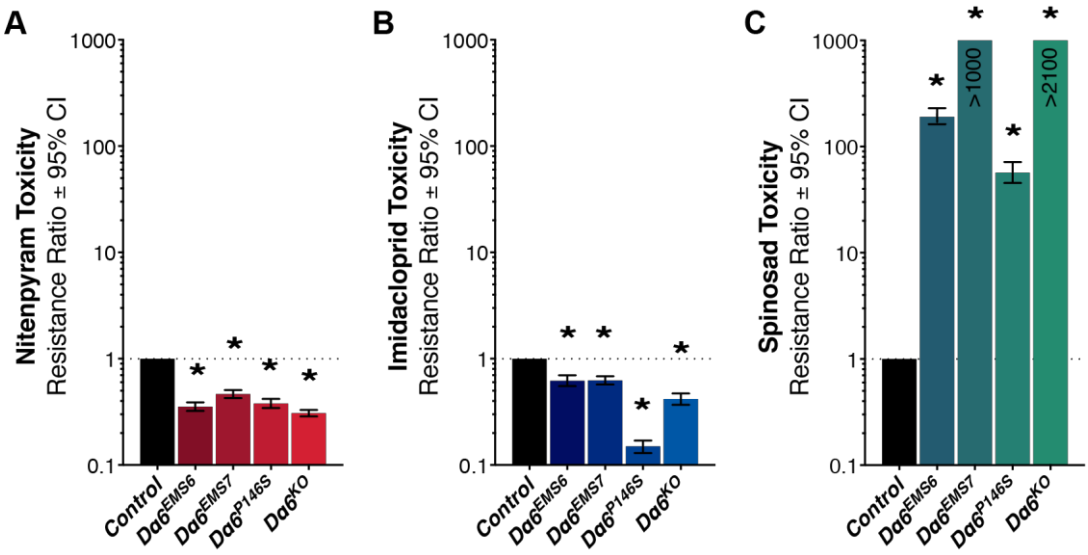

Figure 2.5 Insecticide toxicity for four *Dα6* mutants

Bar graphs showing the resistance ratio for (A) nitenpyram, (B) imidacloprid and (C) spinosad, measured using toxicology bioassays on first instar larvae of multiple four *Dα6* mutants, compared to their respective background strain. Graphs were plotted on a $\log_{10}$ scale and error bars indicate 95% confidence limits of the ratio, where intervals excluding 1 (dotted line) are considered statistically significant (*). *n.s.*, not significant

2.4 Discussion

2.4.1 Neonicotinoid resistance

The results presented in this study indicate that the Dα1, Dα2 and Dβ2 subunits are the main constituents of the one or more major nAChR subtypes targeted by neonicotinoids. This contention is supported by various studies on the heterologous expression of these subunits and the neonicotinoid resistance observed in other strains tested (Ihara et al. 2003; Lansdell and Millar 2000b; Perry et al. 2008, 2012; Somers, Luong, Batterham, et al. 2017). Although the *Dα3*, *Dα4*, *Dα7* and *Dβ3* mutants tested were resistant, the level of neonicotinoid resistance observed (less than 2-fold) was much lower than that observed for *Dα1*, *Dα2* and *Dβ2* (Figure 2.1). These subunits might contribute to receptor subtypes that are either less abundant or bind neonicotinoids less efficiently. The combination of Dα3/rat β2 in heterologous system was evidenced to provide a high affinity binding site for imidacloprid (Lansdell and Millar 2000b), but it is not known to what implications this has in evaluating the function of *Drosophila*-only nAChR subunit combinations.

Dα2 mutations in the subunit confer resistance to imidacloprid, but not nitenpyram. These two neonicotinoid insecticides are classified by Insecticide Resistance Action Committee (IRAC) as having the same mode of action (Sparks and Nauen 2015), but it would seem that there may be a difference in the efficiency with which they bind different nAChR subtypes. Target site resistance involving the *α2* subunit has not been previously reported in *Drosophila*, but a study on thiamethoxam- and imidacloprid-resistant field strains of *M. domestica* reported 60% lower copy number of *Mdα2* transcript in some of the strains compared to the susceptible control (Markussen and Kristensen 2010b). The level of nitenpyram toxicity to these strains was not examined. That the Dα2 subunit may be included in imidacloprid but not nitenpyram targets, suggests that there could be two different receptor subtypes; one including Dα1, Dα2 and Dβ2 subunits targeted by both neonicotinoids and another consists of only Dα1 and Dβ2 targeted by imidacloprid, not nitenpyram. In suggesting that imidacloprid has more targets than nitenpyram, this hypothesis could, at least in part, explain why

imidacloprid is typically significantly more toxic than nitenpyram in *Drosophila*. Consistent with this hypothesis, co-immunoprecipitation studies on native protein preparations identified Dα1/Dα2/Dβ2 and Dα1/Dβ2 native receptors, but not a Dα2/Dβ2 subtype (Chamaon et al. 2002). In discussing receptor subtypes there is a complicating factor. A receptor is composed of five subunits, so in considering heteromeric receptors such as Dα1/Dβ2 we do not know how many subunits of Dα1 and Dβ2 are included, or whether other subunits such as Dβ1 are also co-assembled.

Compared to earlier studies, an extensive range of *Dα1* mutant alleles has been assayed here with two neonicotinoids. While all mutant strains showed neonicotinoid resistance, the levels of resistance varied (Figure 2.3A-B). This may be an indicator of variation in the severity of the impact of the lesions on the functional capacity of Dα1. $Dα1^{EMS1}$ and $Dα1^{Nit11}$ both described as truncation mutants have a significant level of resistance to both neonicotinoids. The level of resistance in both cases is less than that observed for the knockout mutant, $Dα1^{KO}$, possibly suggesting that some Dα1 function is retained in the truncation mutants. In a heterologous expression system, it has been shown that the co-expression of a truncated Dα1 along with Dα2 and chicken β2 subunit is assembled into functional, but impaired, receptors (Schulz et al. 2000). It is therefore possible that these truncated subunits are still providing some level of function, mechanically or structurally, to the receptor complex.

$Dα1^{P141S}$ was generated to create a single amino acid replacement analogous to $Dα6^{P146S}$ in the Dα1 subunit. The P146S replacement in *Drosophila* Dα6 was associated with spinosad resistance and this phenotype was characterised as an incompletely dominant trait (Somers et al. 2015). The proline residue at this site is highly conserved. It sits in a conserved region located just before the Cys-loop motif and contributes to the complementary face of orthosteric ligand-binding pocket (Chiara, Xie, and Cohen 1999). Here, a Proline to Serine amino acid replacement at P146 analogous site for Dα1 subunit, P141, was introduced using CRISPR/Cas9. The mutant allele, $Dα1^{P141S}$, conferred resistance to both neonicotinoids at levels similar to that of the truncation alleles, $Dα1^{EMS1}$ and $Dα1^{Nit11}$ (Table 2.6, Figure 2.3). That the resistance level is lower than that

observed with *Dα1^{KO}* suggests that this mutant does not have a complete loss of function. It is likely that the mutant subunit is being assembled into nAChR complexes. A replacement of Proline, adjacent to orthologous P141 site in human muscle-type nAChR subunit, εP121L was associated with congenital myasthenic syndrome, where it was found that the mutation affects nAChR opening (Ohno et al. 1996). Although a mutation engineered into the orthologous P141 site (εP120) in the same muscle-type subunit did not lead to as large an effect, reduced ligand gating was still recorded (Gupta, Purohit, and Auerbach 2013).

The neonicotinoid resistance for *Dα1^{P141S}* was characterised as an incomplete recessive trait, but the analysis of concentration-dependent dominance level of the phenotype suggests that the resistance is partially dominant at a low insecticide concentration (Table 2.4 and Table 2.5). This is similar to the dominance profile reported for *Dα6^{P146S}* (Somers et al. 2015) and is consistent with the hypothesis that the mutated subunit is incorporated into receptors targeted by these insecticides (Somers et al. 2015). The concentration-dependent dominance can be understood in terms of the proposed role that P141S mutation impacts, i.e. gating. If the Dα1 subunit is incorporated into heteromeric receptors, in heterozygotes at least 50% of these will contain the mutated subunit and have reduced gating function. Hence, a higher concentration of neonicotinoids will be required to mediate a similar response to one provided by the wildtype. Of course, in homozygotes this value will be 100%, and thus, leading to even higher neonicotinoid resistance levels.

Interestingly, the full knockout allele, *Dα1^{KO}* showed an even higher resistance level on nitenpyram compared to the other *Dα1* alleles, but this was not observed with imidacloprid (Figure 2.3A-B). One possible explanation is that the receptor subunit with high affinity for nitenpyram failed to form in the absence of Dα1, whereas a subtype that is targeted by imidacloprid may still be present, possibly in a modified form. For example, Dα1 may be replaced by another subunit that is normally present in the impacted nAChR subtype e.g. Dα2 might replace Dα1 in the Dα1/Dα2/Dβ2 nAChR complex. This could account for the resistance data if Dα1/Dα2/Dβ2 subtypes have the highest affinity for both neonicotinoids and the newly formed Dα2/Dα2/Dβ2 nAChRs are responsive to imidacloprid, but not

nitenpyram. However, it was demonstrated that although the Dα2/Dβ2 receptor is formed in a heterologous expression system, the complex was insensitive to α-BTX, so a native Dα2/Dβ2 subtype consisting of only these two subunit types was suggested to not likely to exist in flies (Chamaon et al. 2002). We do not know to what level this holds true. It could be that another nAChR subunit is required to stabilise this combination of subunits. An examination a double-knockout of *Dα1* and *Dα2* to determine whether levels of imidacloprid resistance are elevated would be revealing.

2.4.2 Spinosyn resistance

Studies on a range of insect species and *D. melanogaster* have associated the loss of α6 subunit function with spinosyn resistance (Bao et al. 2014; Perry et al. 2015; Perry, McKenzie and Batterham 2007; Puinean et al. 2013; Wang et al. 2016; Watson et al. 2010). Indeed, to date, only mutants of *α6* orthologs have been shown to be spinosyn resistant, suggesting α6 is the principle nAChR subunit targeted by spinosyn. Here mutants of the Dα2, Dα3, Dα4, Dα7 and Dβ3 subunits showed very low-level resistance in comparison to the 2000-fold observed for Dα6 knockout mutant (Figure 2.1). Thus, it is unlikely that any of these subunits contribute to a significant percentage of the nAChRs targeted by spinosad. The Dα6 subunit may form a homomeric nAChR subtype targeting spinosad, given that the closely related subunits, Dα5 and Dα7, were previously shown to successfully form functional homomeric nAChRs that is functional (Lansdell et al. 2012). It should be noted that attempts to produce functional homomeric Dα6 receptors in the same study failed. In contrast, previous radioligand-binding assays showed that both Dα6 and Dα7 chimeric subunits (fused to the C-terminal domain of the 5-HT_3 receptor) form a functional αBTX-binding homomeric receptors in *Drosophila* S2 cell line (Lansdell and Millar 2004). It is not clear that the results from these experiments can be definitive in assessing the likelihood of homomeric Dα6 receptors forming *in vivo.*

One nAChR subunit, Dα5, has not been assessed for insecticide responses. The Dα5 subunit has proven difficult to study due to lethality or infertility issues of *Dα5* knockout flies (Christesen et al. manuscript in preparation), so testing with toxicity

bioassays has not been possible. Thus, the Dα5 subunit cannot be excluded as a possible spinosad target, particularly given evidence that Dα5 and Dα6 subunits form a heteromeric nAChR spinosyn-responsive subtype when expressed in *Xenopus* oocytes (Watson et al. 2010).

A range of different *Dα6* mutation alleles generated in different genetic backgrounds are described in this study. All of these mutants are highly resistant to spinosad (Figure 2.5C). The $D\alpha6^{EMS7}$ had been previously reported to have a spinosad resistance level of over 1000-fold (Perry et al. 2015). That finding was replicated here. This mutant was generated with EMS mutagenesis. While the causative lesion remains unknown, there is no *Dα6* transcript that can be detected in this mutant using real-time qPCR (Perry et al. 2015). $D\alpha6^{EMS7}$ is therefore classified as a full knockout allele. The discrepancy in resistance levels between $D\alpha6^{EMS7}$ (~1200 fold) and $D\alpha6^{KO}$ (~2100 fold) may indicate a very low level of expression from the $D\alpha6^{EMS7}$ allele. The other two alleles, $D\alpha6^{EMS6}$ (truncated subunit) and $D\alpha6^{P146S}$ (single amino acid replacement in ligand binding domain) both showed lower resistance levels compared to the two knockouts, again suggesting that there may be some retained function of the impaired nAChR subunit that allows the insecticide to act, albeit at a low level.

2.4.3 Negative cross-resistance relationships

Mutants for three different subunits, Dα1, Dα2 and Dα6, were shown to have negative cross-resistance phenotypes. Negative cross-resistance was observed between the neonicotinoid and spinosyn insecticides in the *Dα1* and *Dα6* mutants. In contrast to earlier studies, here different mutant alleles for each nAChR subunit gene were examined to ascertain whether the negative cross-resistance phenomena are allele specific. It appears that the phenotype is fairly consistent where almost all *Dα1* and *Dα6* mutants examined here were negative cross-resistant. In general, the negative cross-resistance phenotype does not appear to be an allele-specific phenomenon, but the level of negative cross-resistance does vary between alleles.

Four of the five *Dα1* mutants tested were resistant to the two neonicotinoids, while showing elevated sensitivity towards spinosad (Figure 2.3C). This was not true

for *Dα1*^{KO} which was highly resistant to neonicotinoids but yielded a non-significant reduction in LC_{50} for spinosad. This allele-specific observation will be discussed in Section 2.4.4.

All four *Dα6* mutants tested here were highly resistant to spinosad while being hypersensitive to both neonicotinoids (Figure 2.5). In examining these mutants, there was no correlation between the level of resistance to neonicotinoids and the level of sensitivity to spinosad.

The examination of the two *Dα2* mutants produced a surprising outcome. The mutants were resistant to imidacloprid. This led to an expectation that they would also be resistant to the other neonicotinoid, nitenpyram, but when tested they proved to be hypersensitive (Figure 2.4). Again, as the two different *Dα2* mutants showed negative cross-resistance, the phenotype is likely not allele specific. Further, these mutants showed wildtype sensitivity to spinosad. As suggested in Section 2.4.1, it is likely that Dα1, Dα2 and Dβ2 subunits form multiple nAChR subtypes, and that each has a different affinity for different neonicotinoids. This may provide a foundation understanding the negative cross-resistance phenotype observed in the *Dα2* mutants.

Based on these, we might have expected the *Dβ2* mutant would lead to the same negative cross-resistance phenotype given the fact that the subunit is among the targets for neonicotinoids. However, loss of Dβ2 did not result in negative cross-resistance to another insecticide. Given that mutation in *Dβ2* led to the same neonicotinoid resistance to when *Dα1* is mutated, Dα1 and Dβ2 are both likely to participate in the same neonicotinoid binding site. This is supported by the fact that imidacloprid resistance level of a double mutant of *Dα1* and *Dβ2* did not deviate significantly from the level seen for *Dα1* or *Dβ2* mutant alone (Perry et al. 2012). As mentioned previously, unlike other non α-subunits, Dβ2 is more closely related to the α-subunit, α8 in other insect species (Figure 1.4B). Evolutionary speaking, the case could be different for when *Dβ2* is completely deleted. The lack of negative cross-resistance to spinosad may be due to the fact that the Dβ2 subunit is more dispensable compared to the other subunits observed with the phenotype. However, given there is insecticide resistance when the subunit is affected, it should not be the case.

2.4.4 Possibility for nAChR compensation

None of the published mechanisms (Section 1.3.4.1) fully explain the examples of negative cross-resistance identified here. As neonicotinoids and spinosyns are known to have different targets, a mutation that changes binding affinity for neonicotinoids would not result in increased binding affinity for spinosyn, and vice versa. Here, negative cross-resistance was observed for mutations that impacted the insecticide binding site and those that did not. Further, many of the mutant alleles were generated through targeted mutation, ensuring that only a single mutation was created in a single nAChR subunit gene. The change in binding site mechanism would require mutations in two nAChR subunit genes. In its simplest form a mechanism underpinned by changes in metabolism can be rejected as the genes conferring negative cross-resistance do not encode metabolic enzymes, but it is possible that a mutation in a nAChR gene may initiate metabolic changes that lead to insecticide hypersensitivity although direct evidence of this has not been previously reported.

Considering the nAChR gene family is highly conserved in protein structure, it is also possible that a mutation in one nAChR subunit may impact the expression of other subunits. This compensation mechanism could have impacts at the nAChR subunit or subtype level that lead to the negative cross-resistance phenotype (Figure 2.6). A precedent for a compensation in response to loss of nAChR subunits has been previously documented in mammals. Mouse α6 subunits (not orthologous to Dα6) were previously shown to co-assemble together with α4 and β2 subunits (Klink et al. 2001). A study using a mouse *α6* knockout strain detected an increase in the amount of other nAChR subtypes with different pharmacological properties (Champtiaux et al. 2002). In the study, the authors described a replacement α6 by α4 in $\alpha4\alpha6\alpha5(\beta2)_2$ receptor complexes in the *α6* knockout mice, following an increase in αCTXMII-resistant, epibatidine binding sites (Champtiaux et al. 2002). However, the exact molecular mechanism behind this is unknown. It is not known whether this is through assembly of additional α4 into the nAChR subtype, or simply an upregulation of an existing nAChR subtype with the αCTXMII-resistant, epibatidine binding sites. A similar

compensation mechanism was proposed for *α4* knockout mice, but this has not been investigated further (Klink et al. 2001).

Applying the compensation hypothesis to the current context, a mutation in a single nAChR subunit would change the population of nAChR subtypes at the membrane, in tissues targeted by insecticides, leading to the observed negative cross-resistance phenotype (Figure 2.6). A mutation in an nAChR subunit targeted by one insecticide would lead to a compensatory increase in the number of nAChRs of a subtype(s) targeted by a second insecticide, and thus, lead to hypersensitivity.

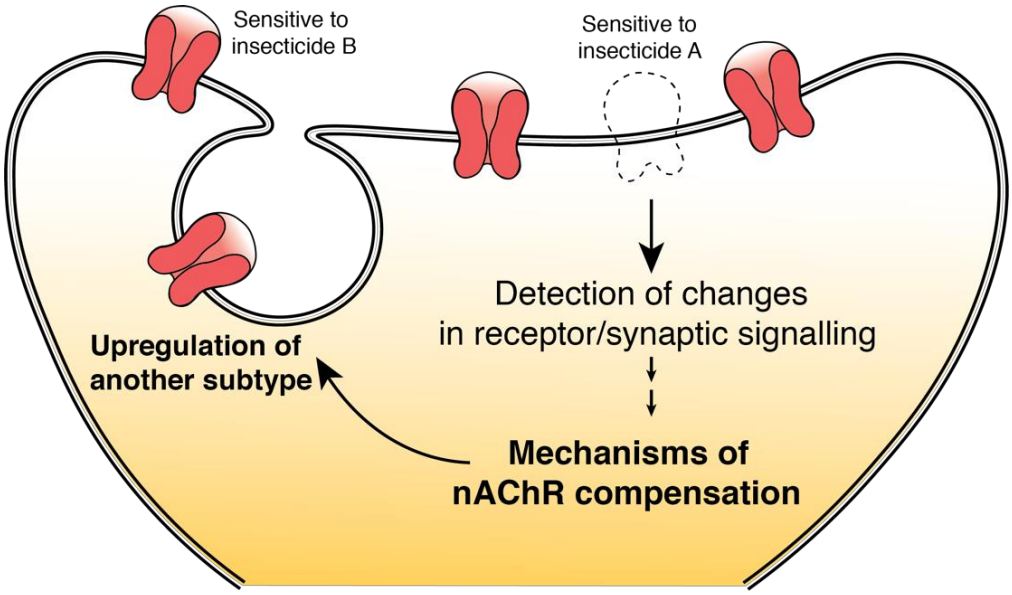

Figure 2.6 A mechanism by which nAChR compensation could lead to negative cross-resistance

Figure illustrates a detection of; mutated receptor subunit in nAChR subtype(s) that is target for an insecticide A, or the resulting dysregulation in synaptic signalling, as a mechanism triggering nAChR compensation leading to upregulation of nAChRs of a subtype(s) targeted by an insecticide B. Hence, this would lead to negative cross-resistance, where the mutant confers resistance to the insecticide A but is hypersensitive to the insecticide B.

In accounting for the negative cross-resistances observed here with a compensation hypothesis some predictions can be made. *Dα1* mutants would lead to an upregulation of Dα6-containing subtype conferring spinosad

hypersensitivity (Figure 2.7). Conversely, an upregulation of Dα1-containing subtypes in *Dα6* mutants would lead to nitenpyram and imidacloprid hypersensitivity. *Dα2* mutants require a more complex explanation given that both neonicotinoids, imidacloprid and nitenpyram seem to target the Dα1 and Dβ2 subunits. It is proposed that the loss of Dα2 leads to an increase in the proportion of Dα1/Dβ2 subtypes that may provide lower binding affinity for imidacloprid than Dα1/Dα2/Dβ2 subtype (Figure 2.7). This would result in increased sensitivity to nitenpyram, but not imidacloprid. Compensation may occur at a subunit level (Dα1 replacing Dα2 subunit in the original Dα1/Dα2/Dβ2 subtype) or at a subtype level (upregulation of native Dα1/Dβ2 subtype to compensate for the loss of Dα1/Dα2/Dβ2 subtype), assuming the presence of Dα1/Dβ2 subtype in wildtype flies.

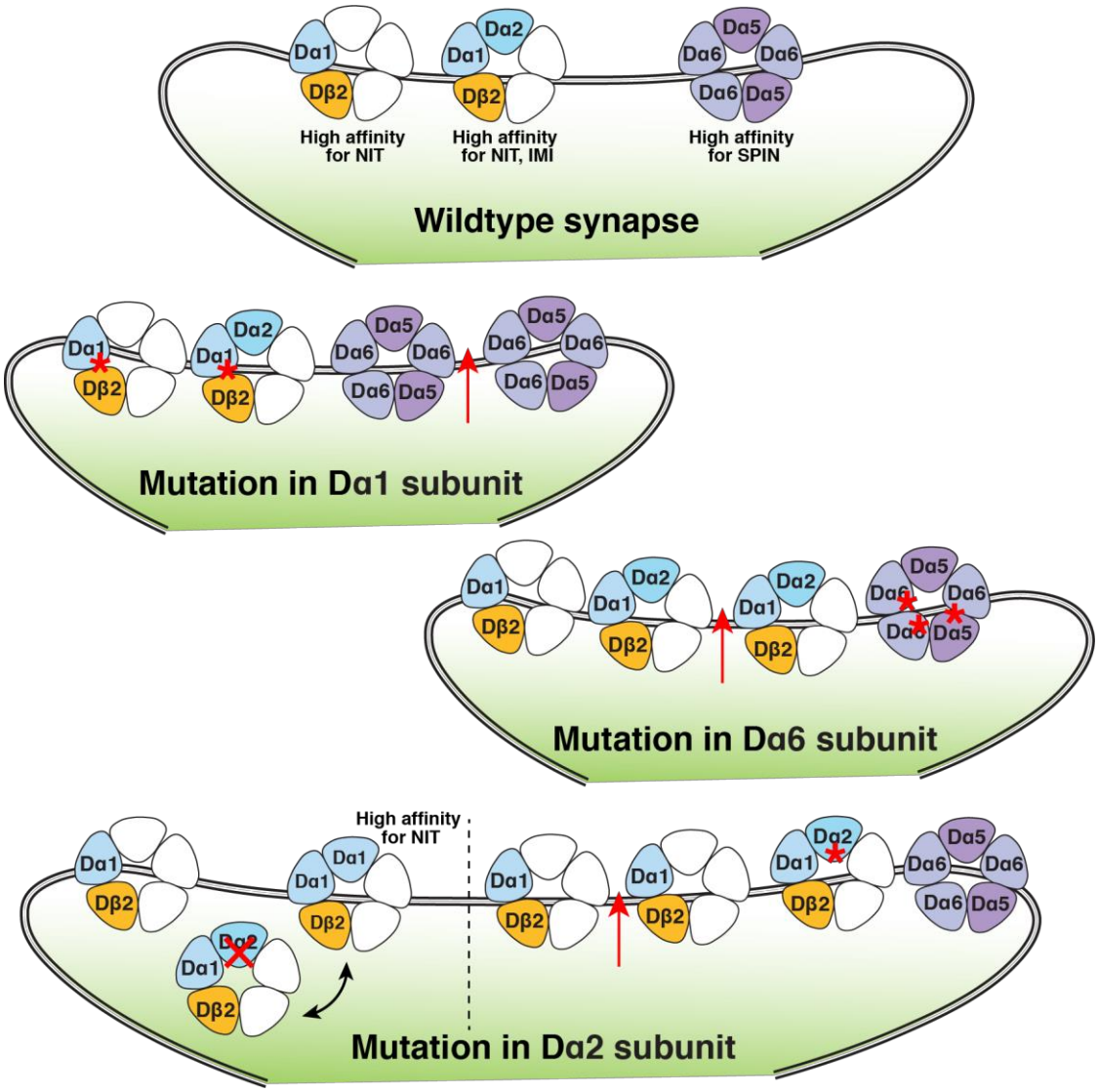

Figure 2.7 Proposed nAChR combinations for insecticide targets in subunit mutants

Opposite. Diagram illustrates the proposed nAChR subtypes, exist in the wildtype flies, that are targets for neonicotinoids (Dα1/Dα2/Dβ2 subtype that provides high affinity binding site for both nitenpyram (NIT) and imidacloprid (IMI), and Dα1/Dβ2 subtype that provides high affinity binding for NIT only). Meanwhile, homomer of Dα6, or heteromer of Dα5/Dα6 maybe exist as nAChR subtypes that are targets for spinosad (SPIN). In *Dα1* mutants, upregulation of the Dα6-containing subtype by mechanism of nAChR compensation could lead to the observed SPIN hypersensitivity. Similarly, in *Dα6* mutants, upregulation of the Dα1-containing subtypes by the same mechanism could result in the NIT and IMI hypersensitivity. In *Dα2* mutants, loss of Dα2 may lead to compensation at subunit or subtype levels, leading to an increase in the proportion of Dα1/Dβ2 subtypes, thus, the NIT hypersensitivity.

These hypotheses could be tested using the appropriate mutants for the nAChR subunits and antibodies for the individual subunits. The use of tagged receptor subunits would also allow changes in protein levels to be examined. There are complicating factors in testing these predictions. Firstly, to explain for the observation of negative cross-resistance, this nAChR compensation only needs to occur in the neurons targeted by these insecticides. At this point, it is not clear whether this involves all neurons or subsets of them. If it is specific to a subset of neurons, changes in the levels of a particular nAChR may be difficult to detect. Secondly, while the compensation hypothesis points to changes in expression, this could occur at many different levels – transcriptional, translational or post-translational levels. Testing at any one of these levels may not resolve the question of whether compensation is occurring or not. The second point is underscored by the lack of a negative cross-resistance phenotype for $D\alpha1^{KO}$ mutant. That negative cross-resistance occurs in *Dα1* mutants where protein is produced suggests that protein expression of the mutated subunit is required for the negative cross-resistance mechanism to occur. In mutants that still express a modified or truncated Dα1 protein the sensing of defects in the receptor complex or in synaptic signalling may be sensed, triggering compensation. The strongest support for this comes from the result testing dominance, where the presence of the allele that showed negative cross-resistance ($D\alpha1^{EMS1}$) in the

Dα1^{KO} background leads to the negative cross-resistance phenotype (Section 2.3.3.2). By way of contrast, there is evidence that protein expression is not required for the negative cross-resistances observed for *Dα2* and *Dα6* mutants. In both cases, negative cross-resistance is observed in full gene deletion mutants. These differences point to the possibility that different mechanisms may explain the examples of negative cross-resistance identified here.

2.4.5 Negative cross-resistance insecticides for pest control

Negative cross-resistance may be useful to complement other resistance management strategies, helping to supress the development of resistance and thus extending the life of insecticides in the field. It may be possible to manage existing resistance to an insecticide A by applying a different insecticide B to which field populations have been rendered hypersensitive. Under these circumstances the 'resistance' allele for insecticide A will be selected against, offering the opportunity to again use insecticide A. Rotation would be one of a number of options possible where negative cross-resistance exists. The potential for exploiting negative cross-resistance for control has been demonstrated in various studies as presented in Section 1.3.5, where the frequency of resistance alleles has been easily manipulated with the application of the negative cross-resistance compounds (Kamidi and Kamidi 2005; Pedra et al. 2004; Yamamoto et al. 1993).

Applying this to our findings, the observed negative cross-resistance relationship between neonicotinoids and spinosyns could benefit the management of resistance to these two insecticide classes simultaneously, extending their current life in the field. In some cases, allele specificity may be a barrier but, in the case of target site resistances to neonicotinoids and spinosyns studied here, almost all of the alleles tested had the same negative cross-resistance relationships. While the research conducted here has used *Drosophila*, the targets are conserved in insects. Field strains resistant to either of these insecticide classes due to target site mutations could be tested for negative cross-resistance.

Understanding the mechanism(s) that underlie negative cross-resistance may assist with an informed approach to identifying which combinations of insecticides and mutations might have a negative cross-resistance relationship. The following chapters of this thesis investigates the negative cross-resistance relationships identified here, aiming to associate changes in protein and gene expression with this phenomenon.

Chapter 3 : Dissecting mechanisms for negative cross-resistance through transcriptional analysis

3.1 Introduction

The composition of native nAChR complexes and the regulatory mechanisms for their expression are still largely unknown (refer Section 1.2.2). The complexity of the *Drosophila* CNS, as well as the diverse cell types in the brain, make it hard to pinpoint where the nAChRs are specifically expressed. Regulation of nAChR expression is likely to occur at a number of levels, one of which is certain to be transcription. Thus, analysis of transcriptomes of the insect model in specific cell types and life stages is likely to be useful in determining the distribution of nAChRs, as well as the regulatory factors behind their expression. The negative cross-resistance phenomenon provides a useful set of alleles that can be studied for changes in gene expression patterns. The compensation mechanism proposed to explain negative cross-resistance, could occur at the transcriptional level. This possibility will be investigated here.

3.1.1 Transcriptional profile of the *Drosophila* nAChR family

Previous transcriptional analyses in *Drosophila* have shed some light on localisation of nAChR gene expression. Single-cell transcriptome analysis of the adult *Drosophila* midbrain generated from a Drop-seq experiment has allowed for expression comparisons to be made for specific genes (including the nAChR subunit genes) in different neuronal cell types (Croset, Treiber, and Waddell 2018). Most of the nAChR genes were shown to be broadly expressed across the different neuronal cell types of the midbrain. The *Dα1, Dα5, Dα6, Dα7* and

Dβ1 genes were expressed in more cells than the other subunits. Patterns of co-expression limit the range of receptor subtypes that could be present in a given cell type. The expression of the *Dα1, Dα5, Dα6* and *Dβ1* genes is highly correlated as is the expression of the *Dα1, Dα2* and *Dβ1* genes (Figure 3.1, Croset et al. 2018). These combinations of co-expressed subunits show that the nAChR subtypes proposed to be targeted by the neonicotinoid and spinosyn classes could be formed (refer Section 2.4.1, Section 2.4.2 & Figure 2.7).

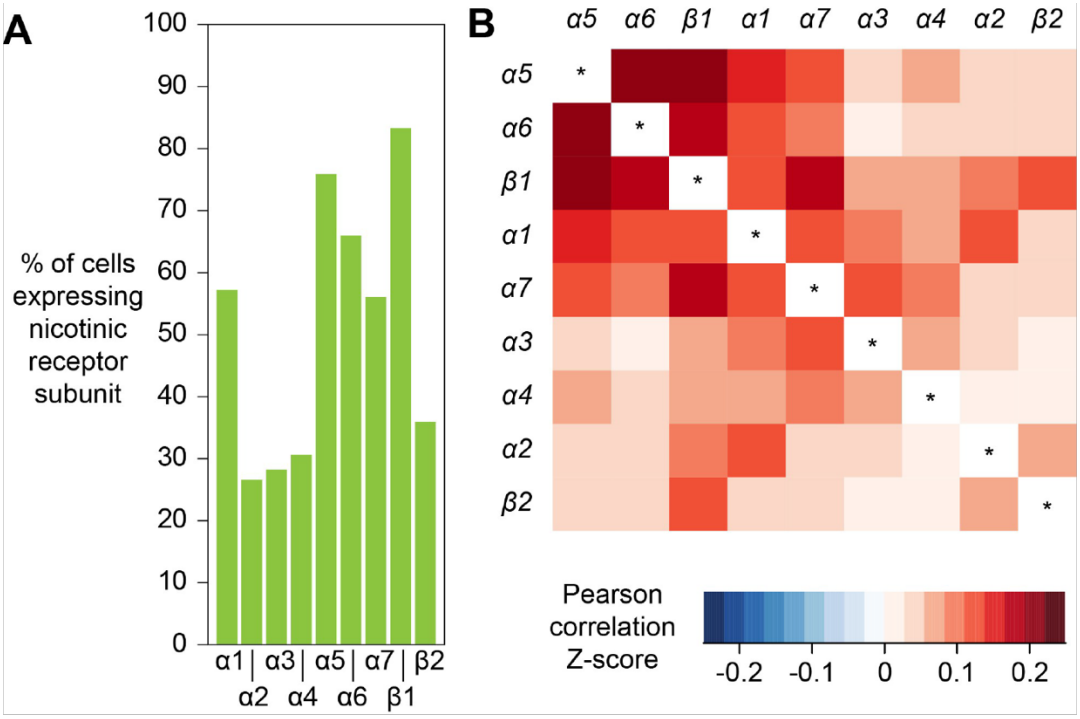

Figure 3.1 Single-cell transcript analysis of nAChR gene expression

(A) Bar graph shows percentage of cells of adult *Drosophila* midbrain expressing nAChR subunit genes. (B) Pearson correlation Z-scores for expression correlation between nAChR subunit gene pairs. Figure obtained from Croset et al. (2018).

The expression profile of the nAChR genes change across developmental stages and in response to extrinsic factors. nAChR gene expression was reported to be non-identical at different stages of mammalian cell differentiation and synapse development (Boulter et al. 1990; Kues et al. 1995; Witzemann et al. 1996). Similar observations were described in *Drosophila* larvae, where the *Dα1* and *Dα6* genes were shown to be expressed at different levels in young and mature neurons (Rosenthal et al. 2019). nAChR transcript levels are also modulated by

external factors such as neuronal injury and light conditions (Kelso et al. 2006; Rosenthal et al. 2019). Despite these findings, the biological importance of selective subunit expression for specific functional roles at different stages of development or at different conditions remains poorly understood.

3.1.2 Impact of insecticides on *Drosophila* transcriptome

Transcriptomic profiles of *Drosophila* tissues upon insecticide exposure, have also recently become available (Martelli 2020). Studies of brain and fat body tissue collected from larvae exposed to imidacloprid or spinosad found that various biological functions were disturbed. Specifically, the study identified dysregulated expression of genes involved in metabolism of lipids, carbohydrates, amino acids, hormones and xenobiotics, as well as genes associated with pathways related to immune response and oxidative phosphorylation (Martelli 2020). It was also proposed that the signal from the insecticide's action, originating in the brain are transmitted to other tissues such as the midgut and fat body, affecting their function (Martelli 2020). Supporting this, an earlier study showed modifications in the transcriptome profile of mosquitoes, *Aedes aegypti* in response to various insecticides including atrazine, permethrin and imidacloprid, where genes encoding transporters, detoxification enzymes and components of mitochondrial respiratory chain were particularly affected (David et al. 2010). Importantly, similar to the study conducted on *Drosophila* tissues, genes associated with xenobiotic response and tolerance were dysregulated (David et al. 2010). Despite the low concentrations of insecticide used in both studies and the subtle phenotypic effects on the organisms tested, a significant alteration in transcriptome profiles was observed (David et al. 2010; Martelli 2020). This raises concerning questions about the hidden impact of insecticides on non-targeted arthropods species that share ecosystems with pests.

3.1.3 Targeted DamID for cell-specific transcriptional analysis

While single cell sequencing is powerful it has some limitations in that in a complex tissue, such as the brain, it is not yet possible to identify all of the cell

types for which transcriptome sequences are produced (Croset et al. 2018). Methods that allow for the transcriptomes of particular cell types to be characterised such as the use of cell sorting techniques using cell-specific fluorescent markers (Berger et al. 2012) are of value. In this context targeted DamID offers a useful alternative.

DNA adenine methyltransferase (Dam) is a protein from *Escherichia coli* that methylates adenines at the N6 position (m6A) of GATC motifs. Dam identification (DamID) utilises Dam fused to a DNA-binding or chromatin-binding protein of interest to allow for targeted DNA methylation in close proximity of protein binding. This strategy was introduced in *Drosophila* to offer an *in vivo* alternative to the techniques available such as chromatin immunoprecipitation (ChIP) and since then, it has been applied to various other model organisms including mice, *C. elegans*, *Arabidopsis thaliana* and human cells (Germann et al. 2006; Schuster et al. 2010; van Steensel and Henikoff 2000; Tosti et al. 2018; Vogel, Peric-Hupkes, and van Steensel 2007). In comparison to bacteria, the methylation of adenine is almost non-existent in eukaryotes. Indeed it was only relatively recently that evidence of m6A methylation and its potential epigenetic roles in *Drosophila* came to light (Zhang et al. 2015). Unregulated expression of Dam has been found to be toxic, although the basis of this is not fully understood. Thus, DamID necessitates a very low expression of the Dam, achieved by exploiting a basal or ‘leaky’ promoter of transcription (van Steensel and Henikoff 2000). Another strategy makes use of a bi-cistronic construct where Dam is inserted as second open reading frame (ORF) and the expression relies on translational re-initiation between the ORFs (Kozak 2001; Luukkonen, Tan, and Schwartz 1995; Southall et al. 2013). This is the strategy that was utilised in this work.

DamID is becoming a versatile tool in studying protein-DNA interactions and mechanisms of gene regulation (Aughey, Cheetham, and Southall 2019). With recent advances, spatial and temporal control to the system has also been made possible by utilising the sophisticated genetic tools available in *Drosophila*. Accordingly, targeted DamID has allowed for cell-specific profiling of protein-DNA binding without the need for cell isolation (Figure 3.2). This was introduced by Southall et al. (2013) who first performed a cell-specific DamID or ‘targeted

DamID' in *Drosophila* neuroblast and neuroepithelial cells (Southall et al. 2013). The analysis not only provided insights into the transcriptionally active regions of the genome, but also, allowed for differential gene expression analysis between the two different cell types. This strategy provides a powerful method to obtain readouts of cell-specific transcription.

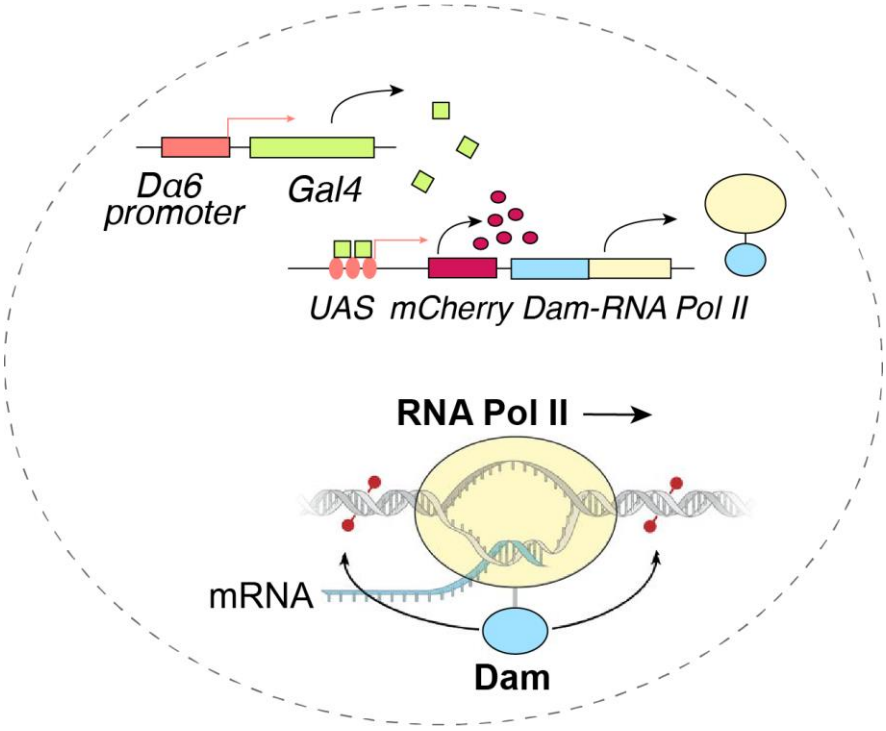

Figure 3.2 Application of targeted DamID for transcriptional analysis

A *Dα6* promoter drives the expression of GAL4 in cells that normally express *Dα6*. GAL4 binding to its UAS leads to the transcription of a bi-cistronic construct with mCherry as the first ORF and Dam fused to RNA Pol II as the second. Translation of Dam-RNA Pol II is greatly reduced, relying on ribosome re-initiation of the second ORF. The RNA Pol II fused to Dam transcribes genes normally expressed in *Dα6* expressing cells and Dam methylates GATC motifs in close proximity of RNA Pol II binding. Methylated DNA regions can be isolated and amplified for whole genome sequencing.

3.1.4 Chapter overview

Chapter 2 identified negative cross-resistance relationships between neonicotinoids and spinosad in *Drosophila* strains carrying mutations in the nAChR Dα1 and Dα6 subunits. In order test whether this negative cross-resistance is due to compensation at the transcript level, DamID was used to

examine the level of RNA Pol II binding to the nAChR subunit genes in larval cells that normally express *Dα6* in mutants for these two genes. While nAChR compensation may occur at other levels (e.g. the post-translational level), the use of target DamID provides a unique opportunity to examine changes in the level of the initiation of transcription across the genome in cells lacking the function of a specific nAChR subunit. It is possible that changes in the expression of genes other than the nAChR subunit genes may confer negative cross-resistance. A broader RNAseq analysis on *Dα1*, *Dα2* and *Dα6* mutant larvae also allows both this and the compensation hypothesis to be tested.

3.1.4.1 Research questions

This chapter will answer the following research questions:

1. What are the nAChR subunit gene expression changes in backgrounds that have the negative cross-resistance phenotype?
2. How does nAChR subunit expression change and does it support the nAChR compensation hypothesis for negative cross-resistance?
3. What functional pathways are affected in the mutants?
4. Do the findings from different transcriptional analyses (RNAseq and Targeted DamID) performed correlate with each other?

3.2 Materials and Methods

3.2.1 Fly strains

All stocks were reared on standard fly food at 18 °C or 25 °C. For RNA sequencing of whole larvae, the mutant strains for Dα1 (*Dα1*$^{\Delta DH}$), Dα2 (*Dα2*$^{\Delta(3)4E}$) and Dα6 (*Dα6*^{KO}) were analysed in comparison to the background control *wAC9* (Section 2.2.1). Fly strains containing a UAS-LT3-NDam (UAS-Dam-only) or UAS-LT3-NDam-RpII215 (UAS-Dam-RNA Pol II) construct on either chromosome II or III were obtained from the Andrea Brand lab, Cambridge, UK (Southall et al. 2013). The flies were crossed into the background the *Dα1* mutant, *Dα1*^{EMS1} and the *Dα6* mutant, *Dα6*^{EMS6} as well as the genetic background control strain, *Armenia*^{14} (Section 2.2.1).

A previously published GAL4 driver strain that contains an enhancer element from the proximal region of the *Dα6* gene locus, *Dα6>GAL4* was used to drive Dam expression (Perry et al. 2015). The *Dα6>GAL4* driver rescues the phenotype of a loss of Dα6 when used to express the wildtype Dα6 subunit in a knockout strain (Perry et al. 2015). A strain expressing GAL80 under the control of tubulin promoter, *tub*>GAL80^{ts} was similarly crossed into the background of *Dα1*^{EMS1}, *Dα6*^{EMS6} and *Armenia*^{14} to allow for temporal control of the GAL4 expression. The fly strains generated through fly crossing are listed in Table 3.1.

Table 3.1 *Drosophila* strains generated for targeted DamID experiment

Strain	Genotype
Control UAS-Dam-only	*w*^{1118}*; UAS-LT3-NDam; Armenia*^{14}
Control UAS-Dam-RNA Pol II	*w*^{1118}*; UAS-LT3-NDam-RpII215; Armenia*^{14}
Dα1^{EMS1} UAS-Dam-only	*w*^{1118}*; UAS-LT3-NDam; Dα1*^{EMS1}
Dα1^{EMS1} UAS-Dam-RNA Pol II	*w*^{1118}*; UAS-LT3-NDam-RpII215; Dα1*^{EMS1}
Dα6^{EMS6} UAS-Dam-only	*w*^{1118}*; Dα6*^{EMS6}*; UAS-LT3-NDam*
Dα6^{EMS6} UAS-Dam-RNA Pol II	*w*^{1118}*; Dα6*^{EMS6}*; UAS-LT3-NDam-RpII215*
Control *Dα6>GAL4* driver	*Dα6>GAL4; tub-GAL80*^{ts}*; Armenia*^{14}
Dα1^{EMS1}*Dα6>GAL4* driver	*Dα6>GAL4; tub-GAL80*^{ts}*; Dα1*^{EMS1}
Dα6^{EMS6} *Dα6>GAL4* driver	*Dα6>GAL4; Dα6*^{EMS6}*; tub-GAL80*^{ts}

3.2.2 RNA extraction

RNA extraction was performed on samples containing dissected tissue or whole larvae. Samples were homogenised in TRIsure (Bioline) for at least 5 minutes. RNA was extracted using 0.2 volumes of chloroform and then precipitated using 1 volume of isopropanol, following manufacturer's instructions. The RNA pellet was washed with 75% ethanol before being resuspended in RNase-free water (Sigma). To remove DNA traces, RNA was treated with RQ1 RNase-free DNase (Promega) and the reaction was stopped using RQ1 Stop solution (Promega). Sample quality was tested by running a 1% agarose gel electrophoresis. RNA purity was evaluated using a Nanodrop spectrophotometer. RNA concentration was quantified using a Qubit 2.0 fluorometer (Thermo Fisher).

3.2.3 RNAseq and analysis

Flies were allowed to lay eggs on a fresh juice plate over a 3-hour laying period. Eggs were left at 25 °C overnight and hatched larvae were cleared the next morning. Freshly hatched larvae over a 3-hour hatching period were collected into new plates to synchronise the larval development stage and after 5 hours, 100 first instar larvae (5 to 8 hours old) were flash-frozen in liquid nitrogen. RNA was extracted as described in the previous section. Library preparation and Illumina sequencing were carried out by Novogene Bioinformatics Technology in Singapore.

For analysis, reads were aligned to the *Drosophila* genome and exons using Tophat2 (Kim et al. 2013). Reads representing gene transcripts were counted using HTSeq (Anders, Pyl, and Huber 2015), and transcript per kilobase per million (TPM) was calculated for gene expression levels. Differential expression analysis was performed using DESeq2 (Anders 2010) and for significant DEGs, adjusted *p*-value was set to $p < 0.05$. Functional gene ontology (GO) enrichment analysis of the DEGs was performed using the Database for Annotation, Visualisation, and Integrated Discovery (DAVID) online tool (https://david.ncifcrf.gov) with a cut-off *p*-value set to $p \leq 0.05$.

3.2.4 Targeted DamID

3.2.4.1 DNA extraction

UAS-Dam-only or UAS-Dam-RNAPolII male flies were crossed to the GAL4 driver females containing GAL80^{ts} for the respective nAChR mutant backgrounds (Table 3.1). The experimental crosses were maintained at 25°C. For egg collection, flies were allowed to lay eggs on a fresh juice plate over a 4-hour laying period to synchronise embryo development. Eggs were then collected and transferred into vials containing standard fly media. Eggs were left to hatch, and larvae were reared at 18°C (restrictive temperature) for 6 days. Larvae were then shifted to 29°C (permissive temperature) for 24hr before dissection. For each sample, 50 brains of third instar larvae were dissected into 1X PBS (phosphate buffered saline, Sigma) and stored at -80°C until ready to be processed. Three replicates of each biological sample were prepared.

Genomic DNA was extracted using pre-made cetyltrimethylammonium bromide (CTAB) extraction buffer (50 mM Tris pH 8.0, 20 mM EDTA, pH 8.0, 1.1 M NaCl, 0.4 M LiCl, 1% CTAB, 2% PVP40, 0.5% Polysorbate TWEEN® 20, 0.2% β-mercaptoethanol). Briefly, the tissue sample was homogenised in CTAB extraction buffer. Proteinase K (Bioline) was added to digest contaminating proteins and then, the sample was treated with RNase A (Thermo Fisher) to remove RNA traces. The mixture was centrifuged at maximum speed for 5 minutes and supernatant was transferred into a fresh tube. Following addition of 1 volume of phenol:chloroform:isoamyl alcohol mixture (Sigma) and centrifugation at maximum speed for 5 minutes, the top aqueous phase containing DNA was transferred into a fresh tube. DNA was precipitated using 1 volume of isopropanol and washed with 75% ethanol. The DNA pellet was resuspended in TE buffer (10mM Tris HCl pH 8.0, 0.1mM EDTA pH 8.0).

3.2.4.2 Methylated DNA processing

Dam-methylated DNA was processed and amplified as previously described (Marshall et al. 2016). Briefly, the DNA sample was digested with DpnI (NEB) overnight. Digested DNA was then purified using a Qiagen PCR Purification kit

following manufacturer's instructions. Up to 750 ng of the purified DNA was used for DamID adaptor ligation reaction. Complementary DamID adaptor oligos (50 µM AdRtop, 50 µM AdRbtm; Integrated DNA Technologies, IDT) were hybridised with an incubation at 95°C which was left to cool down to room temperature. The double-stranded adaptors were ligated to the previously purified DNA sample using T4 DNA Ligase (NEB). The ligated sample was then digested with DpnII (NEB). The DNA fragments were amplified by polymerase chain reaction (PCR) using MyTaq™ DNA Polymerase (Bioline) and DamID-PCR primers (IDT) as detailed in the published protocol (Marshall et al. 2016). Amplified fragments were again purified, and the adaptor sequences were removed by performing AlwI (NEB) digestion. Compared to the original protocol, the DNA sample here was not further fragmented to a mean size of 300bp, thus the final fragments concentrated between 200bp to 1,500bp. Finally, the DNA fragments were size selected using Agentcourt AMPure XP magnetic beads (Beckman Coulter) before library preparation. Sample quality was tested by running an agarose gel electrophoresis. DNA concentration was quantified using Qubit 2.0 fluorometer (Thermo Fisher).

Table 3.2 Adaptors and primers for targeted DamID

Primer	Sequence (5' to 3')	Use
AdRtop	CTAATACGACTCACTATAGGGCA GCGTGGTCGCGGCCGAGGA	DamID adaptors
AdRbtm	TCCTCGGCCG	
DamID-PCR	GGTCGCGGCCGAGGATC	DamID PCR
DamChk_Fwd	AACGGCCTGTGTCGTTACAA	Check *UAS-LT3-NDam* construct
DamChk_Rvs	CCACCTTTTTACGTGTGCCG	
DamPolChk_Fwd	GGACGAACTGCTGGCTTTGTA	Check *UAS-LT3-NDam-RpII215* construct
DamPolChk_Rvs	TTGGATTGTGTGGCGAGACC	

3.2.4.3 Library preparation and sequencing

DNA libraries were prepared using the TruSeq Nano DNA LT Library Prep kit (Illumina) with the 24-barcode kit according to the manufacturer's instructions, apart from the following modification; adaptor enrichment was performed using six cycles of PCR. Libraries were then run on a 5400 Fragment Analyser system

(Agilent) with the High Sensitivity NGS Fragment kit for quality check. 18 indexed libraries were pooled and run with single-end 86bp reads on a NextSeq 550 System (Illumina) with the high-output option to yield at least 400 million reads. The read output numbers that were returned from the DNA sequencing are listed in Table 3.3.

Table 3.3 Amount of reads from targeted DamID sequencing and percentage of read mapped to the reference genome

Sample	Sample ID/ replicate	Read output	Percentage of mapped reads (%)
Control Dam-only	WTC1	32,110,418	94.04
	WTC2	37,281,013	92.03
	WTC3	28,501,695	95.18
Control Dam-RNA Pol II	WTP1	25,000,303	91.38
	WTP2	30,282,821	92.91
	WTP3	27,052,004	91.33
Dα1^{EMS1} Dam-only	A1C1	32,249,348	94.91
	A1C2	31,981,343	94.68
	A1C3	19,395,969	94.08
Dα1^{EMS1} Dam-RNA Pol II	A1P1	22,757,427	70.02
	A1P2	27,308,463	92.69
	A1P3	28,789,626	91.81
Dα6^{EMS6} Dam-only	A6C1	28,475,873	94.55
	A6C2	35,742,737	94.53
	A6C3	31,541,881	94.84
Dα6^{EMS6} Dam-RNA Pol II	A6P1	26,689,475	94.74
	A6P2	31,806,534	95.11
	A6P3	32,317,864	94.66

3.2.4.4 Analysis

FASTQ sequence read files were processed using the damidseq_pipeline Perl script (https://owenjm.github.io/damidseq_pipeline) to generate log2 binding ratio of Dam-RNAPolII/Dam-only and GATC bedgraph as reported previously (Marshall and Brand 2015). Each data set replicate was analysed separately using *Drosophila* genome annotation release 6.17. To test for the consistency between the biological replicates, the generated bedgraphs were compared via Pearson's correlation and a single outlier (with a correlation less than 0.80 between biological replicates) was removed from downstream analysis (Figure 3.3). RNA Pol II-binding enrichment sites were called using the polii.gene.call Perl script (https://github.com/owenjm/polii.gene.call) where each gene transcript was assigned a mean ratio between the biological replicates and a false discovery rate (FDR). FDR threshold of less than 0.05 was set for a significant RNA Pol II-binding enrichment.

A differential expression analysis was conducted using an R package, NOIseq (Tarazona et al. 2015). The Dam-RNA Pol II/Dam-only ratio sets were input into NOIseq-real using the option for upper quartile normalisation. The R script used for this is attached in the Appendix 2. For significant DEG, the probability threshold was set to $q \geq 0.9$. The output was scripted to include a list of significant downregulated and upregulated DEGs with corresponding log2 fold change compared to the control, *Armenia*[14].

GO enrichment analysis of the DEGs was performed using the DAVID online tool with $p \leq 0.05$. Identification of over-represented DNA motifs for transcription factor (TF) binding was performed using Clover tool (Frith et al. 2004). Essentially, sets of promoter sequence (up to 1,000bp upstream of the transcription start site) of the DEGs were extracted using BioMart online tool (https://asia.ensembl.org) and scored for the presence of TF motifs listed on TRANSFAC database (Wingender et al. 1996). For significant overrepresented motifs in the promoter set, the *p*-value was set to $p \leq 0.01$.

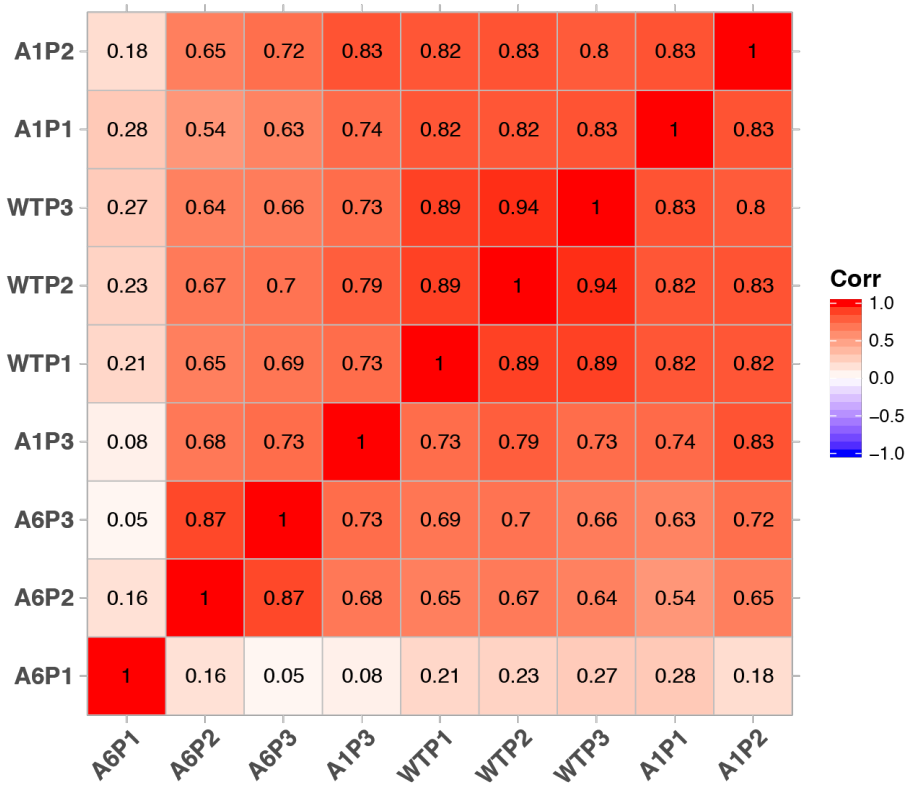

Figure 3.3 Pearson's correlation of Dam-RNAPolII/Dam-only bedgraph files generated for each sample replicate

Only A6P1 was identified as an outlier with correlation below 0.8 between the biological replicates, and thus, excluded from downstream analysis.

3.2.5 Reverse transcription and quantitative real-time PCR

30 brains from third instar larvae were dissected out for RNA extraction (Section 3.2.2). Total RNA up to 2 µg was reverse transcribed to cDNA using GoScript Reverse Transcription System (Promega), following manufacturer's instructions. Quantitative real-time PCR, qPCR was performed with at least three replicates of a 12 µL reaction containing diluted cDNA, 250nM of gene-specific primers and QuantiTect SYBR® Green PCR Master Mix (Qiagen), on a CFX384 Real-time PCR Detection System (Bio-Rad). The samples were subjected to a standard thermal profile: 95 °C for 5 minutes followed by 40 cycles of 95 °C for 10 seconds and 60 °C for 30 seconds. Primer oligos (IDT) used in the study are listed in Table 3.4.

Table 3.4 Primers for real-time qPCR

Gene	Name	Sequence (5' to 3')
nAChR Dα1	Da1 RT F 511	CGCTTAGAGACGTTCCGTTC
	Da1 RT R 511	ATGGTTCGAAGCAATTCCAG
nAChR Dα2	Da2 RT F 0112	AAGTGGGATCCCTCGGAGTA
	Da2 RT R 0112	TGCCGGTATAGTGGAGGATG
nAChR Dα3	Da3 RT F3	GGAAGAGGAGAGCACAAGGG
	Da3 RT R3	AAGATCCACAGGAACAGGCG
nAChR Dα4	Da4 RT F 0712	ACCGTGCATGGGAATATCAT
	Da4 RT R 0712	CCAGCAAAGGAACAACCAAT
nAChR Dα5	Da5 RT ex2 F	CAGCACGCAAATATTAAACGG
	Da5 RT ex3 R	TTTTCATGATATCCTGCTAGGC
nAChR Dα6	Da6 L1	CAATATCTGGCTCCCAAACC
	Da6 R1	TCGTGAAGAGCGTGAAAACAA
nAChR Dα7	Da7 L1	CCCACCAGCCCACATATTAC
	Da7 R1	AATGTCGCTTGTTTCGTCCT
nAChR Dβ1	Db1 R1	AAATCTCGATGATGCGATCC
	Db1 L1	GAGTTCATTGCCGAGCACTT
nAChR Dβ2	Db2 25/8/10 F	GAGCAATGGGTACACCAACG
	Db2 25/8/10 R	GCAGCACTTCGGGTGTTAAG
nAChR Dβ3	Db3 8/10 RT F	CCGTACATCCGAAACAAAGG
	Db3 8/10 RT R	GAAGTCAGCCCCATAAGAAGC
CG13220	CG13220_RT_F	TGGGCAGTGCCTTCTACATTT
	CG13220_RT_R	CGTACGCACCTCGCTTGTT
Rpl11	RpL11_RT_F	CGATCCCTCCATCGGTATCT
	RpL11_RT_R	AACCACTTCATGGCATCCTC
Pcd	RZ_Pcd_FW	CAGCAACGAGTAGAAGCCTGT
	RZ_Pcd_RV	GCGCGTTCCTGTTCGTTTAG
CG43324	RZ_CG43324_FW	CATCAACTTGCAGCTACGGC
	RZ_CG43324_RV	CGCGAAACGGATTCACCTTC
CG13227	RZ_CG13227_FW	GCGGTGGTTTCCAGAGAACT
	RZ_CG13227_RV	TGGGGCAGCACAAAAGAAGT
CG17272	RZ_CG17272_FW	ACATTGATGAGTTCCGTGAGTG
	RZ_CG17272_RV	ATGATGTCCAGGAAGTCGGC
Ocho	RZ_Ocho_FW	GTCGAAGCGAGAACATCCCA
	RZ_Ocho_RV	GAAGAATTGACCGAGCAGCG
Trip1	RZ_Trip1_FW	ACCATCATCACAGGTCACGATAA
	RZ_Trip1_RV	GCACATCAGGGACTCCGAAT

Primer specificity was determined using melting curve analysis. Standard curve was generated to ensure high amplification efficiencies for each primer set. All gene expressions were normalised to two reference genes, *CG13220* and *Rpl11* using standard calculation method published previously (Taylor et al. 2019). The results were analysed using 'comparative ΔΔCt method' and presented as $2^{-\Delta\Delta Ct}$. Student's t-test was performed to test if the difference between two data sets is statistically significant. MIQE checklist of the qPCR analysis is provided in Appendix 3.

3.3 Results

3.3.1 RNAseq analysis of *Dα1*$^{\Delta DH}$, *Dα2*$^{\Delta(3)4E}$ and *Dα6*^{KO} first instar larvae

3.3.1.1 nAChR gene expression levels in *Dα1*$^{\Delta DH}$, *Dα2*$^{\Delta(3)4E}$ and *Dα6*^{KO}

To uncover transcriptional changes in nAChR mutants that showed negative cross-resistance, RNA sequencing (RNAseq) was performed on 5-8 hours old first instar larvae of the *Dα1*$^{\Delta DH}$, *Dα2*$^{\Delta(3)4E}$ and *Dα6*^{KO} mutants and compared to gene expression in the wildtype strain, *wAC9*. The expression of all 10 subunit genes was detected in the wildtype first instar larvae (Figure 3.4A). Most of the transcript levels observed here matched gene expression patterns reported for first instar larvae in the Flybase (Graveley et al. 2011). Notably, the larvae expressed a high level of *Dβ1* and very low levels of *Dα3* and *Dβ3*.

Differential expression analysis was performed using DESeq2 to identify genes that are differentially expressed in the nAChR mutants compared to the wildtype control (Figure 3.4B). Looking at the nAChR gene expression in *Dα1*$^{\Delta DH}$ strain, *Dα7* and Dβ1 mRNA levels were significantly downregulated (log2FC of -0.28 and -0.16, respectively). In *Dα2*$^{\Delta(3)4E}$, *Dα2* mRNA level was significantly reduced (log2FC of -0.70), which can be attributed to the mutation in the gene. In addition, *Dα6* transcript was 1.2-fold upregulated, while *Dα7* transcript was 1.1-fold downregulated in *Dα2*$^{\Delta(3)4}$ strain (log2FC of 0.30 and -0.15, respectively). *Dα6* mRNA level was greatly downregulated in *Dα6*^{KO}, (log2FC of -2.17) due to the null mutation of the *Dα6* gene. Significant downregulation of *Dα5 and Dα7* mRNA expression were also observed in *Dα6*^{KO} strain (log2FC of -0.86 and -0.27, respectively).

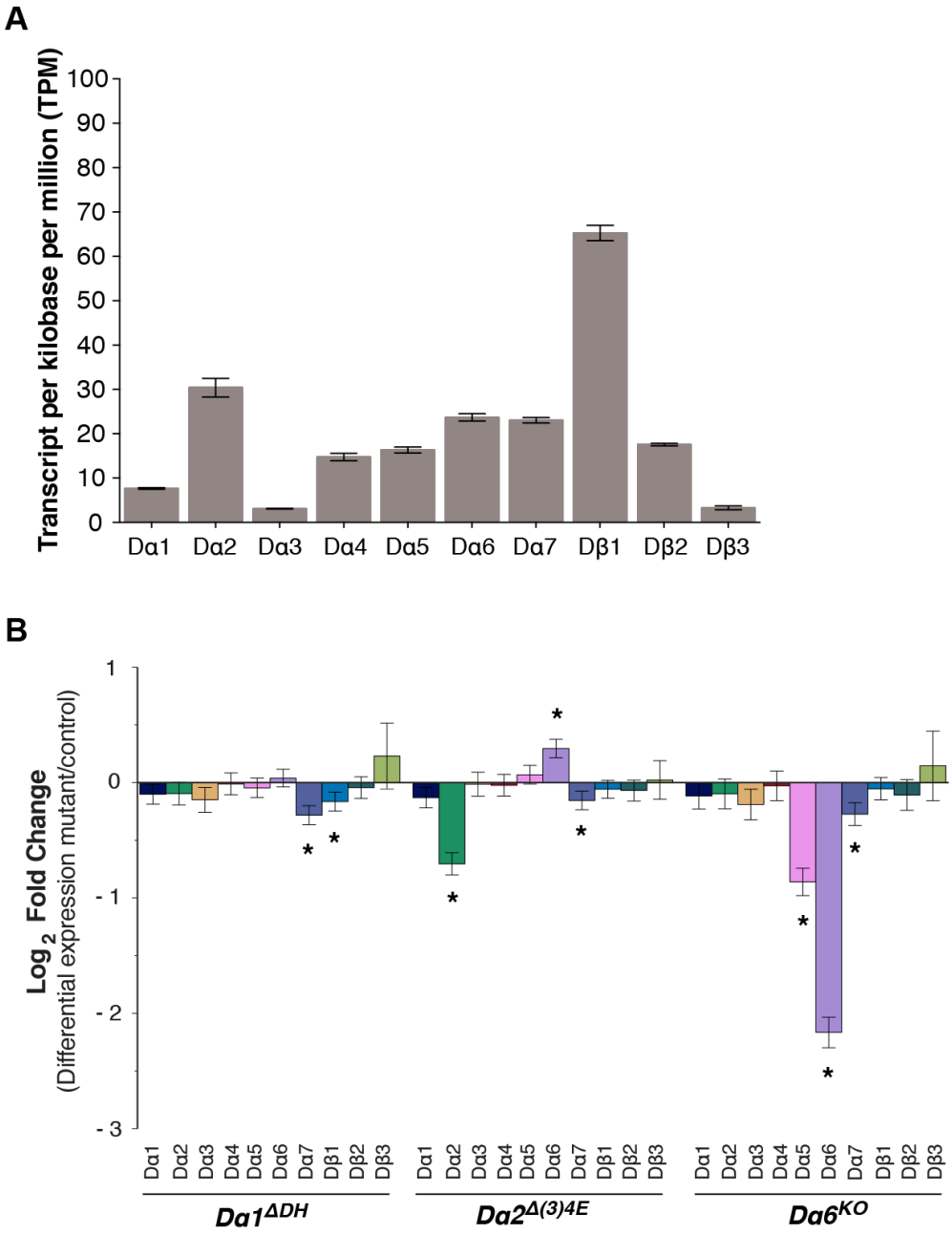

Figure 3.4 Analysis of receptor subunit transcript expression in nAChR mutants exhibiting negative cross-resistance

RNAseq was performed using RNA extracted from whole first instar larvae. (A) Histogram representing relative transcript expression levels of ten nAChR subunit genes in the wildtype strain, *wAC9*. (B) Differential expression of nAChR subunit genes in nAChR mutants, *Dα1*$^{\Delta DH}$, *Dα2*$^{\Delta(3)4E}$ and *Dα6*^{KO} compared to the wildtype strain. Log2 fold change values were plotted and error bars indicate standard error values. Statistical significance was measured by Benjamini-Hochberg adjusted *p*-value from the DESeq2 analysis, where asterisk (*) denotes $P < 0.05$.

Note that *Dα1*$^{\Delta DH}$ and *Dα2*$^{\Delta(3)4E}$ alleles introduced a small deletion in the gene encoding Dα1 and Dα2 respectively, thus, the remaining coding region of the genes are still expected to result in positive transcript expression in the mutants (Appendix 4A-B)(Perry et al. manuscript in preparation). On the other hand, *Dα6*^{KO} allele is deleted for the entire coding region of the *Dα6* gene, with only parts of the 5'UTR and 3'UTR are outside the deletion region (Luong 2018). These regions, apparently, can still be picked up by the RNAseq, giving a positive *Dα6* transcript expression, hence, resulted in just 4.5-fold downregulation of *Dα6* mRNA in *Dα6*^{KO} that could have been higher in magnitude considering the null mutation (Appendix 4C).

3.3.1.2 GO enrichment analysis of DEGs identified in *Dα1*$^{\Delta DH}$, *Dα2*$^{\Delta(3)4E}$ and *Dα6*^{KO} mutants

Differential expression analysis on the RNAseq data identified 1,558 DEGs in the *Dα1*$^{\Delta DH}$ mutant; 913 genes were upregulated, and 645 genes were downregulated. The *Dα2*$^{\Delta(3)4E}$ mutant showed 815 DEGs with 447 upregulated genes and 368 downregulated genes. The *Dα6*^{KO} mutant had 1,096 DEGs with 766 genes that were upregulated and 330 genes that were downregulated. Identification of a larger number of DEGs in *Dα1*$^{\Delta DH}$ may be consistent with that observation that the *Dα1* mutant has more severe fitness cost compared to the other two mutants (Perry et al. manuscript in preparation). To better understand these gene expression changes, GO enrichment analysis was used to place these DEGs into functional groups. The analysis was performed using DAVID online, a functional annotation tool that assigned these genes GO terms for three categories; biological processes, molecular functions, and cellular components. GO terms significantly enriched based on the DEG sets ($p \leq 0.05$) are presented in Figure 3.5.

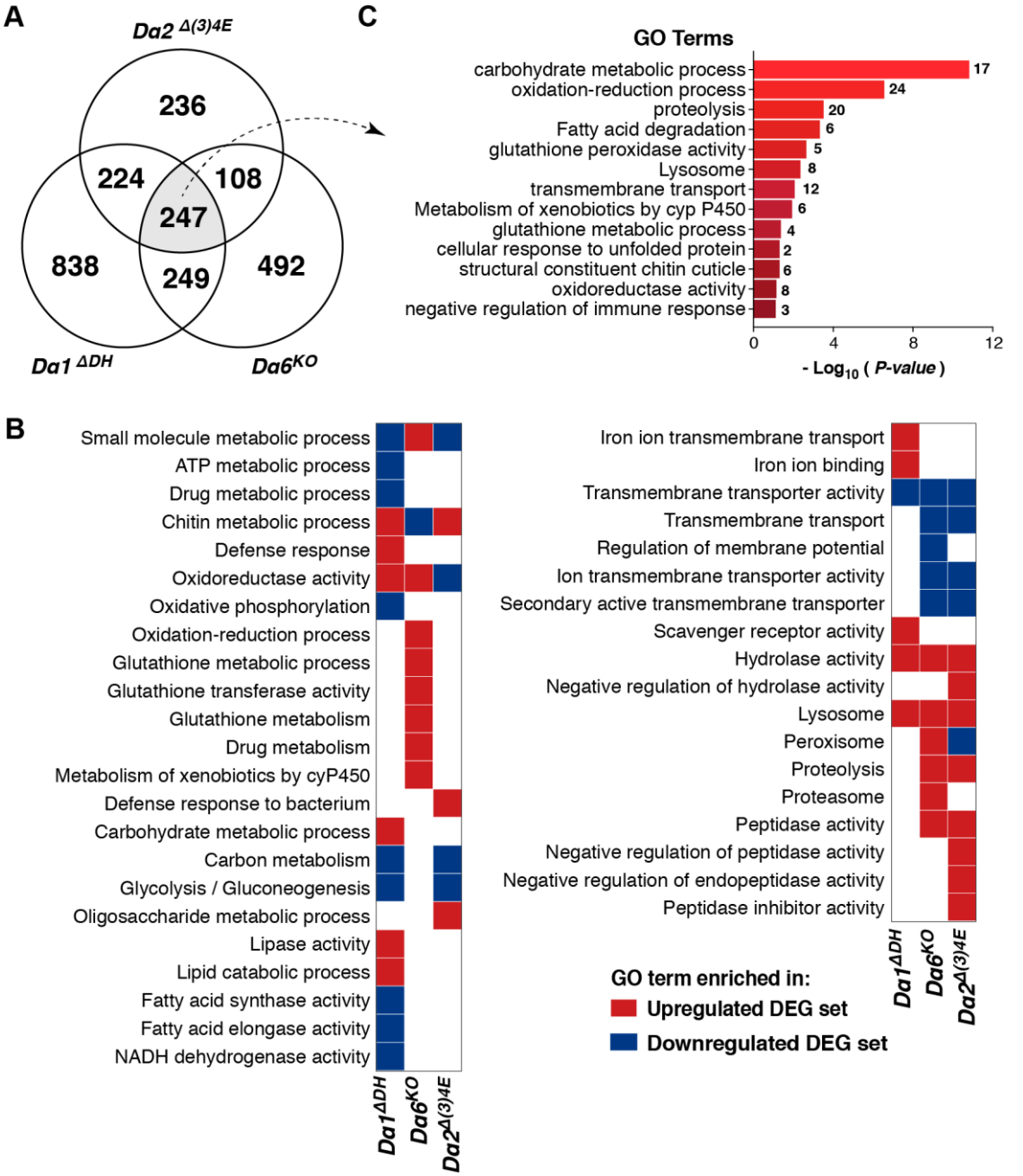

Figure 3.5 Gene ontology analysis of DEGS identified in nAChR mutants, *Dα1*$^{\Delta DH}$, *Dα2*$^{\Delta(3)4E}$ and *Dα6*^{KO}

(A) Venn diagram illustrating the number of DEGs identified in whole first instar larvae of the *Dα1*$^{\Delta DH}$, *Dα2*$^{\Delta(3)4E}$ and *Dα6*^{KO} mutants compared to the wildtype control. (B) Heatmap summarising GO terms enriched in upregulated or downregulated DEGs from each nAChR mutant. (C) Bar chart representing GO terms enriched in 247 DEGs commonly identified in all three mutants. Number of DEGs associated with the terms are listed next to each bar.

GO term enrichment analysis on these DEGs identified pathways that were similarly affected in all three mutants, including terms associated with transmembrane transporter activity, hydrolase activity and lysosomal pathway. In all three mutants, transmembrane transporter activity was enriched in the downregulated DEG sets, while both hydrolase activity and lysosome were enriched in the upregulated DEG sets (Figure 3.5B). DEGs associated with oxidoreductase activity were mainly enriched in upregulated DEG sets in *Dα1*$^{\Delta DH}$ and *Dα6*^{KO}, while enriched in downregulated DEG set in *Dα2*$^{\Delta(3)4E}$. Notably, GO terms associated with fatty acid and lipid metabolism were affected only in *Dα1*$^{\Delta DH}$, while terms associated with oxidative stress and proteolysis were affected mainly in *Dα6*^{KO} (Figure 3.5B). Terms associated with peptidase activity were only enriched in upregulated DEG set of *Dα2*$^{\Delta(3)4E}$. Interestingly, some of these DEGs were commonly identified among the three mutants (Figure 3.5A). Narrowing down the analysis, 247 common DEGs between *Dα1*$^{\Delta DH}$, *Dα2*$^{\Delta(3)4E}$ and *Dα6*^{KO} showed enrichment for GO terms associated with oxidative stress, proteolysis, fatty acid metabolism, glutathione metabolism, lysosomal activity, transmembrane transport activity and regulation of immune response (Figure 3.5C).

3.3.2 Cell-specific transcriptional analysis of *Dα1*^{EMS1} and *Dα6*^{EMS6} using targeted DamID

3.3.2.1 RNA Pol II binding profile of *Dα6*-expressing cells

The transcriptional analysis on whole larvae may not have been sensitive enough to detect cell- or tissue-specific gene expression changes in the nAChR subunit mutants. Therefore, a cell-specific transcription analysis was conducted using targeted DamID and genome-wide DNA sequencing. This was performed on a different *Dα1* allele, *Dα1*^{EMS1} and *Dα6*, *Dα6*^{EMS6} that both have high levels of negative cross-resistance, in comparison to the wildtype control, *Armenia*^{14}. The analysis looked at RNA Pol II occupancy in cells that are expressing *Dα6* in larval brain (Figure 3.2 & 3.6A), taking into account that these cell-types are more likely to have been affected due to the nAChR subunit mutation, particularly in the case of the *Dα6* mutant. Dam protein fused to RNA Pol II was expressed using *Dα6>GAL4* driver and temporally regulated within a 24-hour period (early third instar to wandering third instar larval stages) using temperature-sensitive negative regulator of GAL4, GAL80^{ts} (Matsumoto, Toh-e, and Oshima 1978; McGuire, Roman, and Davis 2004). The 24-hour period of Dam expression is used to minimise saturation and/or toxicity of Dam activity for the analysis. Larval brains were extracted for methylated DNA and these regions were sent for DNA sequencing.

In total, 1,891 protein-coding genes with significant RNA Pol II occupancy were identified in the *Dα6*-expressing cells of *Armenia*^{14}, 1,754 genes in the *Dα1*^{EMS1} and 2,350 genes in the *Dα6*^{EMS6}. Among the genes that were significantly bound by Pol II are genes previously shown to be generally expressed in the larval brain (Figure 3.6A-B). Neuronal markers including *elav*, *CadN* and *nSyb* were significantly bound by RNA Pol II in all three strains, as anticipated since the cell types that are expressing *Dα6* would be expected to be of neuronal lineage (Figure 3.6Bi-ii). A trio of TFs that are important for mushroom body development (*dac, ey* and *toy*) were also significantly occupied by RNA Pol II, indicating expression of the subunit gene in the mushroom bodies (Figure 3.6Biii-v). Reassuringly, lack of RNA Pol II occupancy on glial markers such as *repo* and

nrv2 suggested that the *Dα6* is not expressed in glia cells and the expression is relatively specific to the targeted cells (Figure 3.6Ci-ii). This is consistent with the observation of a very low expression of nAChR genes in cells clustered as glia, in the previous single cell transcriptomic analysis (Croset et al. 2018).

Gene markers for different neuronal cell types including *VAChT* (cholinergic), *VGluT* (glutamatergic), and *Gad1* (GABAergic) were also significantly bound by RNA Pol II in all three strains (Figure 3.6Bvi-viii), indicating expression of the *Dα6* gene in these fast neurotransmitter-releasing neurons. In addition, significant RNA Pol II occupancy on *DAT*, *kek1*, *mub* and *ple* indicate possible *Dα6* expression in the dopamine releasing neurons (Figure 3.6Bix-x). Meanwhile, there was no or low RNA Pol II occupancy on *Tbh*, *tdc2*, *CG34113*, *SerT* and *Trh*, excluding *Dα6* expression in octopamine or serotonin releasing neurons (Figure 3.6Ciii-v). Positive RNA Pol II binding on motor neuron markers, *Futsch* and *Toll-6* (Sanyal, 2009) was also observed (Figure 3.6Bxi-xii). The analysis also identified significant RNA Pol II binding on genes that are mainly enriched in the salivary glands including *Sgs4, Sgs5, Sgs7, Sgs8,* and *ng1* (Furia et al. 1993; Lehmann 1996). It is possible that these genes are also being transcribed in the CNS, although, possible tissue contamination during sample collection cannot be ignored.

Looking at nAChR subunit genes which are anticipated to be expressed in these target cells, only *Dα1* and *Dβ1* were significantly occupied by RNA Pol II in all three strains (Figure 3.7A & G). Statistical analysis suggested that *Dα2*, *Dα5* and *Dα6* were significantly occupied in only $D\alpha6^{EMS6}$ (Figure 3.7A, D & E), while *Dβ3* was significantly occupied in the wildtype strain only (Figure 3.7H). Other nAChR subunit genes showed an RNA Pol II binding ratio and an associated FDR below than what was deemed significant for a positive RNA Pol II occupancy.

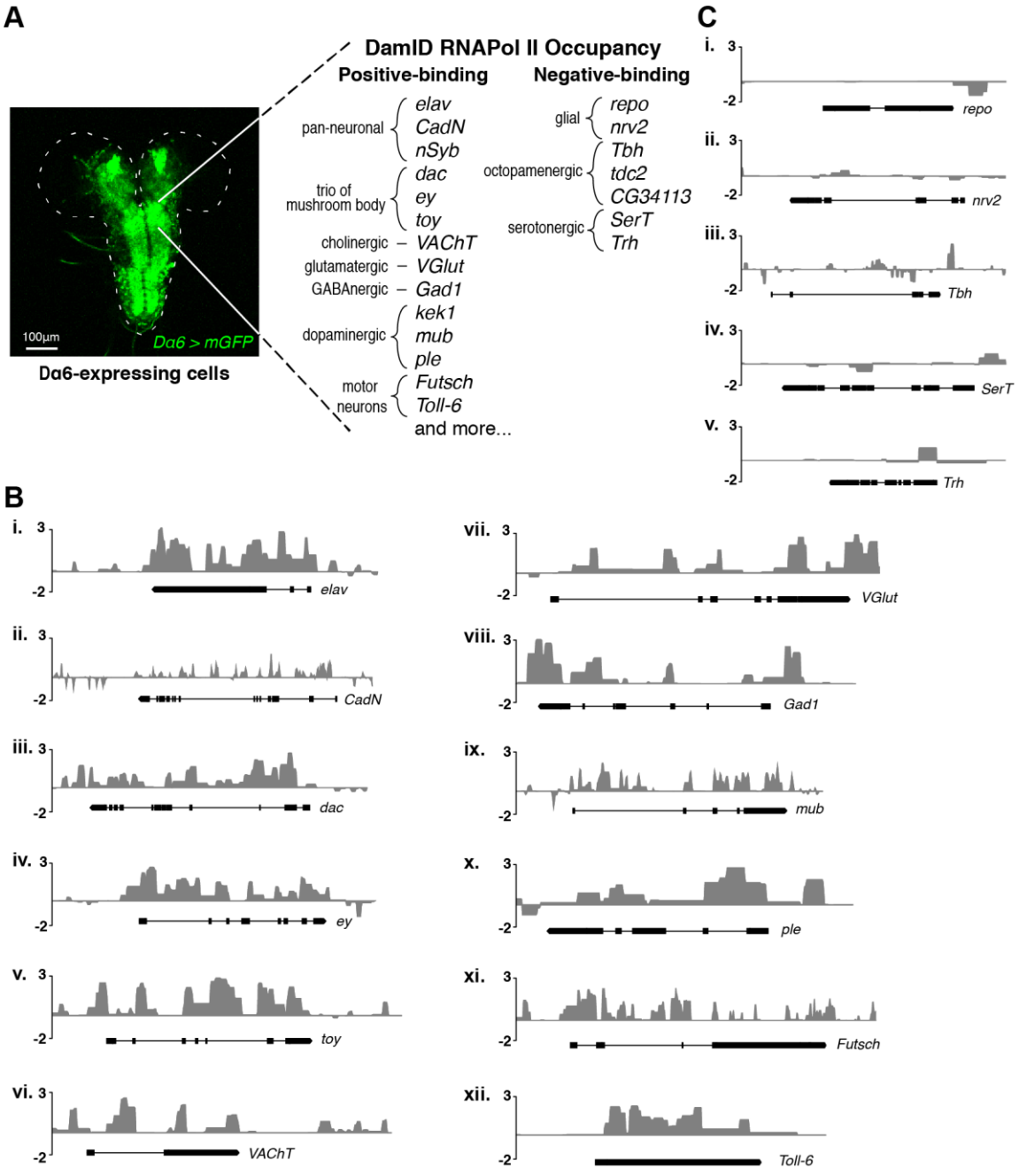

Figure 3.6 RNA Pol II occupancy in *Dα6*-expressing cells revealed co-expression of genes associated with different neuronal cell types

(A) *Dα6* promoter was used to drive Dam-RNA Pol II expression in the third instar larval brain for the targeted DamID analysis. Neuronal markers that are positively or negatively bound by Dam-RNA Pol II in *Dα6*-expressing cells were listed. (B-C) RNA Pol II occupancy/binding peaks on genes associated with neuronal cell type in the wildtype strain, *Armenia*[14]. Y-axis represents log2 ratio change between Dam-RNA Pol II and Dam-only (reference) samples.

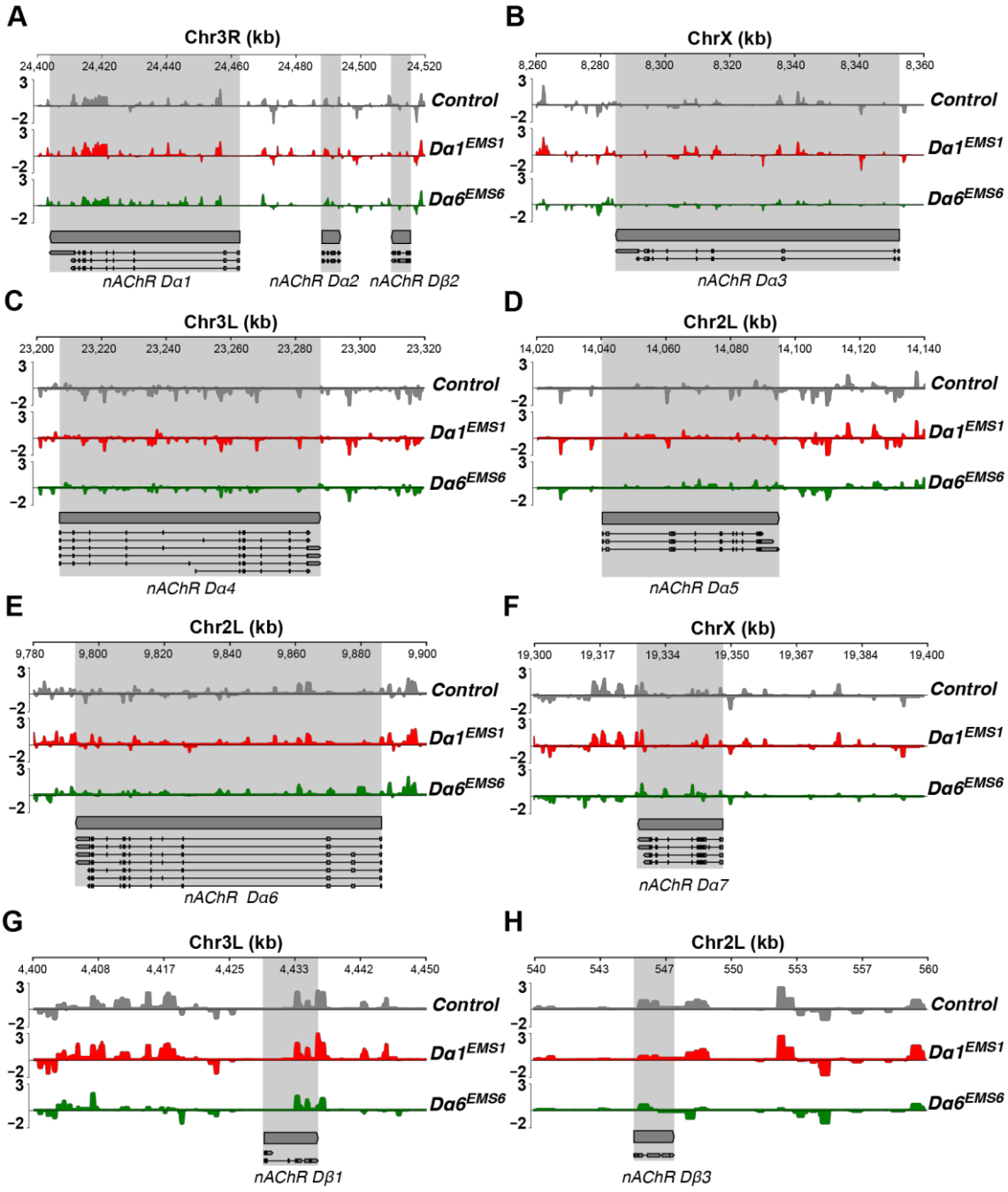

Figure 3.7 Differences in RNA Pol II occupancy on the nAChR subunit genes in neuronal cells of nAChR mutants

(A-H) RNA Pol II occupancy/binding peaks on ten *Drosophila* nAChR subunit genes in the mutants, *Dα1*^{EMS1} (red shading) and *Dα6*^{EMS6} (green shading) compared to the wildtype strain, *Armenia*^{14} (grey shading). Y-axis represent log2 ratio change between Dam-RNA Pol II and Dam-only (reference) samples. Respective gene annotation is indicated below, with all known transcripts illustrated to show exonic and intronic regions of the gene.

3.3.2.2 Differential analysis on RNA Pol II occupancy in nAChR mutants

To identify other genes that were specifically expressed or highly enriched in the mutant strains, RNA Pol II occupancy was compared between the mutants and the wildtype strain. Another R package that is commonly used for RNAseq analysis, NOIseq was adapted to perform the differential analysis following the logic that a DamID analysis on RNA Pol II occupancy would reflect a transcriptomic analysis using RNAseq. While this analysis was employed on a targeted DamID experiment, it is important to note that upregulated DEGs would correspond to genes that are preferentially bound by RNA Pol II in the mutant compared to the control strain. Conversely, the downregulated DEGs correspond to genes that are preferentially bound in the control compared to the mutant strain.

NOIseq probability cut-off was set at 90% ($q \geq 0.9$) for genes that differed significantly between the mutant and the control. The analysis identified 379 protein-coding DEGs in $D\alpha1^{EMS1}$, of which 275 genes were upregulated and 104 genes were downregulated in comparison to the wildtype (Figure 3.8A, List of DEGs is provided in Appendix 5). Meanwhile, of 1,717 protein-coding DEGs that were significant in $D\alpha6^{EMS6}$, 1,001 genes were upregulated and 716 genes were downregulated compared to the control (Figure 3.8B, List of DEGs is provided in Appendix 6). Importantly, none of the nAChR subunit genes were detected as differentially expressed by the statistical analysis.

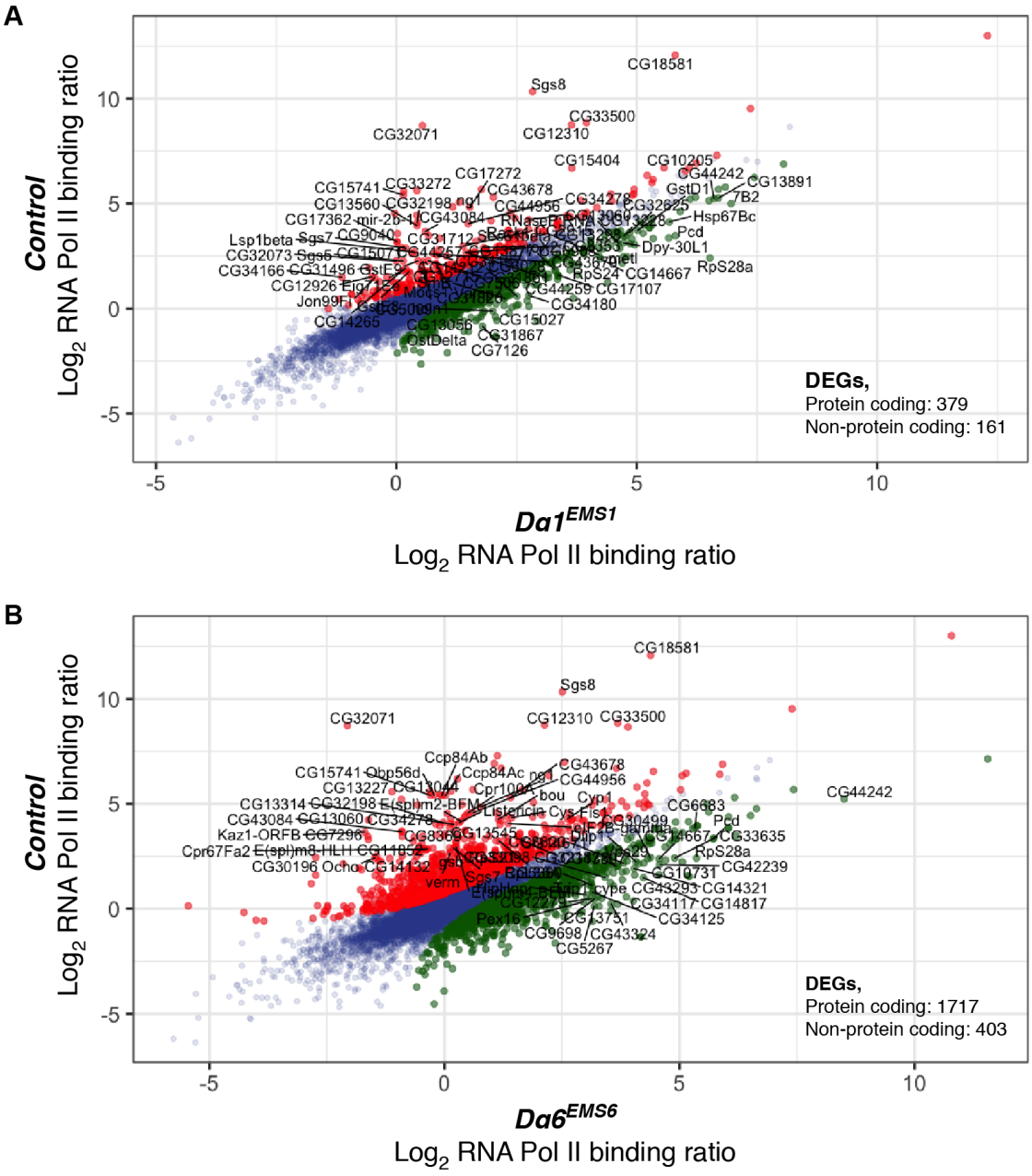

Figure 3.8 Differential analysis of RNA Pol II occupancy revealed dysregulated genes in *Dα6*-expressing neuronal cells of nAChR mutants

Scatter plots represent gene expression values signify by log2 of RNA Pol II occupancy in (A) $D\alpha1^{EMS1}$ and (B) $D\alpha6^{EMS6}$ as output by the NOISeq analysis. Significantly upregulated genes are highlighted in red while significantly downregulated genes are highlighted in green (probability, $q \geq 0.9$).

3.3.2.3 Validation of targeted DamID gene expression using qPCR

To validate the gene expression profile of the targeted DamID analysis, real-time qPCR was used to measure mRNA expression of selected DEGs in whole brains dissected from third instar larvae. Although, the targeted DamID was performed in the specific cells that are expressing *Dα6*, it was hoped that this analysis might be able to pick up some of the gene expression changes if the difference was significant enough. Initially, mRNA expression of the nAChR subunit genes were analysed. Matching this with the data from the targeted DamID, the expression levels of most of these subunit genes did not deviate significantly from the mRNA levels in the wildtype control. Importantly, no expression changes were recorded for *Dα1, Dα2* or *Dα6* genes (Figure 3.9A). This data therefore does not support the hypothesised nAChR compensation, at least at the transcriptional level. Significant upregulation of *Dα3, Dα5* and *Dβ3* transcript were observed in $Dα6^{EMS6}$, although the upregulation levels were less than 2-fold compared to the wildtype expression.

The mRNA expression levels for selected DEGs identified from the targeted DamID analysis were also analysed. Correlated mRNA expression changes in comparison to the preferential RNA Pol II occupancy were observed for some of these genes. For instance, significantly higher mRNA levels of *Pcd* and *CG43324* was recorded in $Dα6^{EMS6}$ mutant compared to the wildtype control, matching the upregulation from the targeted DamID analysis (Figure 3.9B-C). Similarly, significant upregulation of *CG13227* and downregulation of *CG17272* mRNA levels were recorded in $Dα1^{EMS1}$ mutant compared to the wildtype control (Figure 3.9B-C). We also observed an opposite gene expression profile from the two analyses. Several genes including *Ocho* and *Trip1* showed an opposite expression levels to the expression profile presented by the RNA Pol II occupancy data (Figure 3.9B-C). While *Ocho* appeared to be downregulated in $Dα6^{EMS6}$ in term of RNA Pol II occupancy, an increase in mRNA levels was observed in the whole brain of both mutant strains. *Trip1* is upregulated in $Dα1^{EMS1}$ based on targeted DamID analysis but reduced mRNA level was recorded from the whole brain analysis. These discrepancies could be explained by the differences in the cell types that the two analyses were based on. Analysis

of mRNA level from *Dα6*-expressing cells would better reflect the targeted DamID analysis.

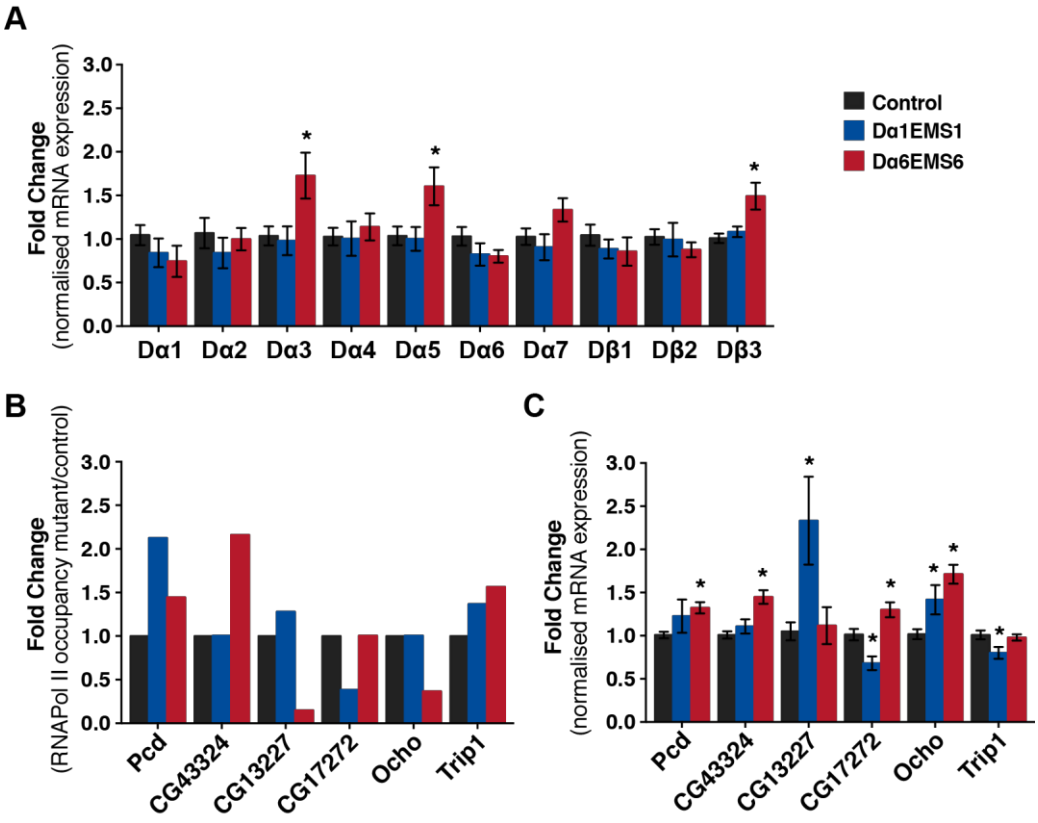

Figure 3.9 Gene expression verification using real-time qPCR

(A) Relative mRNA expression of nAChR subunit genes in third instar brain of $D\alpha1^{EMS1}$ and $D\alpha6^{EMS6}$ compared to the wildtype control. (B) Fold change in RNA Pol II occupancy of selected DEGs identified from the targeted DamID experiment. (C) Relative mRNA expression of the identified DEGs in third instar brain, measured using real-time qPCR. Relative mRNA expression values were normalised to reference genes, *CG13220* and *Rpl11*. Error bars indicate SEM with biological replicates, n > 5. Student's t-test was performed for statistical significance, where asterisk (*) denotes $P < 0.05$.

3.3.3 GO enrichment analysis on *Dα1*^{EMS1} and *Dα6*^{EMS6} DEGs

Among the DEGs identified from the targeted DamID analysis, 274 of the DEGs were shared by the *Dα1*^{EMS1} and *Dα6*^{EMS6} mutants. There were 105 *Dα1*^{EMS1}-specific DEGs and 1443 *Dα6*^{EMS6}-specific DEGs (Figure 3.10A). Again, to better understand the differential RNA Pol II occupancy between the mutants, we looked for functional pathways that correspond to these DEGs using a GO enrichment analysis.

Analysis of the DEGs common to *Dα1*^{EMS1} and *Dα6*^{EMS6} revealed enrichment of GO terms involving translation, glutathione metabolic process, locomotion and reproduction (Figure 3.10C). Meanwhile, analysis of *Dα1*^{EMS1}-specific DEGs revealed enrichment of limited number of GO terms with notably functions in mitochondrial function, endomembrane system and lipid oxidation (Figure 3.10B). We observed many more GO terms for *Dα6*^{EMS6}-specific DEGs, as expected by the huge number of DEGs compared to the other sets. These genes were enriched for functions involved mainly in neuron development, protein folding, vesicle-mediated transport, lysosomal activity, endosomal transport, protein degradation and response to oxidative stress (Figure 3.10D).

Looking at upregulated and downregulated DEG sets separately, GO terms associated with translational process were enriched in upregulated DEG sets from both *Dα1* and *Dα6* mutant (Figure 3.11A). Again, we observed an enrichment of GO terms involved in glutathione metabolism that play important roles in antioxidant defence and xenobiotic metabolism, in the DEG sets of both mutants. Specifically, these terms were significantly enriched in the upregulated DEG set of *Dα1*^{EMS1} while in *Dα6*^{EMS6}, they were enriched in the downregulated DEG set (Figure 3.11A). The genes that were grouped under this term predominately belonged to the GST gene family (Figure 3.11B). In addition, genes involved in lipid metabolism were generally upregulated in both mutants (Figure 3.11A-B), while genes involved in oxidation-reduction processes were only affected in the *Dα6* mutant where they were mainly downregulated (Figure 3.11C).

Previously, the GO term associated with lysosomal activity was only enriched in *Dα6*^{EMS6}-specific DEGs, however, when upregulated and downregulated DEG sets were analysed separately, the GO term was significantly enriched in both the upregulated DEG sets of the *Dα1* and *Dα6* mutants (Figure 3.11A). Several genes associated with lysosome function were upregulated in *Dα6*^{EMS6} while few of these were also upregulated in *Dα1*^{EMS1} (Figure 3.11C). This can indicate oxidative stress or disturbance in normal redox state of cells that may also damage the protein and lipid environment. GO terms associated with protein maturation such as protein folding and transport, as well as protein degradation were generally enriched in the upregulated DEG sets in *Dα6*^{EMS6} and, indeed, these genes were generally upregulated in *Dα6*^{EMS6}, but not *Dα1*^{EMS1} (Figure 3.11A-C).

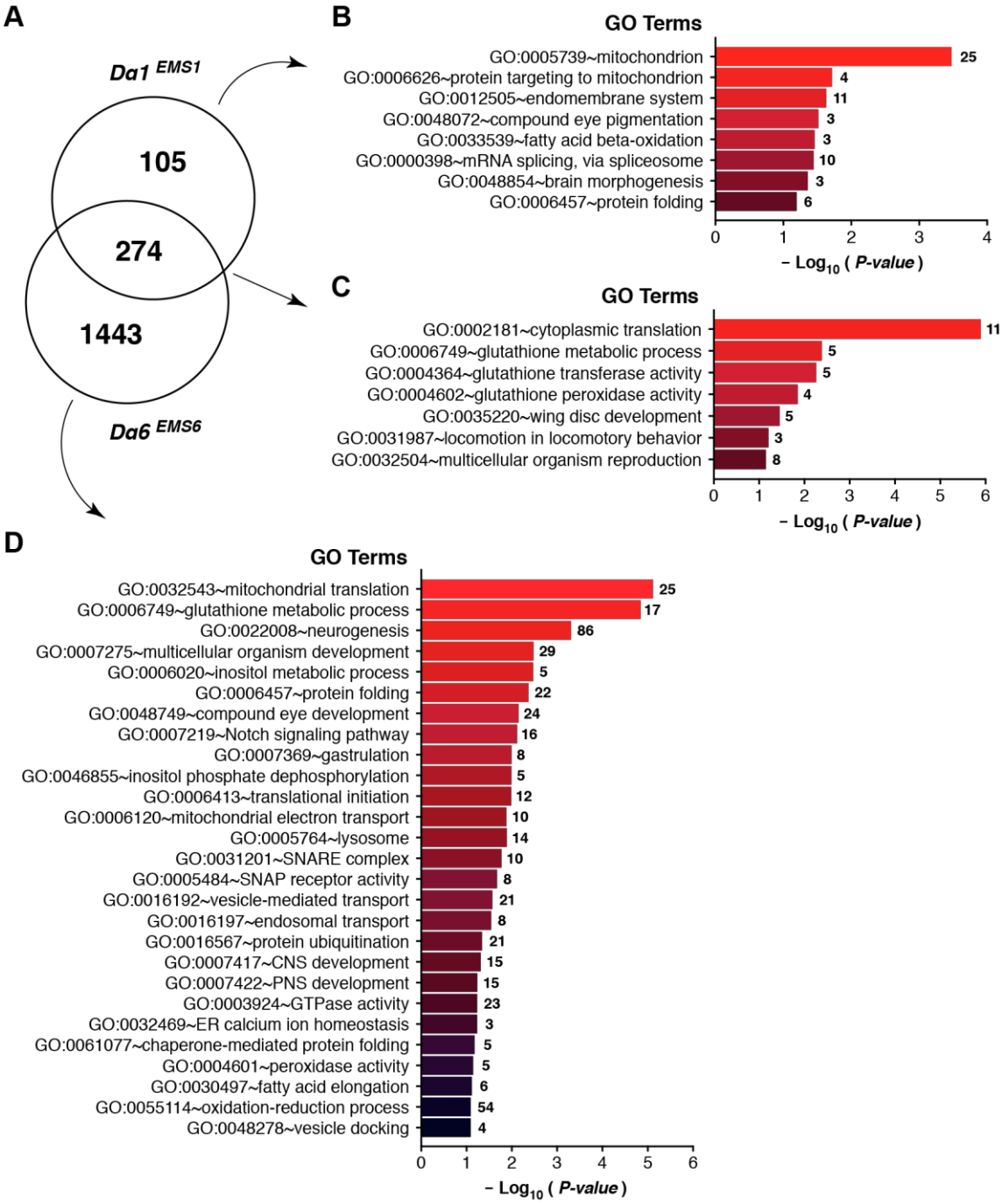

Figure 3.10 GO enrichment analysis of DEGs identified in *Dα6*-expressing neuronal cells of the nAChR mutants

(A) Venn diagram illustrating the number of DEGs identified in *Dα1*^{EMS1} and *Dα6*^{EMS6}, based on differential analysis of the RNA Pol II occupancy in *Dα6*-expressing cells of the third instar larval brain. Bar charts represent significant GO terms enriched in (B) *Dα1*^{EMS1}-specific DEGs, (C) overlapping DEGs, and (D) *Dα6*^{EMS6}-specific DEGs. The number of DEGs associated with the GO terms are listed next to each bar.

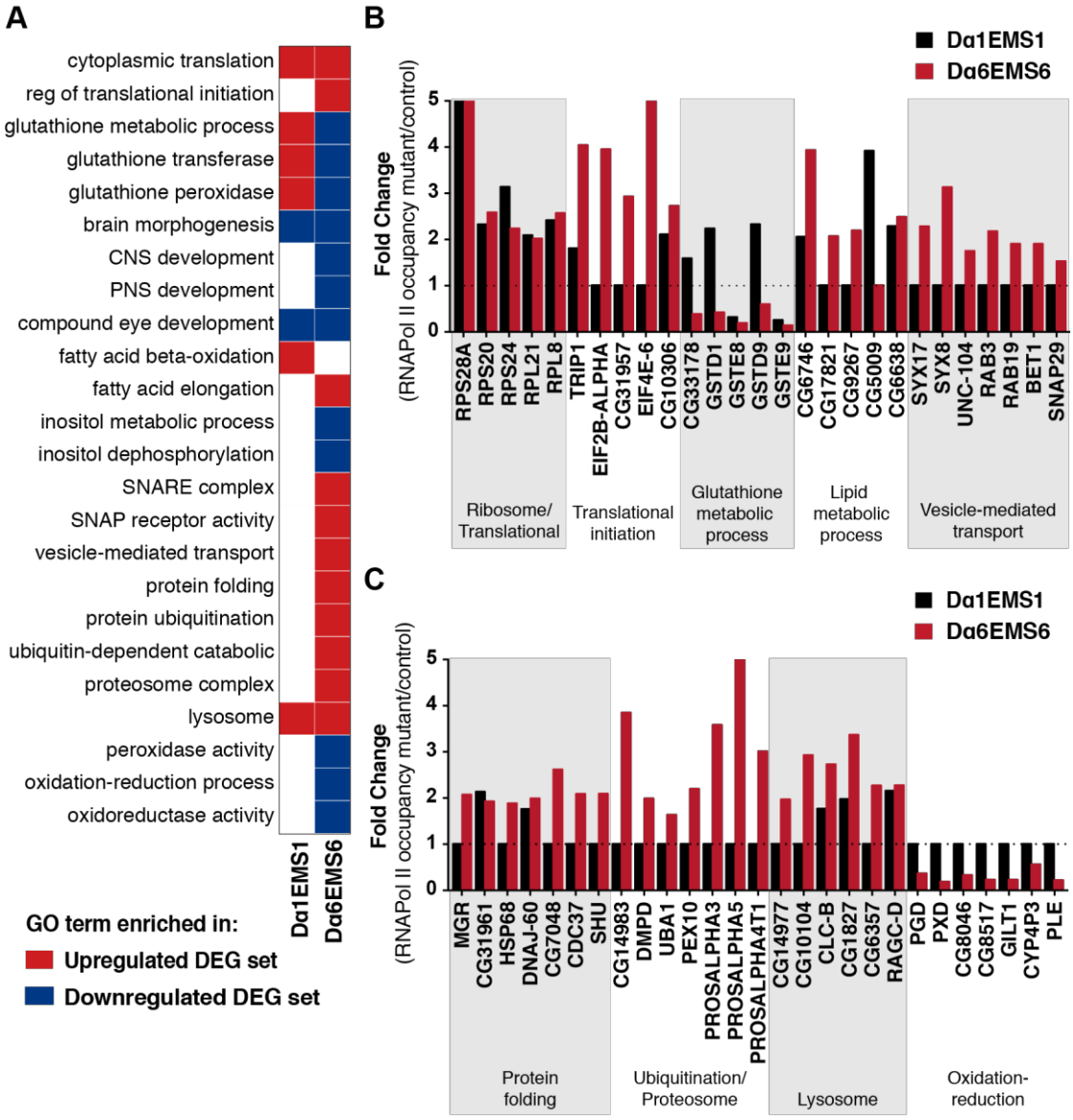

Figure 3.11 Differential RNA Pol II occupancy analysis revealed genes and associated GO terms that are upregulated or downregulated in *Dα6*-expressing neuronal cells of nAChR mutants

(A) The heatmap summarises GO term enrichment in the upregulated or downregulated DEG set of *Dα1*^{EMS1} and *Dα6*^{EMS6}. (B-C) Bar graphs represent the fold change in RNA Pol II occupancy of selected DEGs associated with the dysregulated functional pathways in the nAChR mutants.

3.3.4 Motif enrichment analysis on *Dα1*^{EMS1} and *Dα6*^{EMS6} DEGs

In order to identify TFs that were possibly mediating these gene expression changes, a motif overrepresentation analysis was performed on the promoter sequences of the DEG sets. A computational program called Clover was utilised to analyse these sets of promoter sequences and score for enrichment of recognised TF motifs in the sequences (Frith et al. 2004). This analysis identified a significant number of overrepresented motifs in the promoters of the *Dα1*^{EMS1} DEGS (Table 3.5) and *Dα6*^{EMS6} DEGs (Table 3.6). Common TF binding motifs overrepresented in both of the DEG sets include Br, Slp1, Pnr, Brk, BEAF-32, Mad, Mirr, and Ara which suggest involvement of the corresponding TFs in regulating the gene expression changes. More of these overrepresented motifs, belonging to Fkh, Cf2, Trl, Dl and Deaf1 binding sites, were detected in *Dα6*^{EMS6} DEGs' promoters. In looking for these TFs in the DEG sets, downregulation of *slp1, brk, BEAF-32, fkh* and *mirr* genes was found in the *Dα6* mutant, but not in the *Dα1* mutant (Figure 3.12A).

Table 3.5 Significantly overrepresented motifs in promoters (1 kb upstream of the transcriptional start site) of genes that were differentially expressed in *Dα1*^{EMS1}

Motif	Associated TF	Raw score[a]	*P*-value relative to background[b]	
			chromosome 2R	chromosome 3R
MA0013.1	Br (var.4)	123	<0.001	<0.001
MA0458.1	Slp1	102	<0.001	<0.001
MA0536.1	Pnr	81.8	<0.001	<0.001
MA0012.1	Br (var.3)	76.7	<0.001	<0.001
MA0213.1	Brk	65.9	0.001	0.009
MA0529.1	BEAF-32	62.6	<0.001	<0.001
MA0535.1	Mad	41.0	0.001	0.003
MA0233.1	Mirr	28.5	<0.001	<0.001
MA0210.1	Ara	17.1	<0.001	<0.001

[a] Raw score indicates random fragments matched to the target TF motif

[b] *P*-value is provided by the Clover program. $p<0.01$ indicates statistically significant enrichment of motifs in promoter sequences relative to background

Table 3.6 Significantly overrepresented motifs in promoters (1 kb upstream of the transcriptional start site) of genes that were differentially expressed in *Dα6*^{EMS6}

Motif	Associated TF	Raw score [a]	*P*-value relative to background [b]	
			chromosome 2R	chromosome 3R
MA0010.1	Br	646	<0.001	<0.001
MA0458.1	Slp1	569	<0.001	<0.001
MA0013.1	Br (var.4)	566	<0.001	<0.001
MA0536.1	Pnr	411	<0.001	<0.001
MA0012.1	Br (var.3)	392	<0.001	<0.001
MA0213.1	Brk	370	<0.001	<0.001
MA0529.1	BEAF-32	352	<0.001	<0.001
MA0446.1	Fkh	277	<0.001	<0.001
MA0015.1	Cf2	250	<0.001	<0.001
MA0205.1	Trl	234	<0.001	<0.001
MA0535.1	Mad	216	<0.001	<0.001
MA0233.1	Mirr	164	<0.001	<0.001
MA0210.1	Ara	91.9	<0.001	<0.001
MA0022.1	Dl	62.1	0.001	0.002
MA0185.1	Deaf1	37.8	<0.001	<0.001

[a] Raw score indicates random fragments matched to the target TF motif

[b] P-value is provided by the Clover program. $p<0.01$ indicates statistically significant enrichment of motif in promoter sequences relative to background

The top 5 overrepresented TF motifs shared by both mutants (Br, Slp1, Pnr, Brk and BEAF-32) were analysed using functional enrichment analysis (Figure 3.12B). GOMo tool was used to associate these motifs to GO terms from the database (Buske et al. 2010). The GOMo analysis indicated that isoforms of Br (proteins of Broad-Complex transcription factor) were associated with GO terms related to translational activity, ubiquinone activity, photoreceptor cell development and response to hypoxia. The Fork-head domain transcription factor, Slp1, was associated with GO terms for response to stress and neurogenesis. Here, the GOMo analysis also indicated that Pnr (a zinc-finger transcription factor of GATA family) is involved in mRNA splicing activity, protein folding, translational initiation, ubiquitin-protein ligase activity and vesicle-mediated transport, while Brk (a transcriptional repressor) involves in dendrite morphogenesis, chromatin assembly and also a few GO terms under

reproduction. BEAF-32, an insulator protein known to regulate Hippo pathway activity for neuronal cell fate in the retina (Jukam et al. 2016), was shown in the analysis to associate with GO terms for regulation of signal transduction, spliceosome, ubiquitination and exocytosis.

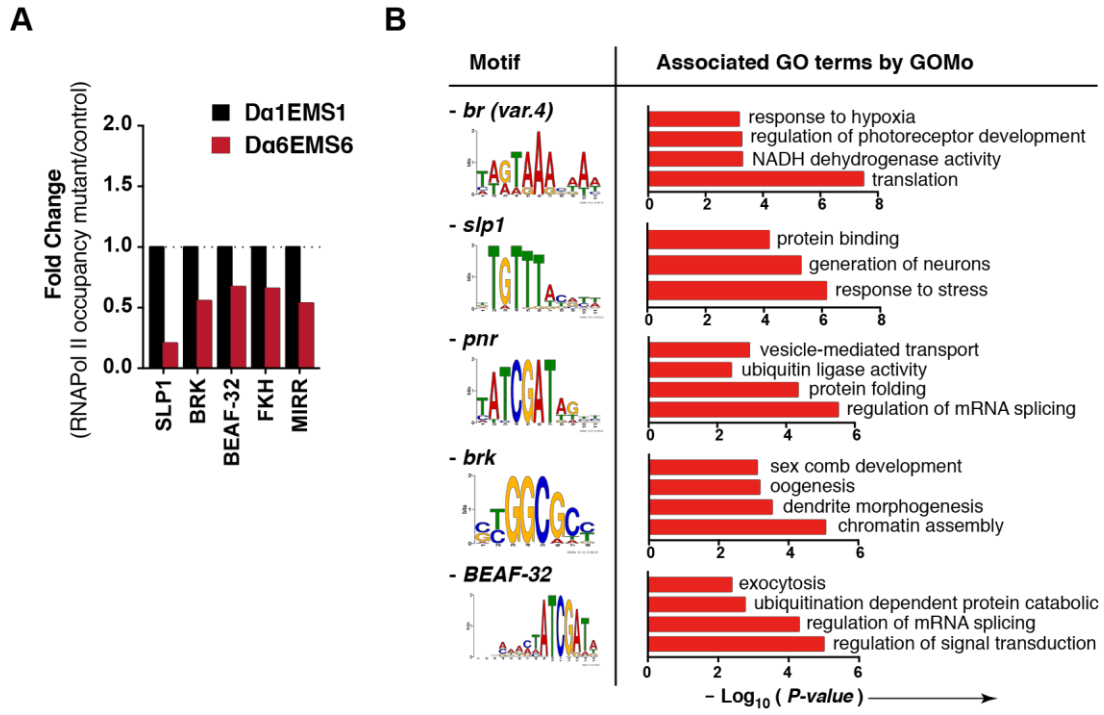

Figure 3.12 Overrepresented motif and its associated TF, on promoters of *Dα1*^{EMS1} and *Dα6*^{EMS6} DEGs

(A) Bar graph shows expression of TF-encoding DEGs associated with overrepresented motifs in *Dα1*^{EMS1} and *Dα6*^{EMS6} DEGs. (B) Top 5 overrepresented motifs in both nAChR mutants DEGs. Logo represents motif associated with TF binding and bar chart shows significant GO terms associated with the motif.

3.4 Discussion

3.4.1 Targeted DamID versus RNAseq for transcriptional analysis

In this chapter, two different techniques were adapted for transcriptional analysis of expression changes occurring in nAChR subunit mutants. Real-time qPCR analysis was also used in an attempt to validate gene expression changes. Although each of these techniques were adapted to different sets of conditions including developmental stages, cell types and mutant alleles, the analyses were all looking at transcriptional changes in nAChR subunit mutants that showed negative cross-resistance. The RNAseq performed here was a broader analysis, looking at transcripts from RNA extracted from whole first instar larvae. On the other hand, the targeted DamID looked at RNA Pol II binding profile in specific *Dα6*-expressing cells of third instar larval brains. In addition, the real-time qPCR was performed on RNA extracted from third instar larval brain in an attempt to cross-validate for gene expression changes observed from the targeted DamID analysis. While the RNAseq looked at first instar larvae as the insecticide toxicology bioassay (refer Chapter 2) reflects insecticide effects on larvae at this developmental stage, other transcriptome analyses were performed in third instar brains to match the protein expression analysis in Chapter 4.

Targeted DamID allows transcriptomic analysis of particular cell types at a specific time point in development without the need for time-consuming techniques such as cell sorting or immunoprecipitation. Based on previous studies (Southall et al. 2013) and the data presented here, this technique is sensitive enough to detect the transcriptional activity of highly expressed genes, but shows limited sensitivity for genes producing stable transcripts that do not require an active transcription. In contrast, RNAseq requires prior steps of cell sorting or enrichment to perform a cell specific transcriptional analysis. This can be time consuming and may disturb gene expression profiles in the process. Despite this, RNAseq provides a more accurate estimation of transcript levels (Wang, Gerstein, and Snyder 2009).

Overall, RNAseq provided a comparable number of DEGs in the first instar larvae of the $D\alpha1^{\Delta DH}$, $D\alpha2^{\Delta(3)4E}$ and $D\alpha6^{KO}$ mutants (Figure 3.5). Given that RNA was

extracted from whole larvae, the results showed general changes in the whole organism due to the receptor subunit mutation. As the nAChR subunit genes are largely expressed in the nervous system, this method will provide a reasonable estimate of their expression levels in that tissue, allowing the levels in the mutants and control to be compared. For genes that have a broader pattern of expression, it is impossible to discern whether observed differences are due to changes in the nervous system or in tissues outside of it or both. Martelli (2020) has provided compelling evidence that the interactions between imidacloprid and spinosad and their respective nAChR targets generates oxidative stress that perturbs metabolism both in the brain and in metabolic tissues (Martelli 2020). The possibility that mutations that change the proportions of nAChR subtypes present in neuronal cells could have downstream impacts outside the brain.

The targeted DamID provided a specific analysis on cells expressing the Dα6 subunit. The gene profile may depict changes that are specific to these cells. The differential analysis of RNA Pol II occupancy revealed almost four times more DEGs in $D\alpha6^{EMS6}$ as were detected for the $D\alpha1^{EMS1}$ mutant (Figure 3.8). This could obviously be a consequence of performing the analysis in *Dα6*-expressing cells only. As indicated by the single cell transcriptomic study on *Drosophila* midbrain, while the majority of *Dα1*-expressing cells (73%) co-express *Dα6*, 27% express *Dα1* but not *Dα6* (Croset et al. 2018). While these estimates come from a study of the adult brain, *Dα6* is also widely expressed in the third instar larval brain (Figure 3.6A). Nonetheless, there will be a significant number of cells that express *Dα1* but not *Dα6*, so the analysis would miss gene expression differences in these cells caused by the presence of the *Dα1* or *Dα6* mutations. The discrepancy in DEG numbers could also indicate that loss of Dα6 function has a more drastic impact on neuronal signalling than the loss of Dα1, precipitating more downstream changes in gene expression. These possibilities are not mutually exclusive. From the outset it needs to be recognised that the downstream changes in expression could reflect a level of chaos introduced by the loss of function or be a part of a controlled response to counterbalance it, or a mixture of the two.

3.4.2 nAChRs are expressed in various neuronal cell types

Examining the distribution of nAChRs in neuronal tissues should provide clues towards their function. Although it is well-known that nAChRs are key elements of the cholinergic neurotransmission, nAChR expression has also been described in other type of neurons including, but not limited to, GABAergic, dopaminergic and glutamatergic neurons (McGranahan et al. 2011; Ngolab et al. 2015; Yan et al. 2018). Perhaps nAChRs play significant roles, not only in the cholinergic neurons, but also globally in mediating responses of other neurotransmitters. Supporting this notion, it was found that a significant number of cells from *Drosophila* adult midbrain are expressing more than one neurotransmitter (Croset et al. 2018). This was also similarly detected in cells from the larval brain (Brunet Avalos et al. 2019).

Our cell-specific transcriptomic analysis identified positive expression of markers for cholinergic, glutamatergic, GABAergic as well as dopaminergic neurons, in cells that are expressing *Dα6* (Figure 3.6A-B). The expression of *Dα6* in these neurons may support the role of nAChRs in modulation of non-cholinergic mediated synaptic transmission. A recent study has found that activation of the nAChR by its agonists mediates dopamine release in *Drosophila* larval brain (Pyakurel, Shin, and Venton 2018). Interestingly, when tested, neonicotinoid-stimulated dopamine release was significantly reduced in the $D\alpha1^{EMS1}$ mutant, suggesting involvement of this nAChR subunit in this process (Pyakurel et al. 2018). Further, the targeted DamID analysis performed here also indicated that the Dα6 subunit is not expressed in octopaminergic or serotonergic neurons (Figure 3.6C). However, whether other nAChR subunit genes are expressed in octopaminergic and serotonergic neurons is not clear. Nicotine mediated nAChR activation can induce serotonin and octopamine neuronal activity (Fuenzalida-Uribe et al. 2013; Garduno et al. 2012). Thus, it is possible that different nAChR subunits are expressed in these neurons.

The study also revealed expression of genes known to be expressed in mushroom bodies and motor neurons in the *Dα6*-expressing cells (Figure 3.6A-B). *Dα6* promoter expression was also shown to be localised in these regions in

the larval brain (Perry et al. 2015). Collectively, this is not unexpected given that mushroom body Kenyon cells are known to be highly cholinergic (Barnstedt et al. 2016). Given mutations on nAChR subunits have been found to affect various behavioural pathways (Fayyazuddin et al. 2006; Luong 2018; Somers, Luong, Mitchell, et al. 2017; Wu et al. 2014), it was not surprising to find expression of genes present in motor neurons.

3.4.3 nAChR genes expression in *Drosophila* larvae

In *Drosophila*, the nAChR genes are expressed in the CNS. The RNAseq analysis on first instar larvae detected expression of all 10 subunit genes. Notably, these genes were expressed at varying levels which may indicate different roles that the subunit plays at this stage of development (Figure 3.4). *Dβ1* is the most highly expressed gene, whereas *Dα3* and *Dβ3* were both lowly expressed. The transcript levels observed here match those reported for first instar larvae in the Flybase database (Graveley et al. 2011). There is one exception. Flybase indicates a higher level of *Dβ3* expression, similar to the level observed for *Dα2*. Given that the two analyses were performed independently with different fly strains, the overall level of concordance is very good.

The cell-specific transcriptional analysis on third instar brains provided more detailed expression levels for the gene family. Most of the nAChR subunit genes showed relatively low levels of RNA Pol II occupancy in *Dα6*-expressing cells, suggesting low levels of active transcription. Across the three *Drosophila* strains analysed, only the *Dα1, Dα2, Dα5*, *Dα6, Dβ1* and *Dβ3* genes showed significant RNA Pol II occupancy in the *Dα6*-expressing cells (Figure 3.7). In some cases, significant levels were only observed in particular strains. *Dα1* and *Dβ1* appeared to be the most highly expressed subunits in the *Dα6*-expressing cells, having high RNA Pol II occupancy in all three strains (Figure 3.7A & G). This is consistent with the single cell transcriptome data indicating co-expression of *Dα1, Dα5* and *Dβ1* are highly correlated with *Dα6* expression in the adult brain (Croset et al. 2018). Nonetheless, the targeted DamID analysis failed to record significant RNA Pol II binding to *Dα6* in the $Dα1^{EMS1}$ and $Armenia^{14}$ strains, despite the analysis being performed in *Dα6*-expressing cells. In contrast to this observation, Flybase

indicates that *Dα6* is expressed at significant levels in the CNS of the third instar larvae. In fact, *Dα6* was shown to be the most highly expressed nAChR gene in the third instar CNS (Brown et al. 2014). Given the low RNA Pol II occupancy on the *Dα6* (Figure 3.4E), it is possible that the mRNA is stable, and that the gene only requires a low level of active transcription to maintain the relatively high transcript levels detected by RNAseq as reported in Flybase.

3.4.4 Differential nAChR gene expression in mutants that showed negative cross-resistance

Transcriptional analyses were performed in *Dα1* and *Dα6* mutant backgrounds to identify gene expression changes that may be responsible for the negative cross-resistance relationship described in Chapter 2, between neonicotinoids and spinosad. Similarly, a *Dα2* mutant was included to identify gene expression changes that may explain the negative cross-resistance relationship between nitenpyram and imidacloprid. The RNAseq data did not reveal any nAChR gene expression changes in first instar larvae that would support the nAChR compensation hypothesis proposed in Chapter 2. Specifically, the analysis did not provide evidence of any significant upregulation of the spinosad target, *Dα6* in $Dα1^{ΔDH}$, or of neonicotinoids targets, *Dα1*, *Dα2*, *Dβ1* or *Dβ2* subunit in $Dα6^{KO}$ mutant (Figure 3.4B). Also, there was no upregulation of transcript levels for the nitenpyram targets, *Dα1* or *Dβ2*, in the $Dα2^{Δ(3)4E}$ mutant (Figure 3.4B). While looking at a subset of cells in the brain in third instar larvae, the targeted DamID data support this conclusion. There was no significant enrichment of RNA Pol II binding for any of these nAChR subunit genes in the $Dα1^{EMS1}$ and $Dα6^{EMS6}$ mutants compared to the wildtype (Section 3.3.2.1). Similarly, the real-time qPCR analysis did not reveal any significant changes in mRNA levels for these genes (*Dα1*, *Dα2*, *Dα6, Dβ1* or *Dβ2*) in the third instar brains of the $Dα1^{EMS1}$ and $Dα6^{EMS6}$ mutants (Figure 3.9A). In summary, no evidence has been found to support the hypothesis that compensation at the transcriptional level is responsible for the observed negative cross-resistance phenotypes, despite having examined two different life stages, whole brains, a subset of cells in the brain and whole animals using qPCR, targeted DamID and RNAseq. Thus, if receptor compensation

involving the nAChR subunits does occur, it must involve post-transcriptional processes.

There were significant nAChR gene expression changes unrelated to the negative-cross resistance phenotype. As expected, the RNAseq analysis showed that *Dα6* was significantly reduced or absent, in $D\alpha6^{KO}$, a full gene deletion mutant (Figure 3.4B). A low transcript expression of *Dα6* however was still detected from the remaining 5'UTR and 3'UTR regions of the gene in the $D\alpha6^{KO}$ strain (Appendix 4)(Luong 2018). There is possibility that these regions are encoding regulatory elements for other subunit genes, but this has not been reported previously. Given that the number of reads mapped to these regions has not changed in comparison to the wildtype background (Appendix 4), it is unlikely that regulatory elements encoded by these UTR regions, if any, would influence the any gene expression in the mutant. Mixed observations were found for the partial deletion mutation alleles, where *Dα1* expression was not affected in $D\alpha1^{\Delta DH}$, while, *Dα2* transcription was significantly reduced in $D\alpha2^{\Delta(3)4E}$ (Figure 3.4B). The *Dα1* mutation in $D\alpha1^{\Delta DH}$ is a small exonic deletion in a region encoding the ligand-binding domain, whereas, the $D\alpha2^{\Delta(3)4E}$ deletion eliminates a substantial Dα2 encoding region that is predicted to truncate the protein after the ligand-binding domain (Appendix 4). The nature of the mutations may influence the level of gene expression observed. In addition, the RNAseq analysis also identified significant downregulation of *Dα7* and *Dβ1* transcripts in $D\alpha1^{\Delta DH}$, downregulation of *Dα7* transcript in $D\alpha2^{\Delta(3)4E}$, and downregulation of *Dα5 and Dα7* transcript in $D\alpha6^{KO}$. However, most of these changes in expression levels are relatively small (less than 2-fold). None of these expression changes can be readily reconciled with the negative cross-resistance phenotype observed for the respective mutants based on our current knowledge of nAChR subunits targeted by neonicotinoids and spinosyns.

The targeted DamID analysis in specific neuronal cells of third instar brain did not identify any transcriptional changes for the nAChR genes. However, the real-time mRNA quantification using whole brain sample indicated significant upregulation of *Dα3, Dα5* and *Dβ3* in $D\alpha6^{EMS6}$ (Figure 3.9A). Again, these are relatively small changes in expression (less than 2-fold). Given that neonicotinoid resistance was

previously recorded when *Dα3* and *Dβ3* were mutated, albeit at low resistance levels (Section 2.3.1), the upregulation of *Dα3* and *Dβ3* transcripts in $D\alpha6^{EMS6}$ could contribute to the elevated neonicotinoid sensitivity. However, again, the lack of evidence that Dα3 and Dβ3 are directly targeted by neonicotinoids provides a setback to this argument.

Notably, an opposite expression change was observed for *Dα5* when comparing findings between the two *Dα6* mutant strains, $D\alpha6^{EMS6}$ and $D\alpha6^{KO}$ from the real-time mRNA quantification and the RNAseq (Figure 3.4B). The discrepancy might be due to the different development stages at which the analyses were performed (first instar larval stage versus third instar stage), particularly given previous analysis of nAChR gene family expression demonstrated that these genes are differentially expressed in different stages of *Drosophila* development (Rosenthal et al. 2019). A compounding factor for the dissimilarities in the gene expression could be due to the differences between mutant alleles of *Dα6*.

In general, gene expression changes in the nAChR mutants examined here suggest that some nAChR subunit mutations can impact transcript levels for other subunits. One example of possible pathways by which these gene expression changes could occur is via nonsense-mediated RNA decay (NMD). NMD provides surveillance pathway on RNA quality in eukaryotes including *Drosophila*, where transcript that harbours premature stop codons is being targeted for degradation (Nickless, Bailis, and You 2017). This pathway has also been known to recruit expression of other genes as part of the compensatory mechanism (Bunton-Stasyshyn, Wells, and Teboul 2019). The premature stop codon introduced by $D\alpha6^{EMS6}$ may trigger NMD, which then recruits expression of the other subunit genes including the *Dα3, Dα5* and *Dβ3* to mitigate the results of the mutation. However, to what extent this hypothesis will be held true requires further investigation. Also, clearly a very small number of subunit mutations have been examined here, so no generalisations can be made about the types of mutations in which genes might trigger such expression changes of other subunit genes. A systematic analysis with a variety of alleles in the different subunit genes would provide some clarity.

3.4.5 Dysregulation of oxidative stress in the nAChR subunit mutants

The analyses performed also aimed to uncover whether overall changes in the transcriptomes of the nAChR mutants would provide clues as on the impact of the absence or reduced function of receptor subunits and how neurons adjust to it. It was hoped that this might provide insights into processes that the nAChR subunits play a role in.

Functional enrichment analyses were performed to identify pathways affected by the loss of receptor subunit function. Various studies in many species including *Drosophila*, have associated nAChRs with regulation of oxidative stress (Krishnaswamy and Cooper 2012; Weber et al. 2012). In *Drosophila*, *Dα6* gene has been specifically associated with oxidative stress (Weber et al. 2012). Here dysregulation of multiple oxidation-reduction processes was observed in all of the nAChR subunit mutant strains tested. RNAseq analysis of the $D\alpha1^{\Delta DH}$, $D\alpha2^{\Delta(3)4E}$ and $D\alpha6^{KO}$ mutants revealed that over 10% of the common DEGs (28 out of 247) were involved in oxidoreductase activity (Section 3.3.1.2). These include the cytochrome P450 family genes - *Cyp4ad1, Cyp6a16, Cyp6g1, Cyp9b1*, *Cyp9h1, Cyp28d2* and *Cyp309a1* and the glutathione-s-transferase genes - *GstD1, GstD3, GstD5* and *GstD10*. These genes have also been associated with other pathways in arthropods, including metabolism of xenobiotics (for example, insecticides) and many other hormonal and chemosensory processes (Chung et al. 2009; Low et al. 2007; Ranson et al. 2001; Ranson and Hemingway 2005; Rewitz, O'Connor, and Gilbert 2007; Tang and Tu 1994). Some GSTs, including GSTD1 have peroxidase activity and can act to ameliorate oxidative stress (Tang and Tu 1994). Interestingly, the genes classified under the term 'oxidoreductase activity' were upregulated in $D\alpha1^{\Delta DH}$ and $D\alpha6^{KO}$ mutant, but generally downregulated in $D\alpha2^{\Delta(3)4E}$ mutant, based on RNAseq on whole first instar larvae (Section 3.3.1.2, Figure 3.5).

Looking at the cell-specific transcriptional analysis we also observed dysregulation of pathways associated with oxidative stress in the $D\alpha6^{EMS6}$ mutant. GO terms associated with glutathione metabolism and oxidation-reduction processes were significantly enriched in DEGs of $D\alpha6^{EMS6}$, with these

genes found to be generally downregulated (Section 3.3.3). *Dα1*^{EMS1} showed less evidence of oxidative stress pathways being affected, although, common glutathione metabolism related terms and corresponding DEGs were also detected in the analysis of *Dα1*^{EMS1} mutant (Section 3.3.3). The opposite direction of gene expression changes in oxidative stress pathways between the RNAseq and the targeted DamID analysis may indicate tissue-specific responses. Tissue-specific variability in oxidative stress associated gene expression have previously been described in mice (Kim, Kim, and Son 2018), and a finding correlated with human gene expression databases (Liu et al. 2008; Xiao et al. 2010). Additionally, genes involved in lipid metabolism, a pathway that has been extensively mentioned to be affected alongside altered oxidative stress levels (Borza 2013; Chen et al. 2019; Logan-Garbisch et al. 2014) were also affected in these neuronal cells of *Dα1*^{EMS1} and *Dα6*^{EMS6} (Figure 3.10 & Figure 3.11).

Based on the pathways we find disrupted in our nAChR subunit mutants, crosstalk likely exists between oxidative stress processes and nAChR cholinergic functions. Various studies have demonstrated modulation of nAChR expression or function by changes in extracellular ROS levels (Campanucci, Krishnaswamy, and Cooper 2008; Gao, Liu, and Guan 2008; Krishnaswamy and Cooper 2012; Yu et al. 2003). In humans, oxidative stress was reported as mechanism connected to the reduced nAChR protein expression in many conditions for example, fluorosis, chronic sleep deprivation and Alzheimer's disease (Gao et al. 2008; Xue et al. 2019; Yu et al. 2003). Elevated ROS levels and oxidative stress were demonstrated to inactivate nAChRs in neurons (indicated by depression of ACh-evoked synaptic currents), thus disrupting cholinergic signalling (Campanucci et al. 2008). This was proposed to be mediated by the conserved Cys residues in the subunit's TM1-TM2 linker that is vulnerable to oxidation (Krishnaswamy and Cooper 2012). On the other hand, neuronal overactivation has been demonstrated to lead to ROS generation in *Drosophila* presynaptic NMJs. This in turn mediates structural plasticity at the synaptic terminals and leads to effects on insect behavioural functions (Oswald et al. 2018).

The nAChR *Dα6* gene has also been directly associated with oxidative stress in a previous genome-wide association study (Weber et al. 2012). When tested, a

Dα6 mutant strain from Drosophila Gene Disruption Project database showed increased susceptibility to an oxidative stress inducing treatment (Weber et al. 2012). Here, this study identifies various dysregulated genes associated with oxidative stress in all of the *Dα6* mutants examined. Although they were generally downregulated in neuronal tissue that is expressing *Dα6*, observations from whole larvae RNAseq indicated overall upregulation of these genes. It is likely that the metabolic tissues are largely impacted by changes in oxidative stress level. Collectively, from the literature and this study, it is anticipated that mutations in Dα6 subunit lead to changes in pathways that alter the capacity of the insect to regulate oxidative stress levels, and thus, would make flies more vulnerable to further changes in oxidative level. Both imidacloprid and spinosad treatments were shown to induce oxidative stress in neuronal and metabolic tissues of *Drosophila* (Martelli 2020), so it is interesting to see that the *Dα6* mutants have increased toxicity only to imidacloprid but not spinosad. This indicates that the subsequent oxidative stress induction was only triggered after the insecticide binding or action on the target receptors. Indeed, spinosad exposure in a *Dα6* knockout was not observed to further increase the oxidative stress level over and above that of the mutant itself (Martelli 2020).

3.4.6 Protein translation, trafficking and degradation were affected in the nAChR subunit mutants

This study observed various other pathways that were affected due to mutations impacting nAChR subunits. Notably, pathways involved in neuronal development and function were affected in the both *Dα1* and *Dα6* mutants, as anticipated due to the localisation of nAChRs and importance at various stages of neuronal development (Rosenthal et al. 2019; Zoli et al. 2018). Interestingly, pathways associated with protein processes including protein translation, maturation, trafficking and degradation were more significantly affected in neuronal cells of $D\alpha6^{EMS6}$ than in the $D\alpha1^{EMS1}$ mutant (Section 3.3.3). The targeted DamID analysis identified GO terms related to translational activity as the most significantly enriched terms and most of the genes under these terms were upregulated in both $D\alpha1^{EMS1}$ and $D\alpha6^{EMS6}$ (Figure 3.11). This may indicate increased translation of proteins that are needed to compensate for loss of the

nAChR subunit, or it may also be an increased translation of proteins that are involved in various biological functions in response to stress. Without proteomic profiles for these mutants, we cannot be sure on what type of proteins are being upregulated in response to the subunit mutation.

These analyses also revealed enrichment for DEGs related to protein processes including protein trafficking and degradation, significantly in the cell-specific transcriptional analysis of the *Dα6*^{EMS6}, but not for the *Dα1*^{EMS1} mutant (Figure 3.11). These pathways however were not detected in RNAseq analysis from whole first instar larvae, indicating tissue-specific changes due to the mutation of Dα6 subunit. Previously, spinosad exposure has been demonstrated to lead to Dα6 protein degradation (Nguyen et al. manuscript in preparation). As spinosad binds allosterically to the C-terminal region of nAChR Dα6 subunit rather than the ligand-binding domain (Puinean et al. 2013; Somers et al. 2015), the structure of the nAChR complex is thought to be disrupted upon the binding, leading to its degradation (Nguyen et al. manuscript in preparation). The same process may be triggered in response to the mutations in the nAChR subunits that lead to mis-folded subunits and/or a dysfunctional receptor complex. Clearance of the dysfunctional nAChR complex from the membrane would explain the observed upregulation of pathways involved in vesicle-mediated trafficking and proteasome-mediated degradation in the *Dα6* mutants.

The proteasome-mediated degradation of Dα6 was further examined and found to involve lysosomal activity. The Dα6-containing receptors have been observed to co-localise with lysosomes after the spinosad exposure (Felipe Martelli, personal communication). Consistent with these data, in addition to upregulation in proteolysis and proteasome activity, our analysis identified upregulation of lysosomal and ubiquitination activity in the neuronal cells of *Dα6*^{EMS6} mutant (Figure 3.11), all of which contribute to protein degradation processes. Endosomal activity, which may play a sorting role in the degradation of dysfunctional synaptic proteins (Uytterhoeven et al. 2011), was also dysregulated in these cells.

The increased proteasome and lysosome activity were also observed in the *Dα6*^{KO} larvae, even though no enrichment of GO term associated with vesicle-

mediated trafficking was represented among the DEGs (Figure 3.5B). Given that a full gene deletion should not produce any protein at all, the need for clearance of dysfunctional Dα6-containing receptors is not expected. This could indicate possible degradation of other unknown proteins due to the loss of this nAChR subunit. It may be that the nAChR subtype that requires Dα6 cannot exist alone, and thus, the rest of subunits or the incomplete nAChR complex are being cleared from the cell when Dα6 is lost. Similarly, these may include chaperone proteins or accessory proteins that are regulating, and specific to, the Dα6-containing nAChRs.

Downregulation of *slp1, brk* and *BEAF-32* in the *Dα6* mutant (where binding motifs of these TFs were also overrepresented in the DEGs in the mutant) were also identified from the targeted DamID analysis (Section 3.3.4). Further, the TFs encoded by these genes may be responsible for mediating the observed expression changes for genes described under pathways such as neuron development, protein transport and protein degradation, based on the GOMo analysis (Section 3.3.4). These regulatory proteins could be acting as a repressor or activator on the genes in mediating the expression changes. Looking at known downstream genes of the TFs that bind to these recognised motifs, many of these genes were not affected in $D\alpha1^{EMS1}$ and $D\alpha6^{EMS6}$. *Dpp* expression is demonstrated to be mediated and maintained by Pnr, while Brk was reported to block *Dpp*, during embryo development (Herranz and Morata 2001; Jazwinska, Rushlow, and Roth 1999). Here, *brk* expression is significantly downregulated in $D\alpha6^{EMS6}$ (Figure 3.12), but no significant changes in *Dpp* gene expression were observed in the mutant. Previous work has also demonstrated that BEAF-32 regulates rhodopsin expression; an RNAi-mediated block in BEAF-32 leads to *Rh5* upregulation and *Rh6* downregulation (Jukam et al. 2016). The analysis here did record a 4.5-fold upregulation of *Rh5* in $D\alpha6^{EMS6}$ (Appendix 6), correlated with the downregulation of *BEAF-32*, but no change in *Rh6* expression was recorded in the mutant. Taking these together, it is difficult to suggest a relative contribution of each TF to the dysregulated pathways in the mutant using data from the targeted DamID and the GOMo analysis alone. Targeting these TFs in the future could shed light on the specific downstream target genes, and thus molecular

pathways, that are responsible for the phenotypic changes observed in the mutant.

3.4.7 Association of the dysregulated pathways with negative cross-resistance

Enrichment of the GO terms associated with protein translation, maturation and trafficking in the nAChR subunit mutants could also be explained by the proposed nAChR compensation mechanism that leads to the negative cross-resistance phenotype. Protein folding and trafficking are important for nAChR subunit maturation and assembly (Brodsky and Skach 2011), and thus, if a compensation mechanism is triggered due to the loss of one of the receptor subunits, it is reasonable for genes involved in regulating these pathways to be upregulated. However, the only significant upregulation of protein folding and trafficking activity observed was in the *Dα6*-expressing neuronal cells of the $D\alpha6^{EMS6}$ mutant, not $D\alpha1^{EMS1}$ (Figure 3.11). This suggests that there are possibly two independent mechanisms in response to the mutations in *Dα1* and *Dα6* that lead to negative cross-resistance, which may or may not involve nAChR compensation. Further examination of these mutants is required.

The transcriptional analyses presented in this chapter also indicated another possible route by which the increased sensitivity to another insecticide may occur. The elevated level of oxidative stress in the mutants may predispose them to increased sensitivity for another insecticide's action, particularly to insecticides that increase oxidative stress. Removing the target for the insecticide would more than compensate for the increased oxidative stress burden, however, for the other compound, the target is still present, but in a hypersensitised insect. Both neonicotinoids and spinosad were shown to increase oxidative stress in cellular environment (Ge et al. 2015; Martelli 2020; Xu et al. 2018). As loss of the insecticide target did not further elevate oxidative stress upon the insecticide exposure (Martelli 2020), it is likely that the oxidative stress is triggered by the binding of the insecticide to its target site. Thus, nAChR mutants that are resistant to insecticides, may be hypersensitive to other insecticides that cause oxidative stress.

For the negative cross-resistance between imidacloprid and nitenpyram in *Dα2* mutants, the fact that the two neonicotinoids are likely to have overlapping targets, further complicates the situation in understanding possible mechanisms behind the phenotype. If oxidative stress is found to be similarly affected in *Dα2* mutant, the observed hypersensitivity to nitenpyram, but not spinosad, would be harder to explain as spinosad is the one that induces oxidative stress (Martelli 2020) and nitenpyram was never examined. The RNAseq analyses highlighted expression changes for genes associated with oxidoreductase activity in $D\alpha2^{\Delta(3)4E}$ (Figure 3.5), but evidence of oxidative stress in this mutant is not as strong as it is for the *Dα1* and *Dα6* mutants. There could be a distinct molecular mechanism responsible for the negative cross-resistance observed between imidacloprid and nitenpram. In addition, the possibility that nAChR compensation occurs at the protein level still needs to be examined in the background of *Dα2* mutant. There could be upregulation of nAChR subtype that is a target for nitenpyram, but not imidacloprid as explained in Chapter 1, that could mediate the negative cross-resistance.

Chapter 4 : Chemical and genetic dissection of mechanisms for negative cross-resistance

4.1 Introduction

The *Drosophila* larval NMJ serves as an ideal model to understand how the synapse functions. The neuronal lineages are well characterised, expression of many genes has been studied both at whole brain (Cahoy et al. 2008; Pacifico et al. 2018; Torres-Oliva et al. 2018) and more recently, at single cell resolution (Brunet Avalos et al. 2019; Croset et al. 2018). The localisation of proteins in this tissue can be studied using many genetic tools. Currently nAChRs are known to play roles in several neuronal pathways associated with visual system, learning and memory, sleep, addiction and motor function (Fayyazuddin et al. 2006; Rosenthal et al. 2019; Somers, Luong, Mitchell, et al. 2017; Su and O'Dowd 2003; Wu et al. 2014). What is poorly understood is how a neuron compensates for the loss of function for an nAChR subunit. In addition to initiating calcium signalling upon its activation, presynaptic and postsynaptic nAChRs also regulate neurotransmitter release and synaptic plasticity (Dani and Bertrand 2007; MacDermott, Role, and Siegelbaum 1999). In addition to influencing the regulation of its own receptor density at the synapse (Section 1.1.5), altered nAChR signalling also dictates synaptic homeostasis. Hence, the absence of specific receptor subunits or receptor subtypes could significantly impact neural signalling through altered expression of other nAChR subunits or cause dysregulation of other cellular processes. Either of which could contribute to the negative cross-resistance mechanism being examined here.

4.1.1 Neuronal synaptic plasticity

A neuron has the capacity to modulate its sensitivity to signalling, and in so doing, its output, in response to external signals. Importantly, adaptive mechanisms enable the nervous system to restore normal functionality in response to perturbations (Davis 2006; Vitureira, Letellier, and Goda 2012). Some of these adaptive changes include modulation of (1) number of receptors at the membrane, (2) the pool of synaptic vesicles, (3) the amount of neurotransmitter released into synapse, or (4) receptor sensitivity to its ligands (Castillo 2012; Gaiarsa, Caillard, and Ben-Ari 2002; Lüscher and Malenka 2012; Scheler 2004). These modulations are collectively described as homeostatic plasticity and have been observed in both vertebrates and invertebrates (Glanzman 2010). This fundamental property is known as synaptic plasticity. It serves to fine tune signalling to optimise various neural and behavioural functions. However, the molecular events that mediate this complex mechanism still elude us. Availability of the *Drosophila* model system has facilitated the detailed investigation of these processes at the NMJ using forward genetic approaches.

4.1.2 Regulation of synaptic plasticity

Various factors have been demonstrated to induce homeostatic synaptic plasticity. Genetic mutations in *Drosophila* glutamate receptors at the NMJ that decrease the receptor sensitivity result in a compensatory increase of presynaptic neurotransmitter release, restoring normal levels of synaptic activity (Davis and Goodman 1998; Petersen et al. 1997). Mutations in other genes (*Pak*, *dorsal*, *cactus* or *nanos*) that reduce clusters of glutamate receptors at the NMJ were reported to have similar effects (Albin and Davis 2004; Heckscher et al. 2007; Menon et al. 2009). Similarly, postsynaptic expression of Kir2.1 potassium channels in muscles, which impairs muscle depolarisation, increases presynaptic neurotransmitter release, a response likely to be compensating for reduced muscle excitability (Paradis, Sweeney, and Davis 2001). Changes in the level of neurotransmitter receptors in response to age-related neuronal damage is another example of neuronal plasticity. Striatum from both animal models and patients with Parkinson's disease indicate upregulation of postsynaptic dopamine

receptors, correlated to dopamine deficiency (Donnan et al. 1991). Meanwhile, a significant decrease in α4β2-nAChR in hippocampus and basal forebrain has been observed in patients with Alzheimer's dementia (Sabri et al. 2018). The findings from these studies have helped to identify pathways and targets for the development of novel treatment strategies for these and other neurological diseases (Hoskin, Al-Hasan, and Sabbagh 2018; Quik et al. 2007; Quik and Wonnacott 2011). In *α6* knockout mice, replacement of α6 by α4 in $\alpha4\alpha6\alpha5(\beta2)_2$ receptor complexes was suggested based on the pharmacological properties of the upregulated nAChR subtype, which may indicate nAChR subunits can directly compensate for each other (Champtiaux et al. 2002; Klink et al. 2001). Other conditions, such as elevated ROS generation, have also been shown to mediate plasticity at presynaptic NMJs (Oswald et al. 2018).

Homeostatic plasticity at the synapse has been observed in the *Drosophila* visual system. Ventral lateral neurons (LNvs) are critical neurons for circadian rhythm and light-related behaviours in larvae (Mazzoni, Desplan, and Blau 2005). Additionally, the structure of LNvs and their physiological response can be modulated by light stimulation (Malpel, Klarsfeld, and Rouyer 2002; Yuan et al. 2011). Increased light exposure reduced the size of dendritic arbors in LNvs and its calcium response (Yuan et al. 2011). Interestingly, a recent study demonstrated that nAChR Dα1 and Dα6 play important roles in LNvs plasticity, with flies carrying mutations in these receptor subunits having a reduced dendrite volume and calcium response in LNvs (Rosenthal et al. 2019). However, neither mutant showed any further reduction in compensatory response upon increased light exposure, indicating that both the light conditions and the nAChR mutations are involved in the same cellular pathway (Rosenthal et al. 2019).

4.1.3 Chapter overview

In Chapter 3, transcriptomic analysis on whole larvae and targeted cells showed significant expression of nAChR subunit genes in the larval brain and differences in gene expression in nAChR mutant backgrounds. The observed changes in nAChR mRNA expression in the mutants did not fit with the hypothesis that the negative cross-resistance is occurring due to compensation at the level of

transcription. Thus, if direct nAChR subunit compensation occurs, it needs to be at the post-transcriptional level. This chapter analyses protein localisation and the expression levels of the nAChR subunits, again using *Dα1* and *Dα6* mutants that exhibit a negative cross-resistance phenotype between neonicotinoids and spinosyn. This chapter also examines candidate pathways revealed through the transcriptional analysis. Using known chemical inhibitors against some of these pathways suggests possible involvement in the negative cross-resistance phenotype.

4.1.3.1 Research questions

This chapter will answer the following research questions:

1. Where in the brain are the nAChR subunits involved with the negative cross-resistance phenotype being expressed? Are they expressed in the same cells?
2. Is there any change in protein level of nAChR subunits that could explain the negative cross-resistance phenotype?
3. Can other pathways possibly involved in negative cross-resistance be targeted for further investigation?

4.2 Materials and Methods

4.2.1 Fly strains

T2AGAL4 or Trojan GAL4 is one of MiMIC-compatible cassettes made available recently. It utilises a SA-T2A-GAL4-polyA cassette that can be exchanged into the MiMIC strains (Diao et al. 2015; Lee et al. 2018). The T2AGAL4 cassette contains a splice acceptor with an in-frame stop codon to truncate the targeted gene, followed by T2A, a ribosomal skipping site that allows translational readthrough of the GAL4 coding region that follows the T2A site (Diao and White 2012). Thus, the system both truncates the original gene product at the insertion site and produces GAL4 protein which essentially places GAL4 expression under the control of a gene's native enhancers.

Previously generated *Drosophila* T2AGAL4 strain of Dα6, *Dα6-T2AGAL4* (Lee et al. 2018) was obtained for this study. T2AGAL4 strains for Dα1 that had been generated using a CRISPR-mediated integration cassette, (CRIMIC) were kindly provided by Wei Chen (personal communication). The T2AGAL4 system disrupts the native subunit gene product and these strains are resistant to respective insecticides that target the nAChR subunit. A reporter strain, *UAS-mCD8::GFP* was used to visualise gene expression localisation of the T2AGAL4 drivers. Fly strains obtained for the study is listed in Table 4.1.

Transgenic flies carrying a yellow fluorescent protein (YFP) tagged Dα1 construct, *UAS-Dα1-YFP* (Somers 2015) or Dα6 construct, *UAS-Dα6-YFP* (Nguyen et al. manuscript in preparation) were used with the corresponding T2AGAL4 drivers to track subunit protein localisation under different conditions. Importantly, these YFP-tagged subunit constructs were validated to restore native levels of susceptibility to neonicotinoid and spinosad, in *Dα1* and *Dα6* mutants respectively (Somers 2015; Nguyen et al. manuscript in preparation). These constructs were also crossed into previously described *Dα1* mutants ($D\alpha1^{EMS1}$ and $D\alpha1^{KO}$) or *Dα6* mutants ($D\alpha6^{EMS6}$ and $D\alpha6^{KO}$) described in Section 2.2.1, to examine subunit expression in the mutant backgrounds (Table 4.2).

Table 4.1 *Drosophila* strains obtained for the study

Strain	Genotype	Stock
Dα1-T2AGAL4	*w; +; Dα1.TG4/TM6b,Tb*	Batterham lab stock
Dα6-T2AGAL4	*yw; Dα6-MI01466.TG4.1; +*	BDSC #76137
UAS-mCD8::GFP	*yw; P{w[+mC]=UAS(FRT.stop)mCD8-GFP.H}11/CyO*	BDSC #30125
UAS-Dα1-YFP	*w; UAS-Dα1-YFP; +*	Batterham lab stock
UAS-Dα6-YFP	*w; +; UAS-Dα6-YFP*	Batterham lab stock

BDSC, Bloomington Drosophila Stock Centre

Table 4.2 *Drosophila* strains generated for *in vivo* tracking of fluorescent tagged subunit in nAChR mutants

Strain	Genotype	Purpose
Control Dα1-T2AGAL4	w^{1118}; +; *Dα1.TG4/TM6b, Tb*	Crossed to express Dα1-YFP in control background
Control UAS-Dα1-YFP	w^{1118}; *UAS-Dα1-YFP; +*	
$Dα6^{EMS6}$ Dα1-T2AGAL4	w^{1118}; $Dα6^{EMS6}$;*Dα1.TG4/TM6b, Tb*	Crossed to express Dα1-YFP in $Dα6^{EMS6}$ background
$Dα6^{EMS6}$ UAS-Dα1-YFP	w^{1118}; $Dα6^{EMS6}$, *UAS-Dα1-YFP; +*	
$Dα6^{KO}$ Dα1-T2AGAL4	w^{1118}; $Dα6^{KO}$;*Dα1.TG4/TM6b, Tb*	Crossed to express Dα1-YFP in $Dα6^{KO}$ background
$Dα6^{KO}$ UAS-Dα1-YFP	w^{1118}; $Dα6^{KO}$, *UAS-Dα1-YFP; +*	
Control Dα6-T2AGAL4	w^{1118}; *Dα6-MI01466.TG4.1; +*	Crossed to express Dα6-YFP in control background
Control UAS-Dα6-YFP	w^{1118}; +; *UAS-Dα6-YFP*	
$Dα1^{EMS1}$ Dα6-T2AGAL4	w^{1118}; *Dα6-MI01466.TG4.1;* $Dα1^{EMS1}$*/TM6b, Tb*	Crossed to express Dα6-YFP in $Dα1^{EMS1}$ background
$Dα1^{EMS1}$ UAS-Dα6-YFP	w^{1118}; +; $Dα1^{EMS1}$, *UAS-Dα6-YFP*	
$Dα1^{KO}$ Dα6-T2AGAL4	w^{1118}; *Dα6-MI01466.TG4.1;* $Dα1^{KO}$*/TM6b, Tb*	Crossed to express Dα6-YFP in $Dα1^{KO}$ background
$Dα1^{KO}$ UAS-Dα6-YFP	w^{1118}; +; $Dα1^{KO}$, *UAS-Dα6-YFP*	

4.2.2 Western blotting

4.2.2.1 Protein extraction

20 adult flies were collected in a fresh tube and flash-frozen in liquid nitrogen. Fly heads were decapitated by vigorous shaking and separated using a mesh sieve on a bed of dry ice. Heads were homogenised in extraction buffer containing 1X RIPA Lysis Buffer (Abcam) and 1X cOmplete™ Mini Protease Inhibitor Cocktail (Sigma) using a bead beater. The sample was boiled at 100°C for 5 minutes before being centrifuged at maximum speed at 4°C for 10 minutes to clear the supernatant from the debris. For larval brain samples, brains from 20 third instar larvae were dissected in 1X PBS. Brains were homogenised in the same extraction buffer by vortexing and left on ice for 15 minutes. The sample was centrifuged at maximum speed at 4°C for 10 minutes. Finally, the supernatant was transferred into a fresh tube. Protein concentration was quantified using Qubit Fluorometric Quantitation.

4.2.2.2 Sodium dodecyl sulfate (SDS)-polyacrylamide gel electrophoresis and blotting

SDS-polyacrylamide gel made up of 4% stacking gel (top) and 10% resolving gel (bottom) was prepared on a 1mm vertical gel cast (Bio-Rad) following manufacturer's instructions. The 10% resolving gel contained 1.8mL of 40% bis-acrylamide solution (Sigma), 1.5mL of 1.5 M Tris-HCl pH 8.8, 60µL of 10% SDS, 60µL of 10% ammonium persulfate, 6µL of TEMED (Sigma) and 2.625mL of water. The 4% stacking gel contained 150µL of 40% bis-acrylamide solution, 375µL of 0.5 M Tris-HCl pH 6.8, 15µL of 10% SDS, 15µL of 10% ammonium persulfate, 1.5µL of TEMED and 97µL of water.

45ug of protein sample was diluted in 1X loading buffer (62.5mM Tris-HCl, pH 6.8, 3% SDS, 10% glycerol, 0.1% bromophenol blue, 100mM dithiothreitol) and heated at 100°C for 5 minutes before loading onto the gel. The sample was run on 1X Tris-Glycine buffer, pH 8.3 (25mM Tris base, 192mM Glycine, 0.1% SDS), in a Mini-PROTEAN Tetra Cell (Bio-Rad) at constant voltage of 70V for 10 minutes, then 150V for 1-2 hours. Resolved proteins were transferred onto an

Immobilon-P PVDF transfer membrane (Thermo Fisher) in transfer buffer containing 25mM Tris base, 192mM glycine and 10% methanol, using an XCell II Blot Module electroblotting set up (Thermo Fisher). The module was run in an XCell Surelock™ Mini-Cell (Thermo Fisher) on ice at a constant current of 250mA for 1.5 hours.

4.2.2.3 Immunostaining and protein detection

The membrane was blocked with 3% BSA or 5% skim milk powder in 1X Tris-Buffered Saline-Tween (10mM Tris-HCL, pH 7.5, 150mM NaCl, and 0.01% w/v Polysorbate TWEEN® 20) for 1 hour at room temperature. Then, the membrane was incubated with a primary antibody overnight at 4°C and washed three times before incubation with a secondary antibody for 1 hour at room temperature. The following primary antibodies; rabbit anti-Dα6 1:1000 (Watson et al. 2010) and rabbit anti-β actin 1:2000 (Abcam), and secondary antibody, HRP-conjugated anti-rabbit IgG 1:5000 (Cell Signaling) were used in the study. Detection of protein bands was performed by chemiluminescence using Clarity™ Western ECL Substrate (Bio-Rad) following manufacturer's instructions and viewed using a ChemiDoc Imaging System (Bio-Rad). Protein bands were analysed and quantified relative to housekeeper, β actin using Image Lab software (Bio-Rad).

4.2.3 Confocal microscopy

For live confocal imaging, third instar larval brains were dissected out in ice-cold 1X PBS. The brains were then mounted in VectaShield® mounting medium (Vector Laboratories) for imaging. All samples were viewed and imaged on Leica SP5 AOBS Inverted Confocal Microscope using Leica Application Suite Advanced Fluorescence software. Images were assembled from a Z-stack with a Z-step interval of 2μm, using the 20x dry objective or 40x oil immersion objective. Further image analysis was performed using Fiji software (Schindelin et al. 2012).

4.2.4 Compounds

Imidacloprid (Confidor®, Bayer Crop Science Australia) and spinosad (Chem Service Inc) were purchased commercially. Imidacloprid was diluted in distilled water, whereas spinosad was diluted in DMSO or ethanol to prepare a 10,000ppm stock solution. Stock solutions were stored at 4°C in the dark. Chemical inhibitors including dynasore (Abcam, ab120192), bortezomib (Abcam, ab142123), nordihydroguaiaretic acid, NDGA (Abcam, ab142582) and PYR-41 (Abcam, ab141469) were also purchased commercially. Dynasore, which is an endocytosis inhibitor, was diluted in ethanol to a 50 mM stock and stored at -20°C. Bortezomib, which is a proteasome inhibitor, was diluted in ethanol to a 1 mM stock and stored in the dark at -20°C. NDGA, which is a naturally occurring antioxidant and an inhibitor of protein transport from the ER to Golgi, was diluted in ethanol to a 1mM stock and stored at room temperature. PYR-41, which is a ubiquitin-activating enzyme E1 inhibitor, was diluted in ethanol to a 1mM stock and stored at -20°C.

4.2.5 Larval movement assay (Wiggle Index)

Larval movement assay or Wiggle Index was performed to measure the response of larvae to insecticide exposure over a period of time as previously described (Denecke et al. 2015). Adult flies were allowed to lay eggs over 24 hours on standard fly media. Eggs were allowed to hatch, and larvae were kept at 25°C for 68 hours. Larvae were washed on mesh and placed onto a 50mm juice plate using the 20% sucrose extraction method (Nichols, Becnel, and Pandey 2012). 25 similar-sized third instar larvae per replicate/well, were collected into a 24-well flat bottom plate filled with 200µL of 5% sucrose solution and left to acclimatise. Larvae were pre-treated with 500µM of dynasore, 10µM of bortezomib, 1mM of NDGA or 500µM of PYR-41 by substituting the appropriate amount of liquid with pre-diluted stock solutions and left in the dark for 1 hour. For control, larvae were pre-treated with the highest ethanol concentration used in the chemical pre-treatment step (10% in this study). 5X insecticide stock solutions were prepared in 5% sucrose and 50µL of the stock was added to each well to make up a desired insecticide concentration (3ppm for imidacloprid and 2ppm for spinosad). After

mixing by agitation, 50µL of total liquid was removed to bring back the final volume to 200µL.

A 30 second video of larval movement was taken for each well at 0, 15, 30, 60, 90, and 120 minutes using a Nikon video recorder. Each of the captured videos was converted to a set of 750 images using Video Jpg Converter (DVDVideoSoft software). The images were input into an R package for Wiggle Index (https://github.com/shanedenecke/WI_Analysis). The package utilised Fiji software to measure light intensity of each image and generate a heat map which was used to calculate movement between the images in the set. The relative movement ratio (RMR) was calculated by comparing the movement at each time point to the baseline movement at time point, 0 min. Data analysis were performed in R studio software.

4.3 Results

4.3.1 Western blot analysis of Dα6 subunit protein level in *Dα1* mutants

The hypothesis that a mutation in a nAChR subunit gene leads to an increase in transcription of another nAChR subunit gene(s) providing an explanation for negative cross-resistance has been rejected (refer Chapter 3). Compensatory expression changes at the translational or post-translational levels could also account for the observed negative cross-resistance. This possibility is investigated here.

A native Dα6 antibody was available for protein quantification (Watson et al. 2010). Dα6 subunit protein levels in the *Dα1* mutants that do and do not exhibit negative cross-resistance, $D\alpha1^{EMS1}$ and $D\alpha1^{KO}$ respectively, were measured. Western blotting analysis of protein extracted from the third instar larval brain and adult brain showed Dα6 specific bands. The band intensities were normalised to those of the housekeeper, β-actin (Figure 4.1). Analysis from the adult brain revealed a 2.3-fold down-regulation of Dα6 protein levels in $D\alpha1^{EMS1}$, meanwhile no significant changes in Dα6 were recorded for $D\alpha1^{KO}$, compared to the wildtype control, $Armenia^{14}$ (Figure 4.1A-B). In examining protein levels in the dissected larval brain, similar trends of reduced expression of Dα6 were observed in both $D\alpha1^{EMS1}$ and $D\alpha1^{KO}$, compared to the control, however, these changes in protein level were not significant (Figure 4.1C-D). In summary, the protein analyses showed no upregulation of Dα6 protein level in $D\alpha1^{EMS1}$ and $D\alpha1^{KO}$ that could support altered protein levels of the subunits as the mechanism underlying spinosad hypersensitivity observed in these mutant strains. Unfortunately, no native Dα1 antibody is currently available for secondary staining for the reverse analysis of Dα1 levels in *Dα6* mutants.

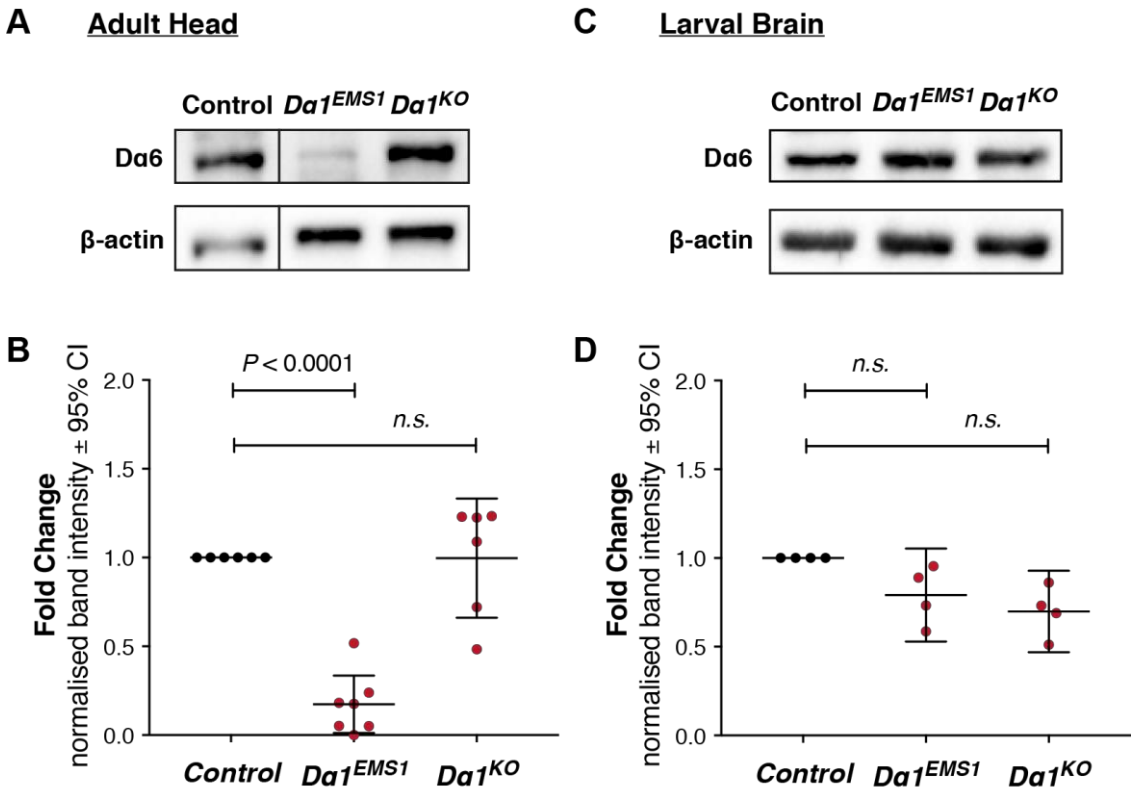

Figure 4.1 Analysis of Dα6 subunit protein level in *Dα1* mutants

Western blots of (A-B) adult head and (C-D) larval brain extracts from *Dα1* mutants, $Dα1^{EMS1}$ and $Dα1^{KO}$ were incubated with anti-Dα6 and the loading control anti-β actin. Graphs show relative expression of the Dα6 bands compared to wildtype control, *Armenia*[14]. Student's t-test was performed for statistical significance, where $P < 0.05$ is considered significant (n ≥ 4). *n.s.*, not significant

4.3.2 Analysis of Dα1 and Dα6 expression in mutants that showed negative cross-resistance using YFP-tagged nAChR subunits

In order to quantify protein expression levels of nAChR Dα1 and Dα6 subunits, an optimised *in vivo* tracking system of YFP-tagged Dα1 and Dα6 subunits, the expression of which could be controlled using the UAS/GAL4 system, was used (Brand and Perrimon 1993). For this, T2AGAL4 strains of *Dα1* and Dα6 which contain a cassette that truncates the subunit gene product at the insertion site and produces GAL4 protein were used (Diao and White 2012). *Dα6-T2AGAL4* strain had a T2A-GAL4 cassette inserted in the intronic region of *Dα6* at position 2L:9,863,534(-) between exon 2 and exon 3, which truncates the subunit product just after residue K22 (Figure 4.2B)(Diao et al. 2015). Meanwhile, the cassette was inserted at position 3R:24,412,847(-) of *Dα1* (between exon 4 and exon 5) using CRIMIC, in the generation of the *Dα1-T2AGAL4* strain and this truncates the protein product at residue Q79 (Figure 4.2A)(Wei Chen, personal communication). This essentially places GAL4 expression under the control of the native enhancers of the nAChR subunit gene being examined. As both T2A-mediated protein truncations occur before loop D inside the extracellular ligand-binding domain of the nAChR subunit, a subunit expression close to a null mutation is expected.

Initially, a UAS-mCD8::GFP reporter was used to visual the gene expression patterns of nAChR *Dα1* and *Dα6* in third instar larval brains. Both subunit genes showed similar fluorescent localisation patterns in the larval brain (Figure 4.3A-F). *Dα1* and *Dα6* showed a very similar localisation of expression in the cortex of the VNC (Figure 4.3B & E) and in the central brain, prominently in cell bodies as well as the mushroom bodies (Figure 4.3C & F). These T2AGAL4 strains are a valuable tool to drive GAL4 expression in the same pattern as the nAChR that it disrupts. Despite observing variations in fluorescence levels for the two genes, it was not possible to compare fluorescence levels due to the nature of GAL4-mediated amplification of the expression and the different laser intensities used in imaging the brains to accommodate the varying intensity of GFP signals.

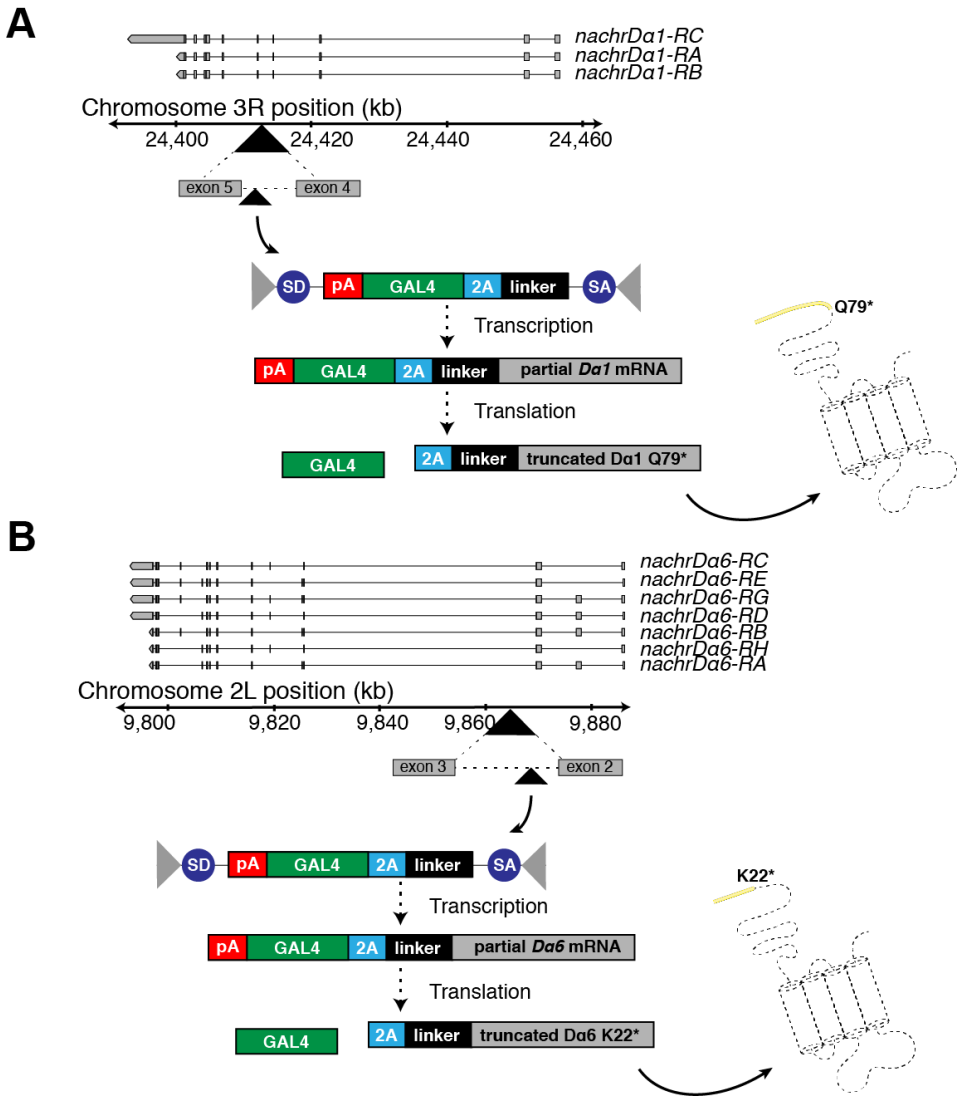

Figure 4.2 T2AGAL4 drivers for *nAChR Dα1* and *Dα6*

Schematic diagrams show sites of T2AGAL4 cassette insertion in coding intron of (A) *nAChR Dα1* and (B) *nAChR Dα6*, which is positioned at 3R:24,412,847(-) and 2L:9,863,534(-) respectively. The T2AGAL4 insertions result in expression of GAL4 under the control of endogenous gene regulatory sequences, while truncating the Dα1 and Dα6 protein products after residue Q79 and K22, respectively.

Figure 4.3 Localisation patterns of GFP reporter under the control of *Dα1* and *Dα6* T2AGAL4 drivers in larval brain

Opposite. Confocal images show expression patterns of UAS-mCD8::GFP reporter driven by (A-C) Dα1-T2AGAL4 and (D-F) Dα6-T2AGAL4 in neurons of third instar larval brain, with magnifications of ventral nerve cord (VNC) and optical lobe. Scale bars are 100μm.

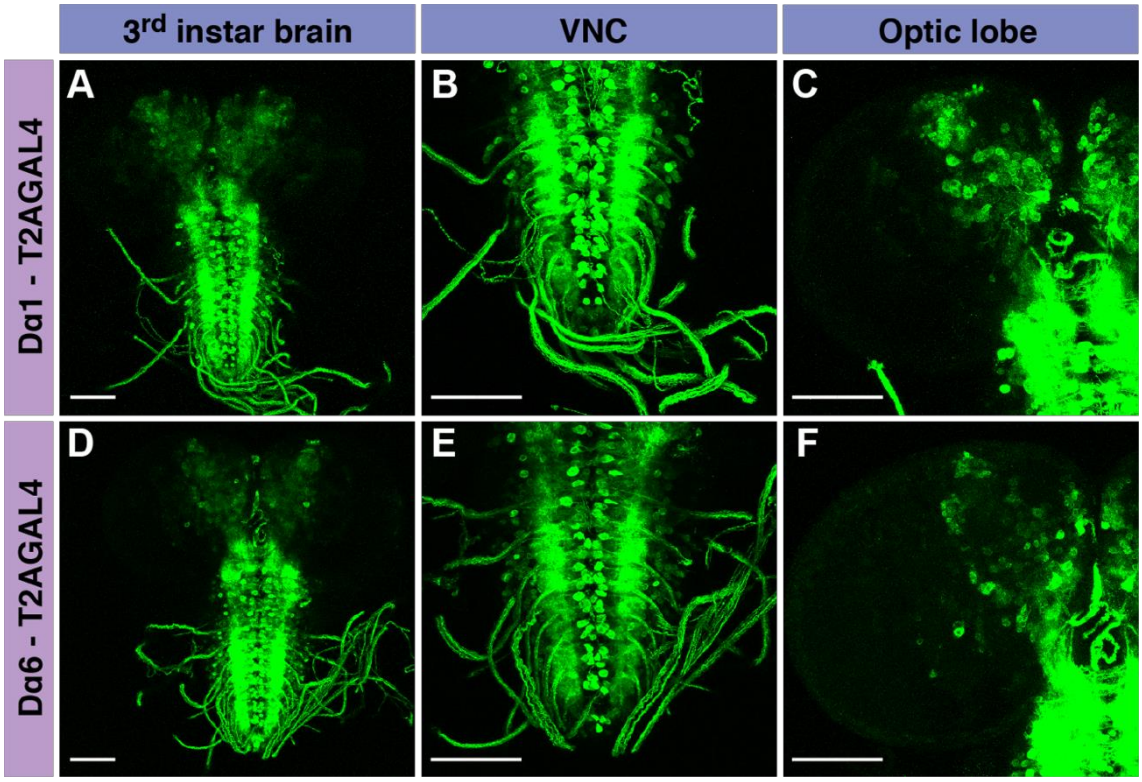

Subsequently, the YFP-tagged Dα1 (Dα1-YFP) and Dα6 (Dα6-YFP) constructs were expressed under the control of the *Dα1-T2AGAL4* or *Dα6-T2AGAL4* drivers, in the *Dα6* and *Dα1* mutant backgrounds, respectively. Again, third instar larval brains were dissected for the analysis. Overall, a similar localisation of fluorescent Dα1 and Dα6 in the larval brain as found for the UAS-mCD8::GFP reporter was observed. The visualisation indicated a similar pattern of Dα1-YFP localisation in all three different genetic backgrounds - wildtype, $Dα6^{EMS6}$ and $Dα6^{KO}$ (Figure 4.4A-C). Similarly, the localisation patterns of Dα6-YFP were very similar in brains of the wildtype, $Dα1^{EMS1}$ and $Dα1^{KO}$ strains (Figure 4.4D-F).

Quantification of the fluorescence signal showed a significant increase in fluorescent signal (~35% increase) in $Dα6^{EMS6}$ brains compared to the wildtype control, suggesting upregulation of Dα1 in the mutant (Figure 4.4G). However, the analysis did not record any significant change in Dα1 signal in the full knockout mutant, $Dα6^{KO}$. Analysis of *Dα1* mutants revealed no significant changes in Dα6-YFP signal, in either $Dα1^{EMS1}$ or $Dα1^{KO}$ brains (Figure 4.4H). The observation of no changes in Dα6 expression in *Dα1* mutants is consistent with results from western blotting analysis on protein extracted from the third instar larval brains (Section 4.3.1).

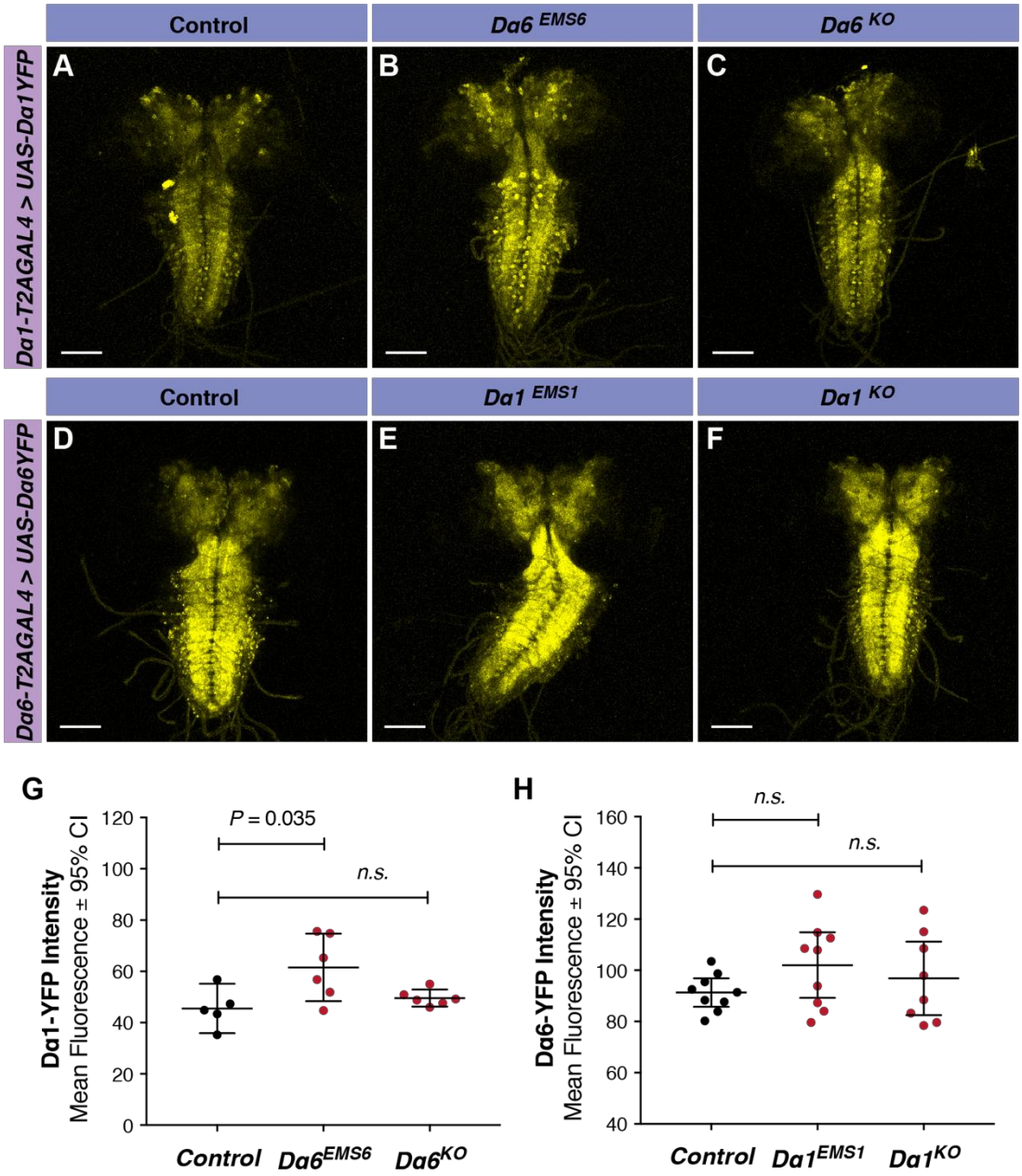

Figure 4.4 Analysis of fluorescently tagged nAChR subunit expression in *Dα1* and *Dα6* mutants

(A-C) *UAS-Dα1YFP* expression driven by *Dα1 T2AGAL4* and (D-F) *UAS-Dα6YFP* expression driven by *Dα6 T2AGAL4*, in third instar larval brain of *Dα6* mutants and *Dα1* mutants, respectively. Comparisons were made to expression of the respective YFP-tagged subunit in the wildtype. Scale bars are 100μm. Graphs show quantification of the fluorescence intensity of (G) Dα1-YFP and (H) Dα6-YFP in the respective nAChR mutants compared to the wildtype control. Student's t-test was used for statistical significance, where $P < 0.05$ is considered significant ($n \geq 6$). *n.s.*, not significant

4.3.3 Larval movement response to inhibition of possible pathways for negative cross-resistance

Given the above results suggest that the negative cross-resistance mechanism is unlikely to be due to altered receptor levels, several candidate pathways identified from the DEGs analysis of *Dα1* and *Dα6* mutants were examined. Chemical inhibitors were used to block these pathways and changes to third instar larvae response to insecticides, imidacloprid and spinosad was recorded. A larval motility assay, the Wiggle Index, was performed to measure the response to the insecticides. Both imidacloprid and spinosad have been shown to reduce larvae motility (Denecke et al. 2015). Bortezomib is a proteasome-specific inhibitor, used to block the proteasomal degradation pathway that might be responsible in the clearance of non-functional nAChR in the mutants (Chen et al. 2011). Similarly, the ubiquitination pathway, which might be involved in ubiquitin-proteasome degradation, was targeted using PYR-41, a ubiquitin-activating enzyme E1 inhibitor. To test for the involvement of protein trafficking, dynasore (dynamin inhibitor) and NDGA (ER-to-Golgi transport inhibitor) were included in the analysis.

Third instar larvae of a wildtype strain, *Armenia*^{14} were pre-treated with the chemical inhibitors for 1 hour prior to measuring larval motility in response to the addition of 3 ppm imidacloprid or 2 ppm spinosad. In the absence of insecticide, no significant differences in larval response to the individual chemical inhibitor compounds were observed when compared with the controls (Figure 4.5A). In examining the impact of the insecticides in isolation, there was a more rapid decline in RMR with imidacloprid than spinosad. The difference between the RMR values for imidacloprid and the control were significant after 15 minutes of exposure. After 60 minutes the decline in RMR was significant for both insecticides (Figure 4.5B). At the 90- and 120-minute time points the RMR values for the two insecticides were the same.

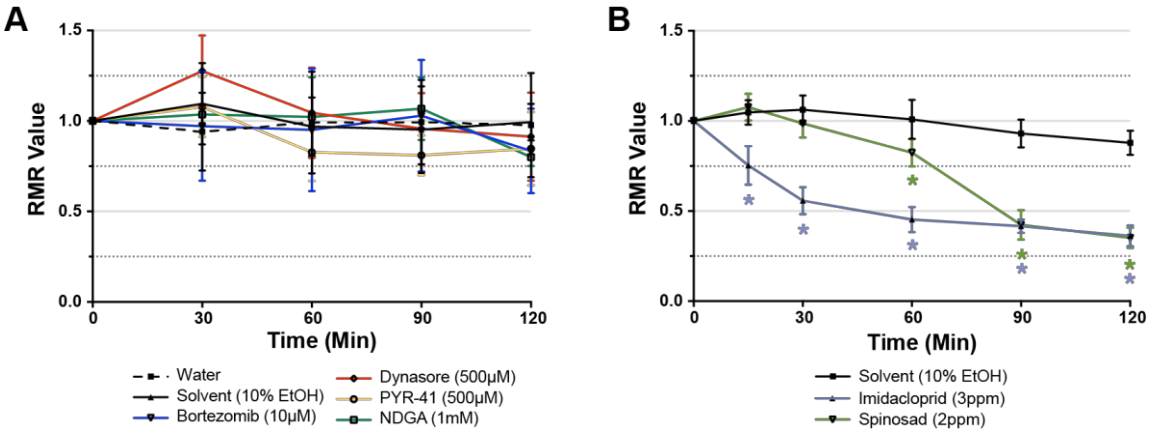

Figure 4.5 Larval motility response to inhibitors and insecticides

(A) Wiggle index analysis of *Armenia*^{14} in response to 1-hour pre-incubation with 10μM bortezomib, 500μM dynasore, 500μM PYR-41 or 1mM NDGA compared to the controls - water or 10% ethanol (EtOH). (B) Wiggle index analysis of *Armenia*^{14} in response to exposure to 3pmm imidacloprid or 2ppm spinosad. Error bars indicate 95% confidence intervals. Statistical significance between the treatment and control was evaluated using two-way ANOVA, followed up with Student's t-test for analysis at specific time points. Asterisk (*) denotes $P < 0.05$.

Pre-treatment with either bortezomib or dynasore, significantly delayed RMR changes in response to spinosad exposure. After 90 minutes of spinosad exposure, the RMR values were 0.72 for bortezomib and 0.88 for dynasore, compared to 0.42 for the control (Figure 4.6E-F). In contrast, only pre-treatment with dynasore significantly delayed the RMR drop in response to imidacloprid exposure (Figure 4.6A-B). After 30 minutes of imidacloprid exposure, the RMR values were 0.81 for dynasore, compared to 0.56 for the control (Figure 4.6B). Pre-treatment PYR-41 or NDGA did not have any significant impact on RMR values for larvae exposed to either imidacloprid or spinosad (Figure 4.6C-D and G-H).

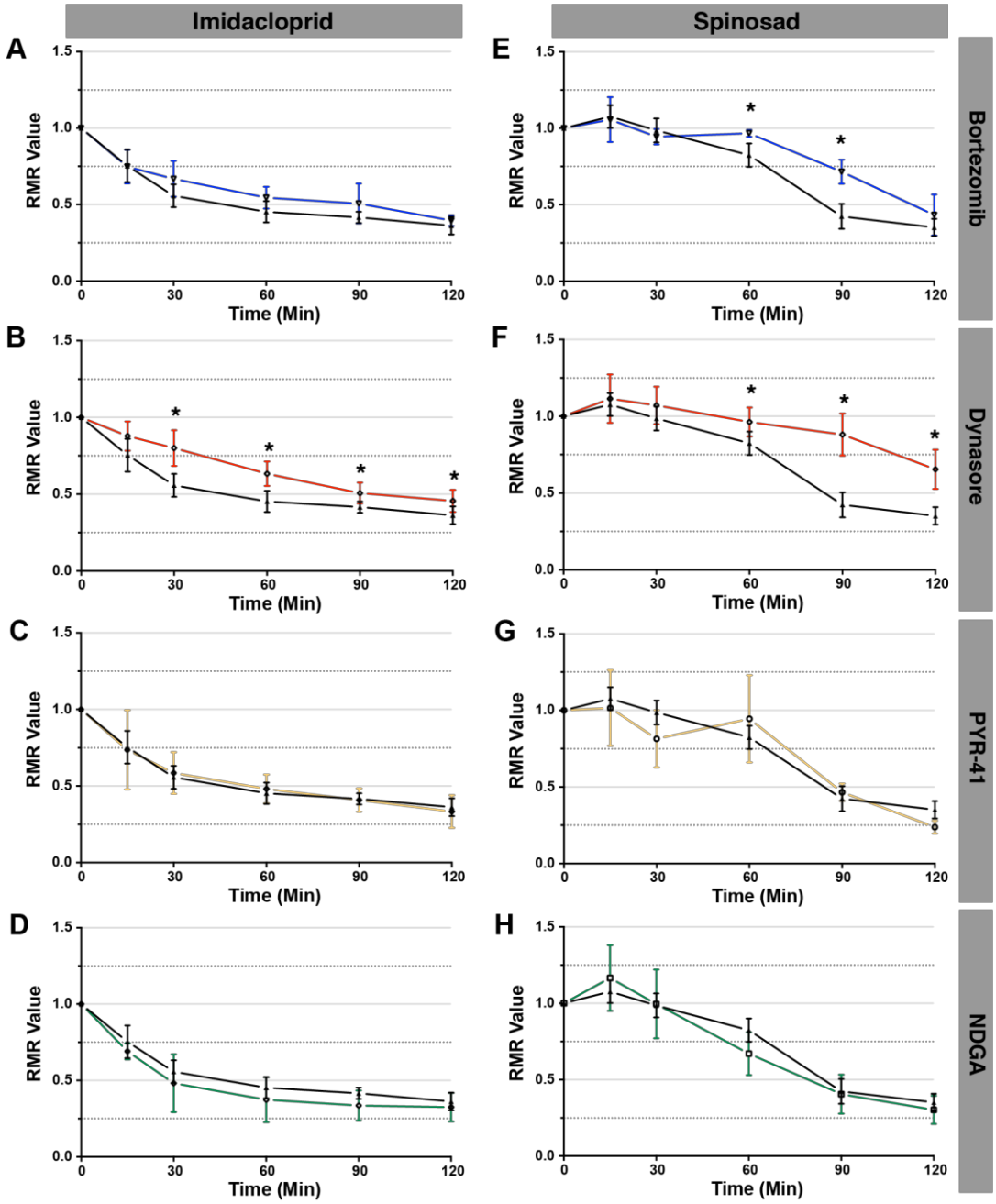

Figure 4.6 Larval motility response to insecticides following pre-treatment of bortezomib, dynasore, PYR-41 and NDGA

Wiggle index analysis of *Armenia*[14] in response to (A-D) 3pmm imidacloprid or (E-H) 2ppm spinosad, after 1-hour pre-incubation with 10μM bortezomib (blue), 500μM dynasore (red), 500μM PYR-41 (yellow) or 1mM NDGA (green) compared to pre-incubation with 10% EtOH as a control. Error bars indicate 95% confidence intervals. Statistical significance between the treatment and control was evaluated using two-way ANOVA, followed up with Student's t-test at specific time points. Asterisk (*) denotes $P < 0.05$.

Dα1^{EMS1} and *Dα6*^{EMS6} larval responses were then analysed using the same methods. When comparing responses at 3 ppm imidacloprid exposure, significantly higher RMR values were recorded for *Dα1*^{EMS1} than *Armenia*^{14}. *Dα6*^{EMS6} showed significantly lower RMR values compared to the *Armenia*^{14}, after 30 minutes of exposure (Figure 4.7A). In response to 2 ppm spinosad, *Dα6*^{EMS6} showed significantly higher RMR values than *Armenia*^{14}. *Dα1*^{EMS1} showed significantly lower RMR value than *Armenia*^{14} but only at the 60-minute time point. The response was similar to that of *Armenia*^{14} at the later time points (Figure 4.7B). These observations further demonstrated that *Dα1*^{EMS1} and *Dα6*^{EMS6} have a reduced response to imidacloprid and spinosad, respectively, matching their resistance phenotypes.

Both bortezomib and dynasore pre-treatment delayed the RMR drop in spinosad-treated *Dα1*^{EMS1} (Figure 4.8E-F). Similarly, dynasore pre-treatment (but not bortezomib), significantly reduces the RMR drop in imidacloprid-treated *Dα6*^{EMS6} (Figure 4.8C-D). Neither of the pre-treatments impacted the RMR values for *Dα1*^{EMS1} larvae in response to imidacloprid or the *Dα6*^{EMS6} larvae in response to spinosad (Figure 4.8A-B and G-H).

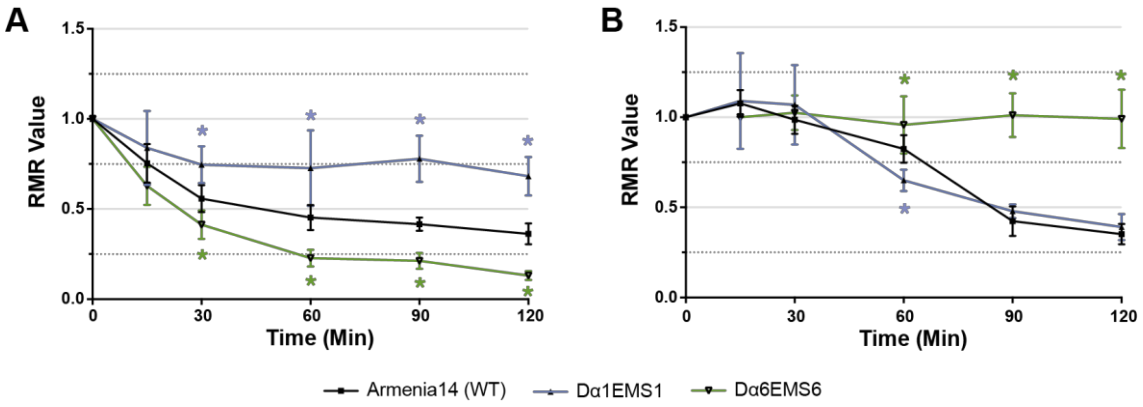

Figure 4.7 Larval motility responses indicate negative cross-resistance between imidacloprid and spinosad in *Dα1*^{EMS1} and *Dα6*^{EMS6}

Wiggle index analysis of *Armenia*^{14}, *Dα1*^{EMS1} and *Dα6*^{EMS6} in response to (A) 3pmm imidacloprid or (B) 2ppm spinosad. Error bars indicate 95% confidence intervals. Statistical significance between the treatments was evaluated using two-way ANOVA, followed up with Student's t-test at specific time points. Asterisk (*) denotes $P < 0.05$.

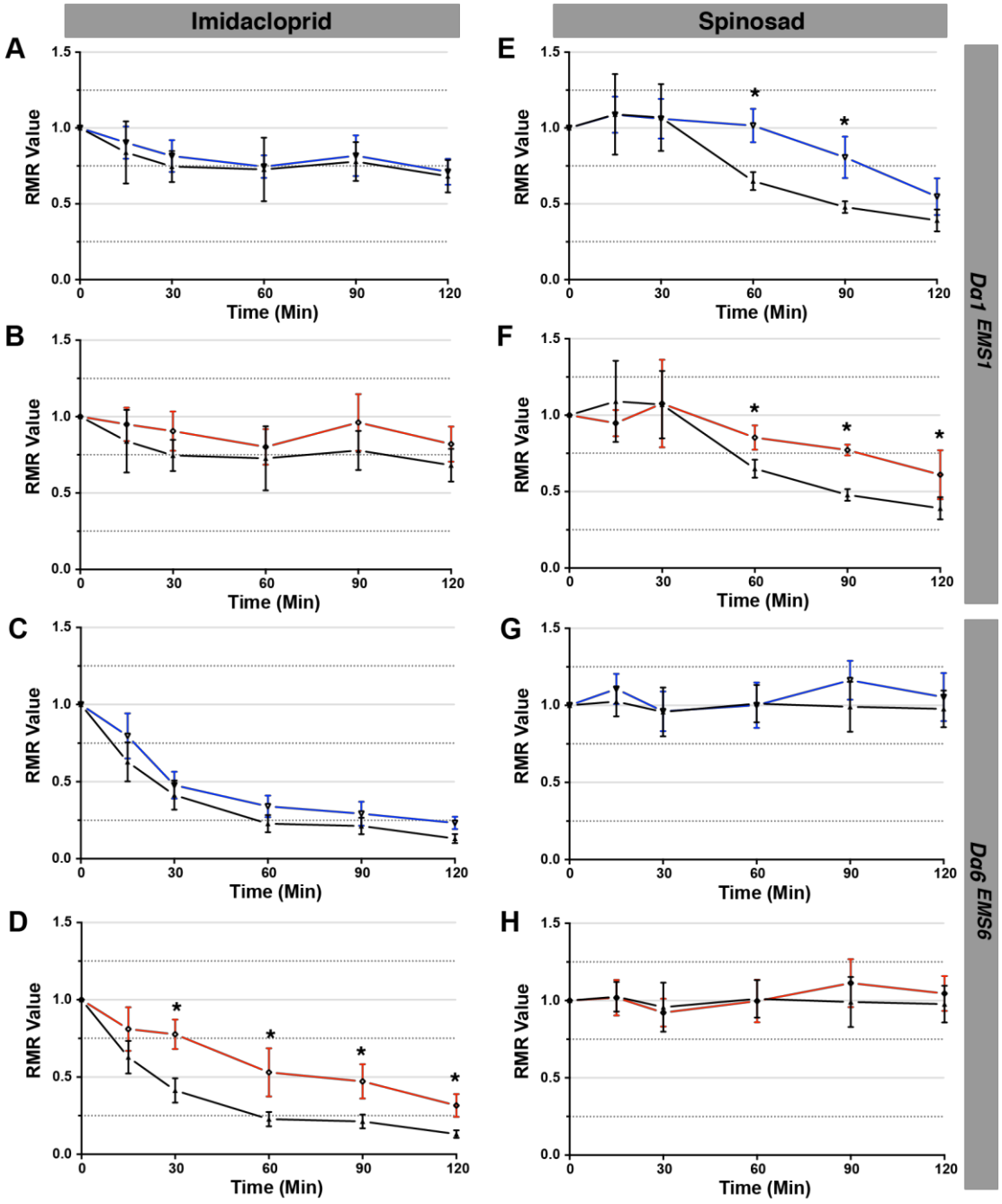

Figure 4.8 *Dα1* and Dα6 mutant's larval motility response to insecticides and inhibitor pre-treatments

Wiggle index analysis of $Dα1^{EMS1}$ and Dα6EMS6 in response to (A-D) 3ppm imidacloprid or (E-H) 2ppm spinosad, after a 1-hour pre-incubation with 10μM bortezomib (blue) or 500μM dynasore (red) compared to pre-incubation with 10% EtOH as control. Error bars indicate 95% confidence intervals. Statistical significance between the treatments was evaluated using two-way ANOVA, followed up with Student's t-test at specific time points. Asterisk (*) denotes $P < 0.05$.

4.4 Discussion

4.4.1 Analysis of nAChR subunits localisation in third instar larval brain using T2AGAL4 strains

The histological localisation of nAChR subunits in *Drosophila* has always required secondary staining, whether using immunohistochemistry, antigen-based detection, *in situ* hybridisation or even when examining the localisation of transcripts (Chamaon et al. 2002; Jonas et al. 1990; Lansdell and Millar 2000a; Sawruk et al. 1990). This requirement has been bypassed for the localisation of *Dα6* expression by cloning the promoter region of the *Dα6* gene to engineer a construct which was used to drive the expression of wildtype *Dα6* cDNA in a pattern that restored spinosad sensitivity to a *Dα6* mutant (Perry et al. 2015). While providing some evidence of appropriate expression, this promoter sequence may not precisely recapitulate the pattern of expression for the endogenous gene, as there may be distal regulatory elements located outside the specific regions cloned into the constructs. To examine whether *Dα1* and *Dα6* are expressed in the same cells, and thus might be co-assembled or have the potential to compensate for each other, T2AGAL4 strains were used to visualise the native expression patterns of the two genes in the larval brain.

Similar gene expression patterns for the *Dα1* and *Dα6* subunits were observed based on the expression of a membrane GFP reporter by the T2AGAL4 drivers (Figure 4.3). The localisation was mainly in the central brain and the VNC of the larval brain, which has been reported for *Dα6* based on its promoter expression (Perry et al. 2015). Noticeably, the fluorescent signals were localised in the cortex of the VNC and in the motor neurons. Expression in the cortex of the central brain, possibly in the cell bodies and the mushroom bodies, was observed for both subunits. A recent study has also demonstrated high expression of *Dα1* and *Dα6* in mushroom bodies of adult brain using a similar T2AGAL4 system (Kondo et al. 2020). This correlates with the findings reported here for larval brains. The targeted DamID analysis also indicated positive transcription of *Dα1* in *Dα6*-expressing neuronal cells (Section 3.3.2.1). Combining these observations, it is highly likely that Dα1 and Dα6 subunits are expressed in a similar subset of

neurons. These T2AGAL4 strains also provided a tool with which we could examine changes in protein levels.

4.4.2 A system to examine Dα1 and Dα6 nAChR subunit protein levels

Fluorescently tagged proteins are valuable tools for the visualisation of proteins in living cells. Here, a strategy that made use of full-length cDNA constructs with the protein tag, in combination with *Dα1* and *Dα6* Minos-mediated transposon gene trapping strains, was employed to express the tagged receptor under the control of the appropriate endogenous regulatory elements (Morin et al. 2001; Venken et al. 2011). The *Dα1-T2AGAL4* and *Dα6-T2AGAL4* express GAL4 while truncating the gene products early, inside the extracellular ligand-binding domain of the nAChR subunits (Figure 4.2). This allowed for expression of the tagged subunit construct in a null background. The YFP tags are located around non-conserved residues inside the large intracellular loop, between the TM3 and TM4 of both Dα1 and Dα6 subunit (Somers 2015; Nguyen et al. manuscript in preparation). This positioning avoided any conserved protein residues or domains known to be important for the receptor function and was informed by the position of tags in vertebrate nAChR subunits (Nashmi et al. 2003). Importantly, these constructs has been demonstrated to restore native levels of susceptibility to neonicotinoids and spinosad, in *Dα1* and *Dα6* mutants respectively (Somers 2015; Nguyen et al. manuscript in preparation), suggesting that the tagged subunits are assembled into functional receptors and are, therefore, a valid alternative to examine the nAChR subunit protein levels.

Despite these, it is important to note that, here, the systems were set up to be heterozygous at both the T2AGAL4 insertion and the protein tag construct insertion. Co-expression of the native, non-tagged subunit alongside the protein tag construct is expected but, assuming that there is no discrimination against expression of either of the two alleles, it still provides a valid system to measure protein expression changes. Expression of Dα1-YFP and Dα6-YFP using the same T2AGAL4 drivers showed that the localisation patterns were very similar to those shown using CD8 reporter expression (Figure 4.3 and Figure 4.4). A lower fluorescence signal was observed for the tagged subunits compared to the

labelled membrane CD8 reporter protein. This could be due to co-expression of the tagged and non-tagged subunit or suggesting that, despite the transcriptional amplification by the UAS/GAL4 system, the level of the tagged nAChR proteins is being tightly regulated.

4.4.3 Negative cross-resistance phenotypes are not correlated with nAChR subunit protein level changes

As the transcriptional analysis did not detect any nAChR gene expression changes that would provide a simple explanation for the negative cross-resistance phenotype, protein levels were examined.

4.4.3.1 Dα6 levels in the *Dα1* mutant backgrounds: -

In the $D\alpha1^{EMS1}$ mutant, that produces truncated Dα1, the upregulation of Dα6 subunit was hypothesised as a possible compensation mechanism that might lead to the spinosad hypersensitivity. Negative cross-resistance was not observed in the full knockout, $D\alpha1^{KO}$, so no compensatory effect expected. These two mutants, therefore, provided an ideal test for the compensation hypothesis. Western blotting analysis using Dα6 specific antibody showed reduced expression of Dα6 in $D\alpha1^{EMS1}$ in adult heads, but no significant changes were observed in dissected third instar larval brains. The result from larval samples was supported by the observation of no significant changes in Dα6 level in larval brains of $D\alpha1^{EMS1}$, in the YFP-tagged subunit analysis (adults were not examined as toxicology was only performed on larvae). Downregulation Dα6 in $D\alpha1^{EMS1}$ in adult may have an impact on spinosad sensitivity, however the level of insecticide sensitivity in adult flies was never measured. It is possible that nAChR compensation may occur at different *Drosophila* life stages based on these observations, however examining this is beyond the scope of this study, focussed on characterising the negative cross-resistance mechanism in *Drosophila* larvae. Thus, in summary, these data provide no support for the compensation hypothesis that predicted an increase in Dα6 protein levels to account for the spinosad hypersensitivity observed in $D\alpha1^{EMS1}$ larvae. Elevated levels of the Dα6 protein were not detected in $D\alpha1^{EMS1}$ larvae. With or without the compensation

hypothesis, there was no reason to expect anything other than the lack of change in Dα6 levels observed in the *Dα1*^{KO} mutant.

4.4.3.2 Dα1 levels in the *Dα6* mutant backgrounds: -

Analysis of YFP-tagged Dα1 subunit in *Dα6* mutants revealed upregulation of Dα1 levels in larval brains of *Dα6*^{EMS6}, consistent with the negative cross-resistance profile and the expectation that an upregulation of Dα1 may compensate for the mutated Dα6 subunit, leading to increased sensitivity to neonicotinoids. However, no significant change in Dα1 level was recorded for the *Dα6*^{KO}, despite the fact that this mutant is also hypersensitive to neonicotinoids. Thus, fluorescent tagged protein quantification showed a compensatory increase of Dα1 in one *Dα6* mutant allele that could explain nitenpyram and imidacloprid hypersensitivity. However, the lack of Dα1 upregulation in the *Dα6* knockout suggests that this is either allele specific or that a different mechanism for the increased neonicotinoid sensitivity exists. Unfortunately, a Dα1 specific antibody could not be obtained to confirm these Dα1 expression changes in the *Dα6* mutants.

The results presented in both Chapter 3 and this chapter suggest that compensation of the nAChR subunits is not involved in the negative cross-resistance phenotypes examined here and that other changes must underlie the phenotype.

4.4.4 Inhibition of candidate functional pathways behind the insecticide hypersensitivity altered larval movement response to insecticides

The lack of evidence for expected changes in nAChR subunit expression raised the possibility that negative cross-resistance may not necessarily be dependent on the nAChR subunit level, but rather an accumulation of other changes at the synapse that contribute to the observed insecticide hypersensitivity. For example, an entirely indirect mechanism stemming from perturbations to oxidative stress and ROS levels in nAChR mutants, identified from transcriptional analysis, may increase their susceptibility to the insecticides (refer Section 3.4.5). Protein trafficking and ubiquitin/proteasome-mediated degradation are pathways associated with nAChR assembly and regulation. The targeted DamID analysis on mutants of *Dα1* and *Dα6* revealed enrichment of DEGs associated with these pathways (refer Section 3.4.6). Hence, in this chapter, endocytic trafficking, ubiquitination and protein degradation were disrupted to determine whether they impacted the insecticide response and could contribute to the mechanism of insecticide hypersensitivity.

The Wiggle Index was utilised to measure larval response following insecticide exposure (Denecke et al. 2015). While the assay showed $D\alpha6^{EMS6}$ hypersensitivity to imidacloprid, $D\alpha1^{EMS1}$ hypersensitivity to spinosad was only observed at the 60-minute time point (Figure 4.7B). At all other time points the responses of the mutant and wild type control were not significantly different. It is possible that the concentration of spinosad used oversaturated the response in both $D\alpha1^{EMS1}$ and wildtype after 60 minutes. A lower concentration of spinosad might be able to better differentiate the spinosad sensitivity levels between the two strains.

The candidate pathways associated with the insecticide hypersensitivity in the mutants were blocked using chemical inhibitors. Significant changes in larval movement response to insecticide were only observed in the wildtype following pre-treatment of dynasore (an inhibitor of dynamin-mediated endocytosis) or bortezomib (an inhibitor of the proteasome), but not PYR-41 (an inhibitor of E1

ubiquitin-activating enzyme) or NDGA (an inhibitor of ER-to-Golgi transport) (Figure 4.6).

4.4.4.1 Pre-treatment of dynamin-mediated endocytosis using dynasore altered larval movement response to imidacloprid and spinosad

Dynamin is essential for clathrin-dependent vesicle formation in endocytosis, as well as in post-Golgi vesicle-mediated transport (Abazeed, Blanchette, and Fuller 2005; Damke et al. 1994). In addition, clathrin-mediated endocytosis has been described to regulate fundamental processes including receptor turnover (McMahon and Boucrot 2011). These activities can be inhibited by dynasore, a compound classified as a dynamin inhibitor and the effect is reversible (Macia et al. 2006). Given vesicle formation is essential for receptor trafficking and turnover, inhibiting dynamin activity was expected to disturb normal nAChR activity and function. Indeed, our study demonstrated a delay in response to insecticides, for both imidacloprid and spinosad exposure (Figure 4.6B & F). Results from our assays using the lipoxygenase inhibitor, NDGA (reported to inhibit ER-to-Golgi protein transport (Fujiwara et al. 1998)) however suggest that clathrin-mediated transport prior to nAChR expression at the membrane is unlikely to be involved in the insecticide response, given that it did not have an effect (Figure 4.6D & H). Thus, it is likely that the dynamin-mediated endocytosis activity is the one essential for insecticide response. It could be that inhibition of this pathway using dynasore may disrupt nAChR internalisation for degradation which appears to be involved in spinosad-mediated insecticidal response (Nguyen et al. manuscript in preparation). Despite that, a similar effect of dynasore pre-treatment was also observed upon imidacloprid exposure, suggesting that this may not be specific to spinosad.

Inhibition of dynamin-mediated endocytosis using dynasore has been shown to decrease the insecticidal toxicity of Vip3Aa (Jiang et al. 2018). Vip3Aa is a vegetative insecticidal protein secreted by *Bacillus thuringiensis* that is toxic to Lepidopteran pests (Bergamasco et al. 2013). Vip3Aa was shown to bind the Sf-SR-C scavenger protein receptor and mediate dynamin-mediated endocytosis in exerting its toxic effect. Treatment of a *Spodoptera frugiperda* cell line with

dynasore reduced Vip3Aa entry into cells, and thus, decreased Vip3Aa toxicity (Jiang et al. 2018). If this is among the mechanisms by which imidacloprid and spinosad mediate their insecticidal activity, this could explain the reduced imidacloprid and spinosad toxicity upon dynasore pre-treatment observed here. However, there is no evidence indicating imidacloprid internalisation into the cell is required for its insecticidal toxicity. Dynasore can also suppress synaptic vesicle endocytosis (Chung et al. 2010). Stimulation of neurotransmission requires rapid recycling of synaptic vesicles and endocytosis (Ertunc et al. 2007; Sara et al. 2002). Exposure to the pyrethroid insecticide, deltamethrin depletes synaptic vesicles at motor nerve terminals of *M. domestica* and this is correlated with the gradual block of neurotransmission (Schouest, Salgado, and Miller 1986). Thus, if the inhibition of endocytosis by dynasore affects vesicle recycling for neurotransmitter release, it may disturb synaptic efficiency, reducing the excitation caused by imidacloprid or spinosad, explaining the slower response to the insecticide that was observed in the assay.

In terms of the requirement for dynamin-mediated endocytosis and trafficking for the mechanism of insecticide hypersensitivity, dynasore did not provide any additional impact on the response to imidacloprid and spinosad, in the imidacloprid-sensitive, *Dα6* mutant and spinosad-sensitive, *Dα1* mutant, respectively (compared to the wildtype control)(Figure 4.8D & F). These mutants are also highly resistant to insecticide that targets the mutated nAChR subunit, evidenced by the lack of any significant reduction in larval movement under conditions of insecticide exposure (Figure 4.8B & H). Under these two circumstances, effect of dynasore may have been masked. In contrast to wildtype, *Dα1* and *Dα6* mutants do not show any further changes in nAChR-mediated plasticity at the synapse upon exposure to light, indicating that both the light condition and the mutations on nAChR are involved in the same cellular pathway (Rosenthal et al. 2019). Similarly here, the endocytic trafficking pathway could be involved in the same cellular pathway as insecticide hypersensitivity. Thus, using a wider range of resistant/sensitive alleles and more concentrations of these compounds perhaps could provide further insight into the role that this mechanism may be playing.

4.4.4.2 Inhibition of proteasome-mediated degradation pathway using bortezomib altered the larval movement response to spinosad

In eukaryotes, the ubiquitin–proteasome system (UPS) regulates multiple cellular processes including signal transduction, cell cycle, transcriptional activation and programmed cell death (Willis et al. 2010). It also functions to eliminate misfolded or damaged proteins in the cell (Adams 2004; Goldberg 2003). UPS-mediated protein degradation has been largely associated with nAChR trafficking. The system regulates the amount of nAChRs that are assembled and the clearance of unassembled subunits in the ER/Golgi compartment, as well as nAChR turnover at the membrane (Christianson and Green 2004; Rezvani et al. 2010). Blocking the UPS pathway inhibits the response of *Drosophila* larvae to spinosad by preventing Dα6 from being removed from the membrane (Nguyen et al. manuscript in preparation). UPS-mediated protein degradation involves two separate steps, ubiquitination and proteasomal degradation (Figure 4.9). In this study, the effect of inhibiting both pathways upon insecticide exposure was examined.

A protective effect against spinosad exposure was observed when proteasome activity was blocked. Bortezomib is a drug designed to bind the proteasome and inhibit its function (Chen et al. 2011). Due to this activity, bortezomib has also been used as a chemotherapy treatment of multiple myeloma and mantle cell lymphoma (Hambley, Caimi, and William 2016). Bortezomib pre-treatment significantly delayed the reduction in larval movement upon spinosad exposure (Figure 4.6E). However, no effect of bortezomib pre-treatment was observed upon imidacloprid exposure (Figure 4.6A). This indicates that the proteasome-mediated degradation plays an important role in the effect of spinosad, but not of imidacloprid. The short period of bortezomib treatment used may not have any effect on expression of receptors that are already at the membrane. Thus, insecticide action on these receptors should not be different, unless the proteasome activity is required in the mode of action.

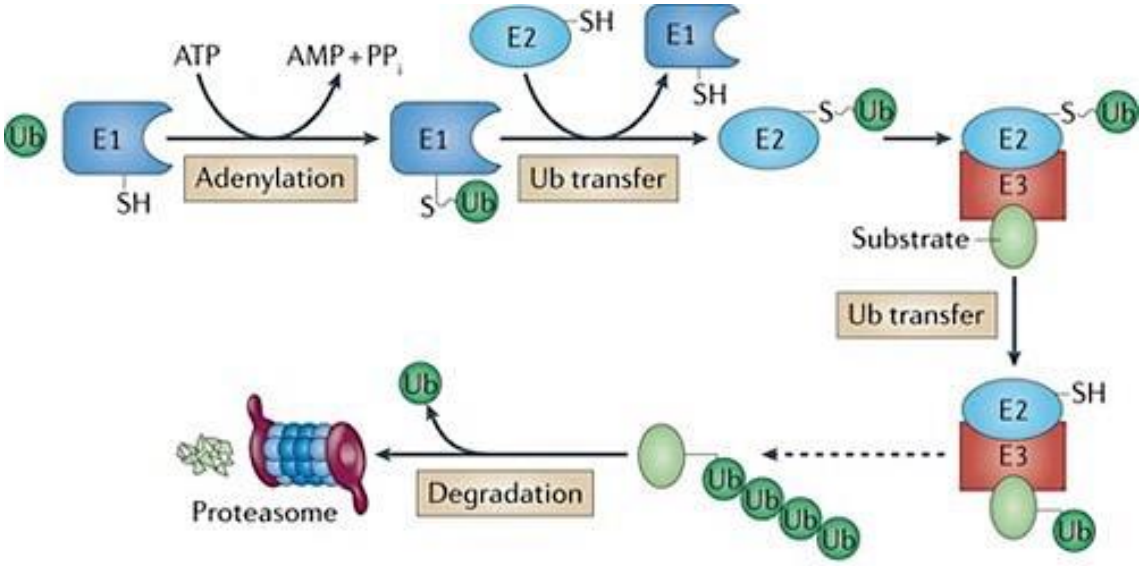

Figure 4.9 Ubiquitin–proteasome system (UPS) in eukaryotes

UPS-mediated protein degradation involves two separate steps, ubiquitination and proteasomal degradation. Ubiquitination involves a cascade of ubiquitin-activating enzymes. Ubiquitin (Ub) is activated by E1 ubiquitin-activating enzyme and conjugated by a thioester bond. This is the transferred to E2 ubiquitin-activating enzyme. Then, with assistance of E3 ubiquitin-activating enzyme it is transferred to the target protein. The growing polyubiquitin chain is recognised by proteasome for protein hydrolysis. Illustration from Maupin-Furlow (2012).

Spinosad's allosteric activity leads to an elimination of Dα6-containing nAChR receptors through UPS-mediated degradation (Nguyen et al. manuscript in preparation). This explains the observation of delayed spinosad-mediated response when proteasome was blocked in this study. By way of contrast, given that imidacloprid acts as nAChR agonist, it is unlikely that the targeted receptors are removed from the membrane or degraded. This is based on the many reports of upregulation of nAChRs in response to chronic stimulation by agonists such as nicotine (Benwell et al. 1988; Marks et al. 1983; Schwartz and Kellar 1983). Again, substantial differences in spinosad-mediated response were not observed after bortezomib treatment in the mutants (Figure 4.8E & G). The same level of protective effect against spinosad response was observed in the spinosad-sensitive mutant *Dα1*^{EMS1} (compared to the response in the wildtype control). The masked response in the mutant suggests the possibility that the protein

degradation pathway involved in the mode of action of spinosad may not be mutually exclusive to the mechanism of insecticide hypersensitivity.

The proteasome has the additional capacity to recognise and degrade proteins, that have been tagged with polyubiquitin chains, which serve as markers for degradation (Voges, Zwickl, and Baumeister 1999). Ubiquitination of receptors at the membrane also provides a mark for internalisation, although ubiquitin independent endocytosis has also been reported (Bulut et al. 2013; Huang, Goh, and Sorkin 2007; Marmor and Yarden 2004). Perturbation of the ubiquitination pathway is common in neurodegenerative diseases. Alzheimer's disease patients were previously described with reduced levels of E1 ubiquitin-activating enzyme (López Salon et al. 2000). E1 ubiquitin-activating enzyme catalyses the first step of the ubiquitination process, followed by ubiquitination by E2 and finally, E3 ubiquitin-activating enzyme (Figure 4.9)(Maupin-Furlow 2012). Theoretically, inhibition of E1 activity should block protein ubiquitination, and thus, prevents UPS-mediated degradation. However, here, no inhibition or delay in spinosad-mediated motility response was observed using pre-treatment with PYR-41, an inhibitor of E1 ubiquitin-activating enzyme (Figure 4.5G). Despite the observation of enrichment of the ubiquitination pathway alongside proteasome-mediated degradation from the cell-specific transcriptional analysis in the *Dα6* mutant (Section 3.3.3), the lack of change in insecticide response following PYR-41 pre-treatment suggests that the Dα6-containing nAChR degradation activated by spinosad exposure is independent of the E1 enzyme. Future investigation could block other ubiquitin-activating enzymes of this pathway, including the E2 and E3 enzyme, to further test the role of protein ubiquitination in nAChR degradation and its role in the mode of action of spinosad.

Chapter 5 : Discussion

5.1 Understanding the nAChR subtypes that are targets for insecticides

Several classes of insecticide, including the neonicotinoids and spinosyns, target nAChRs (Sparks and Nauen 2015). Neonicotinoids alone represent the most used insecticides, occupying more than 26% of the global insecticide market, meanwhile, the market share of the spinosyns is growing, with current demand in more than 80 countries (Santos and Pereira 2020; Sparks et al. 2017). Accordingly, members of the nAChR family have been an important focus for insecticide research to understand the mechanism by which insecticide interacts with the receptor, impacting function. This study, conducted in *D. melanogaster*, has identified an additional nAChR subunit that is targeted by insecticides. It has also provided insights into the subunit combinations that may assemble into pentameric nAChR subtypes that respond to particular insecticides/classes.

5.1.1 Neonicotinoid nAChR targets

In line with previous studies, this study found that the *Drosophila* nAChR subunits, Dα1 and Dβ2 are targets of neonicotinoid insecticides (Perry et al. 2008, 2012; Somers, Luong, Batterham, et al. 2017). Here, mutations that disrupt these receptor subunits were shown to confer a high level of resistance to both nitenpyram and imidacloprid. Significantly, the Dα2 subunit was also identified as a target for imidacloprid. Unlike the *Dα1* and *Dβ2* mutants, the *Dα2* mutants were only resistant to imidacloprid, showing selectivity between neonicotinoid insecticides at the nAChR subtype level. While highly similar at the protein level (~50% similarity Dα1 vs Dα2) there are only a few differences in key residues at the N-terminal loops (A-F) that coordinate ligand binding (Matsuda et al. 2009). Another difference between these subunits is potentially extensive N-glycosylation predicted for the Dα1 subunit (absent from Dα2), that could

influence receptor assembly or selectivity (Tomizawa and Casida 2003). Various combinations of the Dα1, Dα2 and Dβ2 subunits are likely to assemble into the main nAChR subtypes targeted by neonicotinoid compounds in *D. melanogaster*. These subunits were co-immunoprecipitated (Chamaon et al. 2002), and heterologous expression have shown that the Dα1 and Dα2 can co-assemble with a vertebrate β subunit to form an imidacloprid-sensitive receptor (Lansdell and Millar 2000b). Taken together, these support the hypothesis that these subunits are assembled into the same nAChR.

Considering the orthosteric ligand-binding site on the nAChR is provided by an interface between two subunits, there is the additional complication that there could be different interfaces present in a receptor subtype, depending not only on the subunit stoichiometry, but also the order in which the subunits are assembled. Multiple receptor subtypes have been shown to bind neonicotinoids in other insect species (Bass et al. 2011; Lind et al. 1998; Xu et al. 2010). Also, nAChRs with low- and high-affinity binding sites for neonicotinoids can be present in insects (Bass et al. 2011; Xu et al. 2010). Thus, it could be that Dα1, Dα2 and Dβ2 are assembling into multiple nAChR subtypes with different stoichiometries and that these respond to neonicotinoids. Alternatively, different combinations of these subunits may form receptors targeted by neonicotinoids. These possibilities are not mutually exclusive. Combining the findings from this study, with those from heterologous expression studies (Chamaon et al. 2000; Ihara et al. 2003; Lansdell and Millar 2000b; Schulz et al. 2000), there are at least two nAChR subtypes that are responsive to neonicotinoids. One consists of Dα1, Dα2 and Dβ2 and is responsive to both neonicotinoids. Another, consists of only Dα1 and Dβ2, is responsive to imidacloprid but not nitenpyram.

It is important to note that contribution of Dβ1 subunit was not analysed in this study. Homozygous deletion of Dβ1 disrupts pupal eclosion, and adults are poorly viable (Christesen et al. manuscript in preparation). For this reason, a *Dβ1* mutation was made homozygous in the nervous system using somatic CRISPR. These flies were found to have a high level of resistance to both nitenpyram and imidacloprid (Perry et al. manuscript in preparation). Considering this observation, it is likely that Dβ1 also contributes to neonicotinoid targets. Dα3

was also shown to co-immunoprecipitate with Dβ1 (Chamaon et al. 2000), and RNAi knockdown of *Dα3* confers nitenpyram resistance (Mitchell 2012). However, in this study, relatively low level of resistance to nitenpyram (approximately 1.5-fold) was found for the *Dα3* mutant, and the mutant was not resistant to imidacloprid (Figure 2.1). Hence, a direct contribution of Dα3 as neonicotinoids binding site on nAChR is not likely.

5.1.2 Spinosyn nAChR targets

Based on toxicity profiles presented in this study and results from earlier studies, only mutations in the *Dα6* gene are associated with high resistance levels to spinosyns (Perry et al. 2015; Perry, McKenzie and Batterham 2007; Somers et al. 2015; Watson et al. 2010). The α6 subunit is highly conserved among insect species, so it is not surprising that α6-mediated resistance has been discovered in many species (Bao et al. 2014; Baxter et al. 2010; Hsu et al. 2012; Puinean et al. 2013; Wang et al. 2016). It is possible that Dα6 is the only subunit that contributes to the nAChR targeted by spinosyns. However, heterologous expression in *Xenopus* oocytes showed that the Dα6 subunit did not form functional homomeric receptors (Lansdell et al. 2012; Watson et al. 2010). While heterologous expression studies may not always reflect the *in vivo* situation, the possibility that Dα6 forms heteromeric receptors that are targeted by spinosyns needs to be considered. Dα6 has been shown to form functional heteromeric nAChRs with Dα5, and with both Dα5 and Dα7. These studies were conducted using *Xenopus* oocytes with co-expression of a chaperone protein, RIC-3 (Lansdell et al. 2012; Watson et al. 2010). The Dα5/Dα6 receptor was shown to respond to spinosyn A (Watson et al. 2010). Flies carrying a deletion of *Dα7* were analysed in this study and only exhibited a very low level of resistance to spinosad (less than 1.5-fold resistance, compared to the over 2000-fold resistance by the *Dα6* knockout; Figure 2.1). A homozygous *Dα5* mutant strain is not available. MiMIC insertions into the gene that would truncate the protein are homozygous lethal at early larval stages, so this mutant is unsuitable for toxicity assays (Danielle Christesen, personal communication). The lack of data on Dα5 means we cannot discount the possible contribution of this subunit to nAChRs targeted by spinosyns.

5.2 nAChRs are not completely redundant

Functional redundancy is often a feature of multigene families. In the extreme case of some tandemly arrayed families, the DNA sequence of gene family members can be extremely similar due to homologous recombination and gene conversion (Graham 1995; Hurles 2005). In this context, all family members have the same functional capacity. A mutation that eliminated one family member is likely to have no detectable phenotype. The nAChR gene family is very different; there is significant sequence divergence between the family members (Figure 1.4). Nonetheless, functional redundancy could exist. Consider a mutation that eliminates the function of a family member that has a role in maintaining normal patterns of sleep. The mutant may have normal sleep behaviour if the mutation led to the loss of one or more receptor subtypes, but other existing receptor subtypes provided sufficient function to enable normal patterns of sleep to be maintained. An alternate explanation would see the loss of subtype(s) due to the mutation compensated for by other subtypes that included one or more subunits that would not normally function in the maintenance of patterns of sleep. In the circumstance where one receptor subtype is replaced by another, the replacement is unlikely to have precisely the same electrophysiological properties. This would have repercussions for neural signalling, the detection of which would depend on their severity and the sensitivity with which phenotypic change could be measured. A level of functional redundancy is observed when considering viability. While Dβ1 and Dα5 mutants are poorly viable and lethal, respectively, loss-of-function mutants for the other subunits are all viable (Fayyazuddin et al. 2006; Luong 2018; Somers, Luong, Mitchell, et al. 2017; Christesen et al. manuscript in preparation; Perry et al. manuscript in preparation). There is also a level of functional redundancy, in the capacity to bind neonicotinoids. Four subunits (Dα1, Dα2, Dβ1 and Dβ2) have been implicated in neonicotinoid binding. Loss of function of any one of these subunits leads to a moderate level of resistance, as observed here and in earlier studies (Perry et al. 2008, 2012; Somers, Luong, Batterham, et al. 2017), because a population of subtypes capable of binding the insecticide remains present. In stark contrast, there may be no redundancy in terms of spinosad binding. To date,

Dα6 is the sole target identified, although Dα5 warrants further investigation (refer Section 2.4.2). Nonetheless *Dα6* mutants have extremely high levels of resistance.

In terms of compensation, a mechanism involving the upregulation of nAChR subunits was invoked at the outset of this research to explain negative cross-resistance. While there is a similar expression pattern of the Dα1 and Dα6 subunits in the larval CNS (Figure 4.3 and Figure 4.4), suggesting that the neonicotinoid and spinosyn targets are likely being expressed in the same cells, we found that there was not a strong case for the compensation being altered expression at either the transcript or protein level. None of the genes that encode for the nAChR subunits targeted by neonicotinoid and spinosyn were upregulated in the mutants (Chapter 3). The only evidence found, that was consistent with this hypothesis, was the ~35% upregulation of Dα1 protein levels observed in the background of *Dα6* mutant, $D\alpha6^{EMS6}$ (Section 4.3.2, Figure 4.4), supporting a case for it to possibly underlie neonicotinoid hypersensitivity in the mutant. However, as a limited number of alleles for a subset of the nAChR genes has been investigated, the possibility that compensation may occur with loss of function of other alleles or genes cannot be discounted.

In looking for evidence of compensation involving nAChR gene expression, major shifts in the expression of other genes were discovered. Chapter 3 presented evidence that transcriptomic changes occur in first instar larvae when the Dα1, Dα2 and Dα6 subunits are lost. Similar perturbations were observed in the neuronal cells of third instar larval brains of *Dα1* and *Dα6* mutants. Pathways including transmembrane transport, oxidoreductase activity and proteolysis were shown to be affected in first instar larvae based on the analysis of differentially expressed genes in the $D\alpha1^{\Delta DH}$, $D\alpha2^{\Delta(3)4E}$ and $D\alpha6^{KO}$ mutants (Section 3.3.1.2). Evidence of disruption in nervous system development and neuronal cell function was more apparent when specific neuronal cells were analysed, particularly in the $D\alpha6^{EMS6}$ strain (Section 3.3.3). These indicate that the loss of the nAChR subunit function led to dysregulation of the several pathways involved in neuronal activity as well as stress responses in the CNS, something which could possibly lead to neurodegeneration. A recent study found an increase in the size and

number of vacuoles in the adult brain of an *Dα6* knockout mutant. This suggests that accelerated neuronal degeneration may be occurring in the mutant (Martelli 2020).

The *Dα1* and *Dα6* mutants also appear to have very different expression profiles. This probably reflects a difference in their roles in signalling at the synapse. In the cell-specific targeted DamID analysis, both the *Dα1* and *Dα6* mutants affected basic functions linked to nervous system activity (including GO terms for brain development, eye development and locomotor behaviour), but the *Dα6* mutant was shown to affect more processes relevant to neuronal function (Figure 3.10 and 3.11). Combining our data with various previous studies, it is highly likely that these nAChR subunits provide distinct functions in contributing to neuronal activities in the CNS. While significant impacts on gene expression are observed in mutants, it is not clear the extent to which they ameliorate the impact of the loss of subunit function, as compared to compounding it (for further discussion see Section 5.4).

The nAChR genes studied here are widely expressed in the nervous system (Figure 3.6 and Figure 4.3). They also have the potential to be incorporated into multiple receptor subtypes with differing properties. Considering these factors, any given subunit could impact a wide variety of receptor functions and traits. Exemplifying this, a loss of Dα1 function has been associated with defects in sleep, courtship, mating and longevity (Somers, Luong, Mitchell, et al. 2017). But to date none of the nAChR subunit mutants, including this knockout, have been meticulously examined for a wide range of developmental, morphological, behavioural, fitness and life history traits. Both the capacity for individual subunits to have multiple functions and the transcriptional perturbations observed here, suggest that such studies are likely to be revealing. Given that for any give mutant there is both a loss of nAChR subunit function and substantial shifts in gene expression, it may not be possible to unambiguously assign mutant phenotype to the loss of function.

This study also informs discussions on fitness costs associated with insecticide resistance (Somers, Luong, Batterham, et al. 2017). That resistant mutations disrupt nAChR function may well incur fitness cost. Equally, it is likely that there

are optimal patterns of gene expression that allow insects to adapt to their environment. The disruption of gene expression may reduce the capacity to survive and reproduce in the field.

While the research conducted has wider implications, the focus of this thesis was negative cross-resistance, so the balance of this discussion returns to this theme.

5.3 nAChR subunit mutations lead to insecticide hypersensitivity

The nervous system, and in particular synaptic connections, are highly adaptable and plastic (refer Section 4.1.1). This plasticity is essential in maintaining balanced and correct signalling in the nervous system, controlling various important behavioural and motor functions. Deficits in particular signalling pathways may be compensated for by alterations of existing pathways or the addition of novel pathways (refer Section 4.1.2). Here, the perturbations of synaptic signalling due to mutations in nAChR subunits has led to the detection of negative cross-resistance between insecticides. Chapter 2 identified a negative cross-resistance relationship between neonicotinoids and spinosyns in *Dα1* and *Dα6* mutants, while *Dα2* mutants have negative cross-resistance to two neonicotinoids, nitenpyram and imidacloprid. This phenotype was observed for a variety of nAChR subunit mutations, including a single amino acid replacement, an altered ligand-binding domain, truncation of a protein subunit and a complete loss of gene expression. Thus, it is likely that the loss of receptor function, rather than a particular type of mutation, underlies negative cross-resistance. While there was a correlation between the severity of the receptor subunit modifications and the level of insecticide resistance (single amino acid replacement < protein truncation < null expression), the level of hypersensitivity to the second insecticide did not follow a clear pattern.

In seeking to understand the phenomena investigated in this thesis, it is clear that in the subunit mutants, downstream perturbations of gene expression are involved and that nAChR expression changes are not. It may, therefore, be more productive to focus on ‘insecticide hypersensitivity’ rather than negative cross-resistance.

5.4 Expression changes in nAChR mutants implicates several pathways in insecticide hypersensitivity

The targeted DamID analysis identified transcriptional changes that are specific to the neuronal cells (Section 3.3.2). These changes are more likely to result directly from loss of the nAChR subunit than those detected by the RNAseq analysis for whole first instar larvae (Section 3.3.1). The RNAseq analysis reflect changes inside and outside the nervous system. The idea that the loss of nAChR subunit function inside the nervous system could impact gene expression changes outside of it, is extremely interesting and worthy of further investigation. However, some changes outside the nervous system could mask those inside it. Indeed, the targeted DamID analysis demonstrated more obvious evidence for altered gene expression and clearly identified neuronal development and synaptic signalling as pathways that were disrupted in the *Dα1* and *Dα6* mutant, compared to the RNAseq analysis (Figure 3.10 and Figure 3.11).

The targeted DamID analysis identified differentially expressed genes in the neuronal cells, associated with pathways that could be mediating insecticide hypersensitivity in these mutants. Enrichment of pathways indicating an increase in oxidative stress levels was apparent in the *Dα6* mutant and it was also observed in *Dα1* mutant, albeit to a lesser extent. This was also found in the RNAseq analysis of the first instar larvae. The association between nAChRs and oxidative stress has been made before. The *Dα6* gene was associated with increased susceptibility to an oxidative stress inducing treatment (Weber et al. 2012). Interestingly, both imidacloprid and spinosad treatments were shown to induce oxidative stress in neuronal and metabolic tissues of *Drosophila* (Martelli 2020). These mutants, especially the *Dα6* mutant, may have a reduced capacity to deal with oxidative stress, making them vulnerable to further elevation of oxidative stress. An elevation of oxidative stress may contribute to insecticide hypersensitivity. We tested two different classes of insecticide here, however, many other pesticide compounds including organophosphates, permethrins, paraquat as well as ivermectin, have been demonstrated to induce oxidative stress, and thus, the mutants may also be hypersensitive to these compounds (Boussabbeh et al. 2016; Lukaszewicz-Hussain 2010; Ogueji et al. 2020; Tarimo

et al. 2018; Touaylia et al. 2019). *Dα1* and *Dα6* mutants should be tested for sensitivity to these compounds.

The targeted DamID also showed that genes associated with protein regulation, including trafficking, ubiquitination and degradation, were differentially expressed in the neuronal cells of the *Dα6* mutant (Figure 3.10 and Figure 3.11). This was observed to a lesser extent in the *Dα1* mutant. Protein level regulation such as folding and trafficking are important for nAChR subunit maturation and assembly (Brodsky and Skach 2011), meanwhile the ubiquitin-proteasome system (UPS) regulates nAChR assembly, turnover and clearance at the membrane (Christianson and Green 2004; Rezvani et al. 2010). Dysregulation of these functions could disturb insecticide responses of the mutants. Many of these genes were upregulated in the *Dα6* mutant (Figure 3.11).

When the chemical inhibition of these pathways was examined, dynamin-mediated endocytic transport, but not ER-to-Golgi transport, reduced sensitivity of the *Dα6* mutant to imidacloprid (Figure 4.8D). A similar observation was made for the *Dα1* mutant, which became less sensitive to spinosad (Figure 4.8F), indicating involvement of the dynamin-mediated endocytic transport in mediating the response to both insecticide classes. Dynamin is essential for clathrin-dependent endocytosis, as well as vesicle-mediated transport, regulating fundamental processes, including receptor turnover (Abazeed et al. 2005; Damke et al. 1994; McMahon and Boucrot 2011). Inhibition of the proteasome using bortezomib only delayed the larval response to spinosad in the *Dα1* mutant (Figure 4.8E). The results indicate that changes in both endocytic trafficking and proteasome-mediated degradation pathways could play a role in hypersensitivity to spinosad, while only endocytic trafficking pathways appear to be involved in hypersensitivity to imidacloprid.

The extent to which dysregulation of these pathways (oxidative stress, dynamin-mediated endocytosis and proteasome-mediated degradation) may account for the observed insecticide sensitivity is not clear. Further investigations on these dysregulated pathways in the subunit mutants may be able to shed more light on their contribution to the observed insecticide hypersensitivity. A direct assay to test insecticide toxicity level following induction or inhibition of these pathways

may be revealing. For example, including treatment using an antioxidant with the insecticide toxicology bioassay (Section 2.2.5) could indicate if the insecticide hypersensitivity can be modulated by reducing oxidative stress level in the mutants. Insecticide hypersensitivity appears to be a much more complicated mechanism than the initial hypothesis of nAChR subunit compensation proposed and will require a lot more work to unravel.

5.5 Implication of insecticide hypersensitivity for pest control

Insecticide resistance poses a major threat to food and fibre production, rendering insecticides ineffective, placing more pressure on other available chemicals and requiring the development of new chemicals, an expensive task made more difficult due to ever stricter regulatory constraints. Current approaches to delay the evolution of insecticide resistance are the rotation or sequential use of compounds with different modes of action. In recent years these approaches have been recommended by IRAC, which has classified various commercially available insecticides into different groups or subgroups according to their mode of action for this purpose (Sparks and Nauen 2015). However, the combinations of insecticides that work best together were not described in detail.

Chapter 2 provided evidence that the hypersensitivity is present across a range of *Dα1*, *Dα2* and *Dα6* alleles, although levels do vary between them. Therefore, it is reasonable to assume the strategy could apply to a range of nAChR subunit mutations conferring spinosyn or neonicotinoid resistance that might arise in the field. This reciprocal hypersensitivity could manage resistance to these two insecticide classes simultaneously, extending their current life in the field. Application of neonicotinoids and spinosyn in rotation, would be predicted to result in suppression of spinosyn resistant strains by neonicotinoids and vice versa. This strategy focuses on target site resistance, but it should be noted metabolic cross resistance to these insecticides has not been reported. The proposed strategy should not increase risk of metabolic resistance emerging. As this study also provided evidence for nAChR specificity for different insecticides from the neonicotinoid class, substituting different neonicotinoid compounds in turn, as part of a rotational strategy (neonicotinoid-imidacloprid, spinosyn, other

compound, neonicotinoid-nitenpyram, spinosyn, other compound) could also provide some suppression of target site resistance to these compounds. This may not be practical as compounds may not be suitable for the same field application methods or against the same insect pests, hence a broader analysis of hypersensitivity could provide further combinations that may be useful in more situations. Neonicotinoids and spinosyns do share some applications, in particular as flea treatments for companion animals (nitenpyram – Capstar®, imidacloprid – Advantage® and spinosad – Comfortis®)(Vo et al. 2010).

Although the experiments described here have been conducted in an organism that is not a pest, give that (1) the orthology of genes conferring resistance to neonicotinoids and spinosyns in *D. melanogaster* and pest species and (2) resistance to both classes of insecticides exists in pests, these findings should apply to pest species. Furthermore, it should be noted that there are several other classes of insecticides targeting nAChRs - sulfoximines, butenolides, and two newly introduced compounds, cycloxaprid and the mesoionics (Sparks and Nauen 2015). Here, combinations from just two insecticide classes have been tested. There is obviously the potential for other 'negatively cross-resistant' combinations to exist, particularly given that hypersensitivity in testing two chemical compounds of the same class, nitenpyram and imidacloprid. Similarly, if insecticide-induced oxidative stress is the main cause of the insecticide hypersensitivity in these nAChR mutants, hypersensitivity to a variety other insecticide compounds might be identified. Both the mutants used here and the spinosad-resistant field strains of the many pest species that carry *α6* mutations would be useful for this purpose.

5.6 Conclusion and future directions

This study has highlighted the fact that there are still many unknowns in insect nAChR biology and that much more work can be done to addressing questions around nAChR compensation and receptor assembly. It has been established that insecticides, used as (semi-)selective nAChR probes, together with insecticide resistance phenotypes of nAChR mutants, can assist with the task of dissecting which receptor subunits may co-assemble.

Insecticide hypersensitivity does not appear to be due to the receptor but is likely to result from altered gene expression in pathways that are perturbed due to its loss. These pathways may provide new targets for future insecticide development or synergists that could enhance the efficacy of insecticides or assist in overcoming resistance. Although the reciprocal hypersensitivity relationship between *Dα1* and *Dα6* mutants was characterised here, the mechanism behind the insecticide hypersensitivity requires further study. Despite the similar negative cross-resistance phenotypes between mutations in different nAChR subunits, the changes in gene and protein expression observed differed between these mutants. This may indicate an allele-specificity of the molecular changes, complicating our attempts to understand the phenomenon. It is unlikely that the negative cross-resistance phenotype in the nAChR mutants is mediated by the same mechanism, given the observed differences in gene expression. Future studies taking advantage of the sophisticated genetic tools available in *Drosophila* to interrogate the different genes and pathways could help to resolve this.

Insecticide resistance has always been an issue and it is becoming more so for these compounds which have now been in use for the best part of three decades. Some mutations in the nAChRs targeted by insecticides are viable and highly resistant. The *Myzus persicae* $\beta1^{R81T}$ mutation and various *α6* mutations in a range of insect pests are posing problems for pest management in the field. This study highlights the potential for the incorporation of insecticides with reciprocal sensitivities as an option for future resistance management. This could extend life of current generation insecticides in the field. Insecticide resistance through mutations in nAChR subunit targets is likely to come with a cost to synaptic signalling and potentially cause hypersensitivity. Early testing of resistant pests as they arise in the field could lead to the rapid implementation of an effective resistance management strategy. In turn, this will assist in suppressing the frequency of resistant insects and help to safeguard the efficacy of insecticides so that they remain a viable control option.

Bibliography

Abazeed, Mohamed E., Jennifer M. Blanchette, and Robert S. Fuller. 2005. "Cell-Free Transport from the Trans-Golgi Network to Late Endosome Requires Factors Involved in Formation and Consumption of Clathrin-Coated Vesicles." *Journal of Biological Chemistry* 280(6):4442–50.

Abbott, W. S. 1925. "A Method of Computing the Effectiveness of an Insecticide." *Journal of Economic Entomology* 18(2):265–67.

Adams, Julian. 2004. "The Proteasome: A Suitable Antineoplastic Target." *Nature Reviews Cancer* 4(5):349–60.

Albin, Stephanie D. and Graeme W. Davis. 2004. "Coordinating Structural and Functional Synapse Development: Postsynaptic p21-Activated Kinase Independently Specifies Glutamate Receptor Abundance and Postsynaptic Morphology." *Journal of Neuroscience* 24(31):6871–79.

Albuquerque, Edson X., Edna F. R. Pereira, Newton G. Castro, Manickavasagom Alkondon, Sigrid Reinhardt, Hannsjörg Schröder, and Alfred Maelicke. 1995. "Nicotinic Receptor Function in the Mammalian Central Nervous System." *Annals of the New York Academy of Sciences* 757(1):48–72.

Alkondon, Manickavasagom and Edson X. Albuquerque. 2004. "The Nicotinic Acetylcholine Receptor Subtypes and Their Function in the Hippocampus and Cerebral Cortex." *Progress in Brain Research* 145:109–20.

Althoff, Thorsten, Ryan E. Hibbs, Surajit Banerjee, and Eric Gouaux. 2014. "X-Ray Structures of GluCl in Apo States Reveal a Gating Mechanism of Cys-Loop Receptors." *Nature* 512(7514):333–37.

Ambros, Victor. 2004. "The Functions of Animal MicroRNAs." *Nature* 431(7006):350–55.

Anders, Simon. 2010. "Analysing RNA-Seq Data with the DESeq Package." *Mol*

Biol 43(4):1–17.

Anders, Simon, Paul Theodor Pyl, and Wolfgang Huber. 2015. “HTSeq—a Python Framework to Work with High-Throughput Sequencing Data.” *Bioinformatics* 31(2):166–69.

Aughey, Gabriel N., Seth W. Cheetham, and Tony D. Southall. 2019. “DamID as a Versatile Tool for Understanding Gene Regulation.” *Development* 146(6):dev173666.

Bao, W. X., Y. Narai, A. Nakano, T. Kaneda, T. Murai, and S. Sonoda. 2014. “Spinosad Resistance of Melon Thrips, *Thrips palmi*, Is Conferred by G275E Mutation in Alpha6 Subunit of Nicotinic Acetylcholine Receptor and Cytochrome P450 Detoxification.” *Pestic Biochem Physiol* 112:51–55.

Barnstedt, Oliver, David Owald, Johannes Felsenberg, Ruth Brain, John-Paul Moszynski, Clifford B. Talbot, Paola N. Perrat, and Scott Waddell. 2016. “Memory-Relevant Mushroom Body Output Synapses Are Cholinergic.” *Neuron* 89(6):1237–47.

Barros, Antonio Thadeu M., Alberto Gomes, Ana Paula K. Ismael, and Wilson W. Koller. 2002. “Susceptibility to Diazinon in Populations of the Horn Fly, *Haematobia irritans* (Diptera: Muscidae), in Central Brazil.” *Memórias Do Instituto Oswaldo Cruz* 97:905–7.

Bass, Chris, Alin M. Puinean, Melanie Andrews, Penny Cutler, Miriam Daniels, Jan Elias, Verity Laura Paul, Andrew J. Crossthwaite, Ian Denholm, Linda M. Field, Stephen P. Foster, Rob Lind, Martin S. Williamson, and Russell Slater. 2011. “Mutation of a Nicotinic Acetylcholine Receptor Beta Subunit Is Associated with Resistance to Neonicotinoid Insecticides in the Aphid *Myzus persicae*.” *BMC Neuroscience* 12:51.

Baxter, S. W., M. Chen, A. Dawson, J. Z. Zhao, H. Vogel, A. M. Shelton, D. G. Heckel, and C. D. Jiggins. 2010. “Mis-Spliced Transcripts of Nicotinic Acetylcholine Receptor Alpha6 Are Associated with Field Evolved Spinosad Resistance in *Plutella xylostella* (L.).” *PLoS Genet* 6(1):e1000802.

Ben-David, Yael, Tehila Mizrachi, Sarah Kagan, Tamar Krisher, Emiliano Cohen, Talma Brenner, and Millet Treinin. 2016. “RIC-3 Expression and Splicing Regulate NAChR Functional Expression.” *Molecular Brain* 9(1):47.

Benwell, M. E., D. J. Balfour, and J. M. Anderson. 1988. “Evidence That Tobacco Smoking Increases the Density of (-)-[3H]Nicotine Binding Sites in Human Brain.” *J Neurochem* 50(4):1243–47.

Bergamasco, V. B., D. R. P. Mendes, O. A. Fernandes, J. A. Desidério, and M. V. F. Lemos. 2013. “*Bacillus thuringiensis* Cry1Ia10 and Vip3Aa Protein Interactions and Their Toxicity in *Spodoptera spp.*(Lepidoptera).” *Journal of Invertebrate Pathology* 112(2):152–58.

Berger, Christian, Heike Harzer, Thomas R. Burkard, Jonas Steinmann, Suzanne van der Horst, Anne-Sophie Laurenson, Maria Novatchkova, Heinrich Reichert, and Juergen A. Knoblich. 2012. “FACS Purification and Transcriptome Analysis of *Drosophila* Neural Stem Cells Reveals a Role for Klumpfuss in Self-Renewal.” *Cell Reports* 2(2):407–18.

Bertrand, D., F. Picard, S. Le Hellard, S. Weiland, I. Favre, H. Phillips, S. Bertrand, S. F. Berkovic, A. Malafosse, and J. Mulley. 2002. “How Mutations in the NAChRs Can Cause ADNFLE Epilepsy.” *Epilepsia* 43 Suppl 5:112–22.

Bondarenko, Vasyl, David D. Mowrey, Tommy S. Tillman, Edom Seyoum, Yan Xu, and Pei Tang. 2014. “NMR Structures of the Human Alpha7 NAChR Transmembrane Domain and Associated Anesthetic Binding Sites.” *Biochimica et Biophysica Acta (BBA)-Biomembranes* 1838(5):1389–95.

Bondarenko, Vasyl, David Mowrey, Tommy Tillman, Tanxing Cui, Lu Tian Liu, Yan Xu, and Pei Tang. 2012. “NMR Structures of the Transmembrane Domains of the Alpha4beta2 NAChR.” *Biochimica et Biophysica Acta (BBA)-Biomembranes* 1818(5):1261–68.

Borst, J. G. G. and B. Sakmann. 1996. “Calcium Influx and Transmitter Release in a Fast CNS Synapse.” *Nature* 383(6599):431–34.

Borza, Claudia. 2013. “Oxidative Stress and Lipid Peroxidation – A Lipid Metabolism Dysfunction.” P. Ch. 2 in, edited by D. Muntean. Rijeka: IntechOpen.

Boulter, Jim, Anne O’Shea-Greenfield, Robert M. Duvoisin, John G. Connolly, Etsuko Wada, Abbie Jensen, Paul D. Gardner, Marc Ballivet, Evan S. Deneris, and David McKinnon. 1990. “Alpha3, Alpha5, and Beta4: Three Members of the Rat Neuronal Nicotinic Acetylcholine Receptor-Related Gene Family Form a Gene Cluster.” *Journal of Biological Chemistry* 265(8):4472–82.

Bourguet, D., A. Genissel, M. Raymond, and And M. Raymond. 2000. “Insecticide Resistance and Dominance Levels.” *Journal of Economic Entomology* 93(936):1588–95.

Boussabbeh, Manel, Intidhar Ben Salem, Mohamed Hamdi, Salsabil Ben Fradj, Salwa Abid-Essefi, and Hassen Bacha. 2016. “Diazinon, an Organophosphate Pesticide, Induces Oxidative Stress and Genotoxicity in Cells Deriving from Large Intestine.” *Environmental Science and Pollution Research International* 23(3):2882–89.

Bouzat, Cecilia, Mariana Bartos, Jeremias Corradi, and Steven M. Sine. 2008. “The Interface between Extracellular and Transmembrane Domains of Homomeric Cys-Loop Receptors Governs Open-Channel Lifetime and Rate of Desensitization.” *The Journal of Neuroscience : The Official Journal of the Society for Neuroscience* 28(31):7808–19.

Brackmann, M., S. Schuchmann, R. Anand, and K. H. Braunewell. 2005. “Neuronal Ca2+ Sensor Protein VILIP-1 Affects CGMP Signalling of Guanylyl Cyclase B by Regulating Clathrin-Dependent Receptor Recycling in Hippocampal Neurons.” *J Cell Sci* 118(Pt 11):2495–2505.

Brand, A. H. and N. Perrimon. 1993. “Targeted Gene Expression as a Means of Altering Cell Fates and Generating Dominant Phenotypes.” *Development (Cambridge, England)* 118(2):401–15.

Breese, C. R., C. Adams, J. Logel, C. Drebing, Y. Rollins, M. Barnhart, B. Sullivan, B. K. Demasters, R. Freedman, and S. Leonard. 1997. “Comparison of the Regional Expression of Nicotinic Acetylcholine Receptor Alpha7 mRNA and [125I]-Alpha-Bungarotoxin Binding in Human Postmortem Brain.” *J Comp Neurol* 387(3):385–98.

Breitinger, Hans-Georg, Carmen Villmann, Nima Melzer, Janine Rennert, Ulrike Breitinger, Stephan Schwarzinger, and Cord-Michael Becker. 2009. “Novel Regulatory Site within the TM3–4 Loop of Human Recombinant Alpha3 Glycine Receptors Determines Channel Gating and Domain Structure.” *Journal of Biological Chemistry* 284(42):28624–33.

Brejc, K., W. J. van Dijk, R. V Klaassen, M. Schuurmans, J. van Der Oost, A. B. Smit, and T. K. Sixma. 2001. “Crystal Structure of an ACh-Binding Protein Reveals the Ligand-Binding Domain of Nicotinic Receptors.” *Nature* 411(6835):269–76.

Briseño-Roa, Luis and Jean-Louis Bessereau. 2014. “Proteolytic Processing of the Extracellular Scaffolding Protein LEV-9 Is Required for Clustering Acetylcholine Receptors.” *The Journal of Biological Chemistry* 289(16):10967–74.

Brodsky, Jeffrey L. and William R. Skach. 2011. “Protein Folding and Quality Control in the Endoplasmic Reticulum: Recent Lessons from Yeast and Mammalian Cell Systems.” *Current Opinion in Cell Biology* 23(4):464–75.

Brown, James B., Nathan Boley, Robert Eisman, Gemma E. May, Marcus H. Stoiber, Michael O. Duff, Ben W. Booth, Jiayu Wen, Soo Park, Ana Maria Suzuki, Kenneth H. Wan, Charles Yu, Dayu Zhang, Joseph W. Carlson, Lucy Cherbas, Brian D. Eads, David Miller, Keithanne Mockaitis, Johnny Roberts, Carrie A. Davis, Erwin Frise, Ann S. Hammonds, Sara Olson, Sol Shenker, David Sturgill, Anastasia A. Samsonova, Richard Weiszmann, Garret Robinson, Juan Hernandez, Justen Andrews, Peter J. Bickel, Piero Carninci, Peter Cherbas, Thomas R. Gingeras, Roger A. Hoskins, Thomas C. Kaufman, Eric C. Lai, Brian Oliver, Norbert Perrimon, Brenton R. Graveley,

and Susan E. Celniker. 2014. “Diversity and Dynamics of the *Drosophila* Transcriptome.” *Nature* 512(7515):393–99.

Brown, Laurence A., Makoto Ihara, Steven D. Buckingham, Kazuhiko Matsuda, and David B. Sattelle. 2006. “Neonicotinoid Insecticides Display Partial and Super Agonist Actions on Native Insect Nicotinic Acetylcholine Receptors.” *Journal of Neurochemistry* 99(2):608–15.

Brunet Avalos, Clarisse, G. Larisa Maier, Rémy Bruggmann, and Simon G. Sprecher. 2019. “Single Cell Transcriptome Atlas of the *Drosophila* Larval Brain” edited by K. VijayRaghavan. *ELife* 8:e50354.

Bulut, Gamze B., Rita Sulahian, Huiyu Yao, and Lily Jun-shen Huang. 2013. “Cbl Ubiquitination of P85 Is Essential for Epo-Induced EpoR Endocytosis.” *Blood, The Journal of the American Society of Hematology* 122(24):3964–72.

Bunton-Stasyshyn, Rosie K. A., Sara Wells, and Lydia Teboul. 2019. “When All Is Not Lost: Considering Genetic Compensation in Laboratory Animals.” *Lab Animal* 48(10):282–84.

Buske, Fabian A., Mikael Bodén, Denis C. Bauer, and Timothy L. Bailey. 2010. “Assigning Roles to DNA Regulatory Motifs Using Comparative Genomics.” *Bioinformatics* 26(7):860–66.

Cahoy, John D., Ben Emery, Amit Kaushal, Lynette C. Foo, Jennifer L. Zamanian, Karen S. Christopherson, Yi Xing, Jane L. Lubischer, Paul A. Krieg, Sergey A. Krupenko, Wesley J. Thompson, and Ben A. Barres. 2008. “A Transcriptome Database for Astrocytes, Neurons, and Oligodendrocytes: A New Resource for Understanding Brain Development and Function.” *Journal of Neuroscience* 28(1):264–78.

Campanucci, Verónica A., Arjun Krishnaswamy, and Ellis Cooper. 2008. “Mitochondrial Reactive Oxygen Species Inactivate Neuronal Nicotinic Acetylcholine Receptors and Induce Long-Term Depression of Fast Nicotinic Synaptic Transmission.” *Journal of Neuroscience* 28(7):1733–44.

Carson, Rachel, Lois Darling, Louis Darling, Houghton Mifflin Company, and Mass. Riverside Press (Cambridge). 1962. *Silent Spring*.

Cartaud, Jean, E. Luci. Benedetti, Jonathan B. Cohen, Jean-Claude Meunier, and Jean-Pierre Changeux. 1973. “Presence of a Lattice Structure in Membrane Fragments Rich in Nicotinic Receptor Protein from the Electric Organ of *Torpedo marmorata*.” *FEBS Letters* 33(1):109–13.

Castillo, Pablo E. 2012. “Presynaptic LTP and LTD of Excitatory and Inhibitory Synapses.” *Cold Spring Harbor Perspectives in Biology* 4(2):a005728.

Celie, Patrick H. N., Igor E. Kasheverov, Dmitry Y. Mordvintsev, Ronald C. Hogg, Pim van Nierop, Rene van Elk, Sarah E. van Rossum-Fikkert, Maxim N. Zhmak, Daniel Bertrand, Victor Tsetlin, Titia K. Sixma, and August B. Smit. 2005. “Crystal Structure of Nicotinic Acetylcholine Receptor Homolog AChBP in Complex with an Alpha-Conotoxin PnIA Variant.” *Nature Structural & Molecular Biology* 12(7):582–88.

Chamaon, Kathrin, Regine Schulz, Karl-Heinz Smalla, Bert Seidel, and Eckart D. Gundelfinger. 2000. “Neuronal Nicotinic Acetylcholine Receptors of *Drosophila melanogaster*: The Alpha-subunit Dα3 and the Beta-type Subunit ARD Co-assemble within the Same Receptor Complex.” *Febs Letters* 482(3):189–92.

Chamaon, Kathrin, K. H. Smalla, U. Thomas, and E. D. Gundelfinger. 2002. “Nicotinic Acetylcholine Receptors of *Drosophila*: Three Subunits Encoded by Genomically Linked Genes Can Co-Assemble into the Same Receptor Complex.” *J Neurochem* 80(1):149–57.

Champtiaux, Nicolas and Jean-Pierre Changeux. 2004. “Knockout and Knockin Mice to Investigate the Role of Nicotinic Receptors in the Central Nervous System.” *Progress in Brain Research* 145:233–51.

Champtiaux, Nicolas, Zhi-Yan Han, Alain Bessis, Francesco Mattia Rossi, Michele Zoli, Lisa Marubio, J. Michael McIntosh, and Jean-Pierre Changeux. 2002. “Distribution and Pharmacology of Alpha6-Containing Nicotinic

Acetylcholine Receptors Analyzed with Mutant Mice." *The Journal of Neuroscience : The Official Journal of the Society for Neuroscience* 22(4):1208–17.

Changeux, J. P., M. Kasai, and C. Y. Lee. 1970. "Use of a Snake Venom Toxin to Characterize the Cholinergic Receptor Protein." *Proceedings of the National Academy of Sciences of the United States of America* 67(3):1241–47.

Chao, Shirley L., Tim J. Dennehy, and John E. Casida. 1997. "Whitefly (Hemiptera: Aleyrodidae) Binding Site for Imidacloprid and Related Insecticides: A Putative Nicotinic Acetylcholine Receptor." *Journal of Economic Entomology* 90(4):879–82.

Chen, D., M. Frezza, S. Schmitt, J. Kanwar, and Q. P Dou. 2011. "Bortezomib as the First Proteasome Inhibitor Anticancer Drug: Current Status and Future Perspectives." *Current Cancer Drug Targets* 11(3):239–53.

Chen, Qingqiu, Li Tang, Guang Xin, Shiyi Li, Limei Ma, Yao Xu, Manjiao Zhuang, Qiuyang Xiong, Zeliang Wei, Zhihua Xing, Hai Niu, and Wen Huang. 2019. "Oxidative Stress Mediated by Lipid Metabolism Contributes to High Glucose-Induced Senescence in Retinal Pigment Epithelium." *Free Radical Biology & Medicine* 130:48–58.

Chiara, D. C., Y. Xie, and J. B. Cohen. 1999. "Structure of the Agonist-Binding Sites of the *Torpedo* Nicotinic Acetylcholine Receptor: Affinity-Labeling and Mutational Analyses Identify Gamma Tyr-111/Delta Arg-113 as Antagonist Affinity Determinants." *Biochemistry* 38(20):6689–98.

Christianson, J. C. and W. N. Green. 2004. "Regulation of Nicotinic Receptor Expression by the Ubiquitin-Proteasome System." *EMBO J* 23(21):4156–65.

Chung, ChiHye, Barbara Barylko, Jeremy Leitz, Xinran Liu, and Ege T. Kavalali. 2010. "Acute Dynamin Inhibition Dissects Synaptic Vesicle Recycling Pathways That Drive Spontaneous and Evoked Neurotransmission." *Journal of Neuroscience* 30(4):1363–76.

Chung, Henry, Tamar Sztal, Shivani Pasricha, Mohan Sridhar, Philip Batterham, and Phillip J. Daborn. 2009. “Characterization of *Drosophila melanogaster* Cytochrome P450 Genes.” *Proceedings of the National Academy of Sciences of the United States of America* 106(14):5731–36.

Cilek, J. E., D. L. Dahlman, and F. W. Knapp. 1995. “Possible Mechanism of Diazinon Negative Cross-Resistance in Pyrethroid-Resistant Horn Flies (Diptera: Muscidae).” *Journal of Economic Entomology* 88(3):520–24.

Collins, A. C., E. Romm, and J. M. Wehner. 1990. “Dissociation of the Apparent Relationship between Nicotine Tolerance and Up-Regulation of Nicotinic Receptors.” *Brain Res Bull* 25(3):373–79.

Conti-Tronconi, B. M. and M. A. Raftery. 1982. “The Nicotinic Cholinergic Receptor: Correlation of Molecular Structure with Functional Properties.” *Annual Review of Biochemistry* 51:491–530.

Cooper, S. T. and N. S. Millar. 1997. “Host Cell-Specific Folding and Assembly of the Neuronal Nicotinic Acetylcholine Receptor Alpha7 Subunit.” *J Neurochem* 68(5):2140–51.

Corringer, P. J., N. Le Novere, and J. P. Changeux. 2000. “Nicotinic Receptors at the Amino Acid Level.” *Annu Rev Pharmacol Toxicol* 40:431–58.

Crooks, Peter A., Michael T. Bardo, and Linda P. Dwoskin. 2014. “Nicotinic Receptor Antagonists as Treatments for Nicotine Abuse.” *Advances in Pharmacology (San Diego, Calif.)* 69:513–51.

Croset, Vincent, Christoph D. Treiber, and Scott Waddell. 2018. “Cellular Diversity in the *Drosophila* Midbrain Revealed by Single-Cell Transcriptomics.” *ELife* 7:1–31.

Damke, Hanna, Takeshi Baba, Dale E. Warnock, and Sandra L. Schmid. 1994. “Induction of Mutant Dynamin Specifically Blocks Endocytic Coated Vesicle Formation.” *The Journal of Cell Biology* 127(4):915–34.

Dani, John A. and Daniel Bertrand. 2007. “Nicotinic Acetylcholine Receptors and

Nicotinic Cholinergic Mechanisms of the Central Nervous System." *Annu. Rev. Pharmacol. Toxicol.* 47:699–729.

Darsow, T., T. K. Booker, J. C. Pina-Crespo, and S. F. Heinemann. 2005. "Exocytic Trafficking Is Required for Nicotine-Induced Up-Regulation of Alpha4beta2 Nicotinic Acetylcholine Receptors." *J Biol Chem* 280(18):18311–20.

David, Jean-Philippe, Eric Coissac, Christelle Melodelima, Rodolphe Poupardin, Muhammad Asam Riaz, Alexia Chandor-Proust, and Stéphane Reynaud. 2010. "Transcriptome Response to Pollutants and Insecticides in the Dengue Vector *Aedes aegypti* Using Next-Generation Sequencing Technology." *BMC Genomics* 11(1):216.

Davis, Graeme W. 2006. "Homeostatic Control of Neural Activity: From Phenomenology to Molecular Design." *Annu. Rev. Neurosci.* 29:307–23.

Davis, Graeme W. and Corey S. Goodman. 1998. "Synapse-Specific Control of Synaptic Efficacy at the Terminals of a Single Neuron." *Nature* 392(6671):82–86.

Denecke, Shane, Cameron J. Nowell, Alexandre Fournier-Level, Trent Perry, and Phil Batterham. 2015. "The Wiggle Index: An Open Source Bioassay to Assess Sub-Lethal Insecticide Response in *Drosophila melanogaster*." *PLoS One* 10(12):e0145051.

Deutsch, Curtis A., Joshua J. Tewksbury, Michelle Tigchelaar, David S. Battisti, Scott C. Merrill, Raymond B. Huey, and Rosamond L. Naylor. 2018. "Increase in Crop Losses to Insect Pests in a Warming Climate." *Science (New York, N.Y.)* 361(6405):916–19.

Diao, Fengqiu, Holly Ironfield, Haojiang Luan, Feici Diao, William C. Shropshire, John Ewer, Elizabeth Marr, Christopher J. Potter, Matthias Landgraf, and Benjamin H. White. 2015. "Plug-and-Play Genetic Access to *Drosophila* Cell Types Using Exchangeable Exon Cassettes." *Cell Reports* 10(8):1410–21.

Diao, Fengqiu and Benjamin H. White. 2012. “A Novel Approach for Directing Transgene Expression in *Drosophila*: T2A-Gal4 in-Frame Fusion.” *Genetics* 190(3):1139–44.

Dineley, Kelly T., Anshul A. Pandya, and Jerrel L. Yakel. 2015. “Nicotinic ACh Receptors as Therapeutic Targets in CNS Disorders.” *Trends in Pharmacological Sciences* 36(2):96–108.

Donnan, G. A., D. G. Woodhouse, S. J. Kaczmarczyk, J. E. Holder, G. Paxinos, P. J. Chilco, A. J. Churchyard, R. M. Kalnins, G. C. A. Fabinyi, and F. A. O. Mendelsohn. 1991. “Evidence for Plasticity of the Dopaminergic System in Parkinsonism.” *Molecular Neurobiology* 5(2):421.

Drisdel, R. C. and W. N. Green. 2000. “Neuronal Alpha-Bungarotoxin Receptors Are Alpha7 Subunit Homomers.” *The Journal of Neuroscience : The Official Journal of the Society for Neuroscience* 20(1):133–39.

Dupuis, J., T. Louis, M. Gauthier, and V. Raymond. 2012. “Insights from Honeybee (*Apis mellifera*) and Fly (*Drosophila melanogaster*) Nicotinic Acetylcholine Receptors: From Genes to Behavioral Functions.” *Neurosci Biobehav Rev* 36(6):1553–64.

Eimer, S., A. Gottschalk, M. Hengartner, H. R. Horvitz, J. Richmond, W. R. Schafer, and J. L. Bessereau. 2007. “Regulation of Nicotinic Receptor Trafficking by the Transmembrane Golgi Protein UNC-50.” *EMBO J* 26(20):4313–23.

Elliott, Michael, Andrew W. Farnham, Norman F. Janes, Diana M. Johnson, David A. Pulman, and Roman M. Sawicki. 1986. “Insecticidal Amides with Selective Potency against a Resistant (*Super-Kdr*) Strain of Houseflies (*Musca domestica L.*).” *Agricultural and Biological Chemistry* 50(5):1347–49.

Engel, Andrew G. and Steven M. Sine. 2005. “Current Understanding of Congenital Myasthenic Syndromes.” *Current Opinion in Pharmacology* 5(3):308–21.

Ertunc, Mert, Yildirim Sara, ChiHye Chung, Deniz Atasoy, Tuhin Virmani, and Ege T. Kavalali. 2007. “Fast Synaptic Vesicle Reuse Slows the Rate of Synaptic Depression in the CA1 Region of Hippocampus.” *Journal of Neuroscience* 27(2):341–54.

Fagerlund, M. J. and L. I. Eriksson. 2009. “Current Concepts in Neuromuscular Transmission.” *BJA: British Journal of Anaesthesia* 103(1):108–14.

Fayyazuddin, A., M. A. Zaheer, P. R. Hiesinger, and H. J. Bellen. 2006. “The Nicotinic Acetylcholine Receptor Dalpha7 Is Required for an Escape Behavior in *Drosophila*.” *PLoS Biol* 4(3):e63.

Finney, D. J. 1947. *Probit Analysis: A Statistical Treatment of the Sigmoid*.

Fishel, Frederick M. 2013. “Pest Management and Pesticides: A Historical Perspective.” *Publication PI219. Agronomy Department, Florida Cooperative Extension Service, Institute of Food and Agricultural Sciences, University of Florida, Gainesville, FL, USA*.

Flores, C. M., S. W. Rogers, L. A. Pabreza, B. B. Wolfe, and K. J. Kellar. 1992. “A Subtype of Nicotinic Cholinergic Receptor in Rat Brain Is Composed of Alpha4 and Beta2 Subunits and Is Up-Regulated by Chronic Nicotine Treatment.” *Mol Pharmacol* 41(1):31–37.

Foster, James P. 1990. “Device for Killing Arthropods.” *U.S. Patent* No. 4,908,977.

Frith, Martin C., Yutao Fu, Liqun Yu, Jiang-Fan Chen, Ulla Hansen, and Zhiping Weng. 2004. “Detection of Functional DNA Motifs via Statistical Over-representation.” *Nucleic Acids Research* 32(4):1372–81.

Fuenzalida-Uribe, Nicolás, Rodrigo C. Meza, Hernán A. Hoffmann, Rodrigo Varas, and Jorge M. Campusano. 2013. “NAChR-induced Octopamine Release Mediates the Effect of Nicotine on a Startle Response in *Drosophila melanogaster*.” *Journal of Neurochemistry* 125(2):281–90.

Fujii, Takeshi, Masato Mashimo, Yasuhiro Moriwaki, Hidemi Misawa, Shiro Ono,

Kazuhide Horiguchi, and Koichiro Kawashima. 2017. “Expression and Function of the Cholinergic System in Immune Cells.” *Frontiers in Immunology* 8:1085.

Fujiwara, Toshiyuki, Noboru Takami, Yoshio Misumi, and Yukio Ikehara. 1998. “Nordihydroguaiaretic Acid Blocks Protein Transport in the Secretory Pathway Causing Redistribution of Golgi Proteins into the Endoplasmic Reticulum.” *Journal of Biological Chemistry* 273(5):3068–75.

Furia, Maria, Pier Paolo D’Avino, Stefania Crispi, and Dora Artiaco. 1993. “Ecdysone-Regulated 3C Puff of *Drosophila melanogaster*.” *J. Mol. Hiol* 231:531–38.

Fusetto, Roberto, Shane Denecke, Trent Perry, Richard A. J. O’Hair, and Philip Batterham. 2017. “Partitioning the Roles of CYP6G1 and Gut Microbes in the Metabolism of the Insecticide Imidacloprid in *Drosophila melanogaster*.” *Scientific Reports* 7(1):11339.

Gahring, Lorise C., Karina Persiyanov, and Scott W. Rogers. 2004. “Neuronal and Astrocyte Expression of Nicotinic Receptor Subunit Beta4 in the Adult Mouse Brain.” *Journal of Comparative Neurology* 468(3):322–33.

Gaiarsa, Jean-Luc, Olivier Caillard, and Yehezkel Ben-Ari. 2002. “Long-Term Plasticity at GABAergic and Glycinergic Synapses: Mechanisms and Functional Significance.” *Trends in Neurosciences* 25(11):564–70.

Gao, Qin, Yan-Jie Liu, and Zhi-Zhong Guan. 2008. “Oxidative Stress Might Be a Mechanism Connected with the Decreased Alpha7 Nicotinic Receptor Influenced by High-Concentration of Fluoride in SH-SY5Y Neuroblastoma Cells.” *Toxicology in Vitro* 22(4):837–43.

Garduno, Julieta, Luis Galindo-Charles, Javier Jiménez-Rodríguez, Elvira Galarraga, Dagoberto Tapia, Stefan Mihailescu, and Salvador Hernandez-Lopez. 2012. “Presynaptic Alpha4beta2 Nicotinic Acetylcholine Receptors Increase Glutamate Release and Serotonin Neuron Excitability in the Dorsal Raphe Nucleus.” *Journal of Neuroscience* 32(43):15148–57.

Ge, Weili, Saihong Yan, Jinhua Wang, Lusheng Zhu, Aimei Chen, and Jun Wang. 2015. “Oxidative Stress and DNA Damage Induced by Imidacloprid in Zebrafish (*Danio rerio*).” *Journal of Agricultural and Food Chemistry* 63(6):1856–62.

Gehle, V. M., E. C. Walcott, T. Nishizaki, and K. Sumikawa. 1997. “N-Glycosylation at the Conserved Sites Ensures the Expression of Properly Folded Functional ACh Receptors.” *Brain Research. Molecular Brain Research* 45(2):219–29.

Germann, Sophie, Trine Juul-Jensen, Bruno Letarnec, and Valérie Gaudin. 2006. “DamID, a New Tool for Studying Plant Chromatin Profiling in Vivo, and Its Use to Identify Putative LHP1 Target Loci.” *The Plant Journal* 48(1):153–63.

Glanzman, David L. 2010. “Common Mechanisms of Synaptic Plasticity in Vertebrates and Invertebrates.” *Current Biology* 20(1):R31–36.

Gloor, Greg and William Engles. 1992. “Single-Fly DNA Preps For PCR.” *Univ. of Wisconsin Drosophila Information Service* 71:148–49.

Goldberg, Alfred L. 2003. “Protein Degradation and Protection against Misfolded or Damaged Proteins.” *Nature* 426(6968):895–99.

Gopalakrishnan, M., E. J. Molinari, and J. P. Sullivan. 1997. “Regulation of Human Alpha4beta2 Neuronal Nicotinic Acetylcholine Receptors by Cholinergic Channel Ligands and Second Messenger Pathways.” *Mol Pharmacol* 52(3):524–34.

Gott, Ryan C., Grace R. Kunkel, Emily S. Zobel, Brian R. Lovett, and David J. Hawthorne. 2017. “Implicating ABC Transporters in Insecticide Resistance: Research Strategies and a Decision Framework.” *Journal of Economic Entomology* 110(2):667–77.

Gotti, C. and F. Clementi. 2004. “Neuronal Nicotinic Receptors: From Structure to Pathology.” *Progress in Neurobiology* 74(6):363–96.

Gotti, C., F. Clementi, A. Fornari, A. Gaimarri, S. Guiducci, I. Manfredi, M. Moretti,

P. Pedrazzi, L. Pucci, and M. Zoli. 2009. “Structural and Functional Diversity of Native Brain Neuronal Nicotinic Receptors.” *Biochem Pharmacol* 78(7):703–11.

Gotti, C., M. Zoli, and F. Clementi. 2006. “Brain Nicotinic Acetylcholine Receptors: Native Subtypes and Their Relevance.” *Trends in Pharmacological Sciences* 27(9):482–91.

Govind, Anitha P., Heather Walsh, and William N. Green. 2012. “Nicotine-Induced Upregulation of Native Neuronal Nicotinic Receptors Is Caused by Multiple Mechanisms.” *The Journal of Neuroscience : The Official Journal of the Society for Neuroscience* 32(6):2227–38.

Graham, Geoffrey J. 1995. “Tandem Genes and Clustered Genes.” *Journal of Theoretical Biology* 175(1):71–87.

Grando, Sergei A., Robert M. Horton, Edna F. R. Pereira, Brenda M. Diethelm-Okita, Pierre M. George, Edson X. Albuquerque, and Bianca M. Conti-Fine. 1995. “A Nicotinic Acetylcholine Receptor Regulating Cell Adhesion and Motility Is Expressed in Human Keratinocytes.” *Journal of Investigative Dermatology* 105(6).

Grando, Sergei A., Mark R. Pittelkow, and Karin U. Schallreuter. 2006. “Adrenergic and Cholinergic Control in the Biology of Epidermis: Physiological and Clinical Significance.” *Journal of Investigative Dermatology* 126(9):1948–65.

Gratz, Scott J., Alexander M. Cummings, Jennifer N. Nguyen, Danielle C. Hamm, Laura K. Donohue, Melissa M. Harrison, Jill Wildonger, and Kate M. O’connor-Giles. 2013. “Genome Engineering of *Drosophila* with the CRISPR RNA-Guided Cas9 Nuclease.” *Genetics* 194(4):1029–35.

Gratz, Scott J., C. Dustin Rubinstein, Melissa M. Harrison, Jill Wildonger, and Kate M. O’Connor-Giles. 2015. “CRISPR-Cas9 Genome Editing in *Drosophila*.” *Current Protocols in Molecular Biology* 111:31.2.1-31.2.20.

Grauso, M., R. A. Reenan, E. Culetto, and D. B. Sattelle. 2002. “Novel Putative Nicotinic Acetylcholine Receptor Subunit Genes, Dalpha5, Dalpha6 and Dalpha7, in *Drosophila melanogaster* Identify a New and Highly Conserved Target of Adenosine Deaminase Acting on RNA-Mediated A-to-I Pre-MRNA Editing.” *Genetics* 160(4):1519–33.

Graveley, Brenton R., Angela N. Brooks, Joseph W. Carlson, Michael O. Duff, Jane M. Landolin, Li Yang, Carlo G. Artieri, Marijke J. van Baren, Nathan Boley, Benjamin W. Booth, James B. Brown, Lucy Cherbas, Carrie A. Davis, Alex Dobin, Renhua Li, Wei Lin, John H. Malone, Nicolas R. Mattiuzzo, David Miller, David Sturgill, Brian B. Tuch, Chris Zaleski, Dayu Zhang, Marco Blanchette, Sandrine Dudoit, Brian Eads, Richard E. Green, Ann Hammonds, Lichun Jiang, Phil Kapranov, Laura Langton, Norbert Perrimon, Jeremy E. Sandler, Kenneth H. Wan, Aarron Willingham, Yu Zhang, Yi Zou, Justen Andrews, Peter J. Bickel, Steven E. Brenner, Michael R. Brent, Peter Cherbas, Thomas R. Gingeras, Roger A. Hoskins, Thomas C. Kaufman, Brian Oliver, and Susan E. Celniker. 2011. “The Developmental Transcriptome of *Drosophila melanogaster*.” *Nature* 471(7339):473–79.

Grube, Arthur, David Donaldson, Timothy Kiely, and La Wu. 2011. “Pesticides Industry Sales and Usage: 2006 and 2007 Market Estimates.” *U.S. Environmental Protection Agency* 1–41.

Gupta, Shaweta, Prasad Purohit, and Anthony Auerbach. 2013. “Function of Interfacial Prolines at the Transmitter-Binding Sites of the Neuromuscular Acetylcholine Receptor.” *The Journal of Biological Chemistry* 288(18):12667–79.

Halevi, S., J. McKay, M. Palfreyman, L. Yassin, M. Eshel, E. Jorgensen, and M. Treinin. 2002. “The *C. elegans* Ric-3 Gene Is Required for Maturation of Nicotinic Acetylcholine Receptors.” *EMBO J* 21(5):1012–20.

Halevi, S., L. Yassin, M. Eshel, F. Sala, S. Sala, M. Criado, and M. Treinin. 2003. “Conservation within the RIC-3 Gene Family. Effectors of Mammalian Nicotinic Acetylcholine Receptor Expression.” *J Biol Chem* 278(36):34411–

17.

Hambley, Bryan, Paolo F. Caimi, and Basem M. William. 2016. “Bortezomib for the Treatment of Mantle Cell Lymphoma: An Update.” *Therapeutic Advances in Hematology* 7(4):196–208.

Hansen, Scott B., Todd T. Talley, Zoran Radic, and Palmer Taylor. 2004. “Structural and Ligand Recognition Characteristics of an Acetylcholine-Binding Protein from *Aplysia californica*.” *The Journal of Biological Chemistry* 279(23):24197–202.

Harkness, P. C. and N. S. Millar. 2002. “Changes in Conformation and Subcellular Distribution of Alpha4beta2 Nicotinic Acetylcholine Receptors Revealed by Chronic Nicotine Treatment and Expression of Subunit Chimeras.” *J Neurosci* 22(23):10172–81.

Heckscher, Elizabeth S., Richard D. Fetter, Kurt W. Marek, Stephanie D. Albin, and Graeme W. Davis. 2007. “NF-KB, IκB, and IRAK Control Glutamate Receptor Density at the *Drosophila* NMJ.” *Neuron* 55(6):859–73.

Heeschen, Christopher, James J. Jang, Michael Weis, Anjali Pathak, Shuichiro Kaji, Robert S. Hu, Philip S. Tsao, Frances L. Johnson, and John P. Cooke. 2001. “Nicotine Stimulates Angiogenesis and Promotes Tumor Growth and Atherosclerosis.” *Nature Medicine* 7(7):833–39.

Henry, Mickaël, Maxime Beguin, Fabrice Requier, Orianne Rollin, Jean-François Odoux, Pierrick Aupinel, Jean Aptel, Sylvie Tchamitchian, and Axel Decourtye. 2012. “A Common Pesticide Decreases Foraging Success and Survival in Honey Bees.” *Science* 336(6079):348–50.

Herranz, Hector and Ginés Morata. 2001. “The Functions of *Pannier* during *Drosophila* Embryogenesis.” *Development* 128(23):4837 LP – 4846.

Hoffmann, Ary A., B. L. Montgomery, Jean Popovici, Inaki Iturbe-Ormaetxe, P. H. Johnson, F. Muzzi, M. Greenfield, M. Durkan, Y. S. Leong, and Yi Dong. 2011. “Successful Establishment of Wolbachia in Aedes Populations to

Suppress Dengue Transmission." *Nature* 476(7361):454–57.

Hogan, Eric M., Alison P. Casserly, Michael D. Scofield, Zhongming Mou, Rubing Zhao-Shea, Chris W. Johnson, Andrew R. Tapper, and Paul D. Gardner. 2014. "MiRNAome Analysis of the Mammalian Neuronal Nicotinic Acetylcholine Receptor Gene Family." *RNA* 20(12):1890–99.

Homem, Rafael A., Bliss Buttery, Ewan Richardson, Yao Tan, Linda M. Field, Martin S. Williamson, and T. G. Emyr Davies. 2020. "Evolutionary Trade-Offs of Insecticide Resistance - The Fitness Costs Associated with Target-Site Mutations in the NAChR of *Drosophila melanogaster*." *Molecular Ecology*.

Hoskin, Justin L., Yazan Al-Hasan, and Marwan Noel Sabbagh. 2018. "Nicotinic Acetylcholine Receptor Agonists for the Treatment of Alzheimer's Dementia: An Update." *Nicotine & Tobacco Research* 21(3):370–76.

Hsu, J. C., H. T. Feng, W. J. Wu, S. M. Geib, C. H. Mao, and J. Vontas. 2012. "Truncated Transcripts of Nicotinic Acetylcholine Subunit Gene Bdalpha6 Are Associated with Spinosad Resistance in *Bactrocera dorsalis*." *Insect Biochem Mol Biol* 42(10):806–15.

Huang, Fangtian, Lai Kuan Goh, and Alexander Sorkin. 2007. "EGF Receptor Ubiquitination Is Not Necessary for Its Internalization." *Proceedings of the National Academy of Sciences* 104(43):16904–9.

Huang, Y., M. S. Williamson, A. L. Devonshire, J. D. Windass, S. J. Lansdell, and N. S. Millar. 1999. "Molecular Characterization and Imidacloprid Selectivity of Nicotinic Acetylcholine Receptor Subunits from the Peach-Potato Aphid *Myzus persicae*." *J Neurochem* 73(1):380–89.

Hucho, Ferdinand, Walter Oberthür, and Friedrich Lottspeich. 1986. "The Ion Channel of the Nicotinic Acetylcholine Receptor Is Formed by the Homologous Helices M II of the Receptor Subunits." *FEBS Letters* 205(1):137–42.

Hurles, Matthew. 2005. "How Homologous Recombination Generates a Mutable

Genome." *Human Genomics* 2(3):179–86.

Ihara, Makoto, Kazuhiko Matsuda, Maiko Otake, Morihiko Kuwamura, Masaru Shimomura, Koichiro Komai, Miki Akamatsu, Valérie Raymond, and David B. Sattelle. 2003. "Diverse Actions of Neonicotinoids on Chicken Alpha7, Alpha4beta2 and *Drosophila*-Chicken SADβ2 and ALSβ2 Hybrid Nicotinic Acetylcholine Receptors Expressed in *Xenopus laevis* Oocytes." *Neuropharmacology* 45(1):133–44.

Jarman, Walter M. and Karlheinz Ballschmiter. 2012. "From Coal to DDT: The History of the Development of the Pesticide DDT from Synthetic Dyes till Silent Spring." *Endeavour* 36(4):131–42.

Jazwinska, A., C. Rushlow, and S. Roth. 1999. "The Role of Brinker in Mediating the Graded Response to Dpp in Early *Drosophila* Embryos." *Development* 126(15):3323 LP – 3334.

Jeanclos, E. M., L. Lin, M. W. Treuil, J. Rao, M. A. DeCoster, and R. Anand. 2001. "The Chaperone Protein 14-3-3eta Interacts with the Nicotinic Acetylcholine Receptor Alpha4 Subunit. Evidence for a Dynamic Role in Subunit Stabilization." *J Biol Chem* 276(30):28281–90.

Jensen, Marianne L., Arne Schousboe, and Philip K. Ahring. 2005. "Charge Selectivity of the Cys-Loop Family of Ligand-Gated Ion Channels." *Journal of Neurochemistry* 92(2):217–25.

Jeschke, Peter and Ralf Nauen. 2008. "Neonicotinoids—from Zero to Hero in Insecticide Chemistry." *Pest Management Science: Formerly Pesticide Science* 64(11):1084–98.

Jiang, Kun, Xiao-yue Hou, Tong-tong Tan, Zhang-lei Cao, Si-qi Mei, Bing Yan, Jin Chang, Lu Han, Dan Zhao, and Jun Cai. 2018. "Scavenger Receptor-C Acts as a Receptor for Bacillus Thuringiensis Vegetative Insecticidal Protein Vip3Aa and Mediates the Internalization of Vip3Aa via Endocytosis." *PLOS Pathogens* 14(10):e1007347.

Jin, Yongfeng, Nan Tian, Jun Cao, Jing Liang, Zhaolin Yang, and Jianning Lv. 2007. “RNA Editing and Alternative Splicing of the Insect NAChR Subunit Alpha6 Transcript: Evolutionary Conservation, Divergence and Regulation.” *BMC Evolutionary Biology* 7:98.

Jonas, P., A. Baumann, B. Merz, and E. D. Gundelfinger. 1990. “Structure and Developmental Expression of the Dalpha2 Gene Encoding a Novel Nicotinic Acetylcholine Receptor Protein of *Drosophila melanogaster*.” *FEBS Lett* 269(1):264–68.

Jones, A. K., G. Elgar, and D. B. Sattelle. 2003. “The Nicotinic Acetylcholine Receptor Gene Family of the Pufferfish, *Fugu rubripes*.” *Genomics* 82(4):441–51.

Jones, A. K. and David B. Sattelle. 2004. “Functional Genomics of the Nicotinic Acetylcholine Receptor Gene Family of the Nematode, *Caenorhabditis elegans*.” *BioEssays : News and Reviews in Molecular, Cellular and Developmental Biology* 26(1):39–49.

Jones, A. K. and David B. Sattelle. 2010. “Diversity of Insect Nicotinic Acetylcholine Receptor Subunits.” Pp. 25–43 in *Advances in Experimental Medicine and Biology*. Vol. 683, edited by S. H. Thany. New York, NY: Springer New York.

Jukam, David, Kayla Viets, Caitlin Anderson, Cyrus Zhou, Peter DeFord, Jenny Yan, Jinshuai Cao, and Robert J. Johnston. 2016. “The Insulator Protein BEAF-32 Is Required for Hippo Pathway Activity in the Terminal Differentiation of Neuronal Subtypes.” *Development* 143(13):2389 LP – 2397.

Kagabu, Shinzo. 1999. “Discovery of Chloronicotinyl Insecticides.” Pp. 91–106 in *Nicotinoid Insecticides and the Nicotinic Acetylcholine Receptor*. Springer.

Kamidi, R. E. and M. K. Kamidi. 2005. “Effects of a Novel Pesticide Resistance Management Strategy on Tick Control in a Smallholding Exotic-Breed Dairy Herd in Kenya.” *Tropical Animal Health and Production* 37(6):469–78.

Karlin, A. 2002. “Emerging Structure of the Nicotinic Acetylcholine Receptors.” *Nat Rev Neurosci* 3(2):102–14.

Kassner, P. D. and D. K. Berg. 1997. “Differences in the Fate of Neuronal Acetylcholine Receptor Protein Expressed in Neurons and Stably Transfected Cells.” *J Neurobiol* 33(7):968–82.

Kelso, Matthew L., Jeanne M. Wehner, Allan C. Collins, Stephen W. Scheff, and James R. Pauly. 2006. “The Pathophysiology of Traumatic Brain Injury in A7 Nicotinic Cholinergic Receptor Knockout Mice.” *Brain Research* 1083(1):204–10.

Khambay, B. P., I. Denholm, G. R. Carlson, R. M. Jacobson, and T. S. Dhadialla. 2001. “Negative Cross-Resistance between Dihydropyrazole Insecticides and Pyrethroids in Houseflies, *Musca domestica*.” *Pest Manag Sci* 57(9):761–63.

Khamesipour, Faham, Kamran Bagheri Lankarani, Behnam Honarvar, and Tebit Emmanuel Kwenti. 2018. “A Systematic Review of Human Pathogens Carried by the Housefly (*Musca domestica L.*).” *BMC Public Health* 18(1):1049.

Khiroug, Serguei S., Patricia C. Harkness, Patricia W. Lamb, Sterling N. Sudweeks, Leonard Khiroug, Neil S. Millar, and Jerrel L. Yakel. 2002. “Rat Nicotinic ACh Receptor Alpha7 and Beta2 Subunits Co-assemble to Form Functional Heteromeric Nicotinic Receptor Channels.” *The Journal of Physiology* 540(2):425–34.

Kim, Daehwan, Geo Pertea, Cole Trapnell, Harold Pimentel, Ryan Kelley, and Steven L. Salzberg. 2013. “TopHat2: Accurate Alignment of Transcriptomes in the Presence of Insertions, Deletions and Gene Fusions.” *Genome Biology* 14(4):R36.

Kim, Jung Min, Hyeong Geug Kim, and Chang Gue Son. 2018. “Tissue-Specific Profiling of Oxidative Stress-Associated Transcriptome in a Healthy Mouse Model.” *International Journal of Molecular Sciences* 19(10):3174.

Kirst, Herbert A. 2010. “The Spinosyn Family of Insecticides: Realizing the Potential of Natural Products Research.” *The Journal of Antibiotics* 63(3):101–11.

Klink, R., a de Kerchove d’Exaerde, M. Zoli, and J. P. Changeux. 2001. “Molecular and Physiological Diversity of Nicotinic Acetylcholine Receptors in the Midbrain Dopaminergic Nuclei.” *The Journal of Neuroscience : The Official Journal of the Society for Neuroscience* 21(5):1452–63.

Kondo, Shu, Takahiro Takahashi, Nobuhiro Yamagata, Yasuhito Imanishi, Hidetaka Katow, Shun Hiramatsu, Katrina Lynn, Ayako Abe, Ajayrama Kumaraswamy, and Hiromu Tanimoto. 2020. “Neurochemical Organization of the *Drosophila* Brain Visualized by Endogenously Tagged Neurotransmitter Receptors.” *Cell Reports* 30(1):284-297.e5.

Kozak, Marilyn. 2001. “New Ways of Initiating Translation in Eukaryotes?” *Molecular and Cellular Biology* 21(6):1899 LP – 1907.

Kracun, S., P. C. Harkness, A. J. Gibb, and N. S. Millar. 2008. “Influence of the M3–M4 Intracellular Domain upon Nicotinic Acetylcholine Receptor Assembly, Targeting and Function.” *British Journal of Pharmacology* 153(7):1474–84.

Krishnaswamy, Arjun and Ellis Cooper. 2012. “Reactive Oxygen Species Inactivate Neuronal Nicotinic Acetylcholine Receptors through a Highly Conserved Cysteine near the Intracellular Mouth of the Channel: Implications for Diseases That Involve Oxidative Stress.” *The Journal of Physiology* 590(1):39–47.

Kues, W. A., Bert Sakmann, and Veit Witzemann. 1995. “Differential Expression Patterns of Five Acetylcholine Receptor Subunit Genes in Rat Muscle during Development.” *European Journal of Neuroscience* 7(6):1376–85.

Lansdell, S. J., Toby Collins, Jim Goodchild, and Neil S. Millar. 2012. “The *Drosophila* Nicotinic Acetylcholine Receptor Subunits Dα5 and Dα7 Form Functional Homomeric and Heteromeric Ion Channels.” *BMC Neuroscience*

13(1):73.

Lansdell, S. J., V. J. Gee, P. C. Harkness, A. I. Doward, E. R. Baker, A. J. Gibb, and N. S. Millar. 2005. “RIC-3 Enhances Functional Expression of Multiple Nicotinic Acetylcholine Receptor Subtypes in Mammalian Cells.” *Mol Pharmacol* 68(5):1431–38.

Lansdell, S. J. and N. S. Millar. 2000a. “Cloning and Heterologous Expression of Dalpha4, a *Drosophila* Neuronal Nicotinic Acetylcholine Receptor Subunit: Identification of an Alternative Exon Influencing the Efficiency of Subunit Assembly.” *Neuropharmacology* 39(13):2604–14.

Lansdell, S. J. and N. S. Millar. 2000b. “The Influence of Nicotinic Receptor Subunit Composition upon Agonist, α–Bungarotoxin and Insecticide (Imidacloprid) Binding Affinity.” *Neuropharmacology* 39(4):671–79.

Lansdell, S. J. and N. S. Millar. 2002. “Dbeta3, an Atypical Nicotinic Acetylcholine Receptor Subunit from *Drosophila* : Molecular Cloning, Heterologous Expression and Coassembly.” *Journal of Neurochemistry* 80(6):1009–18.

Lansdell, S. J. and N. S. Millar. 2004. “Molecular Characterization of Dα6 and Dα7 Nicotinic Acetylcholine Receptor Subunits from *Drosophila*: Formation of a High-Affinity α-Bungarotoxin Binding Site Revealed by Expression of Subunit Chimeras.” *Journal of Neurochemistry* 90(2):479–89.

Latli, Bachir and John E. Casida. 1992. “[3H] Imidacloprid: Synthesis of a Candidate Radioligand for the Nicotinic Acetylcholine Receptor.” *Journal of Labelled Compounds and Radiopharmaceuticals* 31(8):609–13.

Lee, C. Y. and C. C. Chang. 1966. “Modes of Actions of Purified Toxins from Elapid Venoms on Neuromuscular Transmission.” *Memorias Do Instituto Butantan* 33(2):555–72.

Lee, Pei-tseng, Jonathan Zirin, Oguz Kanca, Wen-wen Lin, Karen L. Schulze, David Li-kroeger, Rong Tao, Colby Devereaux, Yanhui Hu, Verena Chung, Ying Fang, Yuchun He, Hongling Pan, Ming Ge, Zhongyuan Zuo, Benjamin

E. Housden, Stephanie E. Mohr, Shinya Yamamoto, Robert W. Levis, Allan C. Spradling, Norbert Perrimon, and Hugo J. Bellen. 2018. “A Gene-Specific T2A-GAL4 Library for *Drosophila*.” *ELife* (1993):1–24.

Lee, S. H., T. J. Smith, D. C. Knipple, and D. M. Soderlund. 1999. “Mutations in the House Fly Vssc1 Sodium Channel Gene Associated with Super-Kdr Resistance Abolish the Pyrethroid Sensitivity of Vssc1/TipE Sodium Channels Expressed in *Xenopus* Oocytes.” *Insect Biochem Mol Biol* 29(2):185–94.

Lee, Won Yong and Steven M. Sine. 2005. “Principal Pathway Coupling Agonist Binding to Channel Gating in Nicotinic Receptors.” *Nature* 438(7065):243–47.

Lehmann, Michael. 1996. “*Drosophila* Sgs Genes: Stage and Tissue Specificity of Hormone Responsiveness.” *Bioessays* 18(1):47–54.

Lester, Henry A., Mohammed I. Dibas, David S. Dahan, John F. Leite, and Dennis A. Dougherty. 2004. “Cys-Loop Receptors: New Twists and Turns.” *Trends in Neurosciences* 27(6):329–36.

Lester, Henry A., Cheng Xiao, Rahul Srinivasan, Cagdas D. Son, Julie Miwa, Rigo Pantoja, Matthew R. Banghart, Dennis A. Dougherty, Alison M. Goate, and Jen C. Wang. 2009. “Nicotine Is a Selective Pharmacological Chaperone of Acetylcholine Receptor Number and Stoichiometry. Implications for Drug Discovery.” *The AAPS Journal* 11(1):167–77.

Letz, B., C. Schomerus, E. Maronde, H. W. Korf, and C. Korbmacher. 1997. “Stimulation of a Nicotinic ACh Receptor Causes Depolarization and Activation of L-Type Ca2+ Channels in Rat Pinealocytes.” *The Journal of Physiology* 499(2):329–40.

Lin, L., E. M. Jeanclos, M. Treuil, K. H. Braunewell, E. D. Gundelfinger, and R. Anand. 2002. “The Calcium Sensor Protein Visinin-like Protein-1 Modulates the Surface Expression and Agonist Sensitivity of the Alpha4beta2 Nicotinic Acetylcholine Receptor.” *J Biol Chem* 277(44):41872–78.

Lind, Robert J., Martin S. Clough, Stuart E. Reynolds, and Fergus G. P. Earley. 1998. “[3H] Imidacloprid Labels High-and Low-Affinity Nicotinic Acetylcholine Receptor-like Binding Sites in the Aphid *Myzus persicae* (Hemiptera: Aphididae).” *Pesticide Biochemistry and Physiology* 62(1):3–14.

Lindholm, Anna K., Kelly A. Dyer, Renée C. Firman, Lila Fishman, Wolfgang Forstmeier, Luke Holman, Hanna Johannesson, Ulrich Knief, Hanna Kokko, and Amanda M. Larracuente. 2016. “The Ecology and Evolutionary Dynamics of Meiotic Drive.” *Trends in Ecology & Evolution* 31(4):315–26.

Liu, Xiong, Xueping Yu, Donald J. Zack, Heng Zhu, and Jiang Qian. 2008. “TiGER: A Database for Tissue-Specific Gene Expression and Regulation.” *BMC Bioinformatics* 9(1):271.

Liu, Z., M. S. Williamson, S. J. Lansdell, I. Denholm, Z. Han, and N. S. Millar. 2005. “A Nicotinic Acetylcholine Receptor Mutation Conferring Target-Site Resistance to Imidacloprid in *Nilaparvata lugens* (Brown Planthopper).” *Proc Natl Acad Sci U S A* 102(24):8420–25.

Loewi, O. 1921. “Über Humorale Übertragbarkeit Der Herznervenwirkung - I. Mitteilung.” *Pflügers Archiv Für Die Gesamte Physiologie Des Menschen Und Der Tiere* 189(1):239–42.

Logan-Garbisch, Theresa, Anthony Bortolazzo, Peter Luu, Audrey Ford, David Do, Payam Khodabakhshi, and Rachael L. French. 2014. “Developmental Ethanol Exposure Leads to Dysregulation of Lipid Metabolism and Oxidative Stress in *Drosophila*.” *G3 (Bethesda, Md.)* 5(1):49–59.

López Salon, Mariella, Laura Morelli, Eduardo M. Castaño, Eduardo F. Soto, and Juana M. Pasquini. 2000. “Defective Ubiquitination of Cerebral Proteins in Alzheimer’s Disease.” *Journal of Neuroscience Research* 62(2):302–10.

Low, Wai Yee, Hooi Ling Ng, Craig J. Morton, Michael W. Parker, Philip Batterham, and Charles Robin. 2007. “Molecular Evolution of Glutathione S-Transferases in the Genus *Drosophila*.” *Genetics* 177(3):1363–75.

Lukaszewicz-Hussain, Anna. 2010. “Role of Oxidative Stress in Organophosphate Insecticide Toxicity – Short Review.” *Pesticide Biochemistry and Physiology* 98(2):145–50.

Luong, Hang Ngoc Bao. 2018. “In Vivo Functional Characterization of Nicotinic Acetylcholine Receptors in *Drosophila melanogaster* [PhD Dissertation].” Melbourne, AU: University of Melbourne.

Lüscher, Christian and Robert C. Malenka. 2012. “NMDA Receptor-Dependent Long-Term Potentiation and Long-Term Depression (LTP/LTD).” *Cold Spring Harbor Perspectives in Biology* 4(6):a005710.

Luukkonen, B. G., Wei Tan, and Stefan Schwartz. 1995. “Efficiency of Reinitiation of Translation on Human Immunodeficiency Virus Type 1 MRNAs Is Determined by the Length of the Upstream Open Reading Frame and by Intercistronic Distance.” *Journal of Virology* 69(7):4086–94.

MacDermott, Amy B., Lorna W. Role, and Steven A. Siegelbaum. 1999. “Presynaptic Ionotropic Receptors and the Control of Transmitter Release.” *Annual Review of Neuroscience* 22(1):443–85.

Macia, Eric, Marcelo Ehrlich, Ramiro Massol, Emmanuel Boucrot, Christian Brunner, and Tomas Kirchhausen. 2006. “Dynasore, a Cell-Permeable Inhibitor of Dynamin.” *Developmental Cell* 10(6):839–50.

Malpel, Sébastien, André Klarsfeld, and François Rouyer. 2002. “Larval Optic Nerve and Adult Extra-Retinal Photoreceptors Sequentially Associate with Clock Neurons during *Drosophila* Brain Development.” *Development* 129(6):1443–53.

Mamede, M., K. Ishizu, M. Ueda, T. Mukai, Y. Iida, H. Kawashima, H. Fukuyama, K. Togashi, and H. Saji. 2007. “Temporal Change in Human Nicotinic Acetylcholine Receptor after Smoking Cessation: 5IA SPECT Study.” *J Nucl Med* 48(11):1829–35.

Mao, D., D. C. Perry, R. P. Yasuda, B. B. Wolfe, and K. J. Kellar. 2008. “The

Alpha4beta2alpha5 Nicotinic Cholinergic Receptor in Rat Brain Is Resistant to Up-Regulation by Nicotine in Vivo." *J Neurochem* 104(2):446–56.

Marchi, Mario and Massimo Grilli. 2010. "Presynaptic Nicotinic Receptors Modulating Neurotransmitter Release in the Central Nervous System: Functional Interactions with Other Coexisting Receptors." *Progress in Neurobiology* 92(2):105–11.

Marks, M. J., J. B. Burch, and A. C. Collins. 1983. "Effects of Chronic Nicotine Infusion on Tolerance Development and Nicotinic Receptors." *J Pharmacol Exp Ther* 226(3):817–25.

Marks, M. J., J. R. Pauly, S. D. Gross, E. S. Deneris, I. Hermans-Borgmeyer, S. F. Heinemann, and A. C. Collins. 1992. "Nicotine Binding and Nicotinic Receptor Subunit RNA after Chronic Nicotine Treatment." *J Neurosci* 12(7):2765–84.

Marks, M. J., J. A. Stitzel, and A. C. Collins. 1985. "Time Course Study of the Effects of Chronic Nicotine Infusion on Drug Response and Brain Receptors." *J Pharmacol Exp Ther* 235(3):619–28.

Markussen, Mette D. K. and Michael Kristensen. 2010a. "Cytochrome P450 Monooxygenase-Mediated Neonicotinoid Resistance in the House Fly *Musca domestica L.*" *Pesticide Biochemistry and Physiology* 98(1):50–58.

Markussen, Mette D. K. and Michael Kristensen. 2010b. "Low Expression of Nicotinic Acetylcholine Receptor Subunit Mdα2 in Neonicotinoid-resistant Strains of *Musca domestica L.*" *Pest Manag Sci* (June):1257–62.

Markussen, Mette D. K. and Michael Kristensen. 2012. "Spinosad Resistance in Female *Musca domestica L.* from a Field-Derived Population." *Pest Manag Sci* (February 2011):75–82.

Marmor, Mina D. and Yosef Yarden. 2004. "Role of Protein Ubiquitylation in Regulating Endocytosis of Receptor Tyrosine Kinases." *Oncogene* 23(11):2057–70.

Marshall, Owen J. and Andrea H. Brand. 2015. “Damidseq-Pipeline: An Automated Pipeline for Processing DamID Sequencing Datasets.” *Bioinformatics* 31(20):3371–73.

Marshall, Owen J., Tony D. Southall, Seth W. Cheetham, and Andrea H. Brand. 2016. “Cell-Type-Specific Profiling of Protein-DNA Interactions without Cell Isolation Using Targeted DamID with Next-Generation Sequencing.” *Nature Protocols* 11(9):1586–98.

Martelli, Felipe. 2020. “The Systemic Impacts of Low Insecticide Exposures in *Drosophila melanogaster* [PhD Dissertation].” Melbourne, AU: University of Melbourne.

Matsuda, Kazuhiko, Satoshi Kanaoka, Miki Akamatsu, and David B. Sattelle. 2009. “Diverse Actions and Target-Site Selectivity of Neonicotinoids: Structural Insights.” *Molecular Pharmacology* 76(1):1–10.

Matsuda, Kazuhiko and David B. Sattelle. 2004. “Mechanism of Selective Actions of Neonicotinoids on Insect Nicotinic Acetylcholine Receptors.” Pp. 172–82 in *New Discoveries in Agrochemicals*. Vol. 892. American Chemical Society.

Matsuda, Kazuhiko, Masaru Shimomura, Makoto Ihara, Miki Akamatsu, and David B. Sattelle. 2005. “Neonicotinoids Show Selective and Diverse Actions on Their Nicotinic Receptor Targets: Electrophysiology, Molecular Biology, and Receptor Modeling Studies.” *Bioscience, Biotechnology, and Biochemistry* 69(8):1442–52.

Matsumoto, KUNIHIRO, A. Toh-e, and YASUJI Oshima. 1978. “Genetic Control of Galactokinase Synthesis in *Saccharomyces cerevisiae*: Evidence for Constitutive Expression of the Positive Regulatory Gene Gal4.” *Journal of Bacteriology* 134(2):446–57.

Maupin-Furlow, Julie. 2012. “Proteasomes and Protein Conjugation across Domains of Life.” *Nature Reviews Microbiology* 10(2):100–111.

Mazzoni, Esteban O., Claude Desplan, and Justin Blau. 2005. “Circadian

Pacemaker Neurons Transmit and Modulate Visual Information to Control a Rapid Behavioral Response." *Neuron* 45(2):293–300.

McCutchen, B. F., K. Hoover, H. K. Preisler, M. D. Betana, R. Herrmann, J. L. Robertson, and B. D. Hammock. 1997. "Interactions of Recombinant and Wild-Type Baculoviruses with Classical Insecticides and Pyrethroid-Resistant Tobacco Budworm (Lepidoptera: Noctuidae)." *Journal of Economic Entomology* 90(5):1170–80.

McGranahan, Tresa M., Natalie E. Patzlaff, Sharon R. Grady, Stephen F. Heinemann, and T. K. Booker. 2011. "α4β2 Nicotinic Acetylcholine Receptors on Dopaminergic Neurons Mediate Nicotine Reward and Anxiety Relief." *The Journal of Neuroscience : The Official Journal of the Society for Neuroscience* 31(30):10891–902.

McGuire, Sean E., Gregg Roman, and Ronald L. Davis. 2004. "Gene Expression Systems in *Drosophila*: A Synthesis of Time and Space." *TRENDS in Genetics* 20(8):384–91.

McMahon, Harvey T. and Emmanuel Boucrot. 2011. "Molecular Mechanism and Physiological Functions of Clathrin-Mediated Endocytosis." *Nature Reviews Molecular Cell Biology* 12(8):517.

Menon, Kaushiki P., Shane Andrews, Mala Murthy, Elizabeth R. Gavis, and Kai Zinn. 2009. "The Translational Repressors Nanos and Pumilio Have Divergent Effects on Presynaptic Terminal Growth and Postsynaptic Glutamate Receptor Subunit Composition." *Journal of Neuroscience* 29(17):5558–72.

Mertz, F. P. and R. C. Yao. 1990. "*Actinomadura fibrosa* Sp. Nov. Isolated from Soil." *Int J Syst Bacteriol* 40(1):28–33.

Meunier, J. C., M. Huchet, P. Boquet, and J. P. Changeux. 1971. "Separation of the receptor protein of acetylcholine and acetylcholinesterase." *Comptes rendus hebdomadaires des seances de l'Academie des sciences. Serie D: Sciences naturelles* 272(1):117–20.

Millar, N. S. 2003. “Assembly and Subunit Diversity of Nicotinic Acetylcholine Receptors.” *Biochemical Society Transactions* 31(Pt 4):869–74.

Millar, N. S. 2009. “A Review of Experimental Techniques Used for the Heterologous Expression of Nicotinic Acetylcholine Receptors.” *Biochemical Pharmacology* 78(7):766–76.

Millar, N. S. and C. Gotti. 2009. “Diversity of Vertebrate Nicotinic Acetylcholine Receptors.” *Neuropharmacology* 56(1):237–46.

Millar, N. S. and S. J. Lansdell. 2010. “Characterisation of Insect Nicotinic Acetylcholine Receptors by Heterologous Expression.” *Advances in Experimental Medicine and Biology* 683:65–73.

Miller, Paul S. and Trevor G. Smart. 2010. “Binding, Activation and Modulation of Cys-Loop Receptors.” *Trends in Pharmacological Sciences* 31(4):161–74.

Millot, Florian, Anouk Decors, Olivier Mastain, Thomas Quintaine, Philippe Berny, Danièle Vey, Romain Lasseur, and Elisabeth Bro. 2017. “Field Evidence of Bird Poisonings by Imidacloprid-Treated Seeds: A Review of Incidents Reported by the French SAGIR Network from 1995 to 2014.” *Environmental Science and Pollution Research* 24(6):5469–85.

Mishra, Aseem, Pankaj Chaturvedi, Sourav Datta, Snita Sinukumar, Poonam Joshi, and Apurva Garg. 2015. “Harmful Effects of Nicotine.” *Indian Journal of Medical and Paediatric Oncology: Official Journal of Indian Society of Medical & Paediatric Oncology* 36(1):24.

Mitchell, Judith. 2012. “Nitenpyram Resistance in *Drosophila melanogaster* [PhD Dissertation].” Melbourne, AU: University of Melbourne.

Miyazawa, Atsuo, Yoshinori Fujiyoshi, and Nigel Unwin. 2003. “Structure and Gating Mechanism of the Acetylcholine Receptor Pore.” *Nature* 423(6943):949–55.

Morin, Xavier, Richard Daneman, Michael Zavortink, and William Chia. 2001. “A Protein Trap Strategy to Detect GFP-Tagged Proteins Expressed from Their

Endogenous Loci in *Drosophila*." *Proceedings of the National Academy of Sciences* 98(26):15050–55.

Morrissey, Christy A., Pierre Mineau, James H. Devries, Francisco Sanchez-Bayo, Matthias Liess, Michael C. Cavallaro, and Karsten Liber. 2015. "Neonicotinoid Contamination of Global Surface Waters and Associated Risk to Aquatic Invertebrates: A Review." *Environment International* 74:291–303.

Mukherjee, Jayanta, Alexander Kuryatov, Stephen J. Moss, Jon M. Lindstrom, and Rene Anand. 2009. "Mutations of Cytosolic Loop Residues Impair Assembly and Maturation of Alpha7 Nicotinic Acetylcholine Receptors." *Journal of Neurochemistry* 110(6):1885–94.

Müller, Ulrike. 1999. "Ten Years of Gene Targeting: Targeted Mouse Mutants, from Vector Design to Phenotype Analysis." *Mechanisms of Development* 82(1–2):3–21.

Nakayama, M., E. Suzuki, S. Tsunoda, and C. Hama. 2016. "The Matrix Proteins Hasp and Hig Exhibit Segregated Distribution within Synaptic Clefts and Play Distinct Roles in Synaptogenesis." *Journal of Neuroscience* 36(2):590–606.

Nashmi, R., M. E. Dickinson, S. McKinney, M. Jareb, C. Labarca, S. E. Fraser, and H. A. Lester. 2003. "Assembly of Alpha4beta2 Nicotinic Acetylcholine Receptors Assessed with Functional Fluorescently Labeled Subunits: Effects of Localization, Trafficking, and Nicotine-Induced Upregulation in Clonal Mammalian Cells and in Cultured Midbrain Neurons." *J Neurosci* 23(37):11554–67.

National Research Council. 2000. *The Future Role of Pesticides in US Agriculture*. National Academies Press.

Nauen, Ralf, Ulrich Ebbinghaus-Kintscher, and Richard Schmuck. 2001. "Toxicity and Nicotinic Acetylcholine Receptor Interaction of Imidacloprid and Its Metabolites in *Apis mellifera* (Hymenoptera: Apidae)." *Pest Management Science: Formerly Pesticide Science* 57(7):577–86.

Nery, Arthur A., Rodrigo R. Resende, Antonio H. Martins, Cleber A. Trujillo, Vesna A. Eterovic, and Henning Ulrich. 2010. “Alpha7 Nicotinic Acetylcholine Receptor Expression and Activity During Neuronal Differentiation of PC12 Pheochromocytoma Cells.” *Journal of Molecular Neuroscience* 41(3):329–39.

Ngolab, Jennifer, Liwang Liu, Rubing Zhao-Shea, Guangping Gao, Paul D. Gardner, and Andrew R. Tapper. 2015. “Functional Upregulation of α4* Nicotinic Acetylcholine Receptors in VTA GABAergic Neurons Increases Sensitivity to Nicotine Reward.” *The Journal of Neuroscience : The Official Journal of the Society for Neuroscience* 35(22):8570–78.

Nguyen, M., A. Alfonso, C. D. Johnson, and J. B. Rand. 1995. “*Caenorhabditis elegans* Mutants Resistant to Inhibitors of Acetylcholinesterase.” *Genetics* 140(2):527–35.

Nichols, Charles D., Jaime Becnel, and Udai B. Pandey. 2012. “Methods to Assay *Drosophila* Behavior.” *JoVE (Journal of Visualized Experiments)* (61):e3795.

Nickless, Andrew, Julie M. Bailis, and Zhongsheng You. 2017. “Control of Gene Expression through the Nonsense-Mediated RNA Decay Pathway.” *Cell & Bioscience* 7(1):26.

Noridomi, Kaori, Go Watanabe, Melissa N. Hansen, Gye Won Han, and Lin Chen. 2017. “Structural Insights into the Molecular Mechanisms of Myasthenia Gravis and Their Therapeutic Implications.” *ELife* 6:e23043.

Ogita, Zenichi. 1961a. “An Attempt to Reduce and Increase Insecticide-Resistance in *D. melanogaster* by Selection Pressure : Genetical and Biochemical Studies on Negatively Correlated Cross-Resistance in *Drosophila melanogaster* I.” *Botyu-Kagaku* 26(1):7–18.

Ogita, Zenichi. 1961b. “Genetical Studies on Actions of Mixed Insecticides with Negatively Correlated Substances.: Genetical and Biochemical Studies on Negatively Correlated Cross-Resistance in *Drosophila melanogaster*. III.” *Botyu-Kagaku* 26(1):88–93.

Ogueji, Emmanuel, Christopher Nwani, Christian Mbah, Stanley Iheanacho, and Friday Nweke. 2020. “Oxidative Stress, Biochemical, Lipid Peroxidation, and Antioxidant Responses in *Clarias gariepinus* Exposed to Acute Concentrations of Ivermectin.” *Environmental Science and Pollution Research*.

Ohno, Kinji, Hai-Long Wang, Margherita Milone, Nina Bren, Joan M. Brengman, Satoshi Nakano, Polly Quiram, Jerry N. Pruitt, Steven M. Sine, and Andrew G. Engel. 1996. “Congenital Myasthenic Syndrome Caused by Decreased Agonist Binding Affinity Due to a Mutation in the Acetylcholine Receptor ε Subunit.” *Neuron* 17(1):157–70.

Ortells, Marcelo O. and George G. Lunt. 1995. “Evolutionary History of the Ligand-Gated Ion-Channel Superfamily of Receptors.” *Trends in Neurosciences* 18(3):121–27.

Oswald, Matthew Cw, Paul S. Brooks, Maarten F. Zwart, Amrita Mukherjee, Ryan Jh West, Carlo Ng Giachello, Khomgrit Morarach, Richard A. Baines, Sean T. Sweeney, and Matthias Landgraf. 2018. “Reactive Oxygen Species Regulate Activity-Dependent Neuronal Plasticity in *Drosophila*.” *ELife* 7:e39393.

Pacifico, Rodrigo, Courtney M. MacMullen, Erica Walkinshaw, Xiaofan Zhang, and Ronald L. Davis. 2018. “Brain Transcriptome Changes in the Aging *Drosophila melanogaster* Accompany Olfactory Memory Performance Deficits.” *PloS One* 13(12):e0209405–e0209405.

Palma, E., L. Maggi, B. Barabino, F. Eusebi, and M. Ballivet. 1999. “Nicotinic Acetylcholine Receptors Assembled from the Alpha7 and Beta3 Subunits.” *The Journal of Biological Chemistry* 274(26):18335–40.

Paradis, Suzanne, Sean T. Sweeney, and Graeme W. Davis. 2001. “Homeostatic Control of Presynaptic Release Is Triggered by Postsynaptic Membrane Depolarization.” *Neuron* 30(3):737–49.

Pedra, Joao H. F., Andrew Hostetler, Patrick J. Gaffney, Robert A. Reenan, and

Barry R. Pittendrigh. 2004. “Hyper-Susceptibility to Deltamethrin in Parats-1 DDT Resistant *Drosophila melanogaster*.” *Pesticide Biochemistry and Physiology* 78(1):58–66.

Perry, D. C., D. Mao, A. B. Gold, J. M. McIntosh, J. C. Pezzullo, and K. J. Kellar. 2007. “Chronic Nicotine Differentially Regulates Alpha6- and Beta3-Containing Nicotinic Cholinergic Receptors in Rat Brain.” *J Pharmacol Exp Ther* 322(1):306–15.

Perry, Trent, Phil Batterham, and P. J. Daborn. 2011. “The Biology of Insecticidal Activity and Resistance.” *Insect Biochem Mol Biol* 41(7):411–22.

Perry, Trent and Philip Batterham. 2018. “Harnessing Model Organisms to Study Insecticide Resistance.” *Current Opinion in Insect Science* 27:61–67.

Perry, Trent, Janice Q. Chan, Phil Batterham, Gerald B. Watson, Chaoxian Geng, and Thomas C. Sparks. 2012. “Effects of Mutations in *Drosophila* Nicotinic Acetylcholine Receptor Subunits on Sensitivity to Insecticides Targeting Nicotinic Acetylcholine Receptors.” *Pesticide Biochemistry and Physiology* 102(1):56–60.

Perry, Trent, D. G. Heckel, J. A. McKenzie, and Phil Batterham. 2008. “Mutations in Dalpha1 or Dbeta2 Nicotinic Acetylcholine Receptor Subunits Can Confer Resistance to Neonicotinoids in *Drosophila melanogaster*.” *Insect Biochem Mol Biol* 38(5):520–28.

Perry, Trent, J. A. McKenzie, and Phil Batterham. 2007. “A Dalpha6 Knockout Strain of *Drosophila melanogaster* Confers a High Level of Resistance to Spinosad.” *Insect Biochem Mol Biol* 37(2):184–88.

Perry, Trent, Jason Somers, Y. T. Yang, and Phil Batterham. 2015. “Expression of Insect Alpha6-like Nicotinic Acetylcholine Receptors in *Drosophila melanogaster* Highlights a High Level of Conservation of the Receptor:Spinosyn Interaction.” *Insect Biochem Mol Biol* 64:106–15.

Petersen, Sophie A., Richard D. Fetter, Jasprina N. Noordermeer, Corey S.

Goodman, and Aaron DiAntonio. 1997. “Genetic Analysis of Glutamate Receptors in *Drosophila* Reveals a Retrograde Signal Regulating Presynaptic Transmitter Release.” *Neuron* 19(6):1237–48.

Pistorius, J., G. Bischoff, U. Heimbach, and M. Stähler. 2009. “Bee Poisoning Incidents in Germany in Spring 2008 Caused by Abrasion of Active Substance from Treated Seeds during Sowing of Maize.” *Julius-Kühn-Archiv* 423:118–26.

Pittendrigh, Barry R., Joseph Huesing, Kent R. Walters, Brett P. Olds, Laura D. Steele, Lijie Sun, Patrick Gaffney, and Aaron J. Gassmann. 2014. *Negative Cross-Resistance*. Elsevier Ltd.

Pittendrigh, Barry R., R. Reenan, R. H. Ffrench-Constant, and B. Ganetzky. 1997. “Point Mutations in the *Drosophila* Sodium Channel Gene Para Associated with Resistance to DDT and Pyrethroid Insecticides.” *Molecular and General Genetics MGG* 256(6):602–10.

Pollak, Peter. 2011. “Market Size and Structure.” Pp. 93–99 in *Fine Chemicals: the industry and the business*. John Wiley & Sons.

Pollock, Veronica V, Tina E. Pastoor, and Lynn Wecker. 2007. “Cyclic AMP-dependent Protein Kinase (PKA) Phosphorylates Ser362 and 467 and Protein Kinase C Phosphorylates Ser550 within the M3/M4 Cytoplasmic Domain of Human Nicotinic Receptor A4 Subunits.” *Journal of Neurochemistry* 103(2):456–66.

Puinean, A. M., S. J. Lansdell, T. Collins, P. Bielza, and N. S. Millar. 2013. “A Nicotinic Acetylcholine Receptor Transmembrane Point Mutation (G275E) Associated with Resistance to Spinosad in *Frankliniella occidentalis*.” *J Neurochem* 124(5):590–601.

Pyakurel, Poojan, Mimi Shin, and B. Jill Venton. 2018. “Nicotinic Acetylcholine Receptor (NAChR) Mediated Dopamine Release in Larval *Drosophila melanogaster*.” *Neurochemistry International* 114:33–41.

Quik, Maryka, Tanuja Bordia, and Kathryn O'Leary. 2007. "Nicotinic Receptors as CNS Targets for Parkinson's Disease." *Biochemical Pharmacology* 74(8):1224–34.

Quik, Maryka and Susan Wonnacott. 2011. "A6β2* and A4β2* Nicotinic Acetylcholine Receptors as Drug Targets for Parkinson's Disease." *Pharmacological Reviews* 63(4):938–66.

Ramírez, Omar A. and Andrés Couve. 2011. "The Endoplasmic Reticulum and Protein Trafficking in Dendrites and Axons." *Trends in Cell Biology* 21(4):219–27.

Ranson, H. and J. Hemingway. 2005. "Glutathione Transferases." Pp. 383–402 in *Comprehensive Molecular Insect Science*, edited by L. I. B. T.-C. M. I. S. Gilbert. Amsterdam: Elsevier.

Ranson, H., L. Rossiter, F. Ortelli, B. Jensen, X. Wang, C. W. Roth, F. H. Collins, and J. Hemingway. 2001. "Identification of a Novel Class of Insect Glutathione S-Transferases Involved in Resistance to DDT in the Malaria Vector *Anopheles gambiae*." *Biochemical Journal* 359(2):295–304.

Rauthan, Manish, Jianke Gong, Jinzhi Liu, Zhaoyu Li, Seth A. Wescott, Jianfeng Liu, and X. Z. Shawn Xu. 2017. "MicroRNA Regulation of NAChR Expression and Nicotine-Dependent Behavior in *C. elegans*." *Cell Reports* 21(6):1434–41.

Raymond-Delpech, V., K. Matsuda, B. M. Sattelle, J. J. Rauh, and D. B. Sattelle. 2005. "Ion Channels: Molecular Targets of Neuroactive Insecticides." *Invert Neurosci* 5(3–4):119–33.

Ren, X., J. Sun, B. E. Housden, Y. Hu, C. Roesel, S. Lin, L. P. Liu, Z. Yang, D. Mao, L. Sun, Q. Wu, J. Y. Ji, J. Xi, S. E. Mohr, J. Xu, N. Perrimon, and J. Q. Ni. 2013. "Optimized Gene Editing Technology for *Drosophila melanogaster* Using Germ Line-Specific Cas9." *Proceedings of the National Academy of Sciences* 110(47):19012–17.

Rewitz, Kim F., Michael B. O'Connor, and Lawrence I. Gilbert. 2007. "Molecular Evolution of the Insect Halloween Family of Cytochrome P450s: Phylogeny, Gene Organization and Functional Conservation." *Insect Biochemistry and Molecular Biology* 37(8):741–53.

Rezvani, K., Y. Teng, and M. De Biasi. 2010. "The Ubiquitin-Proteasome System Regulates the Stability of Neuronal Nicotinic Acetylcholine Receptors." *J Mol Neurosci* 40(1–2):177–84.

Rezvani, K., Y. Teng, Y. Pan, J. A. Dani, J. Lindstrom, E. A. Garcia Gras, J. M. McIntosh, and M. De Biasi. 2009. "UBXD4, a UBX-Containing Protein, Regulates the Cell Surface Number and Stability of Alpha3-Containing Nicotinic Acetylcholine Receptors." *J Neurosci* 29(21):6883–96.

Rezvani, K., Y. Teng, D. Shim, and M. De Biasi. 2007. "Nicotine Regulates Multiple Synaptic Proteins by Inhibiting Proteasomal Activity." *J Neurosci* 27(39):10508–19.

Rinkevich, F. D. and J. G. Scott. 2009. "Transcriptional Diversity and Allelic Variation in Nicotinic Acetylcholine Receptor Subunits of the Red Flour Beetle, *Tribolium castaneum*." *Insect Mol Biol* 18(2):233–42.

Robertson, J. L., R. M. Russel, H. K. Preisler, and N. E. Savin. 2009. *Bioassays with Arthropods*. 2nd ed. Boca Raton, FL: CRC Press.

Roe, R. M., H. P. Young, T. Iwasa, C. F. Wyss, C. F. Stumpf, T. C. Sparks, G. B. Watson, J. J. Sheets, and G. D. Thompson. 2010. "Mechanism of Resistance to Spinosyn in the Tobacco Budworm, *Heliothis virescens*." *Pesticide Biochemistry and Physiology* 96(1):8–13.

Rogers, Krysta H., Stella McMillin, Katie J. Olstad, and Robert H. Poppenga. 2019. "Imidacloprid Poisoning of Songbirds Following a Drench Application of Trees in a Residential Neighborhood in California, USA." *Environmental Toxicology and Chemistry* 38(8):1724–27.

Rosenthal, Justin S., Jun Yin, Caixia Long, Emma Spillman, Chengyu Sheng,

and Quan Yuan. 2019. “Temporal Regulation of Nicotinic Acetylcholine Receptor Subunits Supports Central Cholinergic Synapse Development.”

Roush, R. T. and J. A. McKenzie. 1987. “Ecological Genetics of Insecticide and Acaricide Resistance.” *Annual Review of Entomology* 32(1):361–80.

Roush, Richard T. 1989. “Designing Resistance Management Programs: How Can You Choose?” *Pesticide Science* 26(4):423–41.

Sabri, Osama, Philipp M. Meyer, Susanne Gräf, Swen Hesse, Stephan Wilke, Georg-Alexander Becker, Michael Rullmann, Marianne Patt, Julia Luthardt, Gudrun Wagenknecht, Alexander Hoepping, Rene Smits, Annegret Franke, Bernhard Sattler, Solveig Tiepolt, Steffen Fischer, Winnie Deuther-Conrad, Ulrich Hegerl, Henryk Barthel, Peter Schönknecht, and Peter Brust. 2018. “Cognitive Correlates of Alpha4beta2 Nicotinic Acetylcholine Receptors in Mild Alzheimer’s Dementia.” *Brain* 141(6):1840–54.

Salgado, Vincent L. 1998. “Studies on the Mode of Action of Spinosad: Insect Symptoms and Physiological Correlates.” *Pesticide Biochemistry and Physiology* 60(2):91–102.

Salgado, Vincent L. and R. Saar. 2004. “Desensitizing and Non-Desensitizing Subtypes of Alpha-Bungarotoxin-Sensitive Nicotinic Acetylcholine Receptors in Cockroach Neurons.” *J Insect Physiol* 50(10):867–79.

Salgado, Vincent L. and T. C. Sparks. 2005. “The Spinosyns: Chemistry, Biochemistry, Mode of Action, and Resistance.” Pp. 137–73 in *Comprehensive Molecular Insect Science*, edited by L. I. Gilbert. Amsterdam: Elsevier.

Sallette, J., S. Pons, A. Devillers-Thiery, M. Soudant, L. Prado de Carvalho, J. P. Changeux, and P. J. Corringer. 2005. “Nicotine Upregulates Its Own Receptors through Enhanced Intracellular Maturation.” *Neuron* 46(4):595–607.

Santos, Vanessa Santana Vieira and Boscolli Barbosa Pereira. 2020.

"Properties, Toxicity and Current Applications of the Biolarvicide Spinosad." *Journal of Toxicology and Environmental Health, Part B* 23(1):13–26.

Sara, Yildirim, Marina G. Mozhayeva, Xinran Liu, and Ege T. Kavalali. 2002. "Fast Vesicle Recycling Supports Neurotransmission during Sustained Stimulation at Hippocampal Synapses." *Journal of Neuroscience* 22(5):1608–17.

Sawruk, E., C. Udri, H. Betz, and B. Schmitt. 1990. "SBD, a Novel Structural Subunit of the *Drosophila* Nicotinic Acetylcholine Receptor, Shares Its Genomic Localization with Two Alpha-Subunits." *FEBS Lett* 273(1–2):177–81.

Scheler, Gabriele. 2004. "Regulation of Neuromodulator Receptor Efficacy—Implications for Whole-Neuron and Synaptic Plasticity." *Progress in Neurobiology* 72(6):399–415.

Schindelin, Johannes, Ignacio Arganda-Carreras, Erwin Frise, Verena Kaynig, Mark Longair, Tobias Pietzsch, Stephan Preibisch, Curtis Rueden, Stephan Saalfeld, and Benjamin Schmid. 2012. "Fiji: An Open-Source Platform for Biological-Image Analysis." *Nature Methods* 9(7):676–82.

Schmidt, Joshua M., Paul Battlay, Rebecca S. Gledhill-Smith, Robert T. Good, Chris Lumb, Alexandre Fournier-Level, and Charles Robin. 2017. "Insights into DDT Resistance from the *Drosophila melanogaster* Genetic Reference Panel." *Genetics* 207(3):1181 LP – 1193.

Schouest, L. P., V. L. Salgado, and T. A. Miller. 1986. "Synaptic Vesicles Are Depleted from Motor Nerve Terminals of Deltamethrin-Treated House Fly Larvae, *Musca domestica*." *Pesticide Biochemistry and Physiology* 25(3):381–86.

Schulz, Regine, Sonia Bertrand, Kathrin Chamaon, Karl-Heinz Smalla, Eckart D. Gundelfinger, and Daniel Bertrand. 2000. "Neuronal Nicotinic Acetylcholine Receptors from *Drosophila*." *Journal of Neurochemistry* 74(6):2537–46.

Schuster, Eugene, Joshua J. McElwee, Jennifer M. A. Tullet, Ryan Doonan, Filip

Matthijssens, John S. Reece-Hoyes, Ian A. Hope, Jacques R. Vanfleteren, Janet M. Thornton, and David Gems. 2010. “DamID in *C. elegans* Reveals Longevity-associated Targets of DAF-16/FoxO.” *Molecular Systems Biology* 6(1).

Schwartz, R. D. and K. J. Kellar. 1983. “Nicotinic Cholinergic Receptor Binding Sites in the Brain: Regulation in Vivo.” *Science* 220(4593):214–16.

Shang, Qingli, Yiou Pan, Kui Fang, Jinghui Xi, and James Andrew Brennan. 2012. “Biochemical Characterization of Acetylcholinesterase, Cytochrome P450 and Cross-Resistance in an Omethoate-Resistant Strain of *Aphis gossypii* Glover.” *Crop Protection* 31(1):15–20.

Shao, Y. M., K. Dong, and C. X. Zhang. 2007. “The Nicotinic Acetylcholine Receptor Gene Family of the Silkworm, *Bombyx mori*.” *BMC Genomics* 8:324.

Sharma, Anket, Vinod Kumar, Babar Shahzad, Mohsin Tanveer, Gagan Preet Singh Sidhu, Neha Handa, Sukhmeen Kaur Kohli, Poonam Yadav, Aditi Shreeya Bali, Ripu Daman Parihar, Owias Iqbal Dar, Kirpal Singh, Shivam Jasrotia, Palak Bakshi, M. Ramakrishnan, Sandeep Kumar, Renu Bhardwaj, and Ashwani Kumar Thukral. 2019. “Worldwide Pesticide Usage and Its Impacts on Ecosystem.” *SN Applied Sciences* 1(11):1–16.

Sharma, Smriti, Rubaljot Kooner, and Ramesh Arora. 2017. “Insect Pests and Crop Losses.” Pp. 45–66 in *Breeding insect resistant crops for sustainable agriculture*. Springer.

Sheppard, D. C. and A. A. Marchiondo. 1987. “Toxicity of Diazinon to Pyrethroid Resistant and Susceptible Horn Flies, *Haematobia irritans* (L.): Laboratory Studies and Field Trials” edited by F. A. O. of the UN. 4(3):262–70.

Shi, XuGen, YuKun Zhu, XiaoMing Xia, Kang Qiao, HongYan Wang, and KaiYun Wang. 2012. “The Mutation in Nicotinic Acetylcholine Receptor B1 Subunit May Confer Resistance to Imidacloprid in *Aphis gossypii* (Glover).” *Journal of Food, Agriculture & Environment* 10(2 part 3):1227–30.

Shimomura, Masaru, Maiko Yokota, Makoto Ihara, Miki Akamatsu, David B. Sattelle, and Kazuhiko Matsuda. 2006. “Role in the Selectivity of Neonicotinoids of Insect-Specific Basic Residues in Loop D of the Nicotinic Acetylcholine Receptor Agonist Binding Site.” *Molecular Pharmacology* 70(4):1255 LP – 1263.

Sine, Steven M., Hai-Long Wang, and Nina Bren. 2002. “Lysine Scanning Mutagenesis Delineates Structural Model of the Nicotinic Receptor Ligand Binding Domain.” *The Journal of Biological Chemistry* 277(32):29210–23.

Smit, A. B., N. I. Syed, D. Schaap, J. van Minnen, J. Klumperman, K. S. Kits, H. Lodder, R. C. van der Schors, R. van Elk, B. Sorgedrager, K. Brejc, T. K. Sixma, and W. P. Geraerts. 2001. “A Glia-Derived Acetylcholine-Binding Protein That Modulates Synaptic Transmission.” *Nature* 411(6835):261–68.

Smith, R. F., R. Van Den Bosch, W. W. Kilgore, and R. L. Doutt. 1967. “Pest Control: Biological, Physical, and Selected Chemical Methods.” *Integrated Control* 295–340.

Somers, Jason. 2015. “Using Insecticides to Probe Nicotinic Acetylcholine Receptors in *Drosophila melanogaster* [PhD Dissertation].” Melbourne, AU: University of Melbourne.

Somers, Jason, Hang Ngoc Bao Luong, Philip Batterham, and Trent Perry. 2017. “Deletion of the Nicotinic Acetylcholine Receptor Subunit Gene *Dα1* Confers Insecticide Resistance, but at What Cost?” *Fly* 0(0):00–00.

Somers, Jason, Hang Ngoc Bao Luong, Judith Mitchell, Philip Batterham, and Trent Perry. 2017. “Pleiotropic Effects of Loss of the Dα1 Subunit in *Drosophila melanogaster* : Implications for Insecticide Resistance.” *Genetics* 205(1):263–71.

Somers, Jason, J. Nguyen, C. Lumb, P. Batterham, and Trent Perry. 2015. “In Vivo Functional Analysis of the *Drosophila melanogaster* Nicotinic Acetylcholine Receptor Dα6 Using the Insecticide Spinosad.” *Insect Biochem Mol Biol* 64:116–27.

Southall, Tony D., Katrina S. Gold, Boris Egger, Catherine M. Davidson, Elizabeth E. Caygill, Owen J. Marshall, and Andrea H. Brand. 2013. “Resource Cell-Type-Specific Profiling of Gene Expression and Chromatin Binding without Cell Isolation : Assaying RNA Pol II Occupancy in Neural Stem Cells.” *Developmental Cell* 26(1):101–12.

Sparks, Thomas C., James E. Dripps, Gerald B. Watson, and Doris Paroonagian. 2012. “Resistance and Cross-Resistance to the Spinosyns - A Review and Analysis.” *Pesticide Biochemistry and Physiology* 102(1):1–10.

Sparks, Thomas C., Donald R. Hahn, and Negar V. Garizi. 2017. “Natural Products, Their Derivatives, Mimics and Synthetic Equivalents: Role in Agrochemical Discovery.” *Pest Management Science* 73(4):700–715.

Sparks, Thomas C. and Ralf Nauen. 2015. “IRAC: Mode of Action Classification and Insecticide Resistance Management.” *Pesticide Biochemistry and Physiology* 121:122–28.

van Steensel, B. and S. Henikoff. 2000. “Identification of in Vivo DNA Targets of Chromatin Proteins Using Tethered Dam Methyltransferase.” *Nature Biotechnology* 18(4):424–28.

Su, Hailing and Diane K. O’Dowd. 2003. “Fast Synaptic Currents in *Drosophila* Mushroom Body Kenyon Cells Are Mediated by Alpha-Bungarotoxin-Sensitive Nicotinic Acetylcholine Receptors and Picrotoxin-Sensitive GABA Receptors.” *The Journal of Neuroscience : The Official Journal of the Society for Neuroscience* 23(27):9246–53.

Sumikawa, K. and Vaughn M. Gehle. 1992. “Assembly of Mutant Subunits of the Nicotinic Acetylcholine Receptor Lacking the Conserved Disulfide Loop Structure.” *Journal of Biological Chemistry* 267(9):6286–90.

Tang, A. H. and C. P. Tu. 1994. “Biochemical Characterization of *Drosophila* Glutathione S-Transferases D1 and D21.” *The Journal of Biological Chemistry* 269(45):27876–84.

Tarazona, Sonia, Pedro Furi, David Turr, Alberto Ferrer, Ana Conesa, Eduardo Primo Y, De Vera, Universidad De C, Rabanales Edificio, and Gregor Mendel. 2015. “Data Quality Aware Analysis of Differential Expression in RNA-Seq with NOISeq R / Bioc Package.” *Nucleic Acids Research* 43(21):e140.

Tarimo, Brian B., Henry Chun Hin Law, Dingyin Tao, Rebecca Pastrana-Mena, Stefan M. Kanzok, Joram J. Buza, and Rhoel R. Dinglasan. 2018. “Paraquat-Mediated Oxidative Stress in *Anopheles gambiae* Mosquitoes Is Regulated by an Endoplasmic Reticulum (ER) Stress Response.” *Proteomes* 6(4):1–15.

Tatfeng, Y. M., M. U. Usuanlele, A. Orukpe, A. K. Digban, M. Okodua, F. Oviasogie, and A. A. Turay. 2005. “Mechanical Transmission of Pathogenic Organisms: The Role of Cockroaches.” *Journal of Vector Borne Diseases* 42(4):129.

Taylor, Sean C., Katia Nadeau, Meysam Abbasi, Claude Lachance, Marie Nguyen, and Joshua Fenrich. 2019. “The Ultimate QPCR Experiment: Producing Publication Quality, Reproducible Data the First Time.” *Trends in Biotechnology* xx:1–14.

Teng, Y., K. Rezvani, and M. De Biasi. 2015. “UBXN2A Regulates Nicotinic Receptor Degradation by Modulating the E3 Ligase Activity of CHIP.” *Biochem Pharmacol* 97(4):518–30.

Thany, Steeve Hervé. 2010. “Neonicotinoid Insecticides: Historical Evolution and Resistance Mechanisms.” *Advances in Experimental Medicine and Biology* 683:75–83.

Tierney, M. L. and N. Unwin. 2000. “Electron Microscopic Evidence for the Assembly of Soluble Pentameric Extracellular Domains of the Nicotinic Acetylcholine Receptor.” *Journal of Molecular Biology* 303(2):185–96.

Tomizawa, Motohiro and John E. Casida. 2001. “Structure and Diversity of Insect Nicotinic Acetylcholine Receptors.” *Pest Manag Sci* 57(10):914–22.

Tomizawa, Motohiro and John E. Casida. 2003. “Selective Toxicity of Neonicotinoids Attributable To Specificity of Insect and Mammalian Nicotinic Receptors.” *Annual Review of Entomology* 48(1):339–64.

Tomizawa, Motohiro and John E. Casida. 2004. “NEONICOTINOID INSECTICIDE TOXICOLOGY: Mechanisms of Selective Action.” *Annual Review of Pharmacology and Toxicology* 45(1):247–68.

Tomizawa, Motohiro, Bachir Latli, and John E. Casida. 1996. “Novel Neonicotinoid-agarose Affinity Column for *Drosophila* and *Musca* Nicotinic Acetylcholine Receptors.” *Journal of Neurochemistry* 67(4):1669–76.

Tornøe, C., D. Bai, L. Holden-Dye, S. N. Abramson, and D. B. Sattelle. 1995. “Actions of Neurotoxins (Bungarotoxins, Neosurugatoxin and Lophotoxins) on Insect and Nematode Nicotinic Acetylcholine Receptors.” *Toxicon* 33(4):411–24.

Torres-Oliva, Montserrat, Julia Schneider, Gordon Wiegleb, Felix Kaufholz, and Nico Posnien. 2018. “Dynamic Genome Wide Expression Profiling of *Drosophila* Head Development Reveals a Novel Role of Hunchback in Retinal Glia Cell Development and Blood-Brain Barrier Integrity.” *PLoS Genetics* 14(1):e1007180–e1007180.

Tosti, Luca, James Ashmore, Boon Siang Nicholas Tan, Benedetta Carbone, Tapan K. Mistri, Valerie Wilson, Simon R. Tomlinson, and Keisuke Kaji. 2018. “Mapping Transcription Factor Occupancy Using Minimal Numbers of Cells in Vitro and in Vivo.” *Genome Research* 28(4):592–605.

Touaylia, Samir, Mezni Ali, Khazri Abdellhafidh, and Mustapha Bejaoui. 2019. “Permethrin Induced Oxidative Stress and Neurotoxicity on the Freshwater Beetle *Laccophilus minutus*.” *Chemistry and Ecology* 35(5):459–71.

Unwin, Nigel. 2005. “Refined Structure of the Nicotinic Acetylcholine Receptor at 4 Å Resolution.” *Journal of Molecular Biology* 346(4):967–89.

Unwin, Nigel. 2013. “Nicotinic Acetylcholine Receptor and the Structural Basis of

Neuromuscular Transmission: Insights from Torpedo Postsynaptic Membranes." *Quarterly Reviews of Biophysics* 46(4):283–322.

Uytterhoeven, Valerie, Sabine Kuenen, Jaroslaw Kasprowicz, Katarzyna Miskiewicz, and Patrik Verstreken. 2011. "Loss of Skywalker Reveals Synaptic Endosomes as Sorting Stations for Synaptic Vesicle Proteins." *Cell* 145(1):117–32.

Venken, Koen J. T., Karen L. Schulze, Nele a Haelterman, Hongling Pan, Yuchun He, Martha Evans-Holm, Joseph W. Carlson, Robert W. Levis, Allan C. Spradling, Roger a Hoskins, and Hugo J. Bellen. 2011. "MiMIC: A Highly Versatile Transposon Insertion Resource for Engineering *Drosophila melanogaster* Genes." *Nature Methods* 8(9):737–43.

Vijverberg, H. P., J. M. van der Zalm, and J. van der Bercken. 1982. "Similar Mode of Action of Pyrethroids and DDT on Sodium Channel Gating in Myelinated Nerves." *Nature* 295(5850):601–3.

Vitureira, Nathalia, Mathieu Letellier, and Yukiko Goda. 2012. "Homeostatic Synaptic Plasticity: From Single Synapses to Neural Circuits." *Current Opinion in Neurobiology* 22(3):516–21.

Vo, D. T., W. H. Hsu, E. A. Abu-Basha, and R. J. Martin. 2010. "Insect Nicotinic Acetylcholine Receptor Agonists as Flea Adulticides in Small Animals." *Journal of Veterinary Pharmacology and Therapeutics* 33(4):315–22.

Vogel, Maartje J., Daniel Peric-Hupkes, and Bas van Steensel. 2007. "Detection of in Vivo Protein-DNA Interactions Using DamID in Mammalian Cells." *Nature Protocols* 2(6):1467–78.

Voges, D., P. Zwickl, and W. Baumeister. 1999. "The 26S Proteasome: A Molecular Machine Designed for Controlled Proteolysis." *Annual Review of Biochemistry* 68(1):1015–68.

Vorley, William T. and Volker Dittrich. 1994. "Integrated Pest Management and Resistance Management Systems." Pp. 179–93 in *Reviews of*

Environmental Contamination and Toxicology: Continuation of Residue Reviews, edited by G. W. Ware. New York, NY: Springer New York.

Wanamaker, Christian P., John C. Christianson, and William N. Green. 2003. "Regulation of Nicotinic Acetylcholine Receptor Assembly." *Annals of the New York Academy of Sciences* 998(1):66–80.

Wang, Jing, Xingliang Wang, Stuart J. Lansdell, Jianheng Zhang, Neil S. Millar, and Yidong Wu. 2016. "A Three Amino Acid Deletion in the Transmembrane Domain of the Nicotinic Acetylcholine Receptor Alpha6 Subunit Confers High-Level Resistance to Spinosad in *Plutella xylostella*." *Insect Biochemistry and Molecular Biology* 71:29–36.

Wang, N., A. Orr-Urtreger, J. Chapman, R. Rabinowitz, R. Nachman, and A. D. Korczyn. 2002. "Autonomic Function in Mice Lacking Alpha5 Neuronal Nicotinic Acetylcholine Receptor Subunit." *J Physiol* 542(Pt 2):347–54.

Wang, Xueyong, J. Michael McIntosh, and Mark M. Rich. 2018. "Muscle Nicotinic Acetylcholine Receptors May Mediate Trans-Synaptic Signaling at the Mouse Neuromuscular Junction." *The Journal of Neuroscience : The Official Journal of the Society for Neuroscience* 38(7):1725–36.

Wang, Zhong, Mark Gerstein, and Michael Snyder. 2009. "RNA-Seq: A Revolutionary Tool for Transcriptomics." *Nature Reviews. Genetics* 10(1):57–63.

Watson, Gerald B., Scott W. Chouinard, Kevin R. Cook, Chaoxian Geng, Jim M. Gifford, Gary D. Gustafson, James M. Hasler, Ignacio M. Larrinua, Ted J. Letherer, Jon C. Mitchell, William L. Pak, Vincent L. Salgado, Thomas C. Sparks, and Geoff E. Stilwell. 2010. "A Spinosyn-Sensitive *Drosophila melanogaster* Nicotinic Acetylcholine Receptor Identified through Chemically Induced Target Site Resistance, Resistance Gene Identification, and Heterologous Expression." *Insect Biochemistry and Molecular Biology* 40(5):376–84.

Weber, Allison L., George F. Khan, Michael M. Magwire, Crystal L. Tabor, Trudy

F. C. Mackay, and Robert R. H. Anholt. 2012. “Genome-Wide Association Analysis of Oxidative Stress Resistance in *Drosophila melanogaster*.” *PloS One* 7(4).

Webster, Richard, Wei-Wei Liu, Amina Chaouch, Hanns Lochmuller, and David Beeson. 2014. “Fast-Channel Congenital Myasthenic Syndrome with a Novel Acetylcholine Receptor Mutation at the Alpha-Epsilon Subunit Interface.” *Neuromuscular Disorders : NMD* 24(2):143–47.

Wells, Gregg B. 2008. “Structural Answers and Persistent Questions about How Nicotinic Receptors Work.” *Frontiers in Bioscience: A Journal and Virtual Library* 13:5479.

Wessler, I. and C. J. Kirkpatrick. 2008. “Acetylcholine beyond Neurons: The Non-Neuronal Cholinergic System in Humans.” *British Journal of Pharmacology* 154(8):1558–71.

Wiesner, Petra and Hartmut Kayser. 2000. “Characterization of Nicotinic Acetylcholine Receptors from the Insects *Aphis craccivora*, *Myzus persicae*, and *Locusta migratoria* by Radioligand Binding Assays: Relation to Thiamethoxam Action.” *Journal of Biochemical and Molecular Toxicology* 14(4):221–30.

Willis, Monte S., W. H. Davin Townley-Tilson, Eunice Y. Kang, Jonathon W. Homeister, and Cam Patterson. 2010. “Sent to Destroy: The Ubiquitin Proteasome System Regulates Cell Signaling and Protein Quality Control in Cardiovascular Development and Disease.” *Circulation Research* 106(3):463–78.

Wingender, E., P. Dietze, H. Karas, and R. Knüppel. 1996. “TRANSFAC: A Database on Transcription Factors and Their DNA Binding Sites.” *Nucleic Acids Research* 24(1):238–41.

Witzemann, Veit, Holger Schwarz, Michael Koenen, Christoph Berberich, Alfredo Villarroel, A. Wernig, Hans R. Brenner, and Bert Sakmann. 1996. “Acetylcholine Receptor Ɛ-Subunit Deletion Causes Muscle Weakness and

Atrophy in Juvenile and Adult Mice." *Proceedings of the National Academy of Sciences* 93(23):13286–91.

Wu, Meilin, James E. Robinson, and William J. Joiner. 2014. "SLEEPLESS Is a Bifunctional Regulator of Excitability and Cholinergic Synaptic Transmission." *Current Biology : CB* 24(6):621–29.

Xiao, Sheng-Jian, Chi Zhang, Quan Zou, and Zhi-Liang Ji. 2010. "TiSGeD: A Database for Tissue-Specific Genes." *Bioinformatics* 26(9):1273–75.

Xu, W., A. Orr-Urtreger, F. Nigro, S. Gelber, C. B. Sutcliffe, D. Armstrong, J. W. Patrick, L. W. Role, A. L. Beaudet, and M. De Biasi. 1999. "Multiorgan Autonomic Dysfunction in Mice Lacking the Beta2 and the Beta4 Subunits of Neuronal Nicotinic Acetylcholine Receptors." *J Neurosci* 19(21):9298–9305.

Xu, Wenping, Mingjun Yang, Jufang Gao, Yang Zhang, and Liming Tao. 2018. "Oxidative Stress and DNA Damage Induced by Spinosad Exposure in *Spodoptera frugiperda* Sf9 Cells." *Food and Agricultural Immunology* 29(1):171–81.

Xu, X., H. Bao, X. Shao, Y. Zhang, X. Yao, Z. Liu, and Z. Li. 2010. "Pharmacological Characterization of Cis-Nitromethylene Neonicotinoids in Relation to Imidacloprid Binding Sites in the Brown Planthopper, *Nilaparvata lugens*." *Insect Molecular Biology* 19(1):1–8.

Xue, Rong, Yahui Wan, Xiaoqian Sun, Xuan Zhang, Wei Gao, and Wei Wu. 2019. "Nicotinic Mitigation of Neuroinflammation and Oxidative Stress After Chronic Sleep Deprivation." *Frontiers in Immunology* 10:2546.

Yamamoto, Izuru, Nobuo Kyomura, and Yoji Takahashi. 1993. "Negatively Correlated Cross Resistance: Combinations of N-methylcarbamate with N-propylcarbamate or Oxadiazolone for Green Rice Leafhopper." *Archives of Insect Biochemistry and Physiology* 22(1-2):277–88.

Yamamoto, Izuru, Goro Yabuta, Motohiro Tomizawa, Takayuki Saito, Toru Miyamoto, and Shinzo Kagabu. 1995. "Molecular Mechanism for Selective

Toxicity of Nicotinoids and Neonicotinoids." *Journal of Pesticide Science* 20(1):33–40.

Yamodo, Innocent H., David C. Chiara, Jonathan B. Cohen, and Keith W. Miller. 2010. "Conformational Changes in the Nicotinic Acetylcholine Receptor during Gating and Desensitization." *Biochemistry* 49(1):156–65.

Yan, Yijin, Can Peng, Matthew C. Arvin, Xiao-Tao Jin, Veronica J. Kim, Matthew D. Ramsey, Yong Wang, Sambashiva Banala, David L. Wokosin, and J. Michael McIntosh. 2018. "Nicotinic Cholinergic Receptors in VTA Glutamate Neurons Modulate Excitatory Transmission." *Cell Reports* 23(8):2236–44.

Yao, X., F. Song, Y. Zhang, Y. Shao, J. Li, and Z. Liu. 2009. "Nicotinic Acetylcholine Receptor Beta1 Subunit from the Brown Planthopper, *Nilaparvata lugens*: A-to-I RNA Editing and Its Possible Roles in Neonicotinoid Sensitivity." *Insect Biochem Mol Biol* 39(5–6):348–54.

Yu, C. Ron and Lorna W. Role. 1998. "Functional Contribution of the Alpha7 Subunit to Multiple Subtypes of Nicotinic Receptors in Embryonic Chick Sympathetic Neurones." *The Journal of Physiology* 509(3):651–65.

Yu, Wen-Feng, Agneta Nordberg, Rivka Ravid, and Zhi-Zhong Guan. 2003. "Correlation of Oxidative Stress and the Loss of the Nicotinic Receptor Alpha4 Subunit in the Temporal Cortex of Patients with Alzheimer's Disease." *Neuroscience Letters* 338(1):13–16.

Yuan, Quan, Yang Xiang, Zhiqiang Yan, Chun Han, Lily Yeh Jan, and Yuh Nung Jan. 2011. "Light-Induced Structural and Functional Plasticity in *Drosophila* Larval Visual System." *Science* 333(6048):1458–62.

Zalucki, M. P. and M. J. Furlong. 2017. "Behavior as a Mechanism of Insecticide Resistance: Evaluation of the Evidence." *Current Opinion in Insect Science* 21:19–25.

Zambrano, Cristian A., Caitlin A. Short, Rakel M. Salamander, Sharon R. Grady, and Michael J. Marks. 2015. "Density of Alpha4beta2 NAChR on the Surface

of Neurons Is Modulated by Chronic Antagonist Exposure." *Pharmacology Research & Perspectives* 3(2):e00111–e00111.

Zhang, Aiguo, Hartmut Kaiser, Peter Maienfisch, and John E. Casida. 2000. "Insect Nicotinic Acetylcholine Receptor: Conserved Neonicotinoid Specificity of [3H] Imidacloprid Binding Site: Conserved Neonicotinoid Specificity of [3H] Imidacloprid Binding Site." *Journal of Neurochemistry* 75(3):1294–1303.

Zhang, Guoqiang, Hua Huang, Di Liu, Ying Cheng, Xiaoling Liu, Wenxin Zhang, Ruichuan Yin, Dapeng Zhang, Peng Zhang, Jianzhao Liu, Chaoyi Li, Baodong Liu, Yuewan Luo, Yuanxiang Zhu, Ning Zhang, Shunmin He, Chuan He, Hailin Wang, and Dahua Chen. 2015. "N6-Methyladenine DNA Modification in *Drosophila*." *Cell* 161(4):893–906.

Zhang, X., Z. H. Gong, E. Hellstrom-Lindahl, and A. Nordberg. 1995. "Regulation of Alpha4beta2 Nicotinic Acetylcholine Receptors in M10 Cells Following Treatment with Nicotinic Agents." *Neuroreport* 6(2):313–17.

Zoli, Michele, Susanna Pucci, Antonietta Vilella, and Cecilia Gotti. 2018. "Neuronal and Extraneuronal Nicotinic Acetylcholine Receptors." *Current Neuropharmacology* 16(4):338–49.

Appendices

Appendix 1: R Script for Toxicology Bioassay

```
ld50.estimate <- function (file, conf.level= 95)
{
## file = .txt file directory
## run the function once and enter file directory using the final line

mydata = read.table(file)

### Columns of data: response(r) = dead; number_obs(n) = total; dose(d) = conc
data = data.frame(conc=    mydata[, 1],
                  total=   mydata[, 2],
                  dead=    mydata[, 3] )

## Abbots correction
subdata= data[ data$conc == 0, ]
N=data$total
mort=data$dead/N
mortcont=mean(subdata$dead)/N
ad.mort=(mort-mortcont)/(1-mortcont)
data$dead=round(N*ad.mort, digits= 0)
data$dead=ifelse(data$dead < 0, 0, data$dead)
data$alive=N-data$dead

mdf = data.frame(conc= c(data$conc), total= c(data$total), dead= c(data$dead))
mdf = mdf[!(mdf$conc==0),]

#  model    (    r          n - r     )    ~  d
mod =glm(cbind(dead, (total-dead))  ~ log10(conc), family=binomial(link="probit"), data=mdf)

conf.level = 95   # intervals at this confidence levels

  ### Calculate heterogeneity correction to confidence intervals according to Finney, 1971, (p.72, eq.
4.27; also called "h")
  het = deviance(mod)/df.residual(mod) ; if(het < 1){het = 1}
  # Heterogeneity cannot be less than 1
  # R sets dispersion paramerter 1 by default #so I use 1, change if needed
  ## Extract slope and intercept
  summary <- summary(mod, dispersion= 1, cor = F) # summary(mod, dispersion= het, cor = F)  # summary
might change if het is lot > 1
  intercept <- summary$coefficients[1] ; interceptSE <- summary$coefficients[3]
  slope     <- summary$coefficients[2] ;     slopeSE <- summary$coefficients[4]
  z.value <- summary$coefficients[6]
  N <- sum(mdf$total) # or for m3 #  N <- nrow(md_binary) #this needs to be fixed: getting data from
outside the supplied variables

  ## Intercept (alpha)  ## Slope (beta)
  b0 <- intercept   ;   b1 <- slope
  ## Slope variance  # Intercept variance  # Slope intercept covariance
  vcov = summary(mod)$cov.unscaled
  var.b0<-vcov[1,1] ;  var.b1<-vcov[2,2] ; cov.b0.b1<-vcov[1,2]

  ## Adjust alpha depending on heterogeneity (Finney, 1971, p. 76)
  #alpha for confidence level not EC level
  alpha= 1-(conf.level/100) #<-adjust to preferred confidence interval level
  #------------------------------ conf.level= 80, 90, 95, 99
  if(het > 1) {talpha = -qt(alpha/2, df=df.residual(mod))} else {talpha = -qnorm(alpha/2)}

  ## Calculate g (Finney, 1971, p 78, eq. 4.36)
  ## "With almost all good sets of data, g will be substantially smaller than 1.0 and  seldom greater
than 0.4."
  g <- het * ((talpha^2 * var.b1)/b1^2)

  ## Estimate for all LD levels based on probits in eta ~~~~~~~~~~~~~~|
  ## (Robertson et al., 2007, pg.27; or "m" in Finney, 1971, p. 78)  |
  eta= family(mod)$linkfun(0.5) # probit distribution curve           |
  # fixed for LD50                                                    |
  theta.hat = (eta - b0)/b1  #  returns the conc or dose at p level  |
  # b0 = intercept ; b1 = slope                                       |
  ##_____ this section is critical to the calculation_________________|

  ## Calculate correction of fiducial limits according to Fieller method (Finney, 1971, p. 78-79. eq.
```

```
4.35)
  const1 <- (g/(1-g))*(theta.hat + cov.b0.b1/var.b1) # const1 <- (g/(1-g))*(theta.hat -   cov.b0.b1/
var.b1)
  const2a <- var.b0 + 2*cov.b0.b1*theta.hat + var.b1*theta.hat^2 - g*(var.b0 - (cov.b0.b1^2/var.b1))
  const2 <- talpha/((1-g)*b1) * sqrt(het * (const2a))

  ## Calculate the confidence intervals LCL=lower, UCL=upper (Finney, 1971, p. 78-79. eq. 4.35)
  LCL <- (theta.hat + const1 - const2)
  UCL <- (theta.hat + const1 + const2)

  ##Calculate var.theta.hat to find conf.int for ratio (Robertson et al., 2007, pg. 27)
  # Based on formula for SD of ratio between two means
  #fixed; for ld.level= 50  # need to figure out this for different ld.level
  var.theta.hat <- ((b0/b1)^2) * ( ((interceptSE/b0)^2) - 2*cov.b0.b1/(b0*b1) + ((slopeSE/b1)^2) )

  # Calculate variance based (Robertson et al., 2007, pg. 27)
  ## var.theta.hat <- (1/(theta.hat^2)) * ( var.b0 + 2*cov.b0.b1*theta.hat + var.b1*theta.hat^2 )
  #---I don't know why this equation is not working to give out the expected value


  ## Make a data frame from the data at all the different values
      xtxt = cbind(
            N=N,
            slope=(slope),
            slopeSE=(slopeSE),
            LD50=(10^theta.hat),
            LCL95=(10^LCL),
            UCL95=(10^UCL),
            theta.hat=theta.hat,
            var.theta.hat=var.theta.hat )

      write.table(xtxt, file=paste(file, ".summary.txt", sep=""), sep="\t", row.names=FALSE,
col.names=TRUE)   ## give out text file of result summary

            return(xtxt)
}

ld50.estimate(file, conf.level = 95)
```

Appendix 2: R Script for NOIseq-real Differential Expression Analysis

```
library(NOISeq)
library(ggplot2)
library(ggrepel)

# grab all csv files in directory
files = Sys.glob("*.csv")

# read in the first file
input = read.table(files[1],header=T)[,1:2]
name = regmatches(files[1],regexpr(".*?(?=[-\\.])",files[1],perl=T))
input$polii = scale(input$polii,center=F)
input$polii = 2^input$polii
names(input)[2] = name

# read all the others
for (file in files[2:length(files)]) {
  tempin = read.table(file,header=T)[,1:2]
  name = regmatches(file,regexpr(".*?(?=[-\\.])",file,perl=T))
  tempin$polii = scale(tempin$polii,center=F)
  tempin$polii = 2^tempin$polii
  names(tempin)[2] = name
  input = merge(input,tempin,by="name")
}

# setup data for NOIseq analysis
mycounts=input[,2:10]
row.names(mycounts)=input$name
myfactors = data.frame(Tissue=
 c("A1","A1","A1","A6","A6","A6","wt","wt","wt"),TissueRun=c("A1_n1","A1_n2","A1_n3","A6_n1","A6_n2","A6
 _n3","wt_n1","wt_n2","wt_n3"))
mydata = readData(data=mycounts,factors=myfactors)

# run NOIseq
mynoiseq = noiseq(mydata,conditions=c("A1","wt"),factor="Tissue",replicates="biological",norm="uqua")

# grab the full dataset
mynoiseq.all = mynoiseq@results[[1]]
mynoiseq.all$log.rat = log2(mynoiseq.all$A1_mean/mynoiseq.all$wt_mean)
mynoiseq.all$log.prob = -log10(1-mynoiseq.all$prob)

# get differentially expressed genes
mydeg = degenes(mynoiseq,q=0.9,M=NULL)
mydeg.up = degenes(mynoiseq,q=0.9,M="up")
mydeg.down = degenes(mynoiseq,q=0.9,M="down")

mydeg095.up = degenes(mynoiseq,q=0.95,M="up")
mydeg095.down = degenes(mynoiseq,q=0.95,M="down")

# calculate means
input$wt = log2(rowMeans(input[,c("WTP1","WTP2","WTP3")]))
input$a1 = log2(rowMeans(input[,c("A1P1","A1P2","A1P3")]))
input$a6 = log2(rowMeans(input[,c("A6P1","A6P2","A6P3")]))

# "classic plot"
p = ggplot(input,aes(a1,wt))
p+theme_bw(base_size=20)+
  #stat_density2d(geom="raster",aes(fill=..density..^0.25,alpha=..density..^0.05),contour=F)+
  #scale_fill_gradientn(colours=colorRampPalette(c("white", blues9))(256))+
  geom_point(color=rgb(0.2,0.3,0.6),alpha=0.15)+
  geom_point(data=subset(input,name %in% rownames(mydeg.down))
 [,c("a1","wt")],color="red",alpha=0.5,size=2)+
  geom_point(data=subset(input,name %in% rownames(mydeg.up))
 [,c("a1","wt")],color="darkgreen",alpha=0.5,size=2)+
  geom_text_repel(data=subset(input,name %in% rownames(mydeg095.down))[,c("a1","wt")],
                  aes(label=subset(input,name %in% rownames(mydeg095.down))$name),size=3,
                  box.padding=unit(0.5,"mm")
                  #nudge_x=0.25,nudge_y=-0.25
                  )+
  geom_text_repel(data=subset(input,name %in% rownames(mydeg095.up))[,c("a1","wt")],
                  aes(label=subset(input,name %in% rownames(mydeg095.up))$name),size=3,
```

```
                  box.padding=unit(0.5,"mm")
                  #nudge_x=0.25,nudge_y=-0.25
                  )+
  xlab(bquote("A1"))+
  ylab(bquote("Wild-type"))+
  ggtitle("Differentially expressed genes")
ggsave("Differentially expressed genes A1 vs wt classic.pdf",device=pdf,width=35,height=35,units="cm")

# volcano plot
p = ggplot(mynoiseq.all,aes(log.rat,log.prob))
p+theme_bw(base_size=20)+
  geom_point(color=rgb(0,0,0),alpha=0.15)+
  geom_point(data=subset(mynoiseq.all,rownames(mynoiseq.all) %in% rownames(mydeg.down))
[,c("log.rat","log.prob")],color="red",alpha=0.5,size=2)+
  geom_point(data=subset(mynoiseq.all,rownames(mynoiseq.all) %in% rownames(mydeg.up))
[,c("log.rat","log.prob")],color="red",alpha=0.5,size=2)+
  geom_text_repel(data=subset(mynoiseq.all,rownames(mynoiseq.all) %in% rownames(mydeg095.down))
[,c("log.rat","log.prob")],
                  aes(label=rownames(subset(mynoiseq.all,rownames(mynoiseq.all) %in%
rownames(mydeg095.down)))),size=3,
                  box.padding=unit(0.5,"mm")
                  #nudge_x=0.25,nudge_y=-0.25
  )+
  geom_text_repel(data=subset(mynoiseq.all,rownames(mynoiseq.all) %in% rownames(mydeg095.up))
[,c("log.rat","log.prob")],
                   aes(label=rownames(subset(mynoiseq.all,rownames(mynoiseq.all) %in%
rownames(mydeg095.up)))),size=3,
                   box.padding=unit(0.5,"mm")
  )+
  xlab(bquote(~log[2]~"(fold change (A1/wt))"))+
  ylab(bquote(~log[10]~"(P)"))+
  ggtitle("Differentially expressed genes of A1 vs WT")
ggsave(filename ,device=pdf,width=35,height=35,units="cm")

# write the differentially expressed genes to file
write.table(rownames(mydeg.up),"A1P_upregulated.csv",quote=F,row.names = F, col.names = F)
write.table(rownames(mydeg.down),"A1P_downregulated.csv",quote=F,row.names = F, col.names = F)
```

Appendix 3: MIQE Checklist for qPCR Analysis

Sample/Template	Details	Checklist
Source	If cancer, was biopsy screened for adjacent normal tissue?	Drosophila melanogaster 3rd instar brain
Method of preservation	Liquid N2/RNAlater/formalin	Liquid N2
Storage time (if appropriate)	If using samples >6 months old	< 2-month-old
Handling	fresh/frozen/formalin	Frozen
Extraction method	TriZol/columns	TRIsure extraction
RNA: DNA-free	Intron-spanning primers/no RT control	Intron-spanning primers, DnaseI, PCR check
Concentration	Nanodrop/ribogreen/microfluidics	Qubit Fluorometric Quantitation
RNA: integrity	Microfluidics/3':5' assay	Agarose Gel
Inhibition-free	Method of testing	Dilution curve, PCR efficiency <100%
Assay optimisation/validation		
Accession number	RefSeq XX_1234567	*Da1*; NM_001275988.2, *Da2*; NM_170146.2, *Da3*; NM_001298086.1, *Da4*; NM_001316465.1, *Da5*; NM_001370005.1, *Da6*; NM_001273373.2, *Da7*; NM_001298507.1, *Db1*; NM_079203.3, *Db2*; NM_170147.3, *Db3*; NM_080359.4, *CG13220*;NM_001273958.1 *RpL11*; NM_001299685.1, *Pcd*; NM_058012.4, *CG43324*;NM_001259470.2 *CG13227*; NM_136802.3, *CG17272*; NM_142660.4, *Ocho*; NM_001259830.1, *eIF3i*; NM_078754.4
Amplicon details	exon location, amplicon size	See Table 3.4
Primer sequence	even if previously published	See Table 3.4
In silico	BLAST/Primer-BLAST/m-fold	Primer-BLAST, electrophoresis, melt curve
empirical	primer concentration/annealing temperature	10µM, 60deg
Priming conditions	oligo-dT/random/combination/target-specific	oligo-dT

PCR efficiency	dilution curve	*Da1* = 1.92, *Da2* = 1.83, *Da3* = 1.98, *Da4* = 1.89, *Da5* = 1.88, *Da6* = 1.79, *Da7* = 1.77, *Db1* = 1.92, *Db2* = 1.88, *Db3* = 1.88, *CG13220* =1.86, *RpL11* =2.03, *Pcd* = 2.02, *CG43324* = 2.05, *CG13227* = 2.10, *eIF3i* = 2.01, *CG17272* = 2.00, *Ocho* = 1.90
Linear dynamic range	spanning unknown targets	2-fold serial dilution
Limits of detection	LOD detection/accurate quantification	*Da1* > CT 31, *Da2* > CT 29, *Da3* > CT 36, *Da4* > CT 29, *Da5* > CT 30, *Da6* > CT 26, *Da7* > CT 27, *Db1* > CT 31, *Db2* > CT 25, *Db3* > CT 28, *CG13220* > CT 35, *RpL11* > CT 30, *Pcd* > CT 32, *CG43324* > CT 29, *CG13227* > CT 28, *CG17272* > CT 29, *Ocho* > CT 31, *eIF3i* > CT 30
Intra-assay variation	copy numbers not Cq	*CG13220*; 0.376, *RpL11;* 1.22
RT/PCR		
Protocols	detailed description, concentrations, volumes	12ul total reaction. 5ul SYBR Green PCR Master Mix, 0.25µl F, 0.25µl R, 4.5µl H2O and 2µl Template
Reagents	supplier, Lot number	QuantiTect SYBR green PCR kit, Qiagen
Duplicate RT	DCq	Triplicate
NTC	Cq & melt curves	CT value or melt curve not detected
NAC	DCq beginning:end of qPCR	N/A
Positive control	inter-run calibrators	Inter-run Calibrator
Data analysis		
Specialist software	e.g., QBAsePlus	$2^{-\Delta\Delta CT}$ method
Statistical justification	e.g., biological replicates	5 biological replicates for each cross
Transparent, validated normalisation	e.g., GeNorm summary	Target and housekeeper validated at the same life stage

Appendix 4: Region spanning gene deletion in *Dα1*$^{\Delta DH}$, *Dα2*$^{\Delta(3)4E}$ and *Dα6*^{KO}

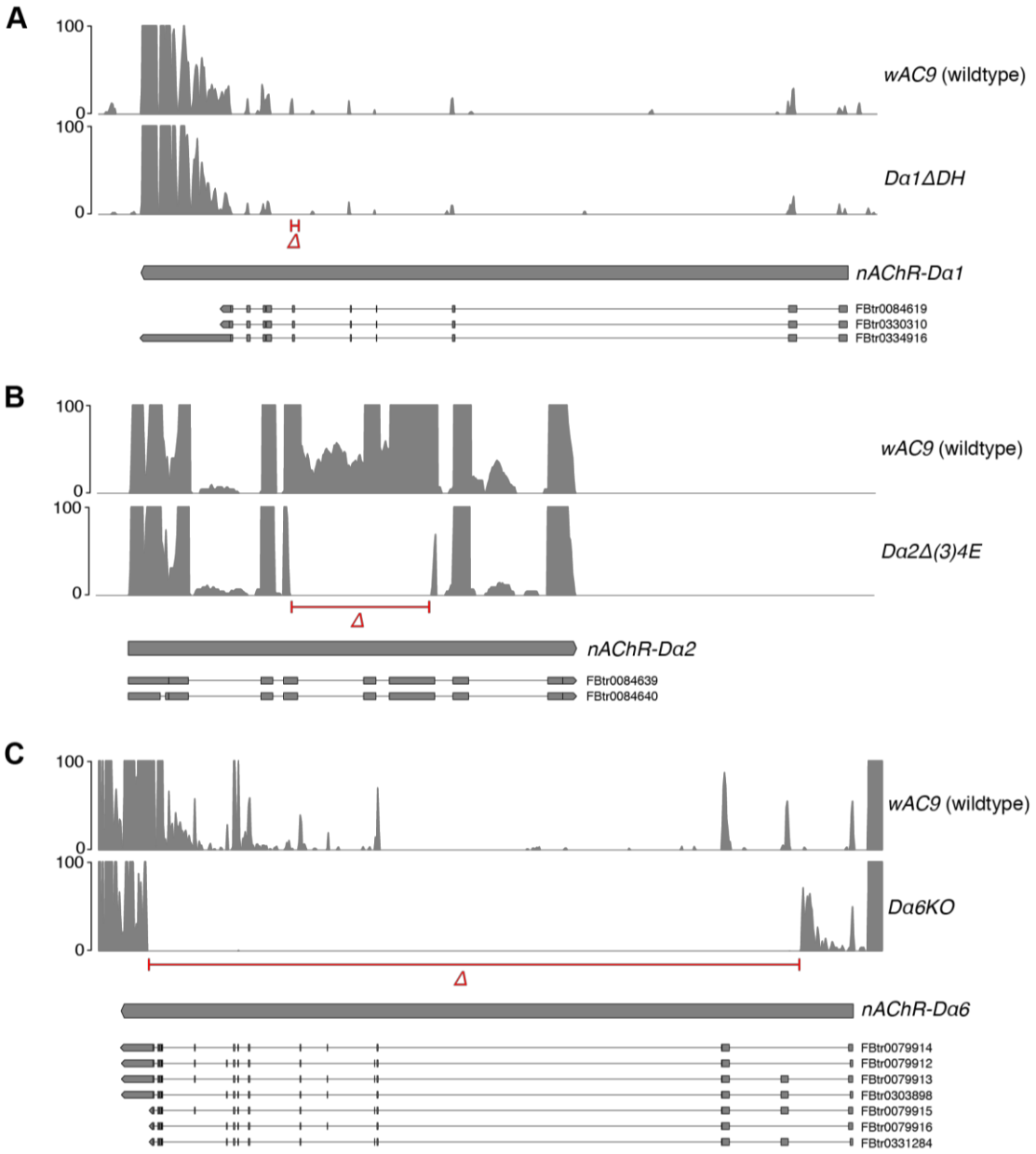

Graphs show read count (y-axis) of RNAseq reads mapped to (A) *Dα1*, (B) *Dα2* and (C) *Dα6* gene, in *Dα1*$^{\Delta DH}$, *Dα2*$^{\Delta(3)4E}$ and *Dα6*^{KO} mutants respectively, in comparison to the wildtype strain, *wAC9*. Red markings indicate region of the gene that was removed using CRISPR/Cas9 in the mutants. RNAseq did not pick up any reads mapped to these regions in the mutants. Respective gene annotation is indicated below the graph, with all known transcripts illustrated to show exonic and intronic regions of the gene.

Appendix 5: List of DEGs in *Dα1*^{EMS1} Mutant

Gene	Log2FC[a]	Probability[b]	Gene	Log2FC[a]	Probability[b]
7B2	1.8820	0.0059	CG44242	1.2784	0.0204
abs	0.9401	0.0847	CG44253	1.9526	0.0295
Acp98AB	1.6976	0.0315	CG44257	1.5652	0.0176
Ady43A	1.6893	0.0588	CG44259	1.8468	0.0119
Ald	-0.8074	0.0654	CG44303	0.7629	0.0920
Arp6	1.2848	0.0368	CG44314	0.8747	0.0583
Arpc1	-1.0623	0.0605	CG44362	1.1704	0.0326
Arpc4	1.2260	0.0625	CG4452	-0.8844	0.0762
AttA	1.8689	0.0624	CG44532	0.7500	0.0873
azot	1.6795	0.0601	CG4725	1.4357	0.0455
b	0.7761	0.0763	CG4860	-1.0470	0.0613
Blos3	1.2053	0.0463	CG4935	1.4041	0.0616
Calr	-0.6509	0.0961	CG5009	1.9696	0.0235
CG10184	1.0848	0.0840	CG5013	0.8161	0.0773
CG10205	-1.3149	0.0190	CG5144	-0.8542	0.0686
CG10222	1.1589	0.0525	CG5210	1.2304	0.0883
CG10286	-1.2509	0.0374	CG5267	1.5367	0.0329
CG10298	-0.8551	0.0674	CG5532	1.3233	0.0389
CG10306	1.0741	0.0496	CG5721	1.0291	0.0918
CG10483	0.7110	0.0968	CG5860	1.0537	0.0940
CG10616	1.1186	0.0722	CG5973	0.8165	0.0829
CG10731	0.8829	0.0575	CG6028	1.2362	0.0290
CG10845	0.8614	0.0917	CG6308	1.2505	0.0456
CG10864	1.3358	0.0688	CG6628	1.1378	0.0468
CG11191	0.6837	0.0931	CG6638	1.1906	0.0965
CG11317	1.3165	0.0343	CG6660	1.3532	0.0604
CG11388	-0.9754	0.0441	CG6686	0.9264	0.0966
CG11577	-0.7512	0.0990	CG6746	1.0376	0.0607
CG11753	-1.0886	0.0389	CG6812	0.9692	0.0455
CG11825	-0.7366	0.0893	CG6908	1.2646	0.0255
CG11858	1.5008	0.0323	CG7126	2.5270	0.0222
CG12016	0.8766	0.0648	CG7133	0.8300	0.0838
CG12091	1.0466	0.0415	CG7203	-0.9134	0.0488
CG12170	-1.1964	0.0385	CG7214	-1.0990	0.0521
CG12264	1.0403	0.0927	CG7289	1.0260	0.0923
CG12279	0.9960	0.0616	CG7296	1.0537	0.0356
CG12309	0.9131	0.0651	CG7299	1.1013	0.0445
CG12321	1.2826	0.0547	CG7506	1.5281	0.0248

CG12926	-2.1710	0.0269	CG7593	0.9639	0.0544
CG12948	0.9830	0.0520	CG7967	-0.7247	0.0954
CG13042	0.9047	0.0573	CG8004	-1.1711	0.0586
CG13050	1.2817	0.0535	CG8066	0.7246	0.0867
CG13056	2.1420	0.0266	CG8206	-0.7373	0.0925
CG13058	0.8627	0.0836	CG8245	0.9478	0.0570
CG13060	-1.6975	0.0105	CG8248	0.9764	0.0638
CG1307	-0.6976	0.0932	CG8319	1.3698	0.0386
CG13108	1.2394	0.0306	CG8353	-1.4124	0.0246
CG13110	2.0084	0.0898	CG8372	2.1406	0.0478
CG13123	1.1119	0.0500	CG9016	0.7233	0.0908
CG13151	1.1793	0.0665	CG9263	1.3733	0.0585
CG13228	1.1482	0.0284	CG9471	1.2688	0.0844
CG13255	-0.7485	0.0850	CG9570	1.2464	0.0367
CG13298	1.3313	0.0198	CG9669	-0.6984	0.0992
CG13437	1.1505	0.0552	CG9890	1.3093	0.0733
CG13484	-1.0334	0.0420	CG9922	1.0000	0.0755
CG13541	0.9755	0.0551	CG9960	0.6869	0.0881
CG13562	1.0048	0.0833	ClC-b	0.8172	0.0967
CG13748	0.9798	0.0574	Cpr67Fa1	1.0934	0.0406
CG13751	1.2614	0.0477	Cpr92F	1.3035	0.0488
CG13807	-1.0128	0.0420	Cpr97Ea	0.7175	0.0983
CG13877	1.2726	0.0265	Cpr97Eb	0.9567	0.0440
CG13891	1.3267	0.0182	CREG	0.7891	0.0773
CG13994	1.8742	0.0350	croc	0.7918	0.0858
CG14212	1.8369	0.0181	Cyp28a5	0.8302	0.0946
CG14298	1.0649	0.0663	Cyp4p1	1.0406	0.0660
CG14321	0.8569	0.0616	Cyp4p2	1.4534	0.0995
CG14377	-0.8194	0.0619	dgt2	-0.7643	0.0904
CG14419	-1.2352	0.0402	Dim1	1.6717	0.0651
CG1444	-0.7074	0.0870	DnaJ-1	-0.7548	0.0756
CG14488	1.2614	0.0523	DnaJ-60	0.8143	0.0882
CG14550	1.5644	0.0456	dos	-0.8555	0.0733
CG14667	1.7736	0.0096	Dpy-30L1	1.3870	0.0173
CG14795	1.0760	0.0570	Dsor1	-0.8059	0.0802
CG14817	0.9472	0.0532	E(spl)m5-HLH	-1.4691	0.0548
CG15019	0.8354	0.0805	E(spl)m7-HLH	-1.2404	0.0304
CG15027	2.2001	0.0155	E(spl)mγ-HLH	-1.1762	0.0391
CG15071	-2.4585	0.0120	edin	0.8565	0.0896
CG15282	-0.8904	0.0764	eIF-5A	0.8458	0.0653
CG15386	-1.0089	0.0486	emc	0.7251	0.0791

CG15390	-0.7999	0.0845	ems	0.8904	0.0560
CG15482	-0.9182	0.0475	Ercc1	1.7056	0.0911
CG15771	0.6830	0.0941	fan	1.4490	0.0484
CG15863	0.8667	0.0581	Fibp	0.7146	0.0978
CG15908	-1.0372	0.0482	Fis1	-1.0383	0.0369
CG16824	1.0731	0.0358	FRG1	0.8407	0.0865
CG16853	1.1055	0.0909	fzy	0.8683	0.0836
CG17028	0.9751	0.0513	gprs	0.9303	0.0758
CG17107	1.4610	0.0203	Gr2a	1.0890	0.0441
CG17260	0.8102	0.0980	gsb	0.9877	0.0427
CG17272	-3.4455	0.0021	GstD1	1.1586	0.0274
CG17803	0.8758	0.0552	GstD9	1.2162	0.0403
CG17996	1.1673	0.0576	GstE10	1.1540	0.0921
CG1827	0.9787	0.0679	GstE8	-1.6895	0.0284
CG18343	-1.2302	0.0388	GstE9	-2.0087	0.0180
CG18731	0.6867	0.0972	Gyc32E	1.0195	0.0956
CG1882	1.0666	0.0633	Hex-A	0.8843	0.0538
CG2017	0.7103	0.0923	His4r	-0.6962	0.0882
CG2120	1.2956	0.0520	HLH3B	-0.9676	0.0467
CG2316	-0.8599	0.0919	HLH4C	-1.0596	0.0430
CG2680	0.8100	0.0665	holn1	-1.8639	0.0198
CG2911	1.0344	0.0448	Hsc70-3	-0.8413	0.0645
CG2915	-1.7655	0.0144	Hsp67Bc	1.4527	0.0146
CG30178	1.5810	0.0450	Hug	0.7751	0.0758
CG30196	-0.8128	0.0717	Jon99Fi	-2.0704	0.0287
CG30273	1.3840	0.0373	Kaz1-ORFB	0.7720	0.0711
CG30355	1.2721	0.0616	l(2)34Fc	0.6821	0.0985
CG30379	1.0805	0.0618	lectin-33A	1.0952	0.0847
CG30380	0.8832	0.0647	lig3	0.8327	0.0936
CG31088	-0.7092	0.0877	link	1.0803	0.0793
CG31457	1.2657	0.0748	Listericin	-0.9114	0.0504
CG31548	-1.2131	0.0324	Max	0.9044	0.0981
CG31606	3.0061	0.0537	MED21	0.7574	0.0856
CG31642	0.9867	0.0711	metl	1.6778	0.0102
CG31712	-2.0954	0.0125	Mocs1	-1.5980	0.0270
CG31717	0.9296	0.0498	mos	-0.8136	0.0890
CG31812	0.8102	0.0915	mRpL2	0.9663	0.0502
CG31820	1.9856	0.0198	mRpL35	0.8761	0.0641
CG31855	-0.8358	0.0751	mRpL55	0.8648	0.0586
CG31861	-1.7542	0.0208	MSBP	0.6986	0.0916
CG31867	2.5545	0.0181	Nap1	0.7914	0.0741

CG31952	0.7889	0.0742	NC2beta	1.0666	0.0497
CG31961	1.0912	0.0840	ND-13A	-1.0548	0.0461
CG32109	-1.3017	0.0382	ND-30	0.6887	0.0985
CG32147	0.8290	0.0609	ND-42	0.7079	0.0941
CG3222	1.0800	0.0819	Npc2b	0.7326	0.0837
CG32225	0.6992	0.0922	Nup50	0.7980	0.0879
CG32368	1.0628	0.0468	Obp56d	-0.7202	0.0801
CG32625	1.1377	0.0288	Obp56e	-1.3224	0.0298
CG32655	1.3092	0.0532	Obp99a	-1.2013	0.0668
CG32762	1.4566	0.0644	Ocho	-0.9978	0.0483
CG32806	0.9208	0.0479	or	1.0684	0.0702
CG33098	0.7203	0.0892	Or59c	1.3609	0.0642
CG33127	1.6039	0.0504	OstDelta	2.4393	0.0283
CG33178	0.6640	0.0984	Pcd	2.1984	0.0041
CG3348	1.1465	0.0352	Pex16	1.0763	0.0571
CG33644	1.3374	0.0766	PGRP-LF	0.8789	0.0738
CG33774	-0.8530	0.0698	Phm	0.7395	0.0858
CG33785	-1.2711	0.0476	phtf	1.1009	0.0566
CG33786	-1.2711	0.0476	Ppcdc	0.9080	0.0678
CG33946	-1.4283	0.0567	prel	-0.9510	0.0817
CG34008	1.0363	0.0961	Prp38	-0.7759	0.0755
CG34021	1.2535	0.0712	Pu	0.8380	0.0716
CG34045	1.3128	0.0712	qkr58E-1	0.8507	0.0727
CG34117	1.1637	0.0457	qkr58E-3	-0.8016	0.0836
CG34125	0.9255	0.0635	Rack1	-1.7798	0.0120
CG34167	-1.8552	0.0169	Rad51C	1.0229	0.0973
CG34169	1.3175	0.0655	RagC-D	1.1067	0.0802
CG34179	0.8860	0.0926	Ref1	-0.6800	0.0954
CG34180	2.0429	0.0140	Roe1	1.4384	0.0393
CG34215	1.2304	0.0578	RpL18A	-0.9046	0.0526
CG34253	-1.3590	0.0795	RpL21	1.0615	0.0365
CG34264	0.8415	0.0847	RpL23A	-0.7016	0.0899
CG34296	1.0559	0.0344	RpL36	-0.7959	0.0658
CG34445	0.7603	0.0780	RpL39	1.0451	0.0367
CG34446	0.8478	0.0618	RpL8	1.2687	0.0460
CG34457	-1.7562	0.0554	RpLP2	0.8252	0.0603
CG3517	0.8555	0.0862	RpS15Aa	0.7706	0.0878
CG3557	-0.9736	0.0729	RpS20	1.2142	0.0349
CG3609	-0.9922	0.0455	RpS24	1.6485	0.0135
CG3776	0.8539	0.0966	RpS28a	4.0277	0.0006
CG3909	1.2398	0.0344	RpS30	0.8792	0.0574

CG40228	-0.6838	0.0943	Rrp42	0.8096	0.0932
CG4186	1.9936	0.0641	Sc2	1.1562	0.0605
CG42269	0.7310	0.0824	Scox	1.2360	0.0310
CG42371	-1.0089	0.0486	scramb2	0.7407	0.0927
CG42382	1.4867	0.0582	Sec61beta	1.3815	0.0187
CG42456	0.8766	0.0648	SelG	-1.6520	0.0297
CG42489	-0.7887	0.0807	Sfp79B	1.3281	0.0407
CG42495	1.1577	0.0558	SmB	1.5391	0.0276
CG42496	0.9080	0.0678	Snapin	0.6869	0.0881
CG42497	1.2199	0.0421	spict	-0.7601	0.0805
CG42498	1.5644	0.0456	sun	-0.9198	0.0625
CG42562	0.9017	0.0549	Tapdelta	0.6517	0.0971
CG42568	0.8143	0.0882	Tes	-0.7372	0.0904
CG4278	1.0744	0.0987	TfIIB	1.2908	0.0837
CG42847	-1.2533	0.0725	Tgi	0.6823	0.0996
CG43085	-0.9942	0.0935	thoc7	1.2101	0.0638
CG43107	1.1290	0.0938	Thor	-0.9550	0.0551
CG43198	-1.0872	0.0904	Tim10	1.2199	0.0421
CG43245	1.3471	0.0526	Tim8	-1.1134	0.0621
CG43293	0.9161	0.0575	Trip1	0.8516	0.0706
CG43295	-0.9522	0.0854	trus	1.1334	0.0842
CG43350	1.2218	0.0511	Uch	0.9410	0.0554
CG43389	0.8473	0.0814	UQCR-C2	-0.8601	0.0656
CG43400	1.3295	0.0451	Vamp7	-1.4729	0.0277
CG43788	-0.9237	0.0916	VepD	0.8280	0.0673
CG43886	0.9446	0.0673	w	1.4905	0.0296
CG44002	1.4625	0.0716	yellow-d2	0.8395	0.0620
CG4407	1.3690	0.0708	Zip89B	1.2026	0.0367
CG4415	0.9306	0.0539			

[a] Log2 fold change of Dam-RNA Pol II/Dam-only

[b] NOIseq probability = 1-q (q ≥ 0.9)

Appendix 6: List of DEGs in *Dα6^{EMS6}* Mutant

Gene	Log2FC[a]	Probability[b]	Gene	Log2FC[a]	Probability[b]
140up	2.7719	0.0175	CG6138	1.3209	0.0327
7B2	0.5572	0.0902	CG6175	-0.8215	0.0927
AANATL2	0.7370	0.0935	CG6179	-0.6818	0.0837
Aatf	1.0661	0.0527	CG6310	0.9998	0.0593
aay	-0.8212	0.0424	CG6337	0.7913	0.0546
Abp1	1.3502	0.0302	CG6357	1.1794	0.0269
Acp98AB	1.5130	0.0298	CG6398	-1.2641	0.0403
Act42A	1.1162	0.0260	CG6424	0.5944	0.0961
Act5C	-0.7803	0.0518	CG6481	0.8548	0.0733
Ada	0.8813	0.0827	CG6550	1.1421	0.0511
Adam	0.8256	0.0508	CG6567	1.1766	0.0364
AdenoK	-0.6193	0.0987	CG6610	-2.0201	0.0094
Adf1	0.8500	0.0461	CG6621	1.4727	0.0526
Adk2	0.7097	0.0626	CG6628	1.9222	0.0114
AdSL	-1.9679	0.0212	CG6638	1.3115	0.0651
Ady43A	2.0992	0.0297	CG6650	0.7686	0.0862
aft	1.1682	0.0292	CG6660	2.2415	0.0177
AGBE	0.9191	0.0690	CG6674	1.0952	0.0384
akirin	-1.0395	0.0329	CG6683	1.4924	0.0073
alc	-1.3505	0.0191	CG6685	0.6182	0.0929
Ald	-0.9505	0.0296	CG6723	-1.4265	0.0577
Aldh-III	-0.7917	0.0629	CG6724	1.4607	0.0182
AlkB	0.7008	0.0737	CG6726	0.9684	0.0870
alpha-Man-IIa	1.2638	0.0465	CG6738	0.8384	0.0898
alpha-PheRS	0.6207	0.0934	CG6746	1.9749	0.0127
alphaTub67C	0.8889	0.0634	CG6762	0.7380	0.0823
Amyrel	0.7098	0.0735	CG6796	1.9976	0.0160
aop	-0.8075	0.0788	CG6812	0.7513	0.0541
aos	-0.8783	0.0776	CG6834	-1.2835	0.0786
AOX3	-1.1980	0.0733	CG6845	0.9232	0.0898
AP-2mu	1.0686	0.0402	CG6891	-0.9289	0.0642
APC10	-1.0056	0.0478	CG6907	1.0790	0.0764
aph-1	1.2252	0.0391	CG6908	-2.0466	0.0136
Aplip1	1.0551	0.0320	CG7048	1.3862	0.0130
Aprt	0.6797	0.1000	CG7058	0.8942	0.0777
Arc1	-0.6757	0.0760	CG7071	0.6225	0.0897
Arf102F	-0.6657	0.0753	CG7102	-0.7982	0.0817
ArfGAP1	0.7344	0.0851	CG7126	2.9598	0.0114

Arfrp1	0.9300	0.0517	CG7133	1.3228	0.0267
Arl6	1.3030	0.0396	CG7166	0.9610	0.0700
Arp6	1.6351	0.0156	CG7172	3.4087	0.0202
Arpc1	-1.2881	0.0360	CG7200	0.9911	0.0531
Arpc5	1.0582	0.0407	CG7203	-5.1040	0.0005
Asciz	-1.3878	0.0143	CG7214	-2.1002	0.0203
AsnS	0.7739	0.0562	CG7239	0.8949	0.0794
asrij	0.6851	0.0975	CG7265	0.8259	0.0607
Atg12	1.6320	0.0079	CG7275	0.6570	0.0967
Atg4a	0.7331	0.0649	CG7276	1.8420	0.0988
Atg4b	-1.0109	0.0648	CG7296	-5.1431	0.0034
Atpalpha	0.5494	0.0965	CG7299	-1.0480	0.0545
ATPsynC	0.9504	0.0290	CG7329	0.8698	0.0954
ATPsynγ	0.7552	0.0749	CG7352	1.0285	0.0374
AttA	2.2827	0.0318	CG7371	1.5138	0.0608
awd	-1.1728	0.0176	CG7429	1.1274	0.0290
azot	1.4006	0.0656	CG7465	-1.8800	0.0571
b	-1.9216	0.0199	CG7488	2.2801	0.0173
B-H1	-1.3820	0.0253	CG7506	2.0616	0.0088
b6	-0.5880	0.0961	CG7548	-4.0625	0.0209
Bacc	-0.6226	0.0746	CG7556	-0.9000	0.0821
Baldspot	0.7579	0.0634	CG7593	0.9088	0.0429
bap	-1.6529	0.0612	CG7600	0.8770	0.0675
Bap55	1.6595	0.0348	CG7601	1.3603	0.0435
bc10	-1.0920	0.0392	CG7630	0.8309	0.0453
BCL7-like	0.6120	0.0938	CG7656	-0.7979	0.0822
Bdbt	0.8507	0.0850	CG7668	-0.9555	0.0513
BEAF-32	-0.5747	0.0964	CG7702	-1.1246	0.0851
beag	0.9556	0.0694	CG7798	-0.9408	0.0709
Bet1	0.9247	0.0478	CG7810	1.7269	0.0234
BHD	1.0646	0.0369	CG7872	-1.0317	0.0323
bic	-0.6843	0.0692	CG7896	-1.0669	0.0698
Blos3	1.8587	0.0144	CG7963	0.8462	0.0534
blow	-1.1447	0.0841	CG7966	-1.2421	0.0856
bnb	-1.0889	0.0479	CG7974	1.3176	0.0267
boca	-0.6315	0.0763	CG7988	0.9022	0.0597
bonsai	1.1598	0.0475	CG8026	0.8081	0.0697
borr	-1.3526	0.0393	CG8032	1.2636	0.0520
bou	-3.1408	0.0022	CG8038	1.3731	0.0143
bowl	-2.0287	0.0203	CG8046	-1.6296	0.0812
brk	-0.8473	0.0618	CG8066	-1.5726	0.0220

Bro	0.8103	0.0814	CG8072	0.9129	0.0891
BthD	0.8799	0.0585	CG8078	1.2933	0.0331
btl	-1.3982	0.0483	CG8089	0.8904	0.0741
btn	0.9942	0.0929	CG8134	0.6484	0.0925
by	-1.1759	0.0464	CG8180	-0.9139	0.0637
cag	0.7954	0.0597	CG8192	-1.4879	0.0288
CAH1	-1.4597	0.0304	CG8230	-0.8881	0.0790
Calr	-1.2337	0.0137	CG8235	-0.8223	0.0648
cas	-1.2035	0.0757	CG8245	1.5720	0.0134
cathD	-1.1622	0.0274	CG8248	1.1144	0.0378
cav	0.6120	0.0801	CG8303	-1.0732	0.0687
Ccdc56	1.2261	0.0271	CG8317	-1.6532	0.0291
Ccp84Aa	-0.9443	0.0631	CG8319	1.8592	0.0154
Ccp84Ab	-5.5000	0.0006	CG8331	0.7016	0.0762
Ccp84Ac	-5.4119	0.0006	CG8349	4.3169	0.0597
Ccp84Ad	-3.0154	0.0048	CG8353	-2.0827	0.0096
Cda5	-1.0170	0.0802	CG8360	0.6420	0.0988
Cdc37	1.0603	0.0440	CG8369	-2.7622	0.0061
Cdk4	-1.4666	0.0367	CG8372	2.6746	0.0226
Cdk5alpha	1.3850	0.0175	CG8399	-0.9803	0.0930
cdm	1.2184	0.0487	CG8441	-0.7551	0.0663
ced-6	-0.8902	0.0611	CG8460	0.7185	0.0748
cer	-1.4530	0.0093	CG8490	-1.1295	0.0252
CG10026	-1.3015	0.0375	CG8498	1.0078	0.0432
CG10082	0.7058	0.0723	CG8500	1.2013	0.0220
CG10096	0.9200	0.0801	CG8507	0.7738	0.0875
CG10097	0.9200	0.0801	CG8517	-2.1586	0.0192
CG10104	1.5485	0.0627	CG8543	-1.7443	0.0475
CG10163	0.7599	0.0577	CG8563	-1.2878	0.0469
CG10205	-5.5368	0.0002	CG8620	1.6285	0.0074
CG10208	1.1221	0.0386	CG8630	-1.0011	0.0838
CG10211	-1.4007	0.0397	CG8673	0.7903	0.0839
CG10222	1.2068	0.0365	CG8728	1.2528	0.0892
CG10237	-1.0396	0.0652	CG8740	-1.0446	0.0631
CG10252	1.1665	0.0494	CG8745	1.8618	0.0099
CG10262	1.2066	0.0475	CG8788	-1.9190	0.0235
CG10286	-0.9971	0.0378	CG8814	0.8320	0.0801
CG10298	-2.5444	0.0126	CG8891	2.3420	0.0279
CG10306	1.4454	0.0194	CG8916	0.8290	0.0766
CG10326	0.8334	0.0461	CG9030	1.2293	0.0300
CG10336	1.0695	0.0987	CG9117	0.9015	0.0593

CG10343	0.9952	0.0706	CG9134	-1.0776	0.0609
CG10344	-1.0030	0.0832	CG9135	0.8536	0.0569
CG10345	-1.2896	0.0523	CG9246	0.9333	0.0839
CG10347	0.8816	0.0901	CG9254	1.3333	0.0471
CG10348	-0.8857	0.0957	CG9263	1.8151	0.0266
CG10359	-1.0184	0.0772	CG9267	1.1299	0.0562
CG10395	1.4260	0.0579	CG9336	-1.9414	0.0234
CG10405	1.4250	0.0699	CG9338	-2.0641	0.0193
CG10428	1.0116	0.0666	CG9376	0.7411	0.0768
CG10433	-2.0142	0.0252	CG9389	1.9045	0.0080
CG10435	-0.8632	0.0891	CG9391	0.8158	0.0622
CG10466	-0.7022	0.0767	CG9427	-1.0864	0.0629
CG10470	0.8285	0.0888	CG9451	-0.9582	0.0960
CG10483	1.0558	0.0335	CG9471	1.2369	0.0692
CG10495	0.9288	0.0647	CG9570	0.9816	0.0418
CG10527	-0.6266	0.0788	CG9577	-1.3151	0.0427
CG10566	0.9660	0.0324	CG9578	-1.4716	0.0190
CG10570	-1.0783	0.0497	CG9586	0.6660	0.0760
CG10581	1.6403	0.0149	CG9593	1.1140	0.0329
CG10602	1.0323	0.0340	CG9601	0.8068	0.0662
CG10639	1.3400	0.0329	CG9609	0.7173	0.0759
CG10657	-1.4080	0.0767	CG9662	1.1587	0.0389
CG10660	-0.9257	0.0891	CG9666	1.0723	0.0672
CG10663	-1.4490	0.0495	CG9684	1.0730	0.0532
CG10731	2.0581	0.0038	CG9689	-1.5073	0.0457
CG10754	0.8299	0.0431	CG9698	2.7401	0.0051
CG10793	1.3244	0.0258	CG9701	-1.4676	0.0360
CG10809	1.2286	0.0456	CG9717	-0.9843	0.0960
CG10863	0.7026	0.0608	CG9769	0.9123	0.0440
CG10864	2.0156	0.0245	CG9773	0.9717	0.0793
CG10866	-1.0571	0.0975	CG9780	-0.6067	0.0765
CG10898	0.7546	0.0990	CG9782	-1.6532	0.0234
CG10924	-1.0130	0.0732	CG9791	1.1128	0.0776
CG10933	-1.4499	0.0378	CG9799	1.1792	0.0844
CG10939	-1.4770	0.0325	CG9813	1.2079	0.0565
CG10959	1.3213	0.0434	CG9815	-0.9970	0.0672
CG10970	-0.8273	0.0813	CG9855	1.0436	0.0448
CG10973	1.9033	0.0110	CG9865	0.7461	0.0789
CG10984	1.1724	0.0338	CG9890	1.1285	0.0733
CG11052	0.7973	0.0564	CG9899	-0.8191	0.0717
CG11068	-1.3452	0.0601	CG9914	-1.0477	0.0531

CG11095	0.7283	0.0825	CG9917	0.9138	0.0724
CG11103	0.8016	0.0592	CG9919	0.8872	0.0400
CG11127	2.3839	0.0122	CG9922	1.1775	0.0429
CG11137	0.8922	0.0511	CG9948	0.6713	0.0791
CG11170	-1.1422	0.0525	CG9960	1.1008	0.0201
CG11191	1.5922	0.0077	CG9970	0.9291	0.0501
CG11226	1.5716	0.0220	CG9975	1.1078	0.0339
CG1124	-0.7720	0.0887	CG9977	0.6999	0.0915
CG11269	-1.4655	0.0225	CG9986	1.2967	0.0335
CG11275	-2.0322	0.0136	CheB93a	0.9150	0.0850
CG1136	-1.1218	0.0575	Chrac-14	0.9107	0.0442
CG11373	1.2977	0.0224	Ciao1	1.3419	0.0310
CG11438	-2.1401	0.0078	cid	-0.8903	0.0618
CG11449	-0.9554	0.0605	CkIIalpha-i1	1.2652	0.0527
CG11454	2.0727	0.0162	Clamp	0.6737	0.0693
CG1146	-0.9590	0.0771	Clc	0.6370	0.0798
CG11474	1.2421	0.0382	ClC-b	1.4471	0.0271
CG11529	-1.6984	0.0503	CngB	0.8879	0.0658
CG11539	1.1904	0.0419	cnir	1.0290	0.0657
CG11560	0.7106	0.0759	cold	-0.7747	0.0865
CG11563	1.4549	0.0297	Coop	-1.0463	0.0766
CG11668	-1.7586	0.0618	corto	-0.6057	0.0990
CG11710	0.7712	0.0819	COX4	0.7512	0.0737
CG11722	0.8190	0.0786	COX7A	0.8334	0.0797
CG11752	0.9907	0.0264	COX7AL	1.7274	0.0113
CG11756	1.3835	0.0308	COX8	-1.1593	0.0292
CG11777	0.7374	0.0749	cpb	1.2971	0.0311
CG11790	-0.7364	0.0671	Cpr100A	-4.1102	0.0015
CG11791	-1.1790	0.0329	Cpr11A	-1.0048	0.0746
CG11825	-2.5339	0.0147	Cpr57A	-1.8696	0.0593
CG11835	1.1928	0.0384	Cpr62Bb	-1.3600	0.0384
CG11852	-3.2169	0.0065	Cpr62Bc	-2.0874	0.0126
CG11858	1.3699	0.0285	Cpr65Ay	-5.6504	0.0439
CG11975	0.9603	0.0645	Cpr66D	-1.3178	0.0430
CG11983	1.1836	0.0400	Cpr67Fa1	-1.5479	0.0280
CG12006	1.0165	0.0799	Cpr67Fa2	-3.2299	0.0065
CG12016	1.5506	0.0131	Cpr78Cb	-1.3824	0.0505
CG12025	1.1166	0.0454	Cpr92A	-1.4508	0.0538
CG12056	-0.7099	0.0820	Cpr97Ea	-0.8686	0.0750
CG12107	1.2222	0.0192	Cpr97Eb	-3.6865	0.0034
CG12118	0.6671	0.0702	Cralbp	-0.8499	0.0961

CG12171	-2.5323	0.0093	crc	-0.7084	0.0800
CG12173	1.3342	0.0359	CrebA	-1.1694	0.0584
CG12194	0.8513	0.0559	CREG	1.2252	0.0218
CG12207	-0.8912	0.0690	crim	1.1813	0.0462
CG12253	1.0904	0.0392	Crk	-0.6483	0.0967
CG12264	1.5713	0.0349	Csat	-0.7297	0.0955
CG12279	2.6562	0.0055	CSN5	2.0844	0.0188
CG12299	-0.9797	0.0610	Csp	0.7043	0.0677
CG12309	1.6573	0.0134	csul	1.6316	0.0469
CG1231	-1.1391	0.0249	cv	-1.0772	0.0411
CG12320	0.9585	0.0696	CycC	1.0282	0.0525
CG12321	1.5325	0.0301	CycD	0.6926	0.0807
CG12338	1.1760	0.0700	CycH	0.8310	0.0611
CG12341	0.8068	0.0669	Cyp1	-1.6923	0.0058
CG12393	0.9924	0.0593	Cyp18a1	-1.0373	0.0535
CG12481	-3.4971	0.0794	Cyp28a5	-1.1747	0.0835
CG12560	-1.3017	0.0337	Cyp4p3	-0.8456	0.0616
CG12581	-1.8770	0.0357	cype	1.7746	0.0072
CG12637	0.9283	0.0835	Cypl	0.8601	0.0456
CG12643	-1.3855	0.0204	Cys	-2.9271	0.0021
CG1265	0.7882	0.0655	Cyt-c-d	0.7846	0.0729
CG12688	-0.8724	0.0752	D	-0.7300	0.0785
CG12730	-0.7499	0.0986	dac	0.8340	0.0479
CG12784	-0.9216	0.0911	dap	-0.9724	0.0943
CG12795	0.7699	0.0595	daw	-1.0846	0.0805
CG12824	-0.8550	0.0432	Dcp-1	1.4420	0.0122
CG12862	1.3846	0.0785	Debcl	-1.6152	0.0405
CG12868	-0.7685	0.0567	DENR	-0.9772	0.0416
CG1287	0.7021	0.0840	Dim1	1.7830	0.0444
CG12883	1.6545	0.0281	DJ-1alpha	-1.6337	0.0181
CG12909	0.7440	0.0959	Dlc90F	1.4421	0.0096
CG1291	0.9423	0.0695	Dlip1	1.8111	0.0052
CG12926	-2.4135	0.0197	dmpd	0.9890	0.0791
CG12945	1.3290	0.0216	DnaJ-60	0.9904	0.0463
CG12984	0.9571	0.0818	DOR	-0.8414	0.0631
CG1299	-1.0911	0.0594	dos	-0.7597	0.0655
CG13018	0.6559	0.0988	dpn	-0.8752	0.0822
CG13024	-1.4636	0.0380	dpr19	1.4235	0.0240
CG13038	-0.7626	0.0956	dpr7	0.5890	0.0997
CG13039	-1.1079	0.0530	Dpy-30L2	-0.8770	0.0709
CG13040	-2.4528	0.0119	Drsl6	0.6749	0.0988

CG13041	-3.4582	0.0079	Duox	-0.7764	0.0982
CG13042	-2.2395	0.0180	E(spl)m2-BFM	-3.8473	0.0021
CG13044	-5.5659	0.0006	E(spl)m3-HLH	-1.8506	0.0199
CG13049	-1.1086	0.0974	E(spl)m4-BFM	-2.6837	0.0066
CG13050	-1.8663	0.0763	E(spl)m5-HLH	-2.2029	0.0319
CG13053	1.1105	0.0495	E(spl)m7-HLH	-3.2687	0.0071
CG13060	-5.9130	0.0018	E(spl)m8-HLH	-3.2001	0.0064
CG13065	-1.3671	0.0562	E(spl)mα-BFM	-1.2161	0.0531
CG1309	0.6547	0.0872	E(spl)mβ-HLH	-1.6122	0.0099
CG13108	0.8748	0.0448	E(spl)mδ-HLH	-2.2363	0.0986
CG13110	1.7296	0.0948	E(spl)mγ-HLH	-2.3337	0.0128
CG13137	1.0863	0.0801	Eb1	1.2741	0.0601
CG13177	-0.8505	0.0714	Egfr	-0.9343	0.0769
CG13203	-1.0881	0.0965	eIF-5A	1.0394	0.0289
CG13204	-1.0922	0.0290	eIF2B-alpha	1.9813	0.0291
CG13220	-0.7894	0.0592	eIF2B-delta	0.7882	0.0794
CG13223	-2.4387	0.0996	eIF2B-gamma	-2.6893	0.0028
CG13227	-6.7429	0.0005	eIF3-S9	0.7204	0.0674
CG13228	-3.9197	0.0035	eIF3ga	0.7571	0.0617
CG13244	1.0279	0.0267	eIF4E-6	2.8309	0.0283
CG13287	-1.0899	0.0241	eIF5	0.6392	0.0815
CG13314	-3.8177	0.0023	Eip55E	1.0223	0.0401
CG13332	-0.8364	0.0681	EloC	0.6951	0.0711
CG13377	-1.1186	0.0612	Elp3	0.7038	0.0777
CG13390	1.1671	0.0372	emp	-2.4866	0.0224
CG13403	-1.7822	0.0667	ems	-1.2000	0.0261
CG13405	-0.7753	0.0998	en	-0.5989	0.0977
CG13430	-0.9608	0.0701	EndoG	0.7785	0.0896
CG13437	0.7816	0.0808	endos	0.6966	0.0972
CG13481	0.8259	0.0982	Ent1	0.8185	0.0788
CG13516	-1.1275	0.0487	Ercc1	2.9325	0.0220
CG13527	0.9795	0.0551	esg	-1.0903	0.0340
CG13532	1.0444	0.0518	Est-Q	-1.7215	0.0729
CG13539	1.3713	0.0350	Ets21C	-0.7738	0.0838
CG13545	-2.8837	0.0026	Ets98B	-1.4421	0.0345
CG13551	-1.2769	0.0362	eve	-1.0774	0.0480
CG13562	1.4007	0.0357	ex	-1.0359	0.0629
CG13563	0.7842	0.0952	ey	0.9211	0.0475
CG13564	-0.9558	0.0628	Fadd	1.7338	0.0142
CG13566	1.8632	0.0105	fan	1.0437	0.0659
CG13578	0.6638	0.0887	Fatp	-0.9576	0.0593

CG13599	1.0927	0.0615	Fbxl7	-1.0694	0.0744
CG13606	-1.1203	0.0488	fd59A	-1.3552	0.0394
CG13607	-0.8621	0.0957	fd68A	1.0150	0.0435
CG13616	0.7890	0.0628	Fdh	0.9203	0.0524
CG13623	1.4474	0.0155	FeCH	0.9416	0.0489
CG13641	-1.5214	0.0981	Fer1	-0.8824	0.0540
CG13643	-1.0795	0.0621	Fer2	-0.7261	0.0800
CG13676	-2.1241	0.0302	fh	1.6650	0.0153
CG13713	-1.5656	0.0328	Fibp	1.0169	0.0369
CG13716	1.2723	0.0992	Fie	-1.2083	0.0223
CG13741	1.3774	0.0556	fig	-0.7635	0.0847
CG13748	-0.7773	0.0859	Fis1	-1.5297	0.0079
CG13751	3.1340	0.0045	fj	-2.1009	0.0146
CG13773	-1.2956	0.0210	FK506-bp1	0.7942	0.0686
CG13807	-1.7767	0.0078	FKBP59	0.6984	0.0790
CG13856	-2.7054	0.0147	fkh	-0.6041	0.0928
CG13876	0.7481	0.0794	Flo1	0.5676	0.0891
CG13877	-3.6865	0.0130	flr	0.7748	0.0957
CG13920	0.8865	0.0390	Fmo-2	-0.8873	0.0864
CG13962	1.2555	0.0973	foi	-0.6870	0.0934
CG13983	0.9131	0.0657	for	-0.9258	0.0775
CG13994	2.6821	0.0123	foxo	-0.7372	0.0964
CG14102	1.1274	0.0822	fs(1)K10	0.7218	0.0978
CG14104	1.1251	0.0318	fz3	-1.1340	0.0478
CG14107	-2.1262	0.0624	fzy	0.8752	0.0623
CG14132	-2.7545	0.0083	Gadd34	1.1160	0.0352
CG14174	1.0910	0.0312	Gadd45	1.0562	0.0320
CG14182	0.8222	0.0650	galectin	-1.1667	0.0258
CG14212	1.2961	0.0266	Galk	-1.4490	0.0288
CG14231	-0.9255	0.0429	γSnap1	0.9998	0.0385
CG14253	-0.9689	0.0872	γTub23C	1.3487	0.0552
CG14321	2.0872	0.0041	Gapdh1	-1.3563	0.0094
CG14377	-6.2072	0.0002	Gas41	0.8426	0.0774
CG14397	-2.4174	0.0350	Gbeta5	0.7602	0.0590
CG14410	0.8079	0.0928	Gbp	-1.9010	0.0219
CG14419	-3.2779	0.0140	Gbs-70E	-1.2114	0.0805
CG14423	-1.0827	0.0593	gdl	-0.8755	0.0667
CG14439	-1.1273	0.0450	Gel	-1.5777	0.0377
CG14480	2.3208	0.0095	gem	-1.1590	0.0644
CG14550	2.1677	0.0186	GILT1	-2.1676	0.0123
CG14565	-1.9240	0.0208	gkt	1.0740	0.0557

CG14591	0.5845	0.0898	Gld2	1.0108	0.0857
CG14610	-0.9138	0.0646	glob3	-1.6008	0.0982
CG14667	2.1731	0.0029	Gp150	-1.3039	0.0436
CG14671	-1.8927	0.0067	gprs	1.4055	0.0270
CG14688	-1.3140	0.0555	Gr2a	0.7244	0.0688
CG14710	1.0704	0.0568	Gr68a	0.7632	0.0733
CG14721	0.7145	0.0827	Gs2	-0.9961	0.0776
CG14722	1.1838	0.0611	gsb	-2.5943	0.0078
CG14780	0.9761	0.0645	GstD1	-1.2750	0.0145
CG14795	1.1035	0.0409	GstD11	1.7700	0.0744
CG14817	2.7814	0.0023	GstD3	-1.4287	0.0990
CG14818	0.7662	0.0562	GstD4	-3.3207	0.0829
CG14883	0.7082	0.0986	GstD9	-0.7608	0.0945
CG14891	1.1894	0.0435	GstE1	-0.7922	0.0880
CG14903	0.9779	0.0410	GstE2	-1.1681	0.0604
CG14921	0.9638	0.0911	GstE3	-1.9681	0.0187
CG14937	1.0116	0.0757	GstE5	-1.3069	0.0651
CG14968	-0.9977	0.0714	GstE6	-1.7892	0.0260
CG14977	0.9744	0.0524	GstE8	-2.4595	0.0162
CG14983	1.9430	0.0751	GstE9	-2.9281	0.0102
CG15014	0.6905	0.0937	GstO1	0.6765	0.0760
CG15027	1.8873	0.0153	GstT3	-0.8669	0.0609
CG15071	-1.8203	0.0111	GstZ1	0.9968	0.0251
CG15093	-0.8037	0.0662	GstZ2	0.7524	0.0550
CG15185	1.4871	0.0723	GV1	-1.3496	0.0395
CG15258	-1.8496	0.0806	hebe	-1.2342	0.0547
CG15282	-2.6820	0.0211	Hip14	1.1117	0.0475
CG15317	1.4200	0.0123	HipHop	2.3474	0.0068
CG15353	-1.3931	0.0246	HIPP1	0.9179	0.0817
CG15386	-0.9937	0.0348	hkb	-0.8105	0.0612
CG15390	-1.2985	0.0323	HLH3B	-1.2760	0.0172
CG15398	2.0885	0.0664	HLH4C	-1.8963	0.0116
CG15414	-0.8784	0.0920	hng2	1.5697	0.0135
CG15432	0.6606	0.0680	hng3	-0.8773	0.0593
CG15440	1.2332	0.0319	hoe2	0.9532	0.0719
CG15449	0.9341	0.0683	hoip	-0.6904	0.0598
CG15475	-0.7206	0.0866	holn1	0.7763	0.0508
CG15506	-1.4875	0.0290	HP1b	1.3434	0.0156
CG15514	0.9055	0.0467	HPS1	-0.8976	0.0691
CG15517	-2.3393	0.0754	Hsc70-4	-0.7193	0.0557
CG15528	0.9731	0.0555	Hsp67Bc	0.7429	0.0522

CG15535	0.7202	0.0639	Hsp68	0.9123	0.0529
CG15549	-0.8277	0.0662	Hug	0.5904	0.0893
CG15561	1.8486	0.0170	hui	-2.0441	0.0112
CG15611	-1.4263	0.0373	hyx	0.8984	0.0444
CG15614	1.7462	0.0393	Ibf1	1.6691	0.0304
CG15784	-1.1813	0.0540	icln	1.0665	0.0258
CG15861	-1.3611	0.0208	ida	1.0282	0.0708
CG15881	1.5206	0.0171	Idgf4	-2.7756	0.0126
CG15908	-0.5718	0.0967	ifc	0.8361	0.0583
CG15914	1.4484	0.0342	imd	1.0298	0.0342
CG15922	1.4599	0.0081	Ime4	0.7831	0.0968
CG1598	1.5711	0.0592	ImpL3	-1.2023	0.0156
CG16716	1.4140	0.0795	in	-0.8214	0.0900
CG16719	0.6265	0.0961	inaD	0.7644	0.0953
CG16721	0.6072	0.0984	Ing3	-0.7244	0.0832
CG1673	-0.9085	0.0758	Inx2	-1.0239	0.0591
CG16753	0.8036	0.0974	Inx3	-1.1001	0.0500
CG16786	-1.6706	0.0393	Inx5	-0.7679	0.0926
CG16824	-2.1250	0.0094	Ip259	0.8418	0.0485
CG16853	1.3360	0.0512	IP3K1	-1.0028	0.0714
CG16947	-0.8597	0.0882	Ir48c	1.3698	0.0937
CG16986	1.1863	0.0328	Ir56a	0.6865	0.0863
CG16989	0.9814	0.0434	Ir76a	1.3287	0.0744
CG17026	-0.9095	0.0760	Irk1	-0.8910	0.0857
CG17028	-1.4495	0.0323	IscU	-0.8551	0.0602
CG17029	-1.2185	0.0413	janA	1.3254	0.0278
CG17032	-1.8230	0.0373	Jhl-26	-0.8697	0.0747
CG17078	1.2146	0.0405	jigr1	-1.2492	0.0299
CG17104	-1.6294	0.0705	Jon99Fi	-2.1549	0.0215
CG17107	-4.3930	0.0152	Kal1	-1.3416	0.0571
CG17108	-2.0518	0.0144	Kaz1-ORFB	-5.3784	0.0029
CG17110	0.9780	0.0860	ken	-2.3823	0.0233
CG17118	-0.8614	0.0850	Klc	0.7912	0.0542
CG17224	-1.2622	0.0656	Klp67A	1.0021	0.0943
CG17239	-1.4079	0.0867	Kmn1	-0.7876	0.0778
CG1724	0.8605	0.0957	koko	1.0369	0.0471
CG17260	1.0258	0.0500	l(1)G0004	-1.0721	0.0335
CG17265	-1.2472	0.0615	l(1)G0045	1.6586	0.0258
CG17359	0.8353	0.0679	l(2)34Fc	-1.2625	0.0349
CG17486	-1.3268	0.0142	l(2)k09913	0.9208	0.0864
CG1750	0.9556	0.0977	l(2)k10201	0.6449	0.0893

CG17549	-1.7009	0.0165	l(2)SH0834	1.3092	0.0151
CG17565	1.0585	0.0886	l(3)01239	0.6310	0.0946
CG17580	1.7586	0.0361	l(3)03670	0.9546	0.0454
CG17625	1.1967	0.0352	l(3)04053	-1.9582	0.0226
CG17662	-1.0412	0.0966	l(3)j2D3	1.5995	0.0386
CG17672	-0.9852	0.0638	l(3)neo43	0.9755	0.0562
CG17680	0.7194	0.0802	laccase2	-1.2691	0.0568
CG17721	-1.2748	0.0137	lbe	-0.7681	0.0731
CG17754	-0.9678	0.0450	lectin-24Db	1.0126	0.0577
CG17764	-1.4500	0.0671	lectin-29Ca	1.8094	0.0703
CG17803	-1.1018	0.0248	lectin-33A	1.7130	0.0294
CG17806	-1.1641	0.0416	lectin-46Ca	-1.3225	0.0592
CG17821	1.0453	0.0784	Lhr	2.4530	0.0196
CG17829	1.6218	0.0210	lid	0.7858	0.0627
CG17919	-0.8604	0.0733	lig3	0.8794	0.0653
CG17991	0.7705	0.0664	link	1.7969	0.0241
CG17996	2.2023	0.0126	Listericin	-3.8132	0.0021
CG18004	-1.1261	0.0472	lolal	1.0471	0.0692
CG1806	-1.5402	0.0390	Lsd-2	-0.8432	0.0882
CG18065	-0.9608	0.0701	MAGE	1.2961	0.0302
CG18081	1.2575	0.0556	mago	-0.9226	0.0762
CG18178	0.6212	0.0870	magu	-1.0163	0.0886
CG18223	1.3590	0.0495	Mal-B1	0.7523	0.0784
CG1827	1.7514	0.0167	Mal-B2	1.0120	0.0448
CG18343	-2.7127	0.0136	MAN1	0.7663	0.0889
CG1840	-0.8971	0.0817	mats	0.6475	0.0961
CG1847	0.9496	0.0461	mav	-1.0763	0.0391
CG18472	1.0306	0.0373	Max	1.7783	0.0227
CG18473	1.2244	0.0284	mbt	-0.7368	0.0892
CG18619	-1.2570	0.0148	MED18	1.8854	0.0208
CG18641	-1.0771	0.0270	MED20	1.1389	0.0447
CG18643	1.6067	0.0156	MED21	1.4062	0.0177
CG18661	0.8664	0.0761	MED28	1.0140	0.0474
CG18731	1.7154	0.0097	MED9	1.3186	0.0261
CG18810	0.8863	0.0712	Menl-1	0.6789	0.0814
CG18815	1.1076	0.0514	Menl-2	0.6789	0.0814
CG1882	1.0530	0.0485	Mes4	1.2605	0.0394
CG1896	0.9527	0.0355	metl	1.0679	0.0223
CG2017	0.8095	0.0524	mfas	-1.8973	0.0249
CG2021	0.7465	0.0820	MFS14	-1.9239	0.0205
CG2034	-0.6751	0.0835	MFS18	0.8180	0.0703

CG2046	1.5408	0.0294	mgr	1.0483	0.0443
CG2051	1.1846	0.0397	mh	0.7999	0.0813
CG2065	-2.4466	0.0279	mib2	0.6796	0.0818
CG2076	0.7249	0.0949	mip40	0.8873	0.0435
CG2100	1.1814	0.0503	miple2	0.6043	0.0820
CG2104	1.8079	0.0296	mirr	-0.8994	0.0403
CG2116	0.8902	0.0651	Mkp3	0.7734	0.0727
CG2120	1.0984	0.0526	mmy	-1.0782	0.0563
CG2124	0.7475	0.0942	mos	-0.7759	0.0711
CG2126	0.7098	0.0878	Mpp6	1.1782	0.0424
CG2162	-0.8134	0.0712	mr	1.4938	0.0438
CG2218	0.8984	0.0615	MrgBP	0.6141	0.0808
CG2310	-1.2281	0.0620	mRpL11	0.8984	0.0811
CG2321	0.7703	0.0557	mRpL13	0.6535	0.0938
CG2336	1.1662	0.0521	mRpL15	0.9330	0.0401
CG2371	1.4036	0.0205	mRpL16	-0.7694	0.0571
CG2604	1.6370	0.0576	mRpL17	0.7151	0.0978
CG2611	1.0094	0.0392	mRpL18	0.7198	0.0595
CG2614	0.8394	0.0979	mRpL19	1.0208	0.0430
CG2617	1.3903	0.0298	mRpL2	0.6783	0.0710
CG2765	0.7753	0.0659	mRpL20	1.6412	0.0112
CG2781	-0.8247	0.0880	mRpL33	0.6389	0.0896
CG2837	-0.9891	0.0660	mRpL4	-0.6418	0.0889
CG2841	-0.9115	0.0870	mRpL42	0.7855	0.0702
CG2862	0.9347	0.0307	mRpL43	1.5503	0.0329
CG2909	0.6015	0.0955	mRpL55	0.5954	0.0825
CG2911	1.3666	0.0159	mRpS10	1.1794	0.0184
CG2915	-1.7248	0.0099	mRpS16	0.6934	0.0700
CG2975	-1.8073	0.0299	mRpS17	-0.9289	0.0763
CG2991	-1.1167	0.0565	mRpS25	1.4990	0.0105
CG30016	-1.1335	0.0398	mRpS28	0.8902	0.0602
CG30039	1.1674	0.0293	mRpS31	1.5872	0.0216
CG30105	0.6589	0.0950	mRpS6	1.5407	0.0190
CG30110	1.1096	0.0869	Ms	1.1758	0.0722
CG30114	-0.9005	0.0712	ms(3)K81	0.6602	0.0713
CG30159	-4.3222	0.0101	MSBP	1.3380	0.0156
CG30178	1.9546	0.0229	msd5	1.2095	0.0323
CG30184	1.2838	0.0983	Msr-110	-3.0983	0.0086
CG30192	1.4577	0.0963	mthl1	-0.6569	0.0879
CG30195	-2.5856	0.0559	mthl9	-1.4967	0.0587
CG30196	-5.1864	0.0079	Mtl	0.6498	0.0985

CG30270	1.3483	0.0386	mtm	0.9428	0.0968
CG30334	1.1932	0.0532	mtTFB1	1.2261	0.0271
CG30345	-1.8533	0.0295	Muted	0.6225	0.0897
CG30378	0.8404	0.0965	Myb	0.9124	0.0435
CG30380	-0.9164	0.0580	NAA20	-0.6355	0.0817
CG30414	0.9900	0.0573	nac	0.9562	0.0540
CG30429	0.9033	0.0683	nAChRbeta3	-0.7580	0.0782
CG30432	-1.3091	0.0882	nahoda	-1.3665	0.0390
CG30441	1.1212	0.0761	Nap1	1.0596	0.0272
CG3045	0.9180	0.0623	ND-13A	0.5543	0.0976
CG30461	1.0187	0.0379	ND-39	-1.2551	0.0364
CG30479	0.7255	0.0836	ND-42	1.1187	0.0279
CG30480	0.7702	0.0768	ND-51	0.6912	0.0878
CG30499	1.9828	0.0038	ND-AGGG	0.8908	0.0676
CG3091	0.8372	0.0866	ND-ASHI	0.6919	0.0702
CG31008	-0.8826	0.0596	ND-B12	-0.8058	0.0478
CG31030	0.7565	0.0566	ND-B14.5B	0.6127	0.0791
CG31068	0.7611	0.0789	ND-B16.6	0.7348	0.0624
CG31086	-1.7527	0.0191	ND-B22	1.0740	0.0389
CG31088	-0.6412	0.0752	ND-MWFE	1.4180	0.0132
CG31111	0.6269	0.0868	ND-SGDH	1.2728	0.0210
CG31115	1.3996	0.0536	Neb-cGP	0.6006	0.0892
CG31121	-1.0225	0.0712	Nedd8	0.8550	0.0637
CG3119	-0.9044	0.0935	Nf-YA	-1.2783	0.0390
CG31199	1.8077	0.0120	Nf-YB	0.7667	0.0682
CG31229	-0.8468	0.0508	Nfl	0.6044	0.0960
CG3123	-1.2268	0.0466	Nmda1	-1.0525	0.0390
CG31344	0.8632	0.0688	nmdyn-D6	0.6126	0.0957
CG31441	1.1683	0.0402	Noa36	0.7480	0.0690
CG31457	2.3222	0.0180	noi	0.7435	0.0753
CG31468	1.8716	0.0290	Non2	0.9539	0.0458
CG31548	-1.9478	0.0103	Non3	0.9634	0.0726
CG31642	1.4335	0.0275	Nop56	1.2588	0.0386
CG31648	1.3099	0.0327	Notum	-0.8059	0.0972
CG31673	-1.2906	0.0491	NP15.6	-0.6394	0.0727
CG31689	-1.0981	0.0814	Npc1a	1.0517	0.0799
CG31712	-1.7246	0.0109	Npc2b	-2.0992	0.0151
CG31715	0.9438	0.0479	Npc2f	-1.3835	0.0658
CG31717	1.3233	0.0132	Nplp3	-1.2657	0.0555
CG31728	-2.5692	0.0105	Nplp4	-1.5873	0.0242
CG31739	0.8393	0.0610	Ns1	-0.7869	0.0623

CG31777	-1.4701	0.0688	Nse1	1.3298	0.0677
CG31785	0.8210	0.0979	nudC	-1.2988	0.0320
CG31798	1.1037	0.0677	Nup37	1.0012	0.0650
CG31806	1.1401	0.0606	Nup50	1.2420	0.0294
CG31812	2.1311	0.0105	Obp28a	-0.8796	0.0556
CG31820	1.9168	0.0154	Obp56a	-3.4895	0.0036
CG31861	-1.8552	0.0138	Obp56b	-1.2096	0.0598
CG31867	1.9106	0.0252	Obp56d	-5.6794	0.0006
CG31910	1.3782	0.0437	Obp56e	-3.5899	0.0086
CG31915	0.9886	0.0857	Obp56f	-4.1184	0.0585
CG31922	1.2549	0.0208	Obp57d	-1.8696	0.0593
CG31952	-1.6978	0.0214	Obp58b	-1.9385	0.0757
CG31957	1.5481	0.0389	Obp83g	-3.5462	0.0055
CG31961	0.9426	0.0821	Obp99a	-2.4254	0.0311
CG3199	0.9318	0.0567	obst-A	-1.9661	0.0238
CG31997	-1.9374	0.0156	obst-B	-0.8974	0.0947
CG32022	1.1995	0.0371	oc	-0.6631	0.0863
CG32039	-0.5786	0.0985	Ocho	-3.9149	0.0083
CG32069	1.7741	0.0101	ocn	2.3779	0.0830
CG32091	-1.0634	0.0726	Odc2	1.1757	0.0386
CG32095	0.6490	0.0809	opm	0.7135	0.0820
CG32109	-1.1546	0.0328	or	1.7075	0.0225
CG32119	1.2469	0.0248	Or45b	1.7360	0.0502
CG32170	-0.9636	0.0695	Or59c	1.2354	0.0589
CG32187	1.6592	0.0075	Orc2	1.1420	0.0415
CG3222	1.5837	0.0319	Ost48	0.9173	0.0426
CG32221	0.9601	0.0768	out	-1.4200	0.0432
CG32237	-1.0101	0.0556	Oxp	-1.3468	0.0779
CG32246	1.8060	0.0485	P32	0.6193	0.0956
CG32280	-1.1088	0.0337	p47	0.8831	0.0478
CG32391	1.4831	0.0512	pain	-0.9983	0.0699
CG32450	0.6861	0.0650	pasha	0.7825	0.0846
CG32485	-0.7318	0.0732	Pask	0.8421	0.0765
CG32512	-0.7596	0.0850	Pcd	2.3209	0.0015
CG32579	-2.4052	0.0073	PCID2	1.6025	0.0356
CG32603	-2.8954	0.0039	Pcmt	1.0321	0.0612
CG32639	-0.9500	0.0730	PCNA	1.5649	0.0413
CG32645	-1.1052	0.0551	Pen	-0.9824	0.0930
CG32655	1.5552	0.0295	Pex10	1.1337	0.0385
CG32694	-0.9210	0.0681	Pex14	0.7522	0.0788
CG32801	1.4166	0.0405	Pex16	2.6097	0.0066

CG32803	0.9519	0.0581	Pex5	1.5645	0.0398
CG32811	1.3305	0.0487	Pgd	-1.4658	0.0306
CG32829	1.5816	0.0206	Pgi	-0.6915	0.0612
CG32845	0.6585	0.0662	Pgk	0.9268	0.0340
CG3294	-1.2405	0.0961	Pglym78	-1.0457	0.0265
CG33051	1.1342	0.0234	Pgm	0.8124	0.0488
CG33062	-0.8792	0.0570	PGRP-SA	-0.7072	0.0846
CG33098	1.9227	0.0065	PGRP-SD	1.4301	0.0438
CG33107	1.0409	0.0504	Phb2	0.8927	0.0518
CG33127	1.7076	0.0342	PHGPx	-0.9140	0.0808
CG33137	1.3445	0.0230	Phm	1.1300	0.0256
CG33170	0.9812	0.0341	Pi3K21B	0.8818	0.0699
CG33177	-0.9875	0.0548	Pif2	-0.9064	0.0721
CG33178	-1.4129	0.0207	PIG-U	-0.7772	0.0785
CG33228	0.6850	0.0677	Pino	-1.4192	0.0451
CG33234	0.9883	0.0433	pirk	-0.8825	0.0795
CG33310	0.9591	0.0680	Pis	1.5832	0.0217
CG33332	0.9550	0.0732	pita	1.2460	0.0193
CG33474	-2.1662	0.0253	Pld	-1.1041	0.0610
CG3348	-1.1195	0.0379	ple	-2.2364	0.0135
CG33557	-0.9347	0.0751	pot	-1.1954	0.0614
CG3358	0.7568	0.0829	Ppa	-0.7338	0.0809
CG33635	2.5294	0.0017	ppan	0.8651	0.0603
CG33643	2.4903	0.0709	Ppcdc	0.8501	0.0565
CG33644	2.4994	0.0175	ppl	0.9395	0.0487
CG33645	0.8328	0.0818	PpN58A	1.2845	0.0592
CG33713	-0.7994	0.0610	PQBP1	0.8615	0.0795
CG33725	-0.8456	0.1000	Prosalpha3	1.8396	0.0177
CG33785	-1.3488	0.0334	Prosalpha4T1	1.5886	0.0152
CG33786	-1.3488	0.0334	Prosalpha5	2.4192	0.0317
CG33792	1.0023	0.0622	Prosalpha6	1.2890	0.0258
CG33919	0.8938	0.0444	Prosbeta1	1.0014	0.0348
CG33939	-1.8540	0.0184	Prpk	0.8964	0.0746
CG33946	-1.8214	0.0358	prt	0.5769	0.0949
CG33995	0.9518	0.0461	Prx6005	1.4360	0.0458
CG34008	1.8194	0.0276	psh	-1.8280	0.0294
CG34010	-1.0402	0.0498	Psn	1.1887	0.0675
CG34021	2.0406	0.0220	pst	-0.8840	0.0892
CG34028	0.8920	0.0950	ptc	-0.9605	0.0889
CG34038	-1.7256	0.0261	Ptp36E	1.0066	0.0348
CG34045	2.4084	0.0169	put	0.6233	0.0944

CG3407	1.3119	0.0294	Pxd	-2.4566	0.0204
CG34115	-1.0499	0.0502	Pym	-1.4622	0.0361
CG34116	1.6891	0.0143	qkr58E-1	0.8095	0.0583
CG34117	3.3315	0.0027	qkr58E-3	0.7518	0.0591
CG34125	2.3689	0.0059	Rab14	0.6306	0.0778
CG34150	0.8523	0.0901	Rab19	0.9272	0.0625
CG34163	1.1286	0.0205	Rab2	0.8605	0.0422
CG34167	-2.0557	0.0106	Rab3	1.1191	0.0342
CG34169	1.5056	0.0392	Rab39	0.6769	0.0949
CG34179	1.1809	0.0437	Rab4	0.9121	0.0459
CG34180	2.1660	0.0086	RabX6	0.6782	0.0968
CG34185	-1.9462	0.0477	Rack1	-1.1889	0.0190
CG34189	1.7669	0.0185	Rad51C	1.1952	0.0593
CG34190	1.0154	0.0930	RagA-B	-0.7471	0.0618
CG3420	0.8396	0.0557	RagC-D	1.1831	0.0553
CG34200	0.7079	0.0606	Ras85D	0.6175	0.0992
CG34215	1.0220	0.0604	Rb97D	0.7983	0.0937
CG34219	0.7420	0.0925	Rbp1	0.9537	0.0904
CG34221	-0.8452	0.0552	Rbp1-like	0.8425	0.0506
CG34224	-0.8584	0.0788	Rbsn-5	0.6687	0.0766
CG34231	1.3910	0.0915	Rcd-1	-0.8701	0.0430
CG34250	-0.6037	0.0907	Rcd2	-0.9009	0.0989
CG34253	-1.0281	0.0787	Rcd6	-1.4902	0.0403
CG34254	0.7877	0.0977	ref(2)P	0.9000	0.0680
CG34263	1.5927	0.0311	Reg-5	-2.3734	0.0160
CG34264	1.0725	0.0418	rev7	1.4520	0.0287
CG34286	1.3481	0.0804	RfC3	1.5272	0.0814
CG34293	0.6685	0.0925	RfC4	1.6452	0.0126
CG34296	-0.8077	0.0441	Rgk1	0.8957	0.0609
CG34324	1.0343	0.0897	Rh5	2.1538	0.0422
CG34328	2.1969	0.0834	rho-7	1.4100	0.0435
CG34331	-0.9420	0.0893	Rho1	0.6514	0.0825
CG3436	1.5265	0.0160	RhoL	-0.7210	0.0972
CG34402	0.8172	0.0762	rnh1	1.0966	0.0311
CG34423	1.0114	0.0770	robl37BC	1.2159	0.0433
CG34445	-3.0172	0.0133	Roc1a	0.5976	0.0864
CG34446	-3.2258	0.0101	Rpb10	0.6330	0.0924
CG34457	-2.0736	0.0390	Rpd3	0.7977	0.0508
CG3491	0.8960	0.0888	RpL10Ab	1.1454	0.0180
CG3500	1.6046	0.0094	RpL13A	1.0512	0.0291
CG3501	0.8923	0.0380	RpL14	-0.7467	0.0524

CG3517	1.1887	0.0369	RpL21	1.0082	0.0263
CG3527	0.7347	0.0800	RpL23	1.0831	0.0242
CG3534	1.1835	0.0510	RpL23A	-1.6956	0.0115
CG3552	1.0528	0.0377	RpL24-like	0.7203	0.0861
CG3557	-0.7062	0.0843	RpL27	1.1731	0.0373
CG3568	1.4322	0.0217	RpL28	0.9000	0.0351
CG3588	-0.8478	0.0834	RpL3	0.6983	0.0622
CG3594	1.3602	0.0185	RpL35	0.8050	0.0536
CG3598	-1.0732	0.0713	RpL35A	-0.7331	0.0667
CG3603	-0.6857	0.0877	RpL36	-0.5512	0.0932
CG3609	-1.1550	0.0220	RpL36A	1.9895	0.0076
CG3618	0.6823	0.0751	RpL39	0.6191	0.0765
CG3678	0.7680	0.0776	RpL4	-1.3181	0.0209
CG3703	1.0077	0.0503	RpL8	1.3589	0.0304
CG3764	-0.6759	0.0990	RpL9	1.1179	0.0473
CG3770	-2.3593	0.0076	RpLP2	-1.7953	0.0033
CG3792	0.8448	0.0636	Rpn12	0.6967	0.0802
CG3800	-1.1331	0.0267	Rpn7	0.9452	0.0844
CG3829	-1.6605	0.0333	Rpn9	0.9770	0.0387
CG3902	-0.8235	0.0925	RpS10a	1.3579	0.0166
CG3909	1.2216	0.0251	RpS14b	0.6081	0.0837
CG3918	-0.6591	0.0784	RpS15Aa	1.4415	0.0190
CG3955	1.1381	0.0317	RpS17	0.6789	0.0752
CG3982	2.2774	0.0353	RpS19b	1.8963	0.0276
CG40228	-1.0523	0.0280	RpS20	1.3684	0.0185
CG4036	0.9327	0.0566	RpS21	-2.2767	0.0079
CG4042	1.4506	0.0152	RpS24	1.1597	0.0214
CG4050	-1.0543	0.0380	RpS27A	0.6608	0.0753
CG4095	1.0395	0.0690	RpS28-like	0.6840	0.0835
CG4096	-1.2876	0.0499	RpS28a	2.9004	0.0011
CG41128	-0.7587	0.0643	RpS29	0.6465	0.0795
CG4115	-0.9196	0.0760	RpS30	1.2648	0.0162
CG4133	-0.7907	0.0550	RpS4	0.6435	0.0902
CG4159	0.9903	0.0810	RpS5b	-0.9924	0.0856
CG4186	3.9193	0.0091	RpS7	1.1946	0.0416
CG4194	-1.6056	0.0225	RpS9	-0.7146	0.0687
CG42239	2.5016	0.0022	Rpt2	0.9099	0.0486
CG42269	-2.3840	0.0119	Rrp42	2.0151	0.0124
CG4230	0.8642	0.0424	rtet	1.4181	0.0690
CG42361	0.6418	0.0730	S-Lap4	1.3235	0.0359
CG42371	-0.9937	0.0348	sc	-1.0039	0.0912

CG42374	1.0723	0.0672	Sc2	1.8185	0.0197
CG42379	0.7461	0.0789	scaf	-0.8496	0.0931
CG42380	0.7461	0.0789	sced	0.8351	0.0886
CG42381	0.7461	0.0789	Scgalpha	1.1652	0.0237
CG42382	1.4440	0.0473	Scox	1.7067	0.0095
CG42391	-0.8981	0.0964	SelG	-2.4474	0.0169
CG42395	1.4038	0.0485	Ser	-0.9699	0.0785
CG42445	-1.1544	0.0551	Ser12	2.2014	0.0633
CG42456	1.5506	0.0131	serp	-2.0358	0.0187
CG42463	-1.0434	0.0459	Sfp24Ba	-0.7369	0.0816
CG42492	0.7684	0.0644	Sfp24F	0.7048	0.0789
CG42495	2.0359	0.0140	Sfp33A3	1.5942	0.0283
CG42496	0.8501	0.0565	Sfp53D	1.6799	0.0813
CG42498	2.1677	0.0186	Sfp79B	1.6466	0.0198
CG42502	-1.0783	0.0497	Sgf11	0.9813	0.0739
CG42518	1.3114	0.0262	Sgf29	0.8401	0.0470
CG42542	-1.3510	0.0718	Shaw	0.8535	0.0593
CG42554	1.0288	0.0738	shd	-0.9928	0.0830
CG42556	1.2622	0.0740	shu	1.0609	0.0903
CG42557	0.6385	0.0792	sicily	1.2284	0.0378
CG42558	0.6385	0.0792	Skeletor	-1.6163	0.0405
CG42559	-2.0719	0.0362	Slh	-0.9194	0.0975
CG42560	-2.0719	0.0362	slim	1.1678	0.0638
CG42562	-2.2098	0.0131	SLIRP1	-0.7994	0.0610
CG42568	0.9904	0.0463	SLIRP2	0.8729	0.0749
CG42615	-1.4536	0.0251	slmo	1.1715	0.0429
CG42697	-2.0378	0.0219	slp1	-2.2808	0.0194
CG42718	-2.4886	0.0191	SmF	1.2938	0.0266
CG42763	1.4395	0.0977	Snap29	0.6049	0.0889
CG42766	0.8952	0.0517	Snapin	1.1008	0.0201
CG4278	1.5770	0.0394	snf	0.9882	0.0620
CG42808	-1.1460	0.0514	sni	0.6685	0.0682
CG42809	-4.5410	0.0002	Snx1	1.6540	0.0276
CG42821	-0.7835	0.0967	Sod	0.9172	0.0684
CG42824	-2.1820	0.0182	Sox21a	-0.7615	0.0821
CG42830	1.8821	0.0160	SoxN	-0.8794	0.0482
CG42846	-0.7508	0.0636	SpdS	0.8249	0.0533
CG42847	-1.3779	0.0512	Spf45	1.6665	0.0362
CG42852	-1.9016	0.0864	spn-B	2.1227	0.0298
CG4300	0.7554	0.0909	Spn28Dc	-0.7218	0.0974
CG43052	-1.5029	0.0847	Spn42Dd	-1.5475	0.0558

CG43085	1.0109	0.0424	Spn43Ab	-1.5338	0.0479
CG43088	1.2096	0.0987	Spn77Ba	-1.6289	0.0477
CG43091	0.9074	0.0533	Sptr	1.5074	0.0124
CG43092	1.1265	0.0688	spz3	-3.3615	0.0070
CG43093	1.4846	0.0528	spz5	-1.0041	0.0603
CG43116	-1.0525	0.0512	Srp14	1.0633	0.0527
CG4313	-0.7246	0.0992	Srp9	1.0765	0.0501
CG43138	-1.3263	0.0452	SrpRbeta	0.8169	0.0538
CG43156	-1.4516	0.0373	Ssb-c31a	1.2172	0.0277
CG43191	1.1217	0.0382	ssp	1.0506	0.0369
CG43198	-1.1974	0.0649	Stam	0.9051	0.0551
CG43202	-1.2069	0.0391	ste14	1.9103	0.0248
CG43204	1.4964	0.0161	ste24c	1.0187	0.0379
CG43229	0.7726	0.0732	stg	-1.2946	0.0387
CG43232	1.2981	0.0253	Stim	0.8041	0.0910
CG43248	-1.0803	0.0529	stv	0.6797	0.0913
CG43249	-2.0792	0.0230	Su(fu)	0.8184	0.0877
CG43292	2.7483	0.0762	Su(var)205	1.0058	0.0386
CG43293	2.4174	0.0037	Swim	-1.4339	0.0347
CG43324	3.3034	0.0035	Syx16	-0.5835	0.0991
CG43325	-2.0683	0.0215	Syx17	1.1885	0.0301
CG43326	-2.1086	0.0206	Syx1A	0.8421	0.0565
CG43342	1.5666	0.0553	Syx8	1.6452	0.0116
CG4335	0.8823	0.0916	Taf11	1.0242	0.0353
CG4338	0.9964	0.0660	Taf12	1.1170	0.0219
CG43393	-1.3285	0.0532	Taf6	0.7539	0.0774
CG43407	-0.9203	0.0851	tal-1A	-2.1245	0.0084
CG43675	1.0334	0.0470	tal-2A	-2.1245	0.0084
CG43707	0.7261	0.0743	tal-3A	-2.1245	0.0084
CG43788	-0.7791	0.0864	tal-AA	-2.1245	0.0084
CG43886	-1.5056	0.0530	tap	-1.1952	0.0750
CG43925	1.4012	0.0094	Task6	0.9440	0.0513
CG4398	1.1153	0.0233	Taz	0.6045	0.0958
CG44000	0.9518	0.0461	Tcp-1eta	0.6217	0.0938
CG44001	0.9518	0.0461	Tctp	0.6008	0.0853
CG44002	1.3656	0.0631	Tdc2	-1.0063	0.0993
CG4407	1.4183	0.0512	Teh4	0.9099	0.0690
CG44090	-2.2764	0.0359	tej	1.1124	0.0245
CG4415	0.6460	0.0762	Tep4	-1.0310	0.0910
CG44242	3.2828	0.0003	Tes	-1.1198	0.0345
CG44253	-2.3444	0.0859	TFAM	-1.1696	0.0403

CG44259	-1.3359	0.0333	TfIIB	1.0545	0.0908
CG44286	-1.9190	0.0235	TfIIFbeta	1.0668	0.0570
CG44325	-0.7033	0.0973	Tgi	-1.4625	0.0319
CG44329	-0.7864	0.0875	thoc7	2.6291	0.0102
CG44355	-0.7353	0.0808	Thor	-2.1835	0.0128
CG44362	1.4547	0.0127	Tim8	1.5047	0.0146
CG4447	1.7349	0.0445	Tina-1	-0.6680	0.0684
CG4452	-1.0620	0.0437	Tis11	-0.8912	0.0696
CG44532	1.7017	0.0111	tj	-2.0175	0.0091
CG45066	-1.7512	0.0296	TkR99D	0.6299	0.0974
CG45068	-1.3281	0.0329	tll	-1.2083	0.0824
CG45069	-1.3281	0.0329	TM4SF	-0.6151	0.0786
CG45085	0.8081	0.0697	tobi	1.2534	0.0740
CG45307	-0.8233	0.0637	Toll-6	0.6225	0.0791
CG4553	1.8107	0.0884	Toll-7	-0.7744	0.0543
CG4572	-0.7858	0.0820	Tom7	1.1626	0.0196
CG4576	-1.0351	0.0808	tomboy40	0.8750	0.0570
CG4598	-0.7933	0.0739	Torsin	0.7671	0.0548
CG4610	0.7117	0.0890	Traf4	-1.3993	0.0502
CG4617	0.7975	0.0789	Trax	1.1649	0.0482
CG4679	1.0974	0.0504	trbl	-1.7355	0.0245
CG4721	0.7131	0.0835	Trip1	2.0142	0.0076
CG4725	2.5772	0.0102	Trs33	-0.9593	0.0642
CG4788	0.9937	0.0495	trus	1.4341	0.0432
CG4793	0.7349	0.0715	Trx-2	-1.2989	0.0111
CG4860	-1.5069	0.0307	Tsf1	-1.0871	0.0817
CG4866	-0.7975	0.0805	Tsp42Ek	-1.5739	0.0170
CG4882	0.6214	0.0800	Tsp74F	-1.9993	0.0309
CG4927	-0.9945	0.0788	tsr	1.1928	0.0262
CG4935	2.5890	0.0138	twit	-0.9524	0.0741
CG4962	-3.7892	0.0026	Uba1	0.7056	0.0687
CG4982	-0.7904	0.0912	Ubc10	-0.6999	0.0811
CG5010	-1.7669	0.0069	Ublcp1	-1.1739	0.0407
CG5028	0.6677	0.0971	Uch	0.9427	0.0385
CG5033	1.1721	0.0997	unc-104	0.8024	0.0677
CG5056	0.7380	0.0705	und	1.6572	0.0269
CG5144	-1.0505	0.0336	UQCR-6.4	0.8074	0.0582
CG5167	-0.9466	0.0453	UQCR-C1	1.0557	0.0262
CG5188	-0.7616	0.0745	UQCR-C2	-1.1666	0.0267
CG5191	-0.9747	0.0808	Usp14	0.8649	0.0642
CG5210	1.1759	0.0748	Usp16-45	-0.7709	0.0700

CG5214	-0.6487	0.0897	Vamp7	-1.6234	0.0171
CG5245	1.0078	0.0388	VepD	0.8015	0.0504
CG5261	-0.7571	0.0613	verm	-2.5390	0.0083
CG5267	3.0711	0.0049	vfl	-0.5900	0.0904
CG5326	-1.0922	0.0633	Vha100-2	-1.0065	0.0647
CG5346	-0.7684	0.0774	Vha16-1	0.7469	0.0549
CG5361	-1.5229	0.0472	Vha26	0.6704	0.0691
CG5376	2.1337	0.0770	Vha68-2	-1.1651	0.0545
CG5380	-2.1062	0.0065	VhaAC39-2	1.7488	0.0789
CG5390	-1.6817	0.0189	VhaM8.9	1.2496	0.0237
CG5458	2.0227	0.0336	VhaM9.7-b	0.5837	0.0860
CG5509	1.0291	0.0976	VhaM9.7-c	0.5565	0.0956
CG5516	0.8255	0.0532	vih	1.0992	0.0202
CG5532	0.6590	0.0964	Vm32E	2.1702	0.0421
CG5537	0.8448	0.0646	Vps2	-0.8265	0.0578
CG5589	1.0888	0.0515	Vps20	0.6656	0.0882
CG5599	0.8980	0.0831	Vps24	0.8091	0.0642
CG5646	1.3441	0.0691	Vps28	0.9866	0.0282
CG5727	0.7386	0.0524	Vps29	1.9470	0.0041
CG5731	-1.1118	0.0469	vri	-0.7030	0.0827
CG5823	1.2167	0.0936	Vti1b	-1.9395	0.0176
CG5830	0.6804	0.1000	vvl	-0.7095	0.0682
CG5835	-1.2619	0.0545	wac	1.2913	0.0166
CG5853	-1.3221	0.0549	wap	0.9235	0.0549
CG5854	0.8952	0.0480	wcd	1.0464	0.0681
CG5861	0.9501	0.0638	wdp	-1.4159	0.0423
CG5885	1.5273	0.0105	wek	1.5912	0.0732
CG5902	0.9091	0.0911	wg	-0.9203	0.0846
CG5906	1.6471	0.0848	Wnt5	-0.6294	0.0882
CG5916	-0.9052	0.0593	wuho	0.7985	0.0826
CG5928	-1.8129	0.0444	Xbp1	-0.7368	0.0721
CG5938	1.7195	0.0166	yellow-b	-2.1913	0.0236
CG5961	0.9760	0.0819	yellow-c	-1.4945	0.0489
CG5973	-1.4567	0.0497	yellow-d2	-2.3107	0.0093
CG5984	-1.3306	0.0466	yellow-h	-1.5205	0.0677
CG5986	1.3443	0.0288	ZC3H3	0.7484	0.0621
CG5989	0.7747	0.0691	zetaTry	-2.4659	0.0650
CG5991	0.7262	0.0911	Zip89B	-1.3117	0.0419
CG6028	0.5570	0.0987	ZnT33D	0.9790	0.0916
CG6091	0.8191	0.0903	Zpr1	1.0826	0.0515
CG6118	-0.8572	0.0975	Zw	-1.2005	0.0625

CG6136	1.3283	0.0319			

[a] Log2 fold change of Dam-RNA Pol II/Dam-only

[b] NOIseq probability = 1-q (q ≥ 0.9)